IDENTIFICATION OF CHROMATIN RELATED GENES REGULATING TEMOZOLOMIDE RESISTANCE IN GBM

by

Filiz ŞENBABAOĞLU

A Dissertation Submitted to the

Graduate School of Health Sciences

in Partial Fulfillment of the Requirements for

the Degree of

Doctor of Philosophy

in

Cellular and Molecular Medicine

KOÇ
UNIVERSITY

June 24, 2019

Identification of chromatin related genes regulating Temozolomide resistance in GBM

Koç University

Graduate School of Health Sciences

This is to certify that I have examined this copy of a doctoral dissertation by

Filiz ŞENBABAOĞLU

and have found that it is complete and satisfactory in all respects,

and that any and all revisions required by the final

examining committee have been made.

Committee Members:

_____

Assoc. Prof. Tuğba Bağcı-Önder (Advisor)

_____

Assoc. Prof. Tamer Önder

_____

Prof. İhsan Solaroğlu

_____

Prof. Nesrin Özören

_____

Assoc. Prof. Bilal Kerman

Date: _____

To my father Dr. Ali Macit Şenbabaoğlu
and my best friend Giray Sönmez,
both of whom lost the battle against cancer…

ABSTRACT

Identification of chromatin related genes regulating Temozolomide resistance in GBM

Filiz ŞENBABAOĞLU

Doctor of Philosophy in Cellular and Molecular Medicine

June 24, 2019

Glioblastoma multiforme (GBM) is the most common and malignant of all brain tumors. Unfortunately, less than 5% of patients survive five years post diagnosis. Standard-of-care for GBM consists of surgery, irradiation and chemotherapy with Temozolomide (TMZ) and it has remained unchanged in the last 20 years. Recurrence of tumors in a therapy-resistant state is a major contributing factor to the poor prognosis of GBM patients.

In this thesis, new *in vitro* models of acquired TMZ resistance were generated in order to examine the molecular features associated with therapy resistance in GBMs. Transcriptomic differences between paired TMZ-sensitive and TMZ-resistant cell lines were examined by RNA sequencing, which revealed major alterations in the resistant cell populations. Accordingly, our established TMZ-resistant models were found to express high levels of several DNA repair pathway components, as part of an adaptive mechanism to resist TMZ-induced DNA damage. Specifically, they were highly dependent on Direct Reversal Repair enzyme MGMT activity, a known prognostic marker in GBM. In addition, key elements of Base Excision Repair and Double Strand Break Repair pathways were upregulated in these cell lines. In parallel, TMZ-resistant cells were also found to activate/inhibit selected cell-cycle regulators, such as CDK4, CDK6, WEE1 and p21. These adaptive changes were probably key elements to ensure their survival under selective pressure.

As the acquired therapy-resistance involves genetic and epigenetic changes in tumor cells, epigenetic vulnerabilities of these resistant cell lines were thoroughly examined. It is known that cancers show aberrant epigenetic regulation, mostly through global changes in DNA methylation and altered histone modification patterns. Yet, the epigenetic mechanisms that cause therapy resistance are not well-known. To examine epigenetic mechanisms of TMZ-resistance and identify new epigenetic inhibitors, we performed chemical screens on the TMZ-resistant cells and their parental controls. Using a comprehensive epigenetic probe library against chromatin modifiers, we identified several Histone deacetylase inhibitors (HDACi) as potent agents to target TMZ-resistant cells. We then focused on a specific class of HDACs as a target, namely HDAC6, as it was less studied in GBM and its inhibitors were emerging as new anti-cancer agents. Accumulating evidence suggests that HDAC6 has a role in drug resistance and apoptosis in GBM, however its exact role in the therapy-resistant state has remained elusive. Thus, in this thesis the role of HDAC6 inhibition in TMZ resistance was thoroughly studied. Using chemical inhibitors (Ricolinostat, CAY10603) and CRISPR/Cas9-mediated gene silencing, we showed that HDAC6 inhibition caused marked alterations in the DNA Repair pathway, led to cell cycle arrest and ultimately apoptosis in GBM cells.

Together, generating and characterizing new models of TMZ-resistance, we identified HDAC6 as a new therapeutic target for therapy-resistant GBMs.

ÖZETÇE

GBM'de Temozolomid direncini düzenleyen kromatin ile ilişkili genlerin belirlenmesi

Filiz ŞENBABAOĞLU

Hücresel ve Moleküler Tıp, Doktora

24 Haziran 2019

Glioblastoma multiform (GBM), yetişkinlerde beyin tümörleri arasında görülen en yaygın ve en malign tümör tipidir. GBM hastalarının %5'inden daha azı tanıdan beş yıl sonrasında hayatta kalabilmektedir. GBM için standart tedavi yöntemi son 15 yılda değişmemiş olmakla beraber, cerrahi müdahale, radyoterapi ve kemoterapötik ajan Temozolomid (TMZ)'den oluşmaktadır. Ancak, hastaların büyük bir kısmında tümörler tedaviye dirençli olarak nüks etmektedir.

Bu tezde, GBM'lerde terapi direnci ile ilişkili mekanizmaları incelemek için TMZ direnci kazandırılmış özgün *in vitro* modeller üretilmiştir. TMZ'ye duyarlı ve TMZ'ye dirençli hücre diziler arasındaki transkriptomik farklılıklar, RNA dizilim deneyleri ile incelenmiştir. Buna göre, oluşturulan TMZ'ye dirençli modellerimizin, TMZ'nin neden olduğu DNA hasarına karşı direnç kazandıkları ve çeşitli DNA onarım yolaklarını yüksek seviyelerde ifade ettikleri bulunmuştur. Dirençli hücrelerimizin GBM'de bir prognostik belirteç olarak kullanılan MGMT enzim ifadesine yüksek derecede bağımlı oldukları gözlemlenmiştir. Ek olarak, Baz Çıkarma Onarımı ve DNA Çift Zincir Kırıkları Onarım yolaklarının temel öğelerinin bu hücre dizilerinde yüksek oranda ifade edildiği belirlenmiştir. Bunun yanında, TMZ dirençli hücrelerin CDK4, CDK6, WEE1 ve p21 gibi hücre döngüsü düzenleyicilerini aktifleştirdiği/baskıladığı bulunmuştur.

Kazanılmış terapi direnci, tümör hücrelerinde genetik ve epigenetik değişiklikleri içerdiği için, bu projede TMZ-dirençli hücre dizilerinin epigenetik mekanizmaları araştırılmıştır. Kanser hücrelerinin çoğunlukla DNA metilasyonunda ve değişmiş histon modifikasyon modellerinde değişiklikler yoluyla, anormal epigenetik düzenleme gösterdiği bilinmektedir. Ancak, terapi direncine neden olan epigenetik mekanizmalar iyi bilinmemektedir. Bu tez kapsamında, kanserlerin, TMZ direncine yol açan epigenetik mekanizmalarını incelemek ve yeni epigenetik inhibitörler tanımlamak için, TMZ-dirençli hücreler ve kontrolleri üzerinde kimyasal kütüphane taramaları yapılmıştır. Sonuç olarak, TMZ-dirençli hücreleri hedef alan güçlü ajanlar olarak histon deasetilaz inhibitörleri (HDACi) tanımlanmış ve GBM'de az çalışılan HDAC6 inhibisyonuna odaklanılmıştır. Literatürde HDAC6'nın GBM'de ilaç direnci ve apoptozda bir rolü olduğu gösterilmiş, ancak tedaviye dirençli durumdaki kesin rolü detaylı çalışılmamıştır. Bu nedenle, bu tezde HDAC6 inhibisyonunun TMZ direncindeki rolü incelenmiştir. HDAC6 inhibisyonu kimyasal inhibitörler (Ricolinostat, CAY10603) ve CRISPR/Cas9 gen susturma yöntemi kullanarak sağlanmış ve bu inhibisyonun DNA tamir mekanizmalarında değişikliklere, hücre döngüsünü yavaşlatmasına ve sonuçta apoptoza neden olduğunu gösterilmiştir.

Sonuç olarak, bu tez kapsamında, özgün TMZ-direnç modelleri üretilmiş, detaylıca karakterize edilmiş ve HDAC6 tedaviye dirençli GBM hastaları için yeni bir tedavi hedefi olarak belirlenmiştir.

ACKNOWLEDGMENTS

First of all, I would like to thank my advisor Dr. Tuğba Bağcı-Önder. She has been a really important role model and her endless support was really valuable during my PhD. Words cannot describe the way her presence has shaped my life both scientifically and personally. I am utterly grateful to her.

I wish to thank my committee members Prof. Dr. Nesrin Özören, Prof. Dr. İhsan Solaroğlu, and Dr. Tamer Önder for their scientific suggestions throughout this thesis. In addition, I thank Dr. Bilal Kerman for his valuable time.

I would like to thank Koç University Research Center for Translational Medicine (KUTTAM), The Scientific and Technological Research Council of Turkey (TÜBİTAK) and EMBO short term fellowship for the financial support. In addition, I owe a lot to Darüşşafaka Foundation, they have supported my education from the age of 11 to the end of my undergraduates. I do not think I could have pursued my dream to become a scientist if I was not a member of the Daçka family.

I need to thank Prof. Dr. Udo Oppermann, Dr. Jim Dunford, Dr. Martin Philpott, Dr. Adam Cribbs, Graham Wells and the rest of the Oppermann Group for the lovely environment and scientific help during my research visit.

I would like to thank KUTTAM family, especially Lack Lab and TO Lab members. Ceren Şeref deserves special thanks for being by my side from the first day of METU to our journey in Koç University, it was a bumpy and long road, but we finally are going to make it. I would also like thank Dr. Fatma Özgün and Dr. Burcu Özçimen for being my closest friends in this journey, and their helpfulness throughout the years.

I would always remember my fellow labmates and appreciate the family we have built together called TBO lab. Ahmet Cingöz, who has been my comrade in this journey. From the time we studied for qualifiers together up to the defending our thesis on the same day, he was the calmest colleague one can hope for. Özlem Yedier-Bayram has helped me a lot during last years, and she was a delight to have around. Ali Cenk Aksu deserves special thanks, because of his wonderful support, endless friendship and remarkable mind. He has been the best friend I have needed for so long. Fidan Şeker, Alişan Kayabölen, Ezgi Özyerli-Göknar, İlknur Sur-Erdem, Nareg Pınarbaşı, Seher Emreoğlu, Birsu Kölemen, Göktuğ Karabıyık and Yağmur Kala among others have provided this friendly environment that made coming to work joyful. Lastly, my

undergraduate research assistant Duygu Uçku deserves applause for her tremendous work.

I thank my former flatmates Dr. Eda Mızrak and Dr. Hilal (Filal/Hiliz) Saraç, Dr. Deniz Uğurlu-Çimen and Yasemin İnceoğlu who were there for me whenever I needed, and they were lovely to live with. Ezgi Kaya-Aksoy for being one of my closest friends and being there for me regardless of the distance. My childhood friend Buket Yazıcı for understanding when I had to work, and for forcing me to take a break when I desperately needed. Burcu Kutlu Kocalar from KURES should be noted here due to her exceptional help during the darkest times. She was a perfect guidance counselor when I needed the most.

Lastly, I wish to thank my mother, my brother, and my grandparents for the endless support they have given. Without them, I could not be what I am today.

TABLE OF CONTENTS

ABSTRACT iv
ÖZETÇE v
ACKNOWLEDGMENTS vi
TABLE OF CONTENTS viii
LIST OF TABLES xii
LIST OF FIGURES xiii
NOMENCLATURE xvi
1. INTRODUCTION 1
1.1. Glioblastoma multiforme (GBM) 1
1.1.1. Glioblastoma genetics 2
1.2. Treatment of Glioblastoma 7
1.2.1. Irradiation 8
1.2.2. Temozolomide 10
1.2.3. Nitrosoureas 11
1.2.4. Tumor treating fields 12
1.2.5. Potential targeted therapies for Glioblastoma 13
1.2.5.1. Endothelial Growth Factor Receptor (EGFR) 13
1.2.5.2. Vascular Endothelial Growth Factor (VEGF) 13
1.2.5.3. O-6-Methylguanine-DNA Methyltransferase (MGMT) 14
1.2.6. Therapy resistance in GBM 14
1.2.6.1. Mechanisms of Irradiation resistance 15
1.2.6.2. Mechanisms of Temozolomide resistance 17
1.2.6.2.1. Direct Repair and MGMT 17
1.2.6.2.2. Mismatch Repair 18
1.2.6.2.3. Base Excision Repair and PARP 18
1.2.6.2.4. Tumor suppressors p53 and PTEN 20
1.3. Epigenetic regulation and Glioblastoma multiforme 20
1.3.1. Chromatin regulators 20
1.3.2. Histone acetylation/deacetylation in GBM 21
1.3.2.1. The role of HDAC6 in GBM and Temozolomide resistance 25
1.4. Primary GBM models 28
2. MATERIALS AND METHODS 30
2.1. Cell culture and chemicals 30
2.2. Establishing primary GBM cell lines and their matched fibroblasts 30

2.3. Testing tumor forming capacities of primary cell lines in mice 31
2.4. Cell viability and proliferation assays 32
2.4.1. Cell Titer Glo assay 32
2.4.2. Clonogenic assays 32
2.5. Establishment of Temozolomide-resistant cell lines 32
2.6. A screen with a chemical library targeting histone modifying enzymes 34
2.7. Hit validation for chemical probes screen 34
2.8. RNA sequencing 34
2.9. Assay for Transposable-Accessible Chromatin using sequencing (ATAC-seq) 36
2.9.1. Expression, Purification, Assembly and Assay of Tn5 Transposase 36
2.9.2. ATAC-seq 36
2.10. Processing of next-generation sequencing data 37
2.11. Gene expression detection by qRT-PCR 38
2.12. CRISPR/Cas9 plasmid cloning 38
2.13. Protein detection by Western Blot 39
2.14. Caspase activity and inhibition assays 41
2.15. Cell cycle analysis by propidium iodide 42
2.16. Statistical Analysis 42
3. RESULTS 43
3.1. Establishment of Temozolomide resistant cell lines 43
3.1.1. Determining Temozolomide (TMZ) response of GBM cell lines 43
3.1.2. Establishment of Temozolomide-resistant cell lines 45
3.1.3. Characterization of TMZ-resistant cell lines 47
3.1.3.1. Response to other DNA alkylating agents 47
3.1.3.2. Investigation of transcriptome changes by RNA-seq 47
3.1.3.2.1. Targeting FGFR2 in TMZ-resistant cell lines 50
3.1.3.3. The role of MGMT in TMZ resistance 52
3.2. Identifying the epigenetic regulators of Temozolomide resistance in GBM . 54
3.2.1. Epigenetic probes screens to identify epigenetic vulnerabilities of TMZ-resistant cell lines 54
3.2.2. HDACi is the major group of TMZ-sensitizers in the epigenetic screens 61
3.2.3. The role of HDAC6 and its inhibition in TMZ-Resistant cells 63
3.2.3.1. Endogenous expression levels of HDACs 63
3.2.3.2. HDAC6 Inhibition by Chemical Inhibitors 65
3.2.3.3. HDAC6 Knockout cells by CRISPR/Cas9 65

3.2.3.4. Histone alterations in HDAC6 inhibited cells 67
3.2.3.5. Ricolinostat treatment induces apoptosis in TMZ-resistant cells ... 68
3.2.3.6. Transcriptome changes upon Ricolinostat treatment 70
3.2.3.6.1. Cell cycle is altered with Ricolinostat treatment 72
3.2.3.6.2. DNA damage and repair related pathways are affected by Ricolinostat 77
3.2.4. Genome wide chromatin accessibility detection by ATAC-seq 81
3.2.4.1. Optimization for GBM cell lines 81
3.2.4.2. Chromatin accessibility among cell lines 82
3.2.5. Testing the leads on established primary GBM cell lines 87
3.2.5.1. Establishing primary cell lines from GBM patient biopsies 87
3.2.5.2. Generation of KUGBM8-EF TMZ resistant cell line 90
3.2.5.3. The role of HDAC6 inhibition on KUGBM8-EF cell line 91
4. DISCUSSION 93
HDAC6 inhibition can induce cell death in TMZ-resistant cell lines 98
5. BIBLIOGRAPHY 105
6. APPENDIX A - EPIKOL SCREEN 117
6.1. Introduction 117
6.1.1. Histone methylation/demethylation in GBM 117
6.1.1.1. KDM5A 118
6.1.1.2. CREBBP/P300 119
6.2. Materials & methods 120
6.2.1. Generation of EPIKOL library and screen strategy 120
6.2.2. Cloning of KDM5A, CREBBP and EP300 into plentiCRISPRv2 plasmid 122
6.2.3. T7 Endonuclease assay 123
6.2.4. shRNA cloning of KDM5A 123
6.2.5. Chemical inhibitors 124
6.3. Results & Discussion 125
6.3.1. KDM5A silencing increases TMZ induced cell death 127
1.1.1. EP300 has a role in TMZ resistance 129
7. APPENDIX B - KUGBM8-EF drug screen 157
7.1. Introduction 157
7.2. Materials & methods 157
7.2.1. Cell culture, chemicals and reagents 157
7.2.2. Drug screen 157

7.2.3. Validation of chosen hits 158
7.3. Results & Discussion 158
8. APPENDIX C - VIABILITY RESULTS OF PROBES SCREEN 176

LIST OF TABLES

Table 1.1. Most Frequent Copy Number Alterations (CNAs) and the Corresponding Genes Observed in TCGA Glioblastoma Database 5
Table 1.2 Table of DNA Repair pathways. 9
Table 2.1 Components of epigenetic probes screen 34
Table 2.2 List of epigenetic probes screen 35
Table 2.3 Adapters used in ATAC-seq 37
Table 2.4 qRT-PCR primer sequences 38
Table 2.5 Oligonucleotide sequences of gRNAs 39
Table 2.6 List of antibodies used in Western Blot 41
Table 3.1 Hits of T98G and U373 1st library. 57
Table 3.2 Hits of U373 and established TMZ-Res cells with 2nd library. 59
Table 3.3 List of GBM patient derived primary cell lines. 87
Table 6.1 Contents of EPIKOL 117
Table 6.2 Primers used in nested PCR 122
Table 6.3 Oligos and T7 primers 123
Table 6.4 List of KDM5A oligos and qRT-PCR primers 124
Table 6.5 List of EPIKOL gRNAs 131
Table 7.1 Table of hits divided into therapeutic classes and effects. 160
Table 7.2 List of drugs included in Prestwick Chemical Library 162
Table 8.1 Percent viability results of Epigenetics Probes Screens 176

LIST OF FIGURES

Figure 1.1 MRI image of a GBM patient 2
Figure 1.2 Common acquired mutations of primary and secondary glioblastoma..... 3
Figure 1.3 Major pathways altered in glioblastoma 6
Figure 1.4 Cell cycle progression and DNA Repair 7
Figure 1.5 The DNA damage response (DDR) pathway activated by irradiation..... 10
Figure 1.6 Mechanism of action of TMZ 12
Figure 1.7 Schematic representation of acquired and innate therapy resistance in tumors 16
Figure 1.8 DNA repair mechanisms to repair damage induced by TMZ 19
Figure 1.9 Epigenetic writers, readers and erasers form a dynamic process of regulation 22
Figure 1.10 The role of HATs and HDACs cancer cells 23
Figure 1.11 Double strand break recognition pathway. 24
Figure 1.12 Reactions to histone deacetylase inhibitors (HDACi) 25
Figure 1.13 Structure and function of HDAC6 26
Figure 1.14 HDAC6 Expression in Sun Brain Glioblastoma cohort vs. Normal Brain 27
Figure 2.1 Schematic representation of establishment of TMZ resistant cell lines..... 33
Figure 3.1. IC_{50} values of TMZ treated GBM cell lines 44
Figure 3.2. TMZ response of U373. 44
Figure 3.3. Clonogenic assay to test TMZ resistance 46
Figure 3.4. Clonogenic assay of drug holiday sublines 46
Figure 3.5. Response to other DNA alkylating agents 48
Figure 3.6. RNA-seq analysis of TMZ-resistant cells 49
Figure 3.7. Common changes in the transcriptome of TMZ-resistant cell lines 50
Figure 3.8. Treatment with FGFR inhibitors 51
Figure 3.9 Combination of FGFR inhibitors with TMZ..... 51
Figure 3.10. MGMT expression levels of TMZR cell lines. 52
Figure 3.11. Overexpressing MGMT in U373 causes TMZ resistance. 53
Figure 3.12. MGMT Knockout cells 54
Figure 3.13. Epigenetic probe screen among U373 and T98G cells. 56
Figure 3.14. Epigenetic probe screen among U373 and T98G cells. 58
Figure 3.15. Heat map of top hits of epigenetic probes screen 60

Figure 3.16. All HDACi in epigenetics probes library 62
Figure 3.17. Cell viability of selected HDACi 62
Figure 3.18. Endogenous HDAC expression 63
Figure 3.19. HDAC6 levels detected by qRT-PCR 64
Figure 3.20 HDAC6i combined with TMZ 65
Figure 3.21. HDAC6 Knockout cells 66
Figure 3.22. Proliferation assays of HDAC6 KO cells 67
Figure 3.23. Acetylation marks of histone H3 68
Figure 3.24. PARP cleavage upon TMZ and/or Ricolinostat treatment 68
Figure 3.25. Caspase Glo 3/7 activity assay 69
Figure 3.26. General caspase inhibitor recovers cell viability upon Ricolinostat treatment 70
Figure 3.27 Heatmap and Principal Component Analysis for vehicle or Ricolinostat treated RNA-seq samples. 71
Figure 3.28. MA plots of Control vs Ricolinostat. 71
Figure 3.29. GSEA analysis among Ctrl vs Ricolinostat treated samples 72
Figure 3.30 Heatmap of "G_1/S-Specific Transcription" Reactome dataset 73
Figure 3.31 Major cell cycle regulators 74
Figure 3.32 p21 gene expression levels of 36 hours Ricolinostat treated samples 75
Figure 3.33 p21 Western Blot. 75
Figure 0.1. Cell cycle changes upon TMZ treatment 76
Figure 0.2. Cell cycle changes upon Ricolinostat treatment 76
Figure 3.36. Heatmap of DNA Damage Repair Genes 78
Figure 3.37. qRT-PCR results of MGMT gene expression levels of 36 hours Ricolinostat treated cells 78
Figure 3.38. Additive effect of Ricolinostat on MGMT overexpression and knockout cells 79
Figure 3.39 Western blot of ATM, p-ATM, ATR and p-ATR 80
Figure 3.40 Cell viability of ATM or ATR inhibition 80
Figure 3.41 Cell viability of ATM or ATR inhibition combined with TMZ 80
Figure 3.42. ATAC-seq 81
Figure 3.43. Correlation plots of ATAC-seq 82
Figure 3.44 ATAC-seq results of U373 vs DE-TMZR. 83
Figure 3.45. IGV plot of MGMT gene 84

Figure 3.46 ATAC-seq results of U373 vs TMZR 85
Figure 3.47 ATAC-seq results of Ricolinostat treated samples. 86
Figure 3.48. Representative photos of established cell lines. 88
Figure 3.49 MRI of KUGBM8 patient prior to surgery 88
Figure 3.50 *In vivo* growth capacities of KUGBM8-DMEM and KUGBM8-EF cells.. 89
Figure 3.51 *In vivo* TMZ experiments 90
Figure 3.52 TMZ resistant cell line from KUGBM8-EF was established. 91
Figure 3.53 KUGBM8-EF cells were treated with Ricolinostat and TMZ for 5 days. .. 92
Figure 3.54 HDAC6 silenced KUGBM8-EF cell lines 92
Figure 4.1 Proposed model for TMZ resistant cell lines and changes upon Ricolinostat treatment. 102
Figure 6.1 KDM5A Expression in Sun Brain Glioblastoma cohort vs. Normal Brain 118
Figure 6.2 Schematics of EPIKOL screen 121
Figure 6.3 Representative gel image of EPIKOL sample preparation for NGS. 126
Figure 6.4 Read count distribution for screen time points are plotted. 126
Figure 6.5 Box plot of log2 gRNA counts among DMSO and TMZ treated samples . 126
Figure 6.6 KDM5A is among top hits of U373 depletion screen 127
Figure 6.7 KDM5A silencing induces TMZ sensitivity on U373 cells 128
Figure 6.8 U373 KDM5A knockdown cells 128
Figure 6.9 Cell viability results of KDM inhibition 129
Figure 6.10 Distribution of enriched RRA scores in TMZ-R TMZ treated vs TMZ-R DMSO day 30. 130
Figure 6.11 Silencing of CBP or EP300 enhances TMZ resistance 130
Figure 6.12 Clonogenic assay of cells treated with SGC-CBP30, a CREBBP/EP300-selective chemical probe 131
Figure 7.1 High-throughput drug repurposing screen on KUGBM8-EF cells. 159
Figure 7.2 Selected hits are combined with Temozolomide 161

NOMENCLATURE

53BP1	p53-binding protein 1
ABC	ATP binding cassette
ATM	Ataxia-telangiectasia mutated
ATR	Ataxia telangiectasia and Rad3-related
BBB	Blood Brain Barrier
BCNU	Carmustine
BER	Base Excision Repair
CCNA1	Cyclin A1
CCNE1	Cyclin E1
CCNU	Lomustine
CDC25	Cell division cycle 25
CDK	Cyclin-dependent kinase
CDKN1A	Cyclin Dependent Kinase Inhibitor 1A
CDKN2A/B	Cyclin-dependent kinase inhibitor 2A/B
CNAs	Copy number aberrations
CNS	Central Nervous System
CSC	Cancer stem cells
CTG	Cell Titer-Glo®
DDR	DNA damage response
DNMT	DNA methytransferase
DR	Direct Reversal
DSB	Double Strand Break
DSBR	Double Strand Break Repair
EGFR	Epidermal growth factor receptor
EORTC	European Organization for Research and Treatment of Cancer
ERST	ER-stress tolerance
FBS	Fetal Bovine Serum
FGF	Fibroblast growth factor
Fluc	Firefly Luciferase
GBM	Glioblastoma multiforme
GSC	Glioma stem-like cells
HAT	Histone acetyltransferases
HDAC	Histone deacetylase
HGFR	Hepatocyte growth factor receptor
HMT	Histone methyltransferases
HR	Homologous recombination
IDH1	Isocitrate dehydrogenase 1
IR	Irradiation
KDM	Histone demethylases
KDM	Lysine demethylase
LOH	Loss of heterozygosity

MDR	Multidrug resistance
MGMT	Methylguanine-DNA methyltransferase
MKI67	Marker of proliferation Ki67
MMR	Mismatch Repair
MRN	MRE11–RAD50–NBS1
N3-MeA	N3 methyl adenine
N7-MeG	N7 methyl guanine
NER	Nucleotide Excision Repair
NF1	Neurofibromatosis type 1
NHEJ	Non-homologous end-joining
NSEM	Normalized Standard Error of the Mean
NSTD	Normalized Standard Deviation
O6-BG	O6-benzylguanine
O6-MeG	O6 methylguanine
P/E	Promoter/enhancer
PARP1	Poly(ADP-ribose) polymerase-1
PCA	Principal Component Analysis
PCNA	Proliferating cell nuclear antigen
PDGFRA	Platelet-derived growth factor receptor A
PDX	Patient-derived xenograft
PI	propidium iodide
PI3K	Phosphatidylinositol 3-kinase
PIK3CA	Phosphatidylinositol-4,5-bisphosphate 3-kinase A
PIP3	Phosphatidylinositol (3,4,5)-trisphosphate
PRMT	Protein arginine methyltransferases
RB	Retinoblastoma
RB1	Retinoblastoma protein 1
RPA	Replication protein A
RT	Radiotherapy
RTK	Receptor tyrosine kinases
SEM	Standard Error of the Mean
SSB	Single Strand Break
STD	Standard Deviation
TCGA	The Cancer Genome Atlas
TERT	Telomerase reverse transcriptase
TKI	Tyrosine kinase inhibitor
TMZ	Temozolomide
TTFields	Tumor treating fields
VEGF	Vascular Endothelial Growth Factor
WHO	World Health Organization

1. INTRODUCTION

1.1. Glioblastoma multiforme (GBM)

According to World Health Organization (WHO) 2018 database, brain and central nervous system (CNS) tumors are among the top 20 common and malignant cancers around the world [1]. In Turkey, CNS tumors are in the top 10 most common cancers (2014 Ministry of Health database) [2].

CNS tumors are classified as gliomas and non-gliomas. Gliomas are further divided into several types, determined by the cell types that give rise to the tumor. Astrocytoma, oligodendroglioma, oligoastrocytoma and glioblastoma are acknowledged as gliomas. Together, gliomas consist of 80% of malignant nervous system tumors [3].

The international standard for the nomenclature and diagnosis of gliomas is determined by WHO classification. Accordingly, gliomas are classified into grade I to IV on the level of malignancy, which is determined by the histopathological criteria. Grade I gliomas have low proliferative potential and can be cured by surgery. Grade II, III and IV gliomas are highly malignant and invasive [4]. Glioblastoma multiforme (GBM, WHO astrocytoma grade IV) is the most common of all malignant brain tumors, and it is characterized as the most aggressive, invasive and undifferentiated tumor type.

Considering all cancer types, GBM is a relatively rare tumor. In developed countries, 3.5 per 100.000 GBM cases are diagnosed every year [5]. However, due to its poor prognosis, with median survival rate around 16 months, GBM is among the most deadly cancers [6].

GBM can occur at any age; however, epidemiology studies revealed that 87% of the patients are aged older than 55 years (mean age = 64 years). In addition, the incidence of GBM is 1.6 times higher in males compared to females [7,8]. There are no definite risk factors for GBM, it occurs sporadically without known predisposition, except some patients with hereditary tumor syndromes like Turcot syndrome and Li-Fraumeni syndrome [9]

The hallmarks of GBM can be defined as uncontrolled cell proliferation, diffuse infiltration, tendency for necrosis, angiogenesis, resistance to apoptosis, and genomic instability. The aggressive nature and heterogeneity of GBMs make treatment very difficult: Extensive tumor infiltration in the surrounding healthy brain tissue, tumor mass

formed by distinct cell types and resistance to available therapy options are the major challenges for successful treatment.

For GBM patients, current treatment regimen around the world is restricted to surgery, radiotherapy and the chemotherapeutic agent Temozolomide [10]. Due to frequent recurrence (**Figure 1.1**), relative survival rate estimates for GBM patients are quite low; only 5% of patients survive five years post diagnosis [11].

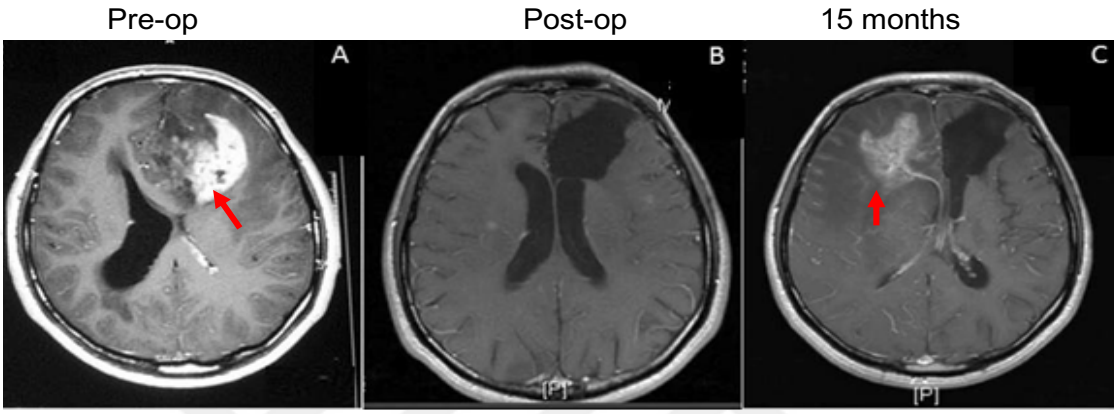

Figure 1.1 MRI image of a GBM patient A) Tumor on the right hemisphere prior to surgery **B)** Cavity due to total tumor removal post-operation **C)** Tumor recurrence observed in the left hemisphere 15 months after the operation. Red arrows indicate the tumor site. Image courtesy of Prof. Dr. İhsan Solaroğlu

1.1.1. Glioblastoma genetics

GBM can arise *de novo* (primary GBM) or progress from a lower grade tumor (secondary GBM). These tumors differ in their mutational and transcriptional landscapes (**Figure 1.2**). 90% of GBM cases are primary GBM, that develop rapidly and mostly in elderly patients.

Promoter methylation in Telomerase Reverse Transcriptase (TERT), the catalytic subunit of Telomerase, is one of the earliest events in gliomagenesis. Due to enhanced TERT activity, telomere length is preserved over cell divisions and cell survival is maintained [12].

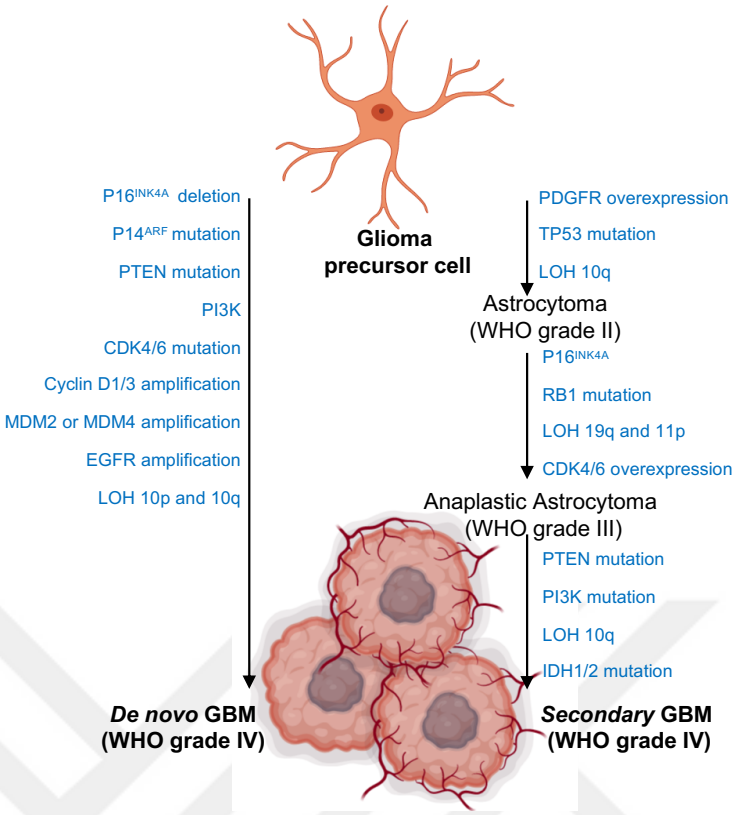

Figure 1.2 Common acquired mutations of primary and secondary glioblastoma. Figure adapted from [13,14]

Primary GBM cases are characterized by loss of heterozygosity (LOH) in 10q (70% of GBM), epidermal growth factor receptor (EGFR) amplification (36%), PTEN mutations (25%) and $p16^{INK4A}$ deletion (31%) [15]. Detailed research on genomic landscape of primary GBM by whole genome sequencing among paired tumor and non-malignant genomic DNA from 291 patients performed by Brennan and colleagues in 2013 revealed significantly mutated genes in GBM [16]. From this comprehensive study, PTEN, TP53, EGFR, phosphatidylinositol-4,5-bisphosphate 3-kinase A (PIK3CA), PIK3R1, NF1, retinoblastoma protein 1 (RB1), isocitrate dehydrogenase 1 (IDH1), and platelet-derived growth factor receptor A (PDGFRA) were identified, hence the importance of these genes in gliomagenesis was validated.

Secondary GBM occurs through the progression of WHO grade II astrocytoma to WHO grade III anaplastic astrocytoma, then to WHO grade IV GBM. For such secondary GBM patients, TP53 mutations are common. Indeed, during tumor progression, many additional mutations occur, such as LOH 10q25 (70% of cases) [15]. Mutations in IDH genes (IDH1 and IDH2) are observed in over 70% of low-grade gliomas and in a subset of the GBM cases [17,18]. IDH1 and IDH2 are mutually exclusive, and the mutations

can occur in one of them [19]. IDH1 catalyzes the oxidative decarboxylation of isocitrate and produces α-ketoglutarate and CO_2. IDH1 and IDH2 catalyze the same reaction outside the context of citric acid cycle and use $NADP^+$ as a cofactor. The most frequent IDH1 mutation (over 95%) occurs at arginine 132 (R132H). The wild-type IDH1 converts isocitrate to α-ketoglutarate, whereas the mutant IDH1 results catalyzes α-ketoglutarate into 2-hydroxyglutarate, which is an oncometabolite that has been associated with genomic hypertension, genetic instability and malignant transformation [17]. It has been found that, IDH1 mutation is one of the most common and earliest genetic alterations in gliomas and is one of the most effective diagnostic and predictive markers used for glioma patients. In addition, IDH mutations are generally associated with a better prognosis [17].

Copy number aberrations (CNAs) are somatic changes in chromosome structure that result in loss or gain of chromosome portions. The most common CNAs observed in GBM are partial loss of chromosome 9 and 10; polysomy of chromosomes 7, 19, and 20; focal deletion of CDKN2A/B locus (9p21.3); and focal amplifications of EGFR locus (7p11.2). Also, CNAs targeting chromosomes 7 and 10 are observed in early GBM tumor evolution. Abnormalities in other known GBM drivers include focal amplification of PDGFRA, SOX2, MDM2 and MDM4 [20] (**Table 1.1**).

Initiatives were taken by the National Institutes of Health's (USA) Cancer Genome Atlas (TCGA) to decipher GBM genetics complexity in the early 2000s. Therefore, GBMs are now the most molecularly profiled of all human tumors [14]. Following TCGA studies, combined efforts around the world revealed a more detailed molecular landscape of GBM. Amplification of EGFR, hepatocyte growth factor receptor (HGFR), PDGFRA, MDM4, MDM2, CCND2, and PIK3CA, among others, and deletion of cyclin-dependent kinase inhibitor 2A/B (CDKN2A/B), CDKN2C, PTEN, RB1, and NFKB1A are often observed in GBM. In addition, somatic mutations of p53, PTEN, neurofibromatosis type 1 (NF1), RB1, IDH1, and IDH2 have been detected with varying frequencies. As a result, genetic alterations in GBM were clustered around three major pathways; RTK/RAS/PI3K signaling, p53 signaling and RB signaling [21,22] (**Figure 1.3**).

Table 1.1. Most Frequent Copy Number Alterations (CNAs) and the Corresponding Genes Observed in TCGA Glioblastoma Database. Adapted from Lombardi et al. [20]

Gene	Cytoband	CNA	Frequency
CDKN2A	9p21	deletion	57%
CDKN2B	9p21	deletion	56%
EGFR	7p12	amplification	44%
MTAP	9p21	deletion	43%
CDK4	12q14	amplification	14%
PDGFRA	4q12	amplification	13%
MLLT3	9p22	deletion	12%
CHIC2	4q11	amplification	12%
KIT	4q12	amplification	12%
MDM4	1q32	amplification	9%
FIP1L1	4q12	amplification	9%
MDM2	12q14.3-q15	amplification	9%
DDIT3	12q13.1-q13.2	amplification	8%
PTEN	10q23.3	deletion	7%
GLI1	12q13.2-q13.3	amplification	7%

The most frequently mutated pathway in GBM patients include receptor tyrosine kinases (RTK), which are cell surface receptors that bind to growth factors. EGFR has a variety of roles including proliferation, migration, differentiation and survival in CNS cells. EGFR is amplified in 40-50% of GBMs [21], via overexpression of the receptor or its ligand, amplification of the *EGFR* locus, and/or receptor mutation. The most common mutation among EGFR in GBM patients is the EGFRvIII, due to the loss of exons 2–7, leading to a deletion of 267 amino-acids in the extracellular domain making the receptor ligand independent and constitutively active. This mutation is not observed in healthy tissues [23]. Wild-type EGFR and EGFRvIII can activate PI3K signaling, enhancing proliferation of GBM tumor cells [24].

Ras pathway is another commonly modified pathway in GBM. Ras functions in a complex signaling network to regulate many cellular functions such as cell proliferation, differentiation, apoptosis, and senescence. Direct Ras mutations are seen rarely in GBM, yet overall activity of Ras pathway is highly enhanced [20]. PI3K is one of the main effectors of RAS and upon growth factor receptor activation, PI3K is drawn to the cell membrane, resulting in the generation of the secondary messenger phosphatidylinositol (3,4,5)-trisphosphate (PIP3). PIP3 activates AKT which in turn leads to cell proliferation

and inhibition of apoptosis. PTEN is the negative regulator of PI3K, thus functions as a tumor suppressor gene[25]. In GBM, the tumor suppressor function of PTEN is frequently inactivated, resulting in increased PI3K function [26].

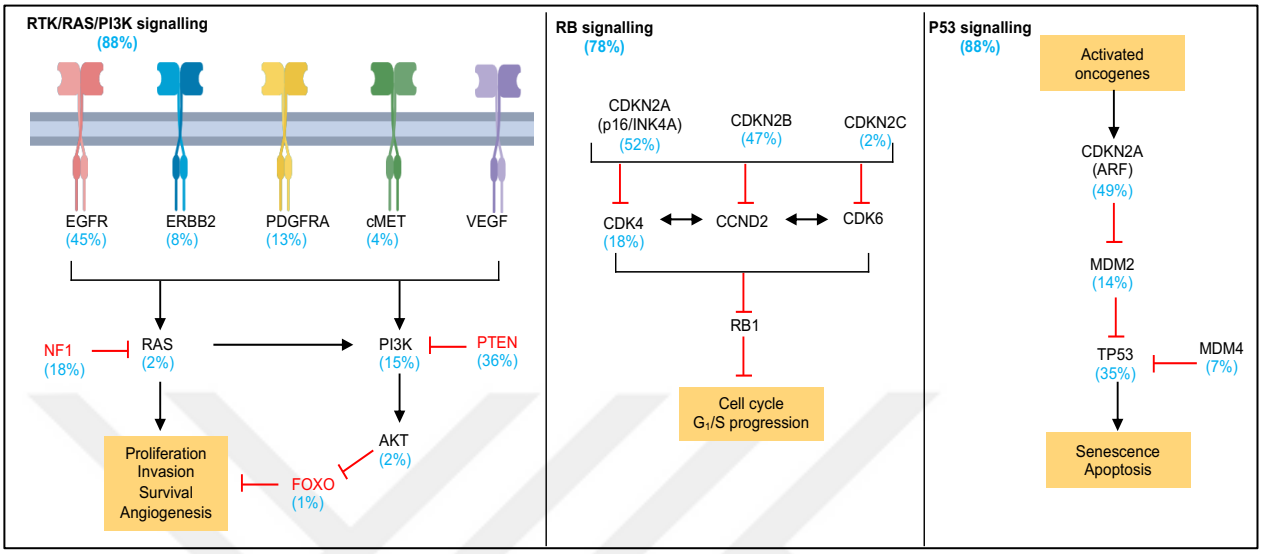

Figure 1.3 Major pathways altered in glioblastoma. Mutations, deletions, and amplifications in RTK/RAS/PI3K, RB, and p53 signaling pathways are shown. Frequency of alterations are indicated as percentages in blue. Adapted from [14].

P53 signaling pathway has a wide range of effects, including cell cycle control, DNA damage response and cell death. When DNA damage occurs, tumor suppressor gene TP53 is expressed, which in turn enhances the transcription of a G_1 phase cell cycle inhibitor, p21 (CDKN1A). If DNA damage cannot be repaired, cell death mechanisms are activated [27]. MDM2, the negative regulator of P53 is inactivated by CDKN2A-p14ARF, so P53 activity is maintained for DNA repair. In gliomas, P53 is often mutated by missense mutations that target exons crucial for DNA binding. MDM2 amplification, and CDKN2A-p14ARF deletion are also commonly observed in gliomas [28,29].

Retinoblastoma (Rb) pathway is the third major altered pathway in GBM. Rb is a known tumor suppressor, controlling cell cycle progression at G_1 phase [30]. In non-proliferating cells, Rb is hypo-phosphorylated and bound to E2F transcription factor. This binding prevents the transcription of genes for cell cycle continuum and mitotic progress. In proliferating cells, growth factors induce Cyclin D1 formation and the activation of cyclin-dependent kinase-cyclin (CDK/cyclin) complexes. Active CDK/cyclin complexes phosphorylate Rb, resulting in the release of transcription factor E2F. Hence cell cycle continues, and proliferation occurs. CDK/cyclin complexes are under tight regulation by

cyclin dependent kinase inhibitor proteins (CDKN). CDKN competes with cyclins, thus inhibiting phosphorylation of Rb [31,32]. Some GBM cells can decrease cell cycle inhibition checkpoints by methylation of *RB* promoter silencing the *RB* gene [33] (**Figure 1.4**).

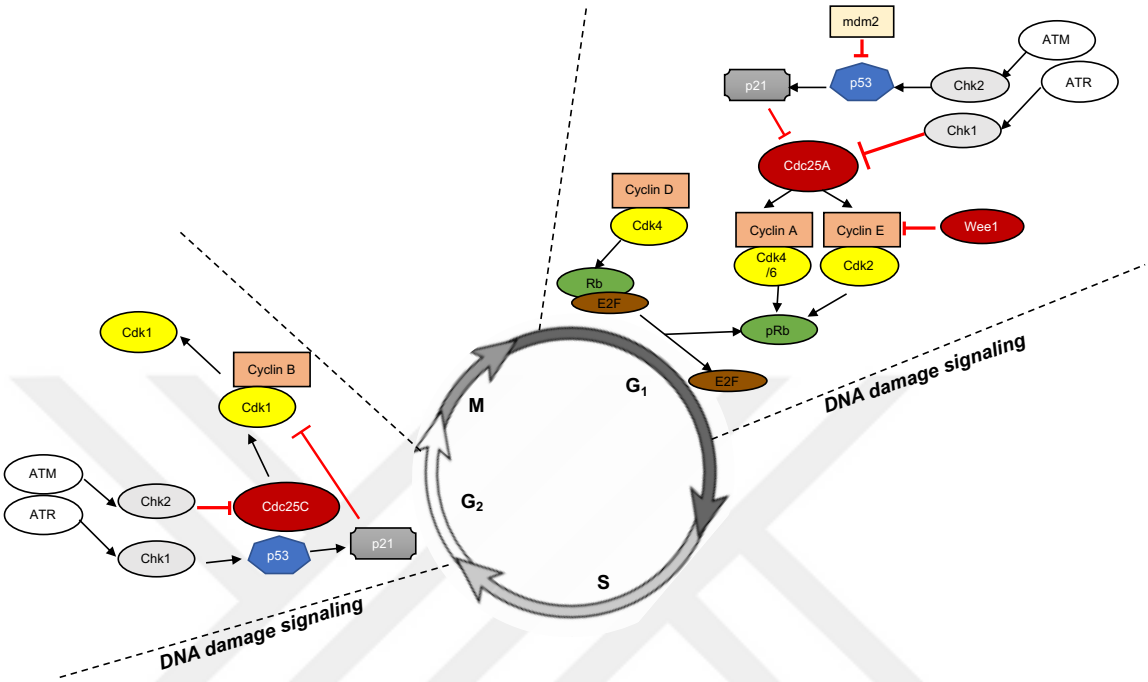

Figure 1.4 Cell cycle progression and DNA Repair. 3 major cell cycle checkpoints are located in G_1/S, intra-S phase and G_2/M phase. Cell cycle checkpoints are controlled by tumor suppressors (p53, p21) and Cdks. Figure adapted from [34,35]

1.2. Treatment of Glioblastoma

Current therapy for GBM was implemented after 2005, according to the results of a phase III study carried out by European Organization for Research and Treatment of Cancer (EORTC) and the National Cancer Institute of Canada. In this trial, after maximum safe surgical resection, concurrent radiation and Temozolomide (TMZ) was administered. TMZ was used at the beginning of GBM treatment at the daily dose of 75 mg/m^2 body surface area in association with radiotherapy (60 Gy in 30 fractions) for six weeks. Then, for maintenance six cycles of TMZ alone at the dose of 150–200 mg/m^2 for five days every 28 days. This aggressive trimodal regimen denoted as "Stupp protocol", improved 2 years survival from 10% for treatment with radiotherapy (RT) alone to 27% compared to treatment with RT and Temozolomide (TMZ) [36]. However, this treatment is still faint against GBM, recurrence occurs within months in 90% of GBM patients [37,38].

Upon recurrence, many patients undergo further surgical resection, and therapy options include re-challenging with alkylating agents, platinum drugs, or VEGF inhibitors [3,39]. Yet, none of these options can currently cure GBM.

Both RT and TMZ induce DNA damages in the tumor cells, which do not have the capacity to repair vast amount of induced damage and therefore undergo senescence and/or apoptosis. However, one major adaptive mechanism of cancer cells is known to be enhancing the DNA repair activity, through genetic and/or epigenetic events [10]. Repair pathways can be grouped into Direct Reversal (DR), Base Excision Repair (BER), Nucleotide Excision Repair (NER), Double Strand Break Repair (DSBR), Mismatch Repair (MMR) and Crosslink Repair [40] (**Table 1.2**).

1.2.1. Irradiation

Radiotherapy (RT) post-surgical resection is the basis of GBM treatment. There are various regimens on radiotherapy, however GBM patients usually receive a series of 2 Gy daily fractions of radiation over several weeks up to a total of 60 Gy. Repetitive but low dose RT application aims to kill greater number of tumor cells and minimize side effects on normal brain cells [35].

The main goal of RT is to deprive tumor cells of their replication potential by inducing DNA damage and cell death. Ionizing radiation can induce base damage, single-strand breaks (SSB), double-strand breaks (DSBs), sugar damage, DNA–DNA and DNA–protein cross-links [41]. DSBs are the most harmful damages, as they are trickier to repair than other DNA lesions and they trigger multifaceted DNA damage response (DDR). DDR is not a single pathway, but a group of highly interrelated signaling pathways including HR and NHEJ, each of which controls different mechanisms in the cell (**Figure 1.5, Table 1.3**).

Upon ionizing radiation administration, DSB and/or SSB occurs in DNA, which triggers DDR. DDR starts either with MRE11–RAD50–NBS1 (MRN) complex with detection of DSBs or replication protein A (RPA) and the RAD9–RAD1–HUS1 (9-1-1) complex spots exposed regions of single-stranded DNA. These sensors recruit the apical

Table 1.2 Table of DNA Repair pathways. Table adapted from the reference [42]

		SSB Repair			DSB Repair		Crosslink Repair
Repair Pathway	**DR**	**BER**	**NER**	**MMR**	**HR**	**NHEJ**	
DNA Damage Source	Alkylating agents	Alkylating agents	Alkylating agents , X-linkers, UV light	DNA Pol proofread errors, Alkylating agents	X-linking agents, replication inhibitors, Topo I inh.	IR, radiomimetics, Topo II inh.	X-linking agents
Type of Damage	Methylation of guanine bases	deamination, oxidation, alkylation of bases	Pyrimidine dimerization,	Mismatch pairing, alkylation of bases	DSB	DSB	DNA interstand crosslinks
Damage Sensors		DNA glycosylases (MBD4, NEIL1), APE1	XPC, DDB2,CSA	MSH2,MSH3, MSH6	MRN	Ku70/Ku80, PARP	FA core complex
Mediators			XPA, XPF, RPA	MLH1, PMS2	ATM,ATR, BRCA1/2, RPA	DNAPK	RAD51C,BRIP1
Effectors	MGMT	XRCC1, PNKP, Polβ, FEN1, TDP1, LIG1, LIG3	XPG,ERCC1, POLE, POLD1, LIG1, LIG3	EXO1, POLD, LIG1	RAD51, POLQ, FANCJ,	XRCC4, XLF, LIG4, Artemis, PAXX, WRN	XPG,ERCC1, POLE, POLD1, LIG1, LIG3

kinases ataxia-telangiectasia mutated (ATM) and ataxia telangiectasia and Rad3-related (ATR). ATM and ATR phosphorylate the histone variant H2AX on Serine 139 (acknowledged as γH2AX). ATM is predominantly activated by DSBs, but ATR responds to DNA replication stress, which is also caused by oncogenes. BRCA1, a tumor suppressor gene, is recruited to the sites of DNA damage on phosphorylation by ATM and ATR. BRCA1 promotes DNA repair by HR and has been reported to block transcriptional elongation at the DNA damage site. p53-binding protein 1 (53BP1) is involved in enduring DDR signaling by enhancing ATM stimulation. DDR signaling expands with downstream kinases CHK2 (phosphorylated by ATM) and CHK1 (phosphorylated by ATR). p53 is a downstream effector of CHK2, whereas cell division cycle 25 (CDC25) phosphatases are affected both by CHK1 and CHK2. CHK1 can also activate RAD51, a protein that has a major role in HR[43]. DDR-mediated response may result in cell cycle arrest followed by repair of damage and resumption of proliferation; senescence, or cell death by apoptosis.

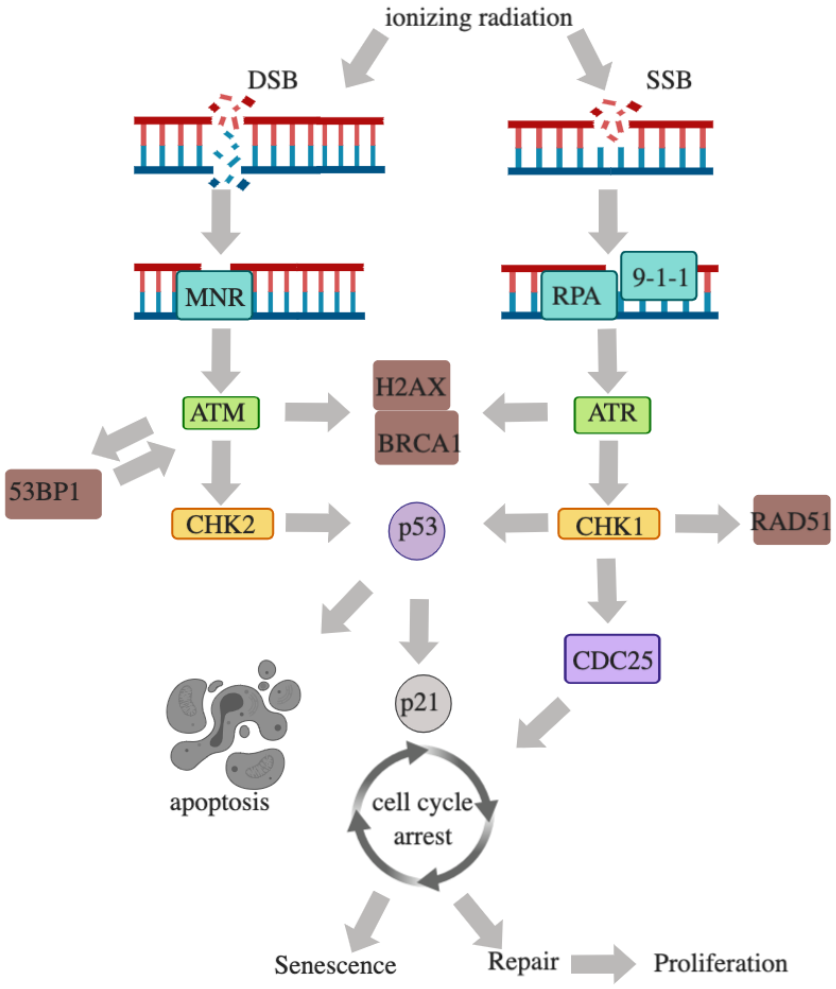

Figure 1.5 The DNA damage response (DDR) pathway activated by irradiation. Adapted from the references [34,35,40].

1.2.2. Temozolomide

TMZ is a small (194 Da) lipophilic molecule, which acts as a DNA alkylating agent that can pass through the Blood Brain Barrier (BBB), and it is stable only at acidic pH. Brain tumors possess a more alkaline pH compared with the surrounding healthy tissue, a situation that favors prodrug activation preferentially within tumor tissue [35,42,44]. TMZ as a prodrug undergoes a chemical conversion to the active form (MTIC), which will react with water to produce a highly reactive methyldiazonium cation (half-life=0.4 seconds). This unstable cation transfers a methyl group to DNA responsible for the cytotoxic effect of TMZ. The methylation occurs at purine bases of DNA at the O6 and N7 positions of guanine and the N3 position of adenine (**Figure 1.6**). N7 site of guanine and N3 site of adenine are strong nucleophilic sites in DNA, so N7 methyl guanine (N7-MeG) and N3 methyl adenine (N3-MeA) by TMZ are very frequent and represent 80–

85% and 8–18% of total alkylations, respectively [45]. N7-MeG and N3-MeA can be repaired by BER Pathway.

O6 methylguanine (O6-MeG) is a weak nucleophile and accounts for 5% of the total lesions caused by TMZ in DNA, but O6-MeG is the main cause of the TMZ cytotoxicity [39,46]. O6-MeG mispairs with thymine instead of cytosine during DNA replication, thus MMR pathway is alerted by this error. MMR excises the mispaired thymine but cannot remove O6-MeG. Repeated cycles of thymine reinsertion and excision result in persistent DNA strand breaks, causing replication fork collapse. This causes cell cycle arrest at G_2/M phase by ATR/CHK1-dependent signaling, finally resulting in activated apoptotic signaling. Methylguanine-DNA methyltransferase (MGMT) can remove the methyl adduct caused by TMZ, thus restoring guanine. So, TMZ cytotoxicity depends on functional MMR and low levels of MGMT [47].

1.2.3. Nitrosoureas

The DNA alkylating agents Carmustine (BCNU) and Lomustine (CCNU) are nitrosoureas that were used as first-line treatment of GBM in the 1970s and 1980s. However, nitrosoureas had undesired side effects such as bone marrow suppression, liver/renal toxicity, and interstitial lung disease. In 1999, two phase II clinical trials changed the therapy of GBM: TMZ was found to be effective for recurrent glioblastoma patients who had received up to one course of nitrosourea-based chemotherapy. Also, compared to other nitrosoureas, TMZ had shown a more tolerable profile. Hence nitrosoureas were moved into second-line therapy as single agents or in combination with TMZ for recurrent high-grade gliomas [45,48].

Carmustine as a biodegradable wafer that can be implanted to resected tumor site during surgery. These wafers provide release of alkylating agents to the surrounding tissue for several weeks, which results in benefit for patients [49]. A phase III clinical trial in 2009 combined Lomustine and TMZ. The trial suggests that Lomustine and TMZ chemotherapy might improve survival compared with TMZ only therapy in patients with newly diagnosed glioblastoma with methylated MGMT promoter [50,51]. Thus, nitrosoureas might be re-incorporated to the standard treatment regimen of GBM patients.

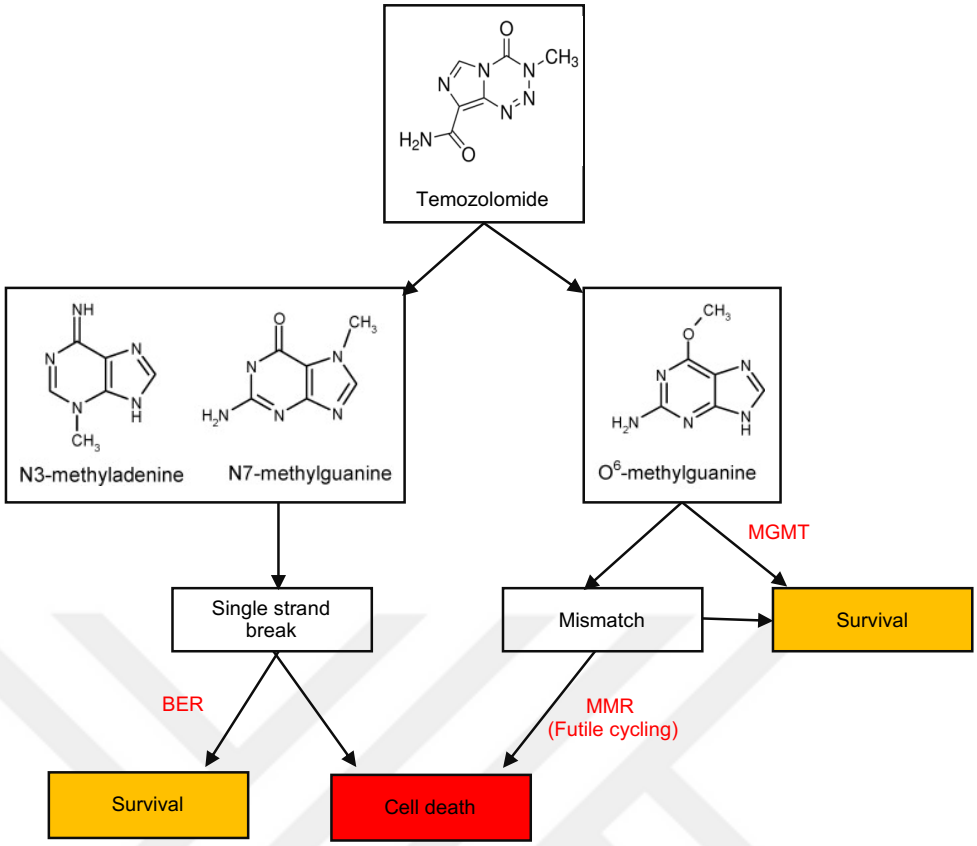

Figure 1.6 Mechanism of action of TMZ. Figure adapted from [52]

1.2.4. Tumor treating fields

Tumor treating fields (TTFields) are low-intensity alternating electric fields delivered at intermediate frequencies to disrupt the division of cancer cells [53]. The USA FDA approved TTFields as a GBM treatment initially in 2011 for recurrent GBM and later in 2015 for primary GBM.

The effect of TTFields was tested in a large cohort of patients (695 GBM patients) whose tumor was resected and had completed concomitant radiochemotherapy. These patients were then either treated with standard TMZ or TMZ and TTFields. Median progression-free survival of TMZ alone group was 4 months, whereas this number was increased to 6.7 months in TMZ and TTFields combination. Overall survival median was increased by 4.9 months in the TTFields combination group [54,55]. Thus, TTFields alongside chemotherapy can be beneficial for GBM patients, unfortunately this treatment option is not currently available in Turkey.

1.2.5. Potential targeted therapies for Glioblastoma

Following the TCGA initiative of genomic profiling of GBM, scientists have been provided with a map of frequent DNA copy number and somatic mutations in GBM. Thus, new classifications for GBM have brought up new potential therapeutic targets.

1.2.5.1. Endothelial Growth Factor Receptor (EGFR)

The common altered element of GBM is EGFR, so targeting EGFR was taught to be a promising approach. Small molecule tyrosine kinase inhibitors (TKIs) such as Erlotinib [56] and Gefitinib [50] are approved for treatments of many diseases, however because of numerous negative outcomes of clinical trials, they are not favored in glioblastoma. Trials in GBM patients have not shown efficacy as single agents or in combination treatments. In addition, major side effects were observed in patients. BBB permeability limitations and lack of selectivity of TKIs are among the reasons for failure of EGFR small molecule inhibitors in clinical studies [57] .

Several monoclonal antibodies targeting EGFR have been used over time for GBM. Cetuximab is an antibody-blocking ligand binding without receptor activation. When Cetuximab is combined with Bevacizumab, a monoclonal antibody against VEGF, tumor shrinkage was observed [58].

Given that EGFRvIII is expressed exclusively in malignant tissue and is highly contributing to tumorigenicity, it was targeted for immunotherapy via vaccinations. PEP-3, a peptide vaccination against the mutated segment of EGFRvIII and anti-EGFVRvIII Dendritic Cell (DC) vaccines were tested in GBM patients in clinical trials. A significant increase in median overall survival (26 months, $p=0.0013$) was observed after vaccination against EGFRvIII in GBM compared to non-vaccinated controls [59]

1.2.5.2. Vascular Endothelial Growth Factor (VEGF)

GBM is one of the most angiogenic solid tumors with vast amount of vasculature around the tumor. Angiogenesis is a pathologic hallmark of GBM, and the angiogenic process is facilitated by hypoxia-dependent and hypoxia-independent mechanisms. Hypoxia-inducible factor-1α (HIF-1α) accumulation leads to activation of Vascular Endothelial Growth Factor (VEGF) production, which is an important regulator of angiogenesis. VEGF is also upregulated in GBM patients via Ras/PI3K pathways. In addition to VEGF, other angiogenic factors fibroblast growth factor (FGF), platelet-

derived growth factor (PDGF), integrins, hepatocyte growth factor (HGF), ephrins, angiopoietins, and interleukin-8 are upregulated in GBM [6,60]. Hence targeting angiogenesis in GBM patients is an important treatment option.

Bevacizumab (Avastin) is a human recombinant monoclonal antibody targeting VEGF. It was FDA-approved in 2009 for recurrent GBM patients for use as a single agent following front-line therapy consisting of surgical resection, radiotherapy, and TMZ [61]. The efficacy of Bevacizumab is limited, and risks include, arterial thromboembolic events, venous thromboembolic events, hypertension, renal injury and proteinuria, ovarian failure, and congestive heart failure. While Bevacizumab is commonly used and known to increase progression free survival, overall survival remains unchanged for GBM patients.

VEGFR tyrosine kinase inhibitors such as Vatalanib, Sorafenib, and Cediranib were also tried in clinical trials. Overall the effect in overall survival was not significantly altered [62].

1.2.5.3. O-6-Methylguanine-DNA Methyltransferase (MGMT)

MGMT works in DR pathway and removes the O6-methylation on guanine. MGMT promoter is frequently hypermethylated in gliomas, resulting in the loss of MGMT expression and activity. Clinical studies have previously demonstrated that MGMT promoter methylation is a positive prognostic marker for the responsiveness of newly diagnosed gliomas to RT and alkylation agents such as TMZ[63,64].

Yet, MGMT mediated therapy resistance is frequently observed in GBM patients. MGMT-depleting agents, such as O6-benzylguanine (O6-BG), a pseudo substrate for MGMT, were tried in phase II clinical trials. O6-BG blocks the active site of MGMT, allowing methyl adducts to accumulate to induce O6-meG adducts. In a preclinical model using xenotransplanted nude mice, the combination of O6-BG with TMZ or Carmustine, augmented the anti-tumor effects [62]. However, preclinical results were unfortunately not replicated [65] at the clinical trial phase and caused hematologic toxicities, a reduced therapeutic window and no clinical benefit compared to TMZ alone [6].

1.2.6. Therapy resistance in GBM

Resistance to anticancer drugs and/or irradiation might be due to a variety of factors, such as individual variations in patients and somatic cell genetic differences in

tumors. Resistance is either intrinsic or tumor cells can acquire resistance over time (**Figure 1.7**). Expression of one or more energy-dependent transporters that detect and eject anticancer drugs from cells is one of the major mechanisms for acquired resistance. In addition, insensitivity to drug-induced apoptosis and induction of drug-detoxifying mechanisms play important roles in acquired drug resistance [38]. Multidrug resistance (MDR) is defined as the resistance to one chemotherapeutic drug accompanied by resistance to others that may have different structures and mechanisms of action [66]. ATP binding cassette (ABC) membrane transporters have roles in the drug efflux mechanism and 3 members of this family (P-gp, MRP1 and ABC- P) have been correlated with resistance to many drugs in variety of cancers [67].

Despite aggressive surgical resection and chemotherapy, tumor recurrence is a major problem for GBM. 90% of GBM tumors have been shown to recur at the primary site [68]. This is caused by the highly infiltrative nature of the tumor, making complete resection with clean margins nearly impossible. In addition, GBM tumors can have extensive regions of hypoxia. This reduction in oxygen may limit the efficacy of IR as the generation of DNA-damaging free radicals is decreased. Thirdly, BBB reduces the capacity of chemotherapeutic drugs to enter the site of the tumor [10,69]. When recurrence occurs in GBM patients, resistance to irradiation and chemotherapy is commonly observed. Therefore, understanding the mechanisms behind innate and acquired resistance to treatment is extremely vital for better therapy design for GBMs.

1.2.6.1. Mechanisms of Irradiation resistance

Due to the infiltrative properties of GBM, radiotherapy after surgical removal of the tumor is an important aspect of the therapy to eliminate remaining tumor cells. However, even high dose radiation treatments fail to improve survival. Interpatient and intratumor heterogeneity of tumor cells are responsible to heterogeneity of sensitivity to ionizing radiation (IR). Thus understanding GBM radiobiology is necessary to identify novel targets for clinical research [6].

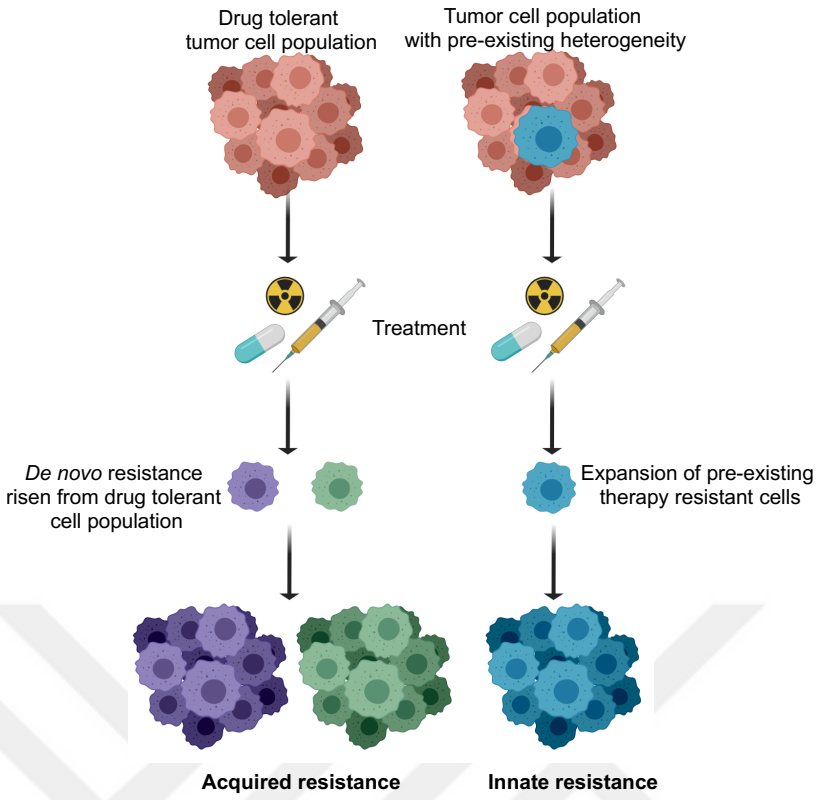

Figure 1.7 Schematic representation of acquired and innate therapy resistance in tumors. Figure adapted from references [70,71].

The principal effect of radiation therapy is to stimulate cell death in rapidly proliferating cancer cells by inducing DNA damage beyond cellular repair capacity. However, multiple factors limit the efficacy of radiation: changes in cell cycle, activation of oncogenes, inactivation of tumor suppressor genes and increased DNA repair capacity [43].

Upon radiation treatment, EGFR and VEGFR signaling pathways are activated in GBM, leading to activation of several downstream survival cascades such as PI3K/AKT/mTOR and MAPK/ERK pathway. A complex survival signaling network is formed and DDR causes cell cycle arrest to allow DNA repair. Normally, with DDR, we expect cancer cells not being able to repair the induced damage and go through apoptosis, however repair proteins such as PARP-1 (BER), ATM, ATR, CHK1 and CHK2 are frequently upregulated in GBM, hence causing constitutively active DDR[70].

Previous studies linked radiation resistant GBM cells to Glioma stem-like cells (GSC) [72]. GSCs are clonal and they have self-renewal and multi lineage differentiation potential, which contribute to radio-resistant recurrent tumors. In addition, when injected in immunodeficient mice, GSCs are able to reconstitute GBM tumors phenotypically

similar to the disease originally present in the patient from which they are derived [73]. Indeed, with *in vitro* and *in vivo* studies, Bao and colleagues showed that after ionizing radiation GBM cells became extremely enriched for GSCs and that irradiated GSCs were more radioresistant as compared to the non-stem cells population. Thus, GSCs may play a pivotal role in GBM radioresistance and tumor aggressiveness [43].

1.2.6.2. Mechanisms of Temozolomide resistance

Intrinsic TMZ resistance can be due to the presence of multi-drug resistance proteins, such as MDR1/ABCB1 encoding multi-drug resistant p-glycoprotein [74].

As an alkylating agent, TMZ acts by methylating adenine and guanine residues in DNA, which induces cell cycle arrest at G_2/M that eventually primes to cell death. The methylated DNA can be repaired by DR, BER or MMR (**Figure 1.8**), and unfortunately GBM cells favor the repair pathways to lessen the effect of TMZ.

1.2.6.2.1. Direct Repair and MGMT

There are several mechanisms suggested for acquired TMZ resistance in GBM. The most explained mechanism of resistance to TMZ is mediated by Direct Repair (DR) protein MGMT, which removes the methyl groups from O6-MeG lesions that arise upon TMZ treatment. The O6-alkyl group is transferred from guanine to the active site cysteine residue (Cys 145) of MGMT [45]. The binding of the methyl group irreversibly inactivates MGMT. Once the methyl group is bound, MGMT is ubiquitinated and degraded by the proteasome.

MGMT expression is inversely correlated with sensitivity to TMZ, cells with elevated levels of MGMT show increased chemoresistance [73]. Promoter/enhancer (P/E) region of MGMT contains a 59 bp cis-acting enhancer element that spans the first exon–intron boundary of MGMT gene and this P/E region is the location where MGMT can be silenced [75]. Patients with MGMT promoter methylation, which occurs around 45% of newly diagnosed GBM, have better prognosis when treated with TMZ [76,77]. There are several transcription factors known to bind to MGMT promoter region such as p53, SP1, GRE, AP-1 and NFkB, thus MGMT can be induced by glucocorticoids, cyclic AMP, protein kinase C activators and NFkB [78].

MGMT promoter status is not the sole determinant of TMZ response. Indeed, discordance between promoter methylation status and MGMT protein expression in

GBM with wild-type MGMT coding sequence is observed in patients: High levels of MGMT expression were detected in patients with DNA methylation at the P/E region. The study reported that an enhancer, located between the promoters of marker of proliferation Ki67 (MKI67) and MGMT genes, is activated in TMZ resistant patient-derived xenograft lines and recurrent tumor samples. So, additional factors can also regulate MGMT expression and confer TMZ resistance [79].

1.2.6.2.2. Mismatch Repair

Another resistance mechanism against TMZ comes from the MMR. O6-MeG lesions mismatched with thymine bases are recognized by the MMR. The thymine residue is removed; however, without MGMT, the O6-MeG cannot be excised. Thymine is reinserted opposite the O6-MeG. These futile cycles of repair result in activation of DDR; ATR and Chk1 kinases, generation DSBs and eventually apoptotic cell death [35,40]. An impaired MMR pathway caused by mutations in MMR protein complexes causes a failure to recognize and repair O6-MeG adducts produced by TMZ. Thus, DNA replication continues and lessens the TMZ effect [6]. For example, a study performed by McFaline-Figueroa *et al*. suggests decreases in MMR protein levels MSH2 and MSH6 in recurrent GBM can be responsible for the observed TMZ resistance at recurrent GBM [80]. These mutations can be present naturally or acquired during TMZ application [81]. Thus, restoring the MMR system in patients could improve the effect of TMZ treatment.

1.2.6.2.3. Base Excision Repair and PARP

Base excision repair (BER) is the major pathway involved in repair of non-bulky damaged nucleotides, abasic sites and DNA SSBs generated by ROS, radiation and alkylating agents. Poly (ADP-ribose) polymerase-1 (PARP1) is a key enzyme in BER and is activated in response to DNA damage. PARP1 binds to DNA and begins synthesis of a PAR from NAD+, which enables the recruitment of BER complex proteins (XRCC1, DNA polymerase, ligase, flap endonuclease 1) and the DNA repair. It was shown that TMZ toxicity increases when components of BER are mutated. Inhibition of PARP increases the frequency of DNA strand breaks, for this reason, PARP inhibitors such as Olaparib and Rucaparib are developed to decrease BER activity [82,83].

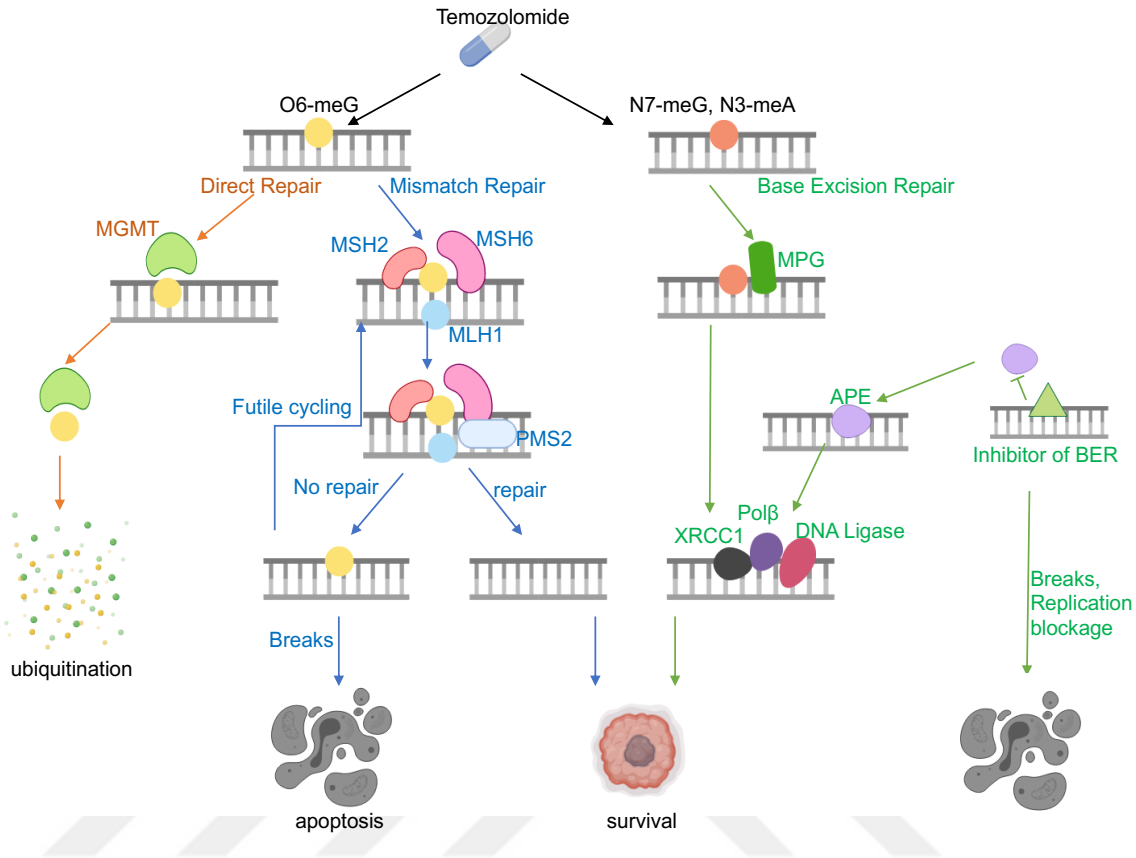

Figure 1.8 DNA repair mechanisms to repair damage induced by TMZ. TMZ produce cytotoxic DNA lesions such as O6-methylguanine (O6-MeG) and N7-methylguanine (N7-MeG) and N3-methyladenine (N3-MeA). Direct Repair; MGMT eradicates the O6-alkylguanine DNA adduct through covalent transfer of the alkyl group to the conserved active-site cysteine and restores the guanine to unmethylated form. After receiving a methyl-group from O6-MeG, MGMT is inactivated, and subjected to ubiquitin-mediated degradation. Mismatch Repair; if an O6-MeG DNA adduct escapes MGMT repair, it would form a base pair with thymine (blue circle) during DNA replication. The mismatched base pair of the persistent O6-MeG with thymine is acknowledged by the MMR, resulting in futile cycles of repair, ultimately leading to cell death. Base Excision Repair; N7-MeG or N3-MeA adducts are efficiently repaired by the BER, and normally they contribute little to the cytotoxicity of TMZ. Methoxyamine (green triangles) binds to AP sites produced by methylpurine glycosylase (MPG), the first step in BER. Methoxyamine-bound AP sites are refractory to AP endonuclease (APE) cleavage, resulting in the blockage of the BER pathway. This leads to strand breaks, disrupted replication, and increased cytotoxicity of TMZ. Figure adapted from reference [78].

1.2.6.2.4. Tumor suppressors p53 and PTEN

The tumor suppressor protein, p53 is a key component in many signaling pathways in the cell. p53 can induce a temporary or permanent cessation of cell growth in response to cellular stress such as DNA damage [84]. Wild-type p53 is under regulation of MDM2, however the mutated p53 cannot undergo this inhibitionand accumulates o in the cells. Both TP53 and MDM2 genes are frequently altered in GBM [85], leading to the promotion of tumor cell growth and a resistance to chemo- and radiotherapy. Restoring the effect of p53 has been a focus for GBM treatment. Targeting MDM2-p53 interaction is also a potential cancer therapeutic strategy, Nutlin-3 is one of the molecules that has been developed for this purpose and has yielded interesting results in preclinical studies. However, this inhibitor's effects are limited since it can only work with wild-type p53 [86].

PTEN is a tumor suppressor gene, frequently mutated in GBM causing enhanced tumor cell proliferation. PTEN protects wild-type p53 from inactivation and degradation through the inhibition of PI3K and inhibition of MDM2 transcription, and p53 can increase PTEN activity by enhancing *PTEN* gene transcription [29].

Very recent findings interestingly show that PTEN can also be found in the nucleus where it is involved in the regulation of DNA damage repair, chromosome stability, and cell-cycle [87–89]. PTEN function can be affected by posttranslational modifications, such as SUMOylation, phosphorylation, ubiquitination oxidation, and acetylation. A 2019 publication by the Furnari group demonstrated that phosphorylation of PTEN on tyrosine 240 (pY240-PTEN) and its translocation into nucleus is observed in GBM samples obtained from patients treated with TMZ and IR, and pY240-PTEN modification is correlated with worse prognosis [88]. Thus, restoration of wild-type PTEN into tumors can promote apoptosis and induce chemosensitivity [29].

1.3. Epigenetic regulation and Glioblastoma multiforme

1.3.1. Chromatin regulators

Epigenetic mechanisms change the gene expression patterns without altering the DNA sequence, but by modifying chromatin structure [89]. Chromatin is the macromolecular complex of DNA and histone proteins, providing the scaffold for the packaging of the genome [90]. Epigenetic mechanisms change the accessibility of chromatin to transcriptional machinery locally and globally via modifications of the DNA and by modification or rearrangement of nucleosomes [91].

There are mainly two types of epigenetic modifications that leads to either a loosened (euchromatin) or a more tightly packed (heterochromatin) chromatin state: i) DNA methylation, ii) Histone modifications [92].

Around 50% of the promoter regions of all human genes have the stretches of DNAs consisting of 60% or more CpG dinucleotides, called CpG islands. These regions act as promoters or enhancers and they are directly responsible for the transcription of their downstream genes. DNA methylation is achieved by DNA methytransferases (DNMT) at the C5 position of cytosine residues in CpG islands in the genome. Hypermethylated CpG islands results in transcriptionally inactive genes [92].

Every 147 bp, DNA is found wrapped around histone octamers that provides the compactness of the genome. However, histones are more than packaging proteins; they are dynamic regulators of gene activity that undergo many post-translational chemical modifications, including acetylation, methylation, phosphorylation, ubiquitylation and sumoylation. The enzymes that add and remove such modifications are, respectively, histone acetyltransferases (HATs), histone deacetylases (HDACs and sirtuins), methyltransferases (HMTs), demethylases (KDMs), kinases, phosphatases, ubiquitin ligases, deubiquitinases, SUMO ligases and proteases (**Figure 1.9**). The acetylation and methylation of specific lysine residues within the tails of nucleosomal core histones have a crucial role in regulating chromatin structure and gene expression [93]. All epigenetic processes work together to establish and maintain the global and local loose or packed chromatin states that eventually determine gene expression. The continuous interplay of all these processes form the epigenetic code [94,95].

1.3.2. Histone acetylation/deacetylation in GBM

Histone acetylation transpires an addition of acetyl group to the lysine residues in the tail domain core histones, especially to Histone H3 and H4. With this addition the charge of lysine residues changes, and interactions between histone and DNA is weakened [96,97]. In general, histone acetylation facilitates the open chromatin configuration and is associated with active gene transcription. Whereas histone deacetylation enables compacted chromatin, and indicates transcriptional repression [98]. Thus, the balance between the activities of HATs and HDACs are important for gene expression (**Figure 1.10**).

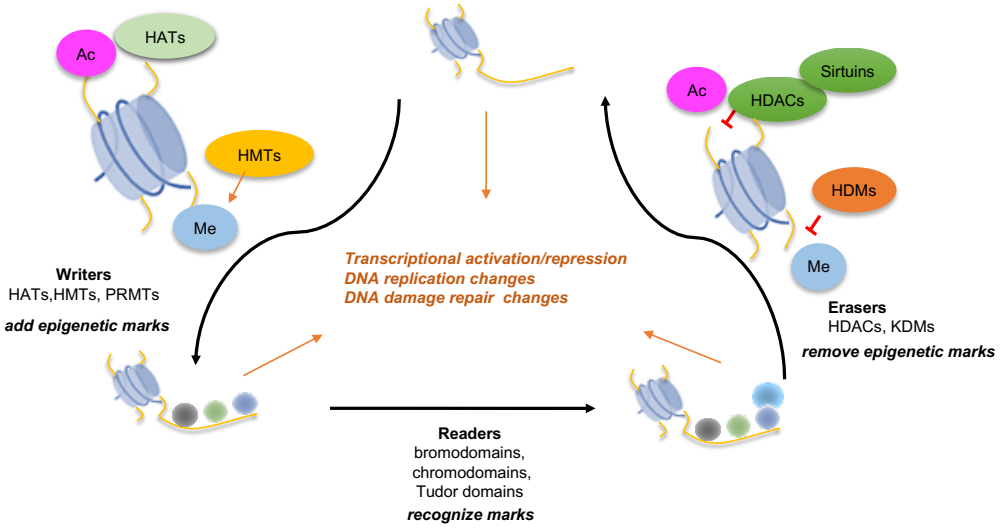

Figure 1.9 Epigenetic writers, readers and erasers form a dynamic process of regulation. Epigenetic writers such as histone acetyltransferases (HATs), histone methyltransferases (HMTs), protein arginine methyltransferases (PRMTs) and kinases lay down epigenetic marks on amino acid residues on histone tails. Epigenetic readers such as proteins containing bromodomains, chromodomains and Tudor domains bind to these epigenetic marks. Epigenetic erasers such as histone deacetylases (HDACs), lysine demethylases (KDMs) and phosphatases catalyze the removal of epigenetic marks. Together, histone modifications regulate various DNA-dependent processes, including transcription, DNA replication and DNA repair. Figure adapted from [99]

HDACs have a variety of roles in the cell, they deacetylate histone lysine residues and non-histone proteins, such as hormone receptors, transcription factors, DNA repair enzymes, inflammation mediators, chaperone proteins and cytoskeleton proteins [100,101]. The human genome comprises 18 identified HDACs, grouped into four classes: class I (HDAC1, 2, 3 and 8), class IIa (HDAC4, 5, 7, 9), class IIb (HDAC6, 10), class III (SIRT1-7) and class VI (HDAC11). Enhanced HDAC expression can promote tumor development [102], and is a common phenomenon among many cancer types including GBM [103]. For GBM, increased HDAC1, HDAC3 and HDAC6 expression levels are observed among GBM cell lines and patient samples [104–106].

With HDACi administration, diverse pathways can be triggered in tumor cells, leading to cell cycle arrest, senescence, differentiation, autophagy and apoptosis. Cell death can be activated by HDACi through accumulation of DNA damage and downregulation of members of HRR and NHEJ DNA Repair pathways such as Ku70, Ku80, RAD50, RAD51, MRE11, DNA-PK, BRCA1, EXO1, CHK1, and CHK2 [107–109] (**Figure 1.11**). HDACi-induced cell cycle arrest can appear at the G_1/S cell cycle or G_2/M

checkpoint, which can lead to apoptosis. G_1/S cell cycle arrest is due to CDK inhibitor p21WAF1/CIP1 encoded by CDKN1A (p21) gene whose expression can be induced by HDACi administration [110,111].

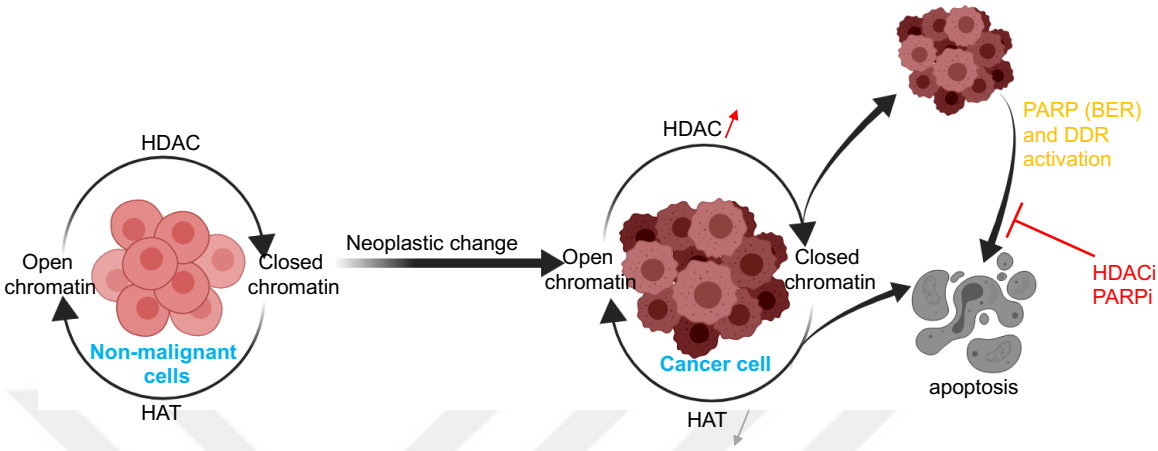

Figure 1.10 The role of HATs and HDACs cancer cells. In non-malignant cells, histone acetyltransferase (HAT) and histone deacetylases (HDAC) are in balance to regulate gene expression. In cancer cells, this balance is disturbed, and DNA repair pathways are enhanced, in addition to decrease in tumor suppressor genes. With HDAC inhibitors and PARP inhibitors DDR and BER can be inhibited, resulting in apoptosis. Adapted from [112–114]

Taken into consideration that irradiation and TMZ are frequently used for GBM patients which generate DNA damage, cell cycle arrest and cell death in tumor cells; combination with HDACi to enhance the effect of current therapy options is rational (**Figure 1.12**). In GBM, inhibitors of HDAC have demonstrated promising preclinical activity, HDACi administration sensitizes tumor cells to radio-chemotherapy and induce apoptosis via increased PTEN, AKT expression, JNK pathway and reduced telomerase activity [101,115,116].

Pan-HDACi Vorinostat, Belinostat, Panobinostat are among FDA approved drugs that were also included in many preclinical and clinical studies with GBM. Vorinostat was found to induce G_2 cell cycle arrest in glioma cells while upregulating p21 levels, with enhanced expression of antiproliferative genes p21WAF1, p27KIP1, DR5 and TNFα *in vitro* [117]. In addition, a study performed in U87MG xenograft model, with combining Vorinostat with tranylcypromine (monoamine oxidase inhibitor) reduced glioma stem cell viability, affecting TP53 and TP73 gene expression *in vivo* [118].

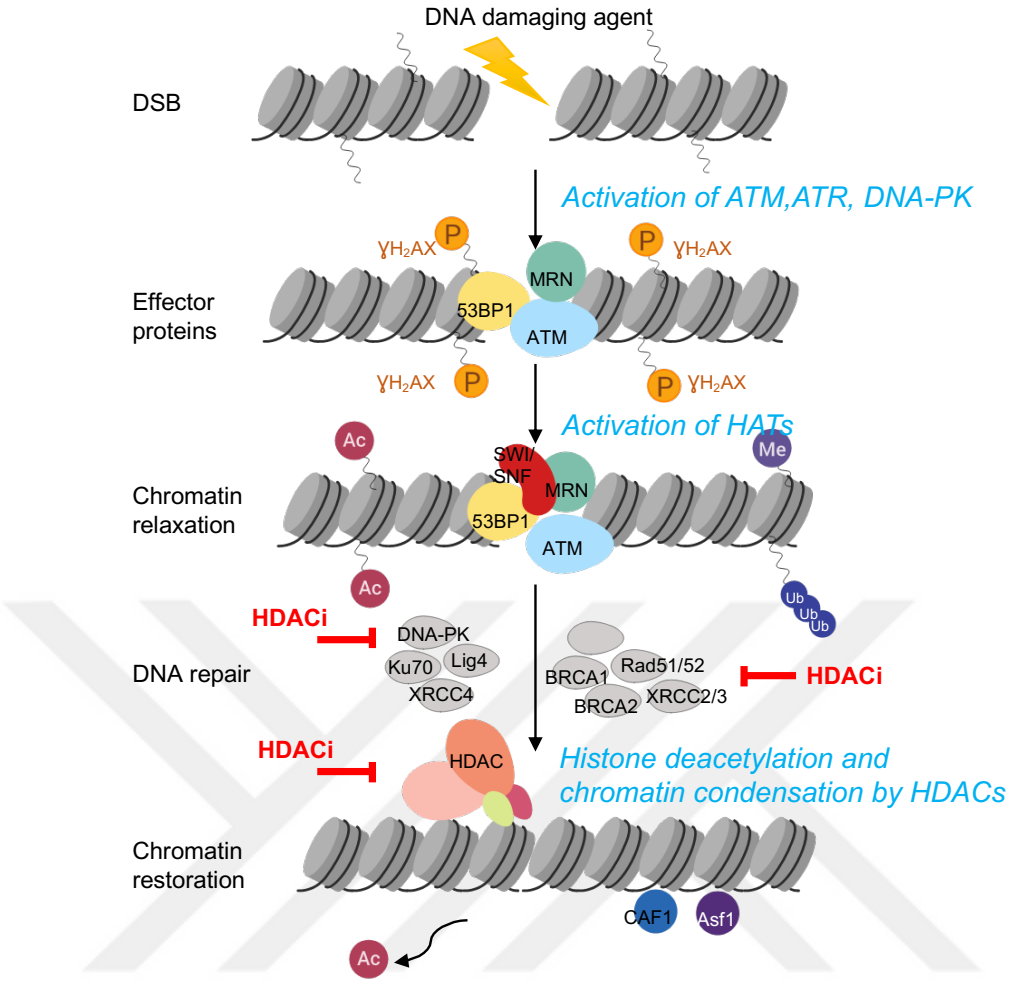

Figure 1.11 Double strand break recognition pathway. Double strand break recognition is followed by recruitment of effector proteins ATM, MRN and 53BP1 and the formation of γH$_2$AX. Chromatin decondensation by HATs, allows DNA repair proteins such as Ku70, DNA-PK, BRCA1/2, Rad51 to be engaged. With HDACs chromatin restoration occurs after DNA repair. When cell is treated with HDACi (denoted in red) DNA repair is blocked and senescence/cell death can be triggered. Figure adapted from [119].

For GBM patients several completed and ongoing clinical trials are performed for general HDAC inhibitors: Vorinostat (14 studies), Belinostat (1 study), Panobinostat (2 studies terminated prior to completion), Valproic acid (6 studies) (https://clinicaltrials.gov, June 2019). Some of the trials have been withdrawn and/or prematurely terminated, whereas others did not show improved prognosis compared to Stupp regimen [101,120]. For example, in one study (Clinical Trial: NCT00238303), in adult patients Vorinostat was utilized as single agent and in combination with standard therapies, but its addition to the standard radio-chemotherapy did not improve survival [121]. Thus, further studies with more selective HDACi are necessary.

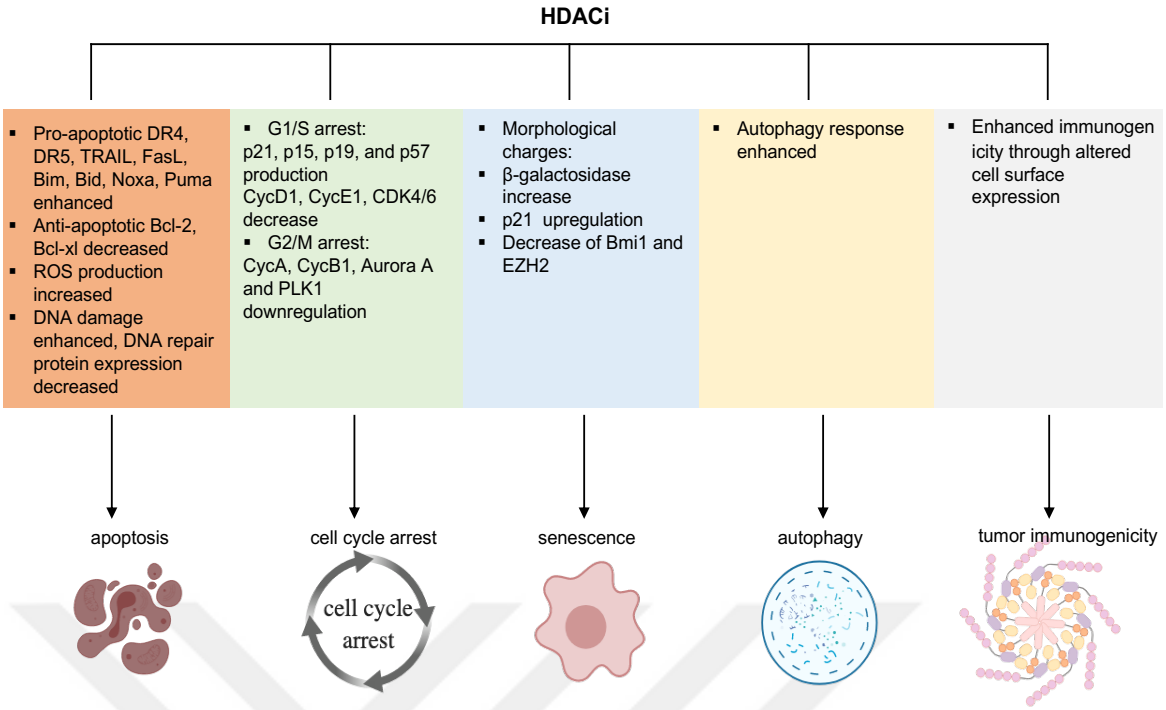

Figure 1.12 Reactions to histone deacetylase inhibitors (HDACi). HDACi can induce various antitumor responses including, cell death, cell cycle arrest at the G_1/S and G_2/M checkpoints, cellular senescence, autophagy and enhanced immunogenicity through altered cell surface expression of immune regulatory molecules. Figure adapted from [116].

1.3.2.1. The role of HDAC6 in GBM and Temozolomide resistance

HDAC6 is a unique member of class II HDAC containing two fully functional homologous catalytic domains and these domains contribute independently to the overall activity of the HDAC6 protein [109]. HDAC6 works in both nucleus and the cytoplasm, controlling epigenetic and non-epigenetic mechanisms. Known targets of HDAC6 include cortactin, Hsp90 and α-tubulin. Furthermore, recent studies have shown links of HDAC6 with EGFR, MAPK, AKT and p53 signaling pathways (**Figure 1.13**).

Pan-HDAC inhibition in the clinic resulted in undesired side effects such as Thrombocytopenia, neutropenia, and anemia, arrhythmias, liver toxicities, etc. alongside the benefits. Thus, to decrease the double edge sword effects of HDAC inhibition, more selective HDACi therapies should be considered in patients. HDAC6 is upregulated in numerous cancer types including GBM [122] (**Figure 1.14**) and thought to be linked to TMZ resistance. So HDAC6 is a promising target for GBM therapy resistance.

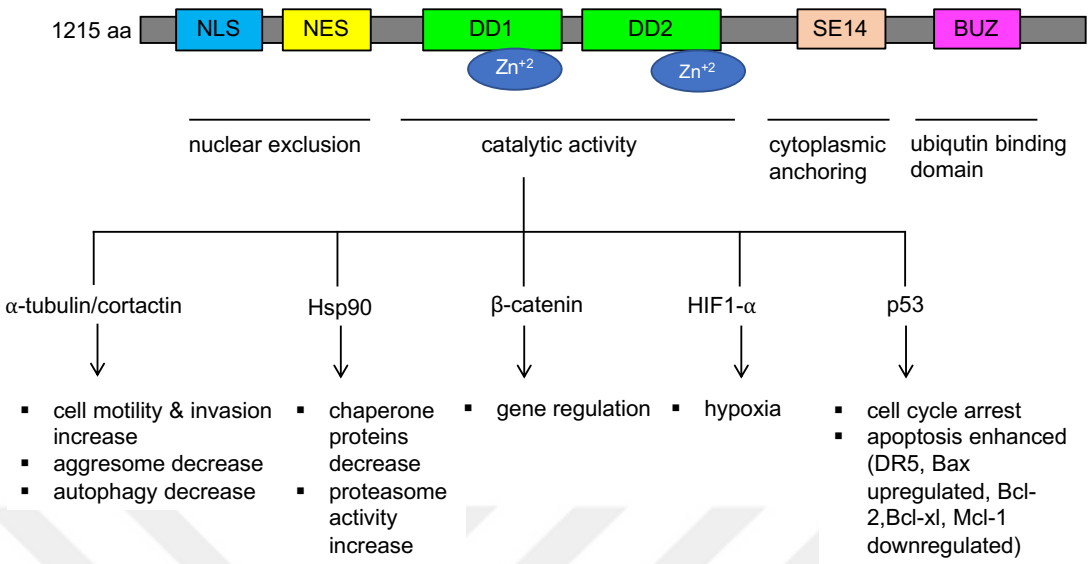

Figure 1.13 Structure and function of HDAC6. HDAC6 deacetylates a number of protein substrates to control several cellular processes. NLS: nuclear localization signal, NES: nuclear export signal, DD1/2: deacetylase domains, SE14: Lysine-specific demethylase. Adapted from [123]

A study performed on mice lacking HDAC6 expression has shown HDAC6-deficient mice are viable, fertile with normal lymphoid development and have moderately affected immune response [109]. Thus, inhibition of HDAC6 might overcome undesired side effects of pan-HDACi.

In GBM cell lines, A172 and U87MG, express significant levels of HDAC6 and when HDAC6 is inhibited by Ricolinostat (ACY-1215), cell growth decreased. Also, SMAD2 phosphorylation results in inhibition of tumor suppressor gene p21. HDAC6 can inhibit the phosphorylation of SMAD2, hence increases the expression of p21[124]. Thus, HDAC6 has a known role in glioblastoma cell growth.

A study in 2016 by Wang *et al*. validated that HDAC6 overexpression increases proliferation in GBM and is also related with TMZ resistance. When HDAC6 was knockdown or inhibited by selective HDAC6i (Ricolinostat, Tubastatin A and CAY10603), they observed sensitization to TMZ. In addition, they reported that HDAC6 inhibitors decrease EGFR protein levels and impair the activation of the EGFR pathway [125].

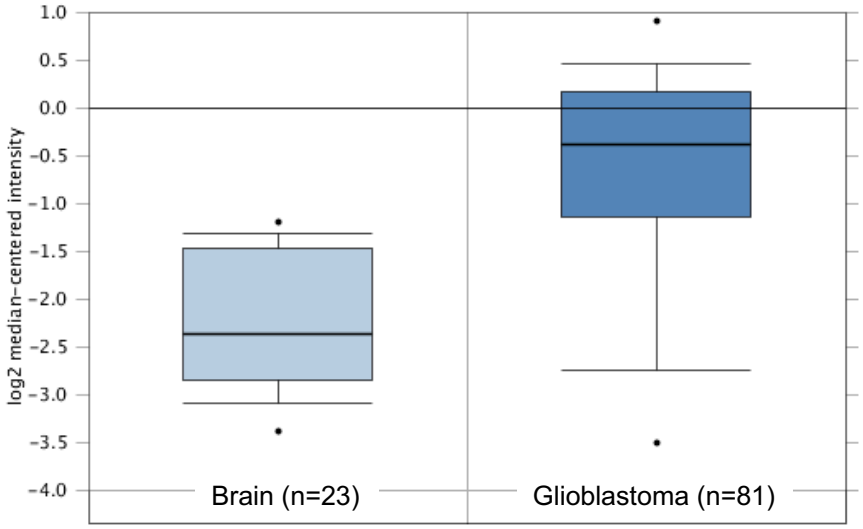

Figure 1.14 HDAC6 Expression in Sun Brain Glioblastoma cohort vs. Normal Brain, p-value 6.66E-13, fold change 3.2. Data obtained from Oncomine [126].

The unfolded protein response (UPR) is a cellular program used by cells to handle protein misfolding stress. In non-malignant conditions when environment-triggered ER stress cannot be fixed, prolonged UPR activation initiates cell death mechanisms. ER stress-induced UPR has been linked to drug resistance in cancer cells in recent years [127]. For GBM cells, Li and colleagues investigated TMZ induced ER-stress tolerance (ERST) in a panel of cell lines including A172, U373, U87MG and U251. They observed that ERST occurs in TMZ-resistant glioma cells, and HDAC6 inhibition can overcome ERST via HSP70 and HSP90 [128].

In the last three years studies by Lin, et al. [129] Yin et al. [130] and Liu, et al. [131] revealed the role of HDAC6 mediated autophagy in GBM. Autophagy in cancer cells maintain metabolism through protein degradation, and can protect cancer cells from IR and alkylating agent damage[130]. Transactive DNA binding protein-43 (TDP-43) is a DNA/RNA binding protein that was found to protect GBM cells from nutrient deprivation induced cell death via inducing autophagy by Lin and colleagues in 2017. In nutrient starved U87MG cells, both expression of TDP-43 and HDAC6 was highly elevated. When these cells were treated with Vorinostat, apoptosis was significantly induced [129]. Yin and Li inhibited autophagy by a specific HDAC6 inhibitor Tubacin A in U251 and LN229 cell lines and observed suppressed growth and drug sensitivity towards TMZ [130]. A more detailed publication by Chern group in 2019, utilized a high-selective HDAC6 inhibitor, J22352, on a panel of various cancer cell lines including U87MG GBM cells. When U87MG cells were treated with J22352, accumulation of autophagic vacuoles at

the time points of absence of apoptotic cell death was observed. In addition, when cells were treated with J22352, LC3 a marker for autophagy was enhanced [131].

Marampon and colleagues' publication in 2017 disclosed that HDAC6 knockdown enhances radiation therapy-induced apoptosis in U251 GBM cell line, while provoking autophagy-mediated cell death in U87MG. Following this in 2018, Yang *et al*. published HDAC6 is upregulated in human GBM stem cells (GSCs) compared to non-stem tumor cells and HDAC6 inhibition decreased DNA damage repair capacity of GSCs through degradation of CHK1 caused by XIAP downregulation, leading to elevated radiosensitivity [108].

Accumulating evidence suggests that HDAC6 has a role in drug resistance, apoptosis and autophagy in GBM, hence investigating the role of HDAC6 in TMZ resistance can be a promising lead for GBM therapy.

1.4. Primary GBM models

For 30 years, commercially available GBM cell lines such as U87MG (>2500 citations in PubMed), U251 (>2700 citations) and T98G (>1200 citations), have been studied extensively, providing valuable information about this cancer type. Cell line-based models are reproducible with reliable growth rate for unlimited number of divisions [132]. However, cell line-based models have also major shortcomings: First, the serum-containing medium alters the genomes and transcriptomes and causes depletion of stem cell-like cells. Secondly, cancer cells injected into the brains of mice fail to develop the defining morphological features of GBM, such as diffuse infiltration into surrounding healthy tissue and microvascular proliferations [133]. Prolonged cell culture changes the genetic and morphological characteristics of cancers, for example for GBM cell lines lack EGFR amplification, whereas more than 40% of primary GBM tumor specimens contain this mutation. In addition, prolonged cell culture leads to progressive hypermethylation of the MGMT promoter, approximately 80% of glioma cell lines are MGMT hypermethylated, as compared to a 40% incidence of promoter hypermethylation in clinical samples [134]. Thus serum-based monolayer cultures are not the best option to investigate therapeutic effects of a new finding in GBM.

GBM cell culture conditions have been shown to improve by culturing GBM cells in serum free condition media as suspension-based cultures. These neurosphere cultures keep a semi-3D environment in which cells deposit ECM to create their own unique microenvironment [135]. Moreover, orthotopic transplantation of such spheres into mice

generated secondary tumors that retained the features of the primary. Orthotopic xenograft models showed that acutely transplanted patient derived GBM cells mimicked well the histopathology, genomics and phenotypic properties of the corresponding patient's primary tumor [136]. Thus, while investigating GBM, it is essential to work with primary cell cultures and/or xenografts. For this purpose, we have been establishing primary GBM cell lines from patient samples in collaboration with Dr. İhsan Solaroğlu and Koç University Neurosurgery department.

To sum up, in the last part of the thesis, we established primary GBM cell lines that are serum based and non-serum based and investigated the capacity of tumor formation in *in vivo* xenografts. The role of HDAC6 in established primary cell line, KUGBM8-EF was studied.

2. MATERIALS AND METHODS

2.1. Cell culture and chemicals

Human GBM cell lines U373, T98G and A172 and human embryonic kidney 293T cells were purchased from American Tissue Type Culture Collection (ATCC). TMZ resistant cell lines were established as described below. Primary GBM cell lines as well as patient-derived fibroblasts were generated in collaboration with Prof. Dr. İhsan Solaroğlu at Koç University. All cells except neurosphere primary cells, were cultured in DMEM medium (Gibco) with 10% fetal bovine serum (Invitrogen) and 1% Penicillin-Streptomycin (Gibco). Primary GBM sphere cells were maintained in EF medium. EF medium components; Neurobasal medium (Gibco), L-Glutamine (Gibco), B27 and N2 supplements (Gibco), Pen-Strep (Gibco), Heparin (Stem Cell Technologies), FGF (Gibco, PHG0266) and EGF (Peprotech, AF-100-15). Cells were kept in 37^0C humidified incubator with 5% CO_2. Cells were routinely checked for mycoplasma contamination by Lonza Mycoplasma Detection Kit.

Temozolomide (TMZ), Ricolinostat, GSK-J4, SGC-CBP30 were purchased from SelleckChem. MGMT overexpression plasmid was purchased from DNAsu (Clone: HsCD00075543) and transduced into U373 cells as described below. Chemical probe library against chromatin modifiers are depicted in **Table 2.2** below.

2.2. Establishing primary GBM cell lines and their matched fibroblasts

Protocol of primary cell line formation was adapted from Xie *et al*. published in 2015[134]. Surgically removed tumor specimens from the incision site were placed in DMEM containing 2.5% Fetal Bovine Serum (FBS) and 5% Pen-strep prior to transfer on ice. Fresh tumor samples were washed with 1X PBS containing 1% Pen-strep several times and minced with a scalpel. Tumor sample was divided into two groups, one part was put into wells of a 6-well plate (depending on the size of the sample) and supplemented with DMEM containing 10% FBS and 1% Pen-strep (Gibco). The plates were incubated at 37°C, 5% CO_2. The attachment of the cells from the dissected tissue was observed and medium was changed 1-2 times a week.

Second group of the dissected tissue was incubated in a mixture of 1:1 Accutase (Stem Cell Technologies) and Trypsin (Gibco) for 10 minutes at 37°C. The dissociated cells were washed twice with DMEM/F12, followed by centrifugation at 600 rpm for 8

minutes. Cells were plated to 25 cm^3 flasks with Neurobasal medium (Gibco) containing N2, B27 supplements (Gibco), EGF (20 ng/ml) (Gibco), FGF (20 ng/ml) (Gibco), Heparin (Stem Cell Technologies) and 0.5% Pen-Strep. After sphere formation (5-7 days), spheres in suspension were centrifuged and manually divided into single cells. Resuspended cells were placed in a new flask containing fresh media.

For the fibroblast establishment, skin biopsy was minced with scalpel, divided into 6 well plates and a coverslips were put on top of the sample for better attachment. Cells were incubated with DMEM containing 10% FBS and 1% Pen-strep. The plates were incubated at 37 °C, 5% CO_2.

2.3. Testing tumor forming capacities of primary cell lines in mice

Tumor forming capacities of primary GBM cell lines were tested in immunocompromised SCID mice. SCID mice were housed and cared in appropriate conditions of Koç University Animal Facility and all protocols were approved by the institution ethics board of Koç University (HADYEK#2014-22). All animal experiments were performed in collaboration with Ahmet Cingöz.

Firefly Luciferase (Fluc) and mCherry expressing [120] stable KUGBM8-DMEM and KUGBM8-EF cells were generated by viral transduction. Initially, mCherry expression was verified under the fluorescence microscope and their Fluc activity was validated by utilizing *in vitro* luminescence assay. Increasing number of Fluc-mCherry expressing cells (0-50,000/well) were seeded on 96-well black-bottom plate and treated with 1000 ug/ml D-Luciferin. Bioluminescence measurements were taken.

For tumor implantation, 4 mice for each condition were used and 120.000 cells per mouse were injected in 7 μl PBS stereotactically into the brain [137]. After injection, tumor cells were visualized by using IVIS Lumina III (Perkin Elmer) equipment. Accordingly, Fluc activity of tumors was measured by injecting mice with 150 ug/g body weight of D-Luciferin intraperitoneally. Approximately 1 month later, mice were sacrificed, and brains were fixed for histological and pathological analyzing. Immunohistochemistry experiments were performed by Fidan Şeker.

2.4. Cell viability and proliferation assays

2.4.1. Cell Titer Glo assay

Cell viability was determined via Cell Titer-Glo® (CTG) Luminescent Cell Viability Assay (Promega, USA). CTG assay determines the number of viable cells via luciferase reaction by measuring ATP amount, which is an indicator of metabolically active cells. CTG reagent lyses cells for ATP release and inhibits endogenous ATPases simultaneously while providing luciferin, luciferase and other reagents for a bioluminescent reaction. CTG assay was slightly modified from the manufacturer's instructions.

Each plate was incubated 10 minutes at room temperature before CTG reagent addition. For 96 well plates, medium was removed and 4 µl + 40 µl of DMEM mix was added per well for attached cells. For spheres 10 µl CTG was directly added to the well. Following CTG addition, the plate was put into Synergy H1 Reader (Biotek, USA) for 2 minutes of shaking and 8 minutes of incubation at dark before luminometric read. Survival was expressed as the percentage of viable cells in the treated sample compared to untreated control samples.

2.4.2. Clonogenic assays

The clonogenic capacity of a cell is by definition, a cell's capacity to survive, proliferate and form a large colony (at least 50 cells). Cells were seeded to 6-well plates in triplicate as 500 cells/well. Next day, Temozolomide was given at different dosages for 48 hours. After 10-14 days cells were fixated with cold methanol for 5 minutes and stained with crystal violet for 30 minutes with gentle shaking [138]. Colony quantifications were done by Image J analysis utilizing ColonyArea plugin [139].

2.5. Establishment of Temozolomide-resistant cell lines

TMZ response of U373, T98G and A172 GBM cell lines were detected after 3 consecutive days of TMZ addition to 6-well plates or 96-well plates. For the 6-well plates, cell viability was then determined by trypan blue cell counting. For 96-well plates CTG (Promega), ATP based luminescence read out was performed. Viability was normalized to untreated controls and/or vehicle treated controls.

U373 TMZ-resistant cells were established by two different methodologies adapted from Banelli *et al*. [140] and Tiek *et al*. [141] (**Figure 2.1A**), dose escalation method and high dose TMZ selection. For dose escalation method, U373 cells were treated TMZ every two days, starting from 25 µM. Every two weeks dosage was doubled (or when cells become resistant to that dosage), these cells are denoted as DE-TMZR^{T}. For high dose TMZ resistant selection, cells were treated with 250 µM TMZ for 15 days, with drug renewal each day. Remaining cell population was left to recover for 15-20 days, they are named as TMZR^{T}. Both cells lines are being treated with 250 µM every 3 days for more than 2 months. After 2 months TMZ pressure was lifted from cells and sublines denoted as drug holiday (named DE-TMZR and TMZR) were established and used in further experiments. U373 parental cells are aged alongside the TMZ resistant cells.

KUGBM8-EF cells were treated with 250 µM TMZ for 10 days, with TMZ renewal each day. Established TMZ-resistant subline was denoted as KUGBM8-EF-TMZR (**Figure 2.1B**).

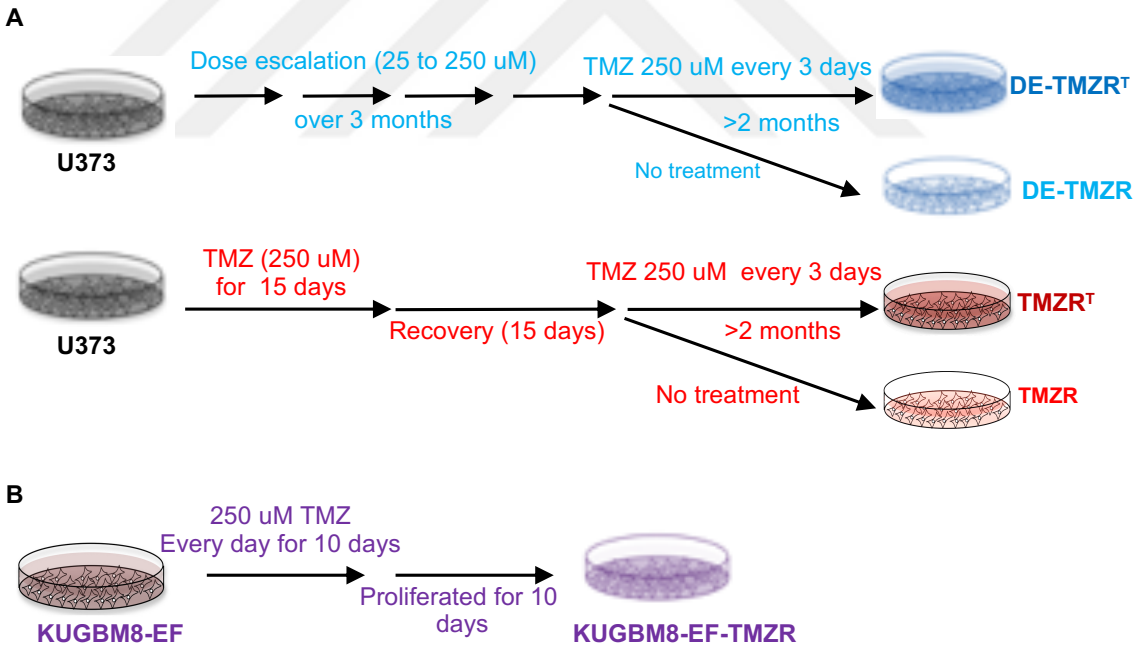

Figure 2.1 Schematic representation of establishment of TMZ resistant cell lines.

2.6. A screen with a chemical library targeting histone modifying enzymes

Our chemical library targeting various histone modifying enzymes is a library consisting of various epigenetic probes (**Table 2.1, Table 2.2**). It was a kind gift from Prof. Udo Opperman (Oxford University). For the screen T98G, U373, DE-TMZR and TMZR cells were seeded 1250 cells/well to black-bottom 96-well plates. Next day, cells were treated with the chemical inhibitors in their individual working concentrations (defined by the Structural Genomics Consortium, SGC) and/or TMZ (250 or 500 μM). Cell viability was detected by CTG assay after 72 hours, and normalization to untreated controls was performed.

Table 2.1 Components of epigenetic probes screen

Target	1st library	2nd library
Bromodomain	22	26
Histone deacetylase	17	18
Histone methyltransferase	14	14
Histone demethylase	11	12
Methyl lysine binder	4	4
Arginine methyltransferase	7	8
Others	11	15
Total	86	97

2.7. Hit validation for chemical probes screen

To determine IC_{50}, cells were treated for 72 hours. For combination treatments viability was detected after 5 days with CTG.

2.8. RNA sequencing

RNA was isolated from 36 hours Ricolinostat treated or untreated control cells using the Quick-RNA Mini Prep kit (Zymogen) according to the manufacturer's protocol. The quality of the RNA samples was verified by electrophoresis on Tapestation (Agilent). The RIN scores for all samples were in the range of 7.5-9.5. RNA-seq libraries were prepared using the NEBNext® Ultra™ RNA library prep kit for Illumina® using TruSeq indexes, according to the manufacturers protocol. The resulting libraries were sequenced on a NextSeq 500 platform (Illumina) using a paired-end run 2 x 80 bp, to an average depth of 112 x 10^6 paired-end reads per sample (range 47 x 10^6 to 168 x 10^6).

Table 2.2 List of epigenetic probes screen

Probe Name	Working concentration (μM)	Class/Target
(+)-JQ1	1	Bromodomains - BRD2, BRD3, BRD4, BRDT (BET)
(-)-JQ1 (inactive)	1	Bromodomains - Negative control
PFI-1	5	Bromodomains - BRD2, BRD3, BRD4, BRDT (BET)
I-BET	1	Bromodomains - BRD2/3/4
Bromosporine	1	Bromodomains - pan-Bromodomain
CBP/BRD4 (0383)	5	Bromodomains - CBP, BRD4(1)
BAZ2-ICR	1	Bromodomains - BAZ2A, BAZ2B
NI-57	1	Bromodomains - pan-BRPF
LP99	1	Bromodomains - BRD9, BRD7
BI-9564	1	Bromodomains - BRD9, BRD7
NVS-CECR2	1	Bromodomains - CECR2
I-BRD9	10	Bromodomains - BRD9
SGC-CBP30	1	Bromodomains - CREBBP, EP300
I-CBP112	1	Bromodomains - CREBBP, EP300
RVX-208	5	Bromodomains - BRD2, BRD3, BRD4, BRDT (BET, BD2)
SMARCA	2.5	Bromodomains - SMARCA, PB1
PFI-3	1	Bromodomains - SMARCA2/4, PB1(5)
GSK2801	1	Bromodomains - BAZ2A, BAZ2B
PFI-4	1	Bromodomains - BRPF1B
CECR2 (control comp.)	1	Bromodomains - CECR2
BAY-299	1	Bromodomains - BRD1, TAF1
OF-1	5	Bromodomains - pan-BRPF
Belinostat	5	HDAC - hydroxamic acids
Valproic acid	1000	HDAC - aliphatic acid compounds
Entinostat	0.5	HDAC - ortho-amino anilides
SAHA	2.5	HDAC - hydroxamic acids
Trichostatin A	0.5	HDAC - hydroxamic acids - Class I & II
SRT1720	1	HDAC - SIRT1 (indirect?) activator
RGFP966	10	HDAC - HDAC3
PCI-34051	5	HDAC - HDAC8
Rocilinostat	10	HDAC - HDAC6
Tubastatin A HCl	10	HDAC - HDAC6
PCI-24781	10	HDAC -
Romidepsin	1	HDAC -
Mocetinostat	10	HDAC -
Santacruzamate	50	HDAC 2?
EX 527	1	HDAC - SIRT1
CI-994	1	HDAC - 1,2,3,(8)
CPI-360	10	Histone methyltransferase - EZH2 and EZH1
UNC0638	1	Histone methyltransferase - G9a, GLP
UNC0642	1	Histone methyltransferase - G9a, GLP
A-366	2	Histone methyltransferase - G9a, GLP
Chaetocin	0.05	Histone methyltransferase - SUV39H1
PFI-2	2	Histone methyltransferase - SETD7
SGC0946	7.5	Histone methyltransferase - DOT1L
GSK343	3	Histone methyltransferase - EZH2
UNC1999	1	Histone methyltransferase - EZH2
LLY-507	1	Histone methyltransferase - SMYD2
Tranylcypromine	20	Lysine demethylases - LSD1
GSK-LSD1 (irreversible)	0,5	Lysine demethylases - LSD1
GSK J4	10	Lysine demethylases - JMJD3, UTX, JARID1B
GSK J5 (inactive)	10	Lysine demethylases - Negative control
IOX1 (5-carboxy-8HQ)	40	Lysine demethylases - pan-2-OG
Methylstat (Ester)	2.5	Histone demethylase
(E)-JIB-04	0.05	Histone demethylase - Pan JmjC
ML324	5	Histone demethylase - JMJD2E
KDOBA67	10	Histone demethylase
KDOAM-25a	1	Lysine demethylases - JARID
KDOAM32	1	Lysine demethylases - JARID
KDOPZ32	1	Lysine demethylases - JARID
KDM5-C70	10	Histone demethylase - JARID1
OICR-9429	1	Methyl Lysine Binder - WDR5
UNC1215	5	Methyl Lysine Binder - L3MBTL3
A-395	1	Methyl Lysine Binder - EED
A-395N	1	Methyl Lysine Binder - EED
MS409N	1	Arginine methyltransferase - PRMT4, PRMT6

TP-064	1	Arginine methyltransferase - PRMT4
TP-064N	1	Arginine methyltransferase - PRMT4
SGC707	1	Arginine methyltransferase - PRMT3
MS049	1	Arginine methyltransferase - PRMT4, PRMT6
MS023	1	Arginine methyltransferase - Type I PRMTs
GSK591	1	Arginine methyltransferase - PRMT5
5-Azacitidine	10	DNA methyltransferase (DNMT) -
5-Azadeoxycitidine	5	DNA methyltransferase (DNMT) - DNMT1/3
A-196	1	Histone methyltransferase - SUV420H1/H2
BAY-598	1	Histone methyltransferase - SMYD2
CPI-169	10	Histone methyltransferase - EZH2, EZH1
UNC2400	1	Histone methyltransferase - EZH2
Olaparib	1	Poly ADP ribose polymerase (PARP)
Rucaparib	10	Poly ADP ribose polymerase (PARP)
C646	1	Histone acetyltransferase (HAT) p300/CBP
GSK484	1	Peptidyl arginine deiminase (PAD4)
GSK106	1	Peptidyl arginine deiminase (PAD4)
MAZ1805	1	tRNA synthehase
GSK864	5	Dehydrogenase
MAZ1392	1	tRNA synthehase
IOX2	10	Prolyl-Hydroxylases - PHD2 (EGLN1)
SGI-1776	10	Kinase inhibitor - Haspin
CHR-6494	1	Kinase inhibitor - Haspin
K00135	1	Kinase inhibitor - ATP competitive - PIM
5-Iodotubercidin	1	Kinase inhibitor - ATP mimetic - Haspin

2.9. Assay for Transposable-Accessible Chromatin using sequencing (ATAC-seq)

2.9.1. Expression, Purification, Assembly and Assay of Tn5 Transposase

Tn5 transposase was manufactured after the method of Picelli, *et al*. [142] with modifications. Briefly, the protein was expressed overnight in *E.coli* at 18°C as a fusion protein with intein/chitin binding protein. The cells were harvested, lysed and a cleared lysate was made by centrifugation. All bacterial DNA was then precipitated with Polyethylenimine and the cleared lysate was then used for Chitin resin chromatography. The bound Tn5 was auto cleaved from the chitin resin by the thiol induced cleavage activity of the intein. Yield was in excess of 15mg/l. The Tn5 can be loaded with double stranded DNA oligo before cleavage from the column or afterwards. Dialysis or concentration/dilution in a centrifugal concentrator can be used to remove unincorporated oligos. These experiments were done with Dr. James Dunford in Oxford University.

2.9.2. ATAC-seq

ATAC-seq was performed using 100.000 cells for the transposition reaction, which was performed based on the protocol by Buenrostro *et al*. [143,144] using in-house produced transposase. Briefly, cells were washed with cold PBS, lysed in 100 μl cold lysis buffer containing 10 mM Tris-HCl pH 8, 10 mM NaCl and 4 mM $MgCl_2$, 0.3% Noniodet NP40 and 0.01% Tween20 for 5 min. After centrifugation of 10 min 500g at 4

°C, cells were resuspended in TD Buffer containing 0.1% Tween20 and 0.05% Digitonin for 5 min at room temperature. After addition of 4 µl Tn5 enzyme incubation at 37 °C for 60 min with 500 rpm shaking was done. Subsequently, the samples were purified. PCR-amplification was performed using the following protocol: 3 min 72°C; 30 sec 98°C; 11 cycles of (10 sec 98°C, 30 sec 63°C, 3 min 72°C). Primers are listed **in Table 2.3**. The samples were then purified and eluted with 20µL of TE buffer. Samples were then validated on a Tapestation (Agilent) to determine library size and quantification prior to paired-end (2x41 bp) sequencing on a NextSeq 500 (Illumina) platform.

Table 2.3 Adapters used in ATAC-seq

Adapter ID	Sequence
Ad1	AATGATACGGCGACCACCGAGATCTACACTCGTCGGCAGCGTCAGATGTG
Ad2	CAAGCAGAAGACGGCATACGAGATTCGCCTTAGTCTCGTGGGCTCGGAGATGT
Ad3	CAAGCAGAAGACGGCATACGAGATCTAGTACGGTCTCGTGGGCTCGGAGATGT
Ad4	CAAGCAGAAGACGGCATACGAGATTTCTGCCTGTCTCGTGGGCTCGGAGATGT
Ad5	CAAGCAGAAGACGGCATACGAGATGCTCAGGAGTCTCGTGGGCTCGGAGATGT
Ad6	CAAGCAGAAGACGGCATACGAGATAGGAGTCCGTCTCGTGGGCTCGGAGATGT
Ad7	CAAGCAGAAGACGGCATACGAGATCATGCCTAGTCTCGTGGGCTCGGAGATGT
Ad8	CAAGCAGAAGACGGCATACGAGATGTAGAGAGGTCTCGTGGGCTCGGAGATGT
Ad9	CAAGCAGAAGACGGCATACGAGATCAGCCTCGGTCTCGTGGGCTCGGAGATGT
Ad10	CAAGCAGAAGACGGCATACGAGATTGCCTCTTGTCTCGTGGGCTCGGAGATGT
Ad11	CAAGCAGAAGACGGCATACGAGATTCCTCTACGTCTCGTGGGCTCGGAGATGT
Ad12	CAAGCAGAAGACGGCATACGAGATTCATGAGCGTCTCGTGGGCTCGGAGATGT
Ad13	CAAGCAGAAGACGGCATACGAGATCCTGAGATGTCTCGTGGGCTCGGAGATGT
Ad14	CAAGCAGAAGACGGCATACGAGATTAGCGAGTGTCTCGTGGGCTCGGAGATGT
Ad15	CAAGCAGAAGACGGCATACGAGATGTAGCTCCGTCTCGTGGGCTCGGAGATGT
Ad16	CAAGCAGAAGACGGCATACGAGATTACTACGCGTCTCGTGGGCTCGGAGATGT
Ad17	CAAGCAGAAGACGGCATACGAGATAGGCTCCGGTCTCGTGGGCTCGGAGATGT
Ad18	CAAGCAGAAGACGGCATACGAGATGCAGCGTAGTCTCGTGGGCTCGGAGATGT
Ad19	CAAGCAGAAGACGGCATACGAGATCTGCGCATGTCTCGTGGGCTCGGAGATGT

2.10. Processing of next-generation sequencing data

Analysis were performed by Dr. Adam Cribbs in Oxford University. A computational pipeline was written calling scripts from the CGAT toolkit to analyze the next generation sequencing data and (https://github.com/CGATOxford/CGATPipelines). For RNA-seq experiments, sequencing reads were mapped to the reference human genome sequence (GRCh37 (hg19) assembly) using hisat v0.1.6. To count the reads mapped to individual genes, the program featureCounts v1.4.6was used. Only uniquely mapped reads were used in the counting step. The counts table that was generated was then used for differential expression analysis. Differential gene expression analysis was performed with DESeq2 v1.12.3 within the R statistical framework v3.3.0. To define differentially expressed genes a threshold of > 2-fold change and FDR < 0.05 was used. For analysis of ATAC-seq data Bowtie software v0.12.5 was used to align the reads to the human hg19 reference genome. Reads were only considered that were uniquely

aligned to the genome with up to two mismatches [145]. Further analysis were performed by Genialis platform [146].

2.11. Gene expression detection by qRT-PCR

To determine the mRNA expression, RNA was isolated from drug treated cells. Cells were seeded to 12 well plates at the density of 10^5 cells/well and treated with the respective drug. RNA was isolated via MN RNA Isolation Kit following manufacturer's instructions (Macheret-Nagel). RNA quality was determined by Nanodrop measurements. 1000 ng cDNA was obtained by reverse transcription of RNA using M-MLV Reverse Transcriptase (Invitrogen). Relative mRNA expression levels were detected by using LightCycler® 480 SYBR Green I Master (Roche). The primers used in these experiments are listed in **Table 2.4**.

Table 2.4 qRT-PCR primer sequences

Gene	Forward primer sequence	Reverse primer sequence
FGFR2	TGCACCCCATCCTTAGTCCA	CCAGAAGAGCCACCAACCAA
GAPDH	AGCCACATCGCTCAGACAC	GCCCAATACGACCAAATCC
HDAC1	CATCTCCTCAGCATTGGCTT	CGAATCCGCATGACTCATAA
HDAC10	GAACAGCCACATCCAGGG	CCTCTTAGATGGGATGCTGG
HDAC2	ATGAGGCTTCATGGGATGAC	ATGGCGTACAGTCAAGGAGG
HDAC3	CTGTGTAACGCGAGCAGAAC	GCAAGGCTTCACCAAGAGTC
HDAC4	CTGGTCTCGGCCAGAAAGT	CGTGGAAATTTTGAGCCATT
HDAC5	GAACTGGGCATGGCTCTTG	GGGAACCATCCTTGGAAATC
HDAC6	GCGGTGGATGGAGAAATAGA	CCGGAGGGTCCTTATCGTAG
HDAC8	GCGTGATTTCCAGCACATAA	ATACTTGACCGGGGTCATCC
HDAC9	GCCCACAGGAACTTCTGACT	GAACTCTAAGCCAGATGGGG
LGR5	CATAAGTGATGCTGGAGCTGGTAA	GAGGATCTGGTGAGCCTGAGAA
MGMT	GGATTGCCTCTCATTGCTCC	CCCGTTTTCCAGCAAGAGTC
p21	GGCAGACCAGCATGACAGATTT	AAGATGTAGAGCGGGCCTTTGA
SEMA5A	TCACACACCAACACAGGTGC	GCTTGGACACCCAACTTTGC

2.12. CRISPR/Cas9 plasmid cloning

Genes indicated in **Table 2.5** targeting gRNAs were chosen from GenScript and cloned into plentiCRISPRv2 backbone according to Zhang Lab's protocol [147] .

Briefly, lentiCRISPRv2 vector was digested with BsmBI Restriction Enzyme and gel purified with MN PCR-Clean Up Kit. Extracted plasmids were treated with Antartic Phosphotase (AP). 1 µl of each oligo (100 µM) was annealed with T4 Polynucleotide

Kinase and T4 DNA Ligase Buffer in 10 µl reaction in a thermal cycler with the following settings: 37°C for 30 min, 95°C for 4 min and then ramp down to 25°C at 5°C/min. Oligos were diluted to 1:200 were used as inserts for cloning. 20 µl ligation reactions were prepared with 50 ng BsmBI-digested, AP-treated vectors, 1 µl of inserts and T4 DNA Ligase (NEB) in 10X T4 DNA Ligase buffer (NEB), respectively. Ligation reaction were incubated for 3 hours at room temperature. 50 µl Stbl3 bacteria was mixed with 5 µl of the ligation reaction for 15 minutes on ice. Heat shock was applied at 42°C for 30 seconds. Later, 250 µl Luria-Bertani (LB) broth was supplemented and cultured in 37°C at 225 rpm in a shaker for an hour. The reaction was spread on Carbenicillin resistant plates and incubated overnight at 37°C. Next day colonies were picked individually, grown in LB and plasmid DNA was extracted by MN Nucleospin Plasmid Kit. To confirm the inserts, samples were sent to sequencing to Macrogen Europe with U6 promoter sequencing (Forward sequencing primer for U6 promoter ACTATCATATGCTTACCGTAAC).

Packaging of plasmids were done in HEK 293T cells. Cells were transfected with the envelope protein (VSVG) and Gag-Pol (8.2 dVPR) utilizing FuGENE Transfection Reagent (Promega) in the afternoon. Next morning, fresh medium was added. Viruses were collected after 48 and 72 hours of transfection.

Table 2.5 Oligonucleotide sequences of gRNAs

Name	Sequence
HDAC6-gRNA-1	CACCGACATGATCCGCAAGATGCGC
HDAC6-gRNA-2	CACCGTCCCTTGCAGTCCCACGATT
MGMT-gRNA-1	CACCGGTGCGCACCGTTTGCGACT
MGMT-gRNA-2	CACCGTATCGAAGAGTTCCCCGTGC

2.13. Protein detection by Western Blot

For whole cell extracts, buffer containing, 1% NP-40, 150 mM NaCl, 1mM EDTA, 50 mM Tris-HCl (pH 7.8), 1 mM NaF, 0.5 mM PMSF, 1X phosphatase inhibitor cocktail (PhosSTOP, Roche) and 1X protease inhibitor cocktail (cOmplete Protease Inhibitor Cocktail Tablets, Roche). Following 30 minutes of incubation on ice, sonication for 60 sec (5 sec on 5 sec off pulse) was performed (Branson Digital Sonifier). Centrifugation at 14,000*g* for 15 min at 4^0C was performed to yield supernatants containing total cell extract.

For histone extraction, cell pellets were resuspended with triton extraction (TE)

buffer and incubated for 10 min on ice on a shaking plate. At the end of incubation, the tubes were centrifuged at 4°C for 10 min at 2000rpm. Supernatant was discarded and the pellet was washed with half volume of triton extraction buffer and centrifuged at 4°C for 10 min at 2000rpm. Supernatant was discarded and the pellet was resuspended in 0.2N HCl. Tubes were incubated at 4°C for overnight on rotating wheel at 10 rpm. At the end of incubation, tubes were centrifuged at 4°C for 10 min at 2000rpm and supernatant was collected in new tube. Acid extractions were neutralized with the addition 0.1M NaOH for 1/5 volume of HCl solution.

Protein amount was detected by Pierce BCA Protein Assay Kit (Thermo Fisher) following manufacturer's instructions. Equal amounts of proteins were heated to 95°C for 10 min with 4X Laemmli sample buffer (Bio-Rad) and loaded onto polyacrylamide gels. Precision Plus Protein Dual Color Standards (Bio-Rad) were used a molecular weight ladder. Proteins were transferred onto Immun-Blot PVDF Membrane (Bio-Rad) by semi-dry or wet transfer technique.

For semi-dry transfer method, Trans-Blot Turbo Transfer System (Bio-Rad) was used. As a transfer buffer, 10% Ethanol added TG buffer (Bio-Rad) was used with standard transfer protocol. Semi-dry transfer method was preferred for all the western blot methods unless the detected protein's size was more than 160 kDa. For larger proteins, wet transfer method was used (Mini Trans-Blot Electrophoretic Transfer Cell - Bio-Rad). As a transfer buffer, Towbin Buffer (25 mM Tris, 192 mM Glycine, 10% ethanol (v/v) -pH 8.3) was used with 12 volts for overnight incubation in cold room. After transfer of proteins on membrane, membrane was incubated with 5% blotting grade blocker (Bio-Rad) dissolved in TBS-T (20 mM Tris, 150 mM NaCl, 0.1% Tween 20 –pH 7.8) for 1-2 hours at room-temperature with gentle stirring. After blocking step, membranes were incubated with primary antibody solution (primary antibody in 5% BSA, 0.02% NaN_3 in TBS-T) at 4°C for 16 hours. Secondary antibody was incubated at room temperature for 1-2 hours. Proteins were visualized with Pierce ECL Western Blotting Substrate (Thermo Scientific) and Odyssey Fc Imaging systems (LiCOR). Used antibodies and their dilutions are indicated in **Table 2.6.**

Table 2.6 List of antibodies used in Western Blot

Antibody target	Brand/Cat. No.	Dilution
HDAC6	Cell Signaling/ 7558	1:1000
ac-α-tubulin	Santa Cruz/sc-23950	1:5000
β-actin	Abcam/ 8227	1:10000
H3K9ac	Cell Signaling/ 9649	1:1000
H3K14ac	Cell Signaling/ 7627	1:1000
H3K18ac	Cell Signaling/ 13998	1:1000
H3K27ac	Cell Signaling/ 8174	1:1000
H3 total	Abcam/ ab9049	1:1000 – 1:5000
cleaved PARP	Cell Signaling/9541	1:1000
GAPDH	Abcam/ab9485	1:5000
ATM	Cell Signaling/2873	1:1000
p-ATM	Cell Signaling/13050	1:1000
ATR	Cell Signaling/2790	1:1000
p-ATR	Cell Signaling/2853	1:1000
p21	Cell Signaling/2947	1:1000
Lamin B1	Abcam/ab16048	1:5000
MGMT	Cell Signaling/ 2739	1:1000
Rabbit secondary (HRP)	Abcam/ab97051	1:5000
Mouse secondary (HRP)	Abcam/ab97023	1:5000
IRDye 800CW anti-rabbit	LICOR/926-32211	1:5000
IRDye 680RD anti-mouse	LICOR/926-68070	1:5000

2.14. Caspase activity and inhibition assays

Caspase-3 and Caspase-7 activation are indicators of late-stage apoptosis. Caspase-3/7 activity was determined by the Caspase-Glo® 3/7 Assay (Promega, USA). The assay provides a proluminescent caspase-3/7 DEVD-aminoluciferin substrate and a proprietary thermostable luciferase in a reagent optimized for caspase-3/7 activity, luciferase activity and cell lysis. With cell lysis, followed by caspase cleavage of the substrates free aminoluciferin, which is consumed by the luciferase, gives out a luminescent signal. The signal is proportional to caspase-3/7 activity. 1000 cells were seeded into 96-well black bottom plates a day prior to drug treatment. Selected drugs were added incubated for 40 hours. Afterwards, The Caspase-Glo® 3/7 reagent was added and incubated for half an hour. Measurement was performed at 560 nm by Synergy H1 Reader (Biotek, USA).

For caspase inhibition assay, cells were seeded to 96-well black plates. Respective wells were pre-treated general caspase inhibitor (z-VAD-FMK (550377, BD Pharmingen) for 24 hours. Next day, cells were treated with Temozolomide and/or Ricolinostat. After 72 hours cell viability was detected by CTG.

2.15. Cell cycle analysis by propidium iodide

Cells were treated with respective drugs for 24, 48 or 72 hours. Afterwards cells were harvested by trypsinization and washed with 1X PBS. Fixation with 70% ice-cold ethanol was performed for 30 minutes at 4°C. Ethanol was washed away by 1X PBS. Pellets were treated with RNAse I (100 μg/ml, Invitrogen) and stained with 50 μg/ml propidium iodide (PI). BD Accuri Flow cytometry was used to quantify cell cycle phases.

2.16. Statistical Analysis

All normalizations were performed to untreated control cells, denoted as 100% using GraphPad Prism version 7.0 and Microsoft Excel 2018. Significance was detected by student's t-test or ANOVA, and at p-value <0.05.

3. RESULTS

3.1. Establishment of Temozolomide resistant cell lines

3.1.1. Determining Temozolomide (TMZ) response of GBM cell lines

In order to establish *in vitro* models of TMZ-resistance, we first characterized our GBM cell lines with respect to their TMZ response. TMZ is a DNA alkylating agent that causes futile cycling of DNA Mismatch Repair Pathway over many cell division cycles leading to cell cycle arrest and ultimately apoptosis. Therefore, cells need to be exposed to TMZ for long term in order to undergo apoptosis. Several GBM cell lines have already been characterized as TMZ-sensitive (A172, U87MG and U373) or TMZ-resistant (LN18 and T98G)[148]. However, there is a dramatic variation in the IC_{50} of cells to TMZ in these reports possibly due to the chosen experimental procedures, such as MTS assay or clonogenic assay. For example, U87MG cells were indicated to have an IC_{50} of ~10 μM [149], or 172 μM [150]. In order to establish a standard for our own studies, we utilized several assays to test the TMZ response of our GBM cell lines. First, we tested the viability of 3 different GBM cell lines (A172, T98G and U373) with Cell Titer Glo (CTG) assay, which measures the effect of repeated TMZ treatment in a 96-well format over 3 days. Accordingly, T98G cell line was validated as TMZ-resistant, requiring >1 mM of TMZ to have significant cell death in this treatment regimen. On the other hand, U373 and A172 cells were found to be sensitive to TMZ, showing around %50 cell death when treated with > 0.5 mM (**Figure 3.1**).

Since TMZ response among cells vary vastly in literature due to the assay used, we further examined the response of U373 cell line to longer duration of treatment. In this regimen, U373 cells were treated with TMZ for 5 consecutive days with daily drug renewal and viability was detected after 7 days with CTG or cell counting by trypan blue. Here, 250 μM TMZ reduced cell viability down to 30-40% and this dose was chosen for later screen assays (**Figure 3.2**).

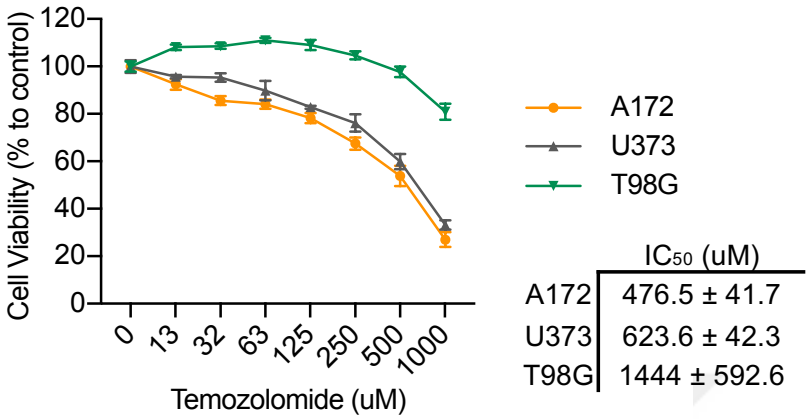

Figure 3.1. IC_{50} values of TMZ treated GBM cell lines. Cells were treated with respective doses for 3 days with drug renewal each day. Cell viability was detected by CTG, normalized to untreated control. Errors bars indicate "% ± NSEM"; n=3 for each condition.

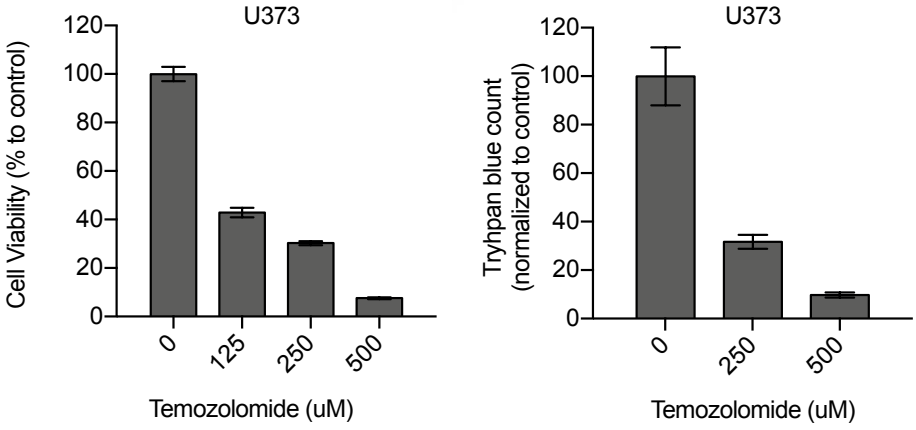

Figure 3.2. TMZ response of U373 tested via **A)** CTG method and **B)** trypan blue assay. U373 cells were treated with TMZ for 5 consecutive days with daily drug renewal and viability was detected after 7 days. Normalized to untreated control, and error bars represent "% ± NSEM"; n=3 for each condition.

3.1.2. Establishment of Temozolomide-resistant cell lines

To generate TMZ-resistant cell lines, we chose U373 that we showed to be sensitive to TMZ. To establish resistance, we employed two different methodologies. Firstly, in dose-escalation method, cells were initially treated with 25 μM TMZ and the dosage was doubled every 2-3 weeks up to 250 μM TMZ. The cells that survived and multiplied over this chronic treatment period of 3 months were as DE-TMZR^T. In the second method, daily high doses (250 μM) of TMZ was acutely applied for 15 days, and remaining U373 cells were expanded. These cells were named as TMZR^T (**Figure 2.1**).

To test whether these cells that survived TMZ treatment were indeed TMZ-resistant, clonogenic assay was performed. In this assay, growth response of cells to increasing doses of TMZ is measured in long term. Accordingly, we observed that both the DE-TMZR^T and TMZR^T cells were capable of forming colonies at the dosages that the parental U373 cells cannot (**Figure 3.3A**, **Figure 3.3B)**. We further validated the resistance by CTG assay, where cell response to an acute single day TMZ treatment was measured. Accordingly, DE-TMZR^T and TMZR^T cells were markedly less responsive to TMZ than U373 cells after 5 days of TMZ treatment (without drug renewal) (**Figure 3.3C**).

To determine whether TMZ resistance is reversible or sustainable, we cultured cells in medium devoid of TMZ for 2 months and examined the TMZ response of resulting cells via clonogenic assays. These sublines were denoted as DE-TMZR and TMZR (**Figure 2.1**). For DE-TMZR cells we observed partial reversal of resistance, TMZR cells were still fully resistant to TMZ (**Figure 3.4A, B**).

In addition, from the clonogenic assay we observed that DE-TMZR^T cells grew slower than TMZR^T cells, as their colony number and size were markedly smaller (**Figure 3.4C**). Thus, we investigated the proliferative capacities of our established resistant cell lines and measured their growth kinetics over 5 days. We observed that TMZR^T cells proliferate at a higher rate than U373, whereas DE-TMZR^T is slower. This trend was similar with their drug holiday sublines DE-TMZR and TMZR (**Figure 3.4C**).

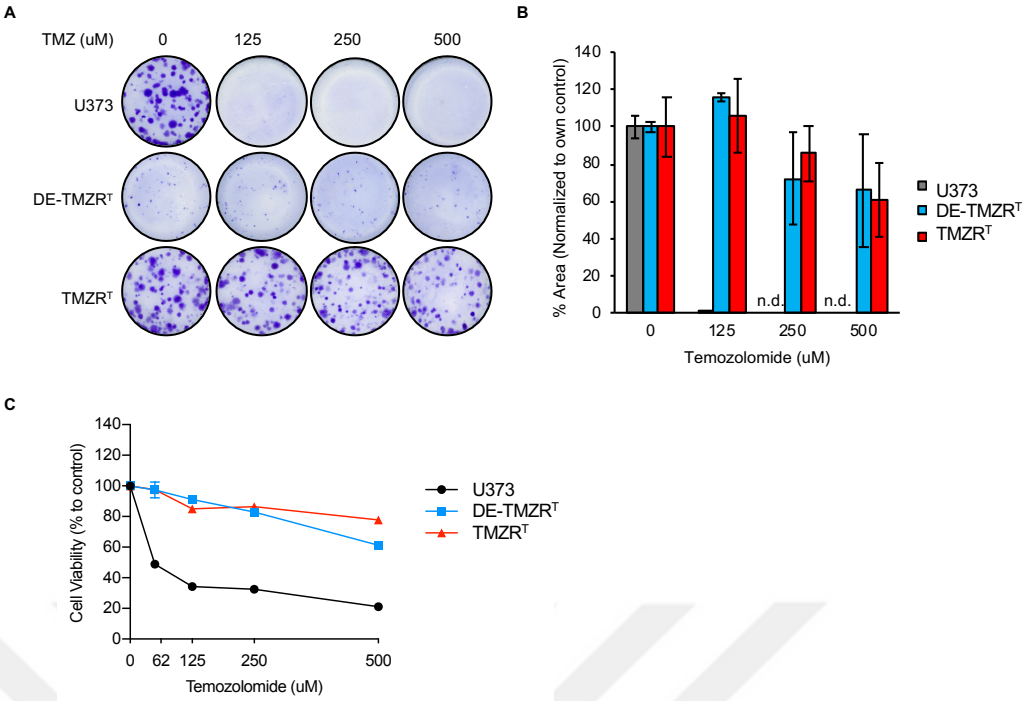

Figure 3.3. Clonogenic assay to test TMZ resistance A, B) Representative photos and bar graph of clonogenic assay. Cells were treated with 0,125, 250 and 500 uM TMZ for 48 hours, afterwards cells were left to proliferate for 10 days. **C)** CTG Cell viability assay, cells were treated with 0,125, 250 and 500 uM TMZ for 5 days (without drug renewal). "% ± NSEM" and n=3 for each condition "n.d." stands for not detected

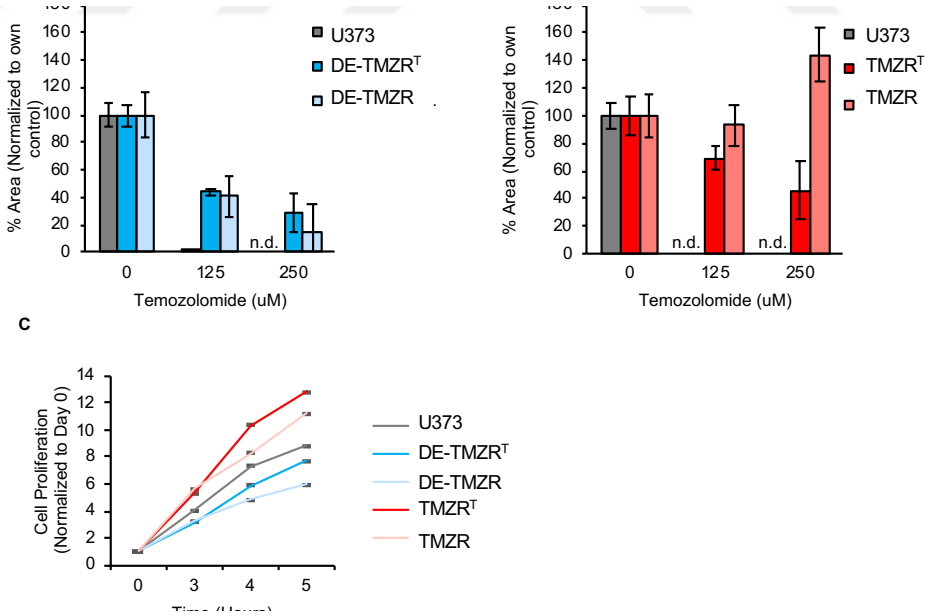

Figure 3.4. Clonogenic assay of drug holiday sublines A, B) Clonogenic assay **C)** Proliferation assay of U373 and TMZ resistant sublines normalized to Day 0. "% ± NSEM" and n=3 for each condition "n.d." stands for not detected

3.1.3. Characterization of TMZ-resistant cell lines

3.1.3.1. Response to other DNA alkylating agents

To test whether our established TMZ resistant cell lines were also cross-resistant to other DNA alkylating agents, we treated the cells with, Cyclophosphamide, Cisplatin, Carboplatin and Lomustine. Cisplatin and Carboplatin are platinum based chemotherapeutic agents that are widely used in oncology. They form DNA crosslinks, which can cause apoptosis upon failure of DNA repair [151]. We did not observe a significant response difference among U373, DE-TMZR and TMZR cells, when we administered Cisplatin or Carboplatin at varying doses (**Figure 3.5A, B**). Cyclophosphamide is a nitrogen mustards-based drug against cancer cells with high levels of phosphamides, which are capable of cleaving the phosphorus–nitrogen (P–N) bond, releasing nitrogen mustard, in turn alkylating DNA guanine residues[152]. Cyclophosphamide did not cause cell death more than 50% even in 100 μM dosages in all cell lines, and there was no significant difference among TMZ-resistant cell lines and the parental U373. (**Figure 3.5C**). Lomustine is an alkylating agent of the nitrosourea type that causes alkylation at O6me-G in DNA, with a similar mechanism of action with TMZ. Lomustine interferes with the function of DNA and RNA and its effect is not cell cycle dependent[150,153]. Interestingly, we observed a similar phenotype of resistance for Lomustine in our TMZ-resistant cell lines. While U373 cells were viable up to 40% at 25 μM, DE-TMZR and TMZR were 90% at this dose. Thus, our TMZ-resistant cell lines exhibited cross resistance to Lomustine (**Figure 3.5D**).

3.1.3.2. Investigation of transcriptome changes by RNA-seq

We hypothesized that transcriptional programs can be rewired during the adaptation of cells to TMZ treatment and acquisition of TMZ resistance. Hence, to investigate the transcriptional changes that operate in TMZ resistance, we performed RNA-seq experiments among U373, our resistant models (DE-TMZR^T and TMZR^T) and their drug holiday sublines (DE-TMZR and TMZR) that were maintained in TMZ-free conditions for more than 3 months.

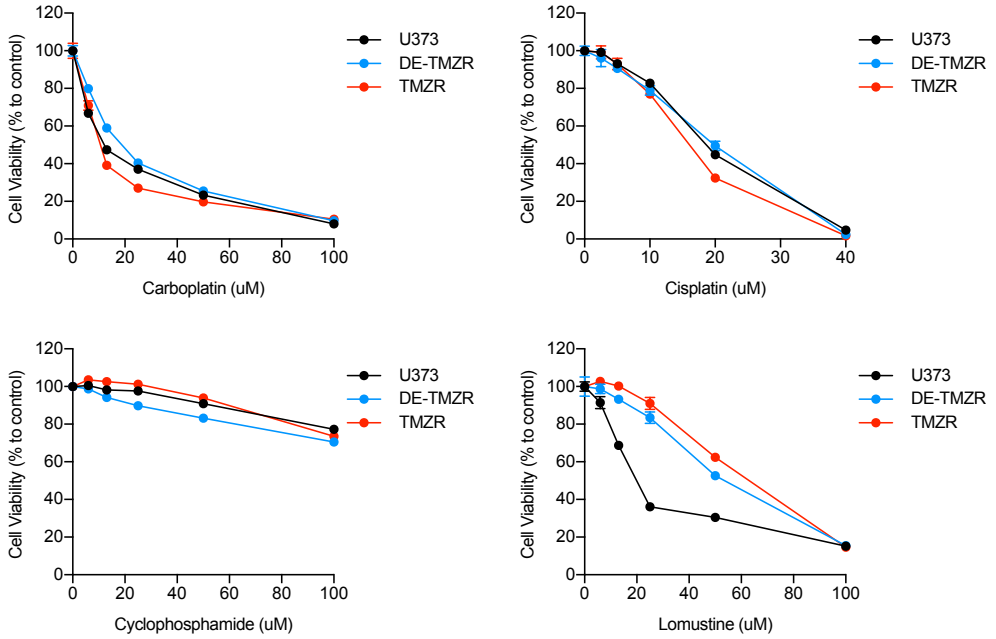

Figure 3.5. Response to other DNA alkylating agents Cell viability was detected by CTG after 5 days. "% ± NSEM" and n=3 for each condition "n.d." stands for not detected

We studied each cell line transcriptome as duplicates and investigated their correlation with PCA analysis. Accordingly, we observed that each duplicate is correlated with its own pair (**Figure 3.6A**) and the parental and TMZ-resistant samples were markedly separated from each other. Indeed, MA plots show that there were 3000 differently expressed genes (DEGs), compared to U373 (**Figure 3.6B**). When we analyze DEGs among groups, we observed that DE-TMZR^{T} has 3518 upregulated, 3245 downregulated genes compared to U373. For TMZR^{T} number of upregulated and downregulated genes are 2263 and 2216 respectively. Number of DEGs significantly decrease in drug holiday sublines DE-TMZR and TMZR (**Figure 3.6C**). A heatmap of the top 200 highly differentially expressed genes among our samples (**Figure 3.6B**) also indicated that DE-TMZR samples were separated the greatest from U373 samples, attesting to their great transcriptome changes compared to TMZR cells. In addition, through this heatmap we observed that DE-TMZR^{T} and DE-TMZR samples, were close to each other. This was also consistent with TMZR^{T} and TMZR samples (**Figure 3.6D**).

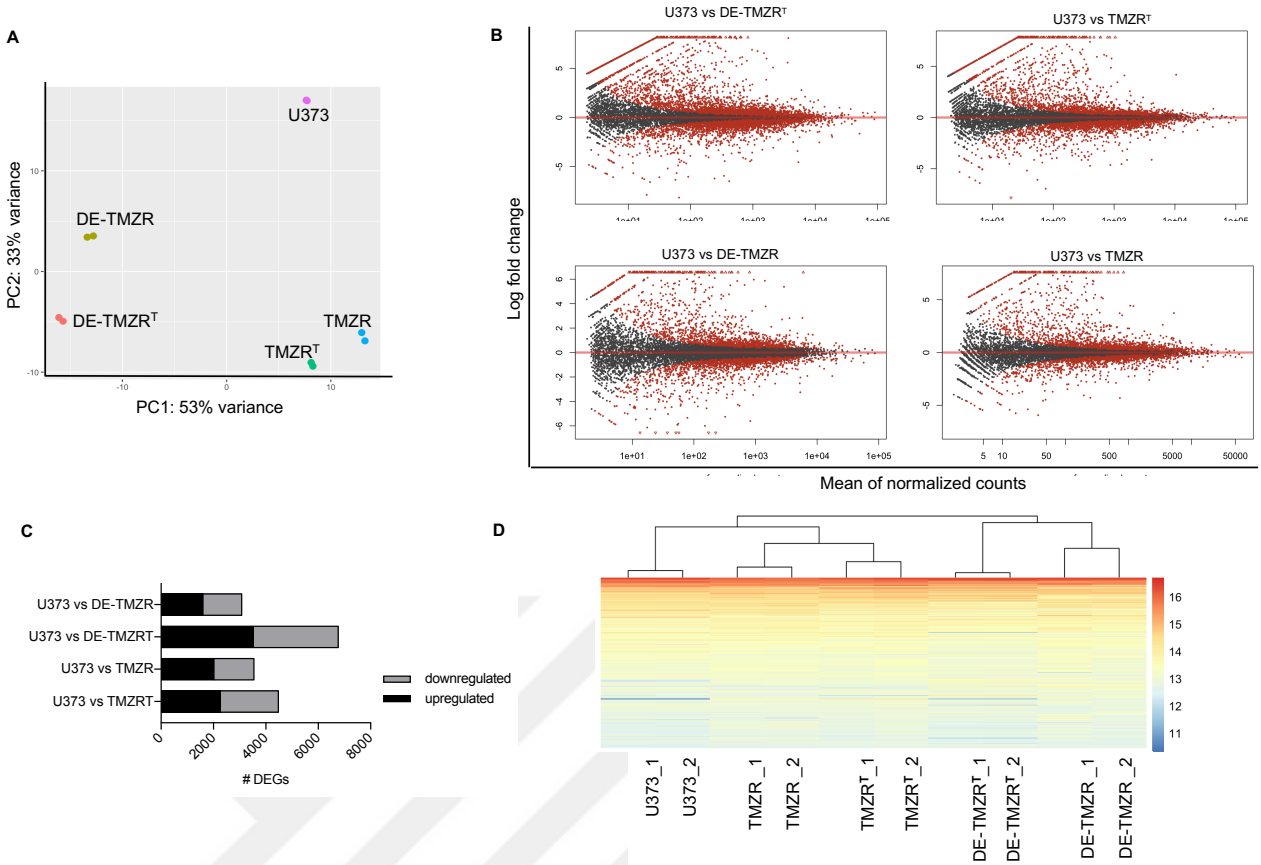

Figure 3.6. RNA-seq analysis of TMZ-resistant cells. A) PCA analysis among duplicates of RNA samples. **B)** MA plots indicating og2 fold changes attributable to a given variable over the mean of normalized counts for all the samples in the DESeqDataSet. Points are colored red if the adjusted p-value is less than 0.1. Points which fall out of the window are plotted as open triangles pointing either up or down. **C)** Bar graph showing DEGs of each group, adjusted p-value is 0.05 **D)** Heatmap depicting top 200 altered gene expressions among RNA-seq samples. (*RNA sequencing and analyses were conducted by Dr. Martin Philpott and Dr. Adam Cribbs, through collaboration with Oppermann Laboratory, Oxford University)*

We aim to investigate the stable transcriptome alterations in our resistant models, hence we focused on the common upregulated and downregulated genes between U373 vs TMZ-resistant models and their drug holiday sublines (**Figure 3.7A**). We observed that 42 genes were commonly upregulated in all TMZ-resistant models compared to U373. Among those the top genes were *CACNA2D1, EFNA5, FGFR2, HGF, MGMT, PTPRM, SEMA3E* and *TLL1*. However, only 5 genes were commonly downregulated, namely, *FMN2, GFAP,*

LGR5, SEMA5A and SPAG17. We validated these expression changes by conducting gene specific qRT-PCR and observed great consistency with RNA-seq results **(Figure 3.7B).**

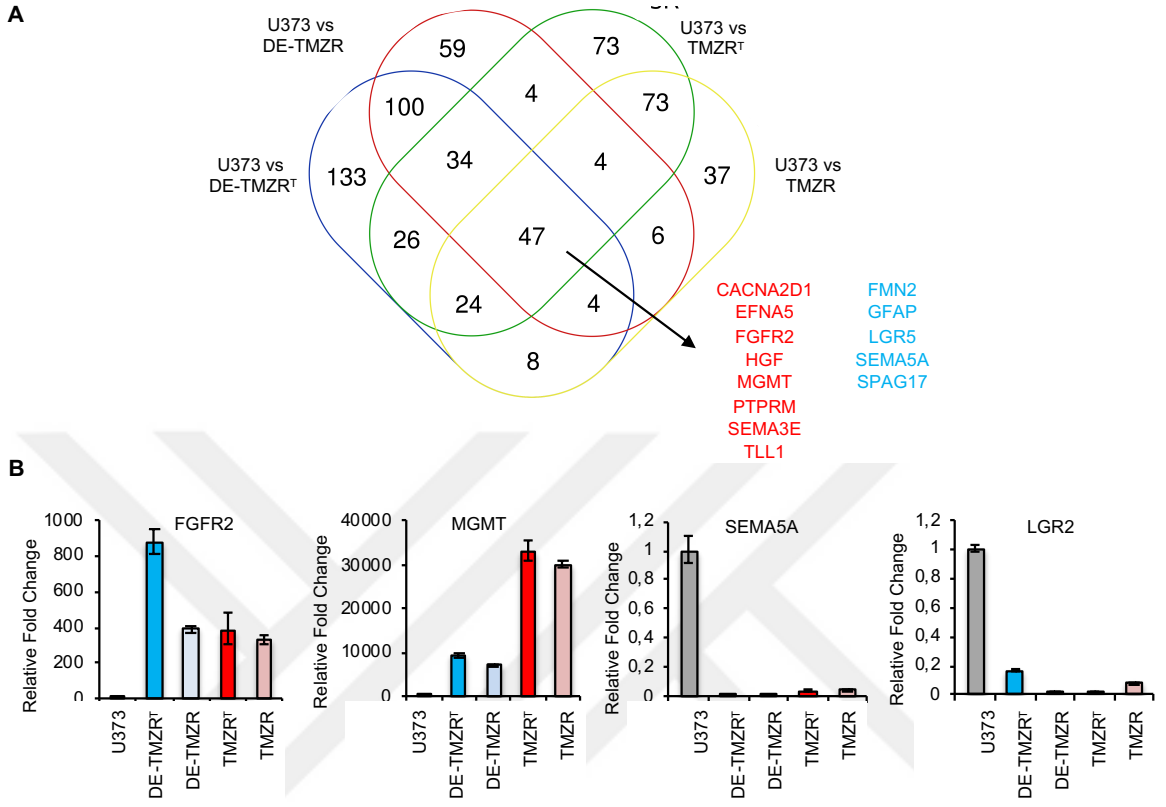

Figure 3.7. Common changes in the transcriptome of TMZ-resistant cell lines A) Venn diagram of common alterations among U373, TMZ resistant cell lines (DE-TMZR^T and TMZR^T) and their drug holiday sublines (DE-TMZR and TMZR).Top upregulated genes are indicated in red, downregulated genes are indicated in blue. **B)** qRT-PCR validation of top 2 upregulated (*FGFR2, MGMT*) and 2 dowregulated (*SEMA5A, LGR2*) genes. Error bars represent "+/-" mean error, n=3.

3.1.3.2.1. Targeting FGFR2 in TMZ-resistant cell lines

We observed that Fibroblast Growth Factor Receptor 2 (FGFR2) was highly elevated in DE-TMZR and TMZR when compared to U373 and this alteration was conserved in drug holiday sublines (**Figure 3.7B**). FGFR2 is a receptor tyrosine kinase that is commonly altered in GBM [16]. Increasing evidence indicates that activation of FGFR pathway plays a critical role in oncogenesis by *FGFR* gene amplification, activating mutations, or translocation [154]. To examine whether FGFR2 was functionally involved in TMZ resistance,

we employed FGFR1,2,3 inhibitor AZD4547 [155] and FGFR2 specific inhibitor Alofanib [156]. Treatment of U373, DE-TMZR and TMZR cells with Alofanib did not lead to notable cell death in any of the cell lines (**Figure 3.8A**). However, pan-FGFR inhibitor AZ4547, lead to significant viability decrease for all three cell lines, at comparable levels (**Figure 3.8B**). Next, we combined these FGFR inhibitors with TMZ to investigate their sensitization capacities. Accordingly, there was no combinatorial effect of FGFR inhibitors and TMZ on any of the cell lines. (**Figure 3.9**). Taken together, these results suggest that although FGFR2 expression in highly elevated in TMZ-resistant state, FGFR2 signaling is unlikely to be a mediator of TMZ-resistance in our cell line models.

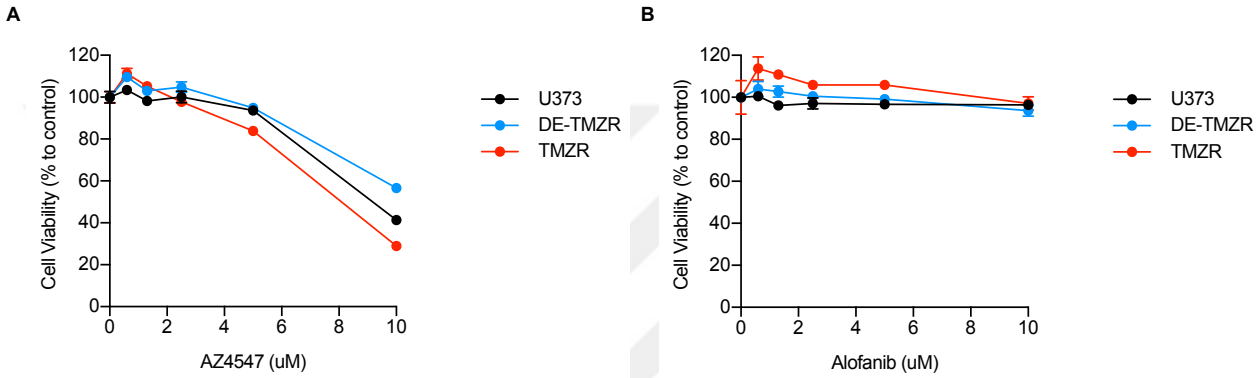

Figure 3.8. Treatment with FGFR inhibitors. Cells were treated with different dosages for 4 days **A)** pan FGFR2 inhibitor AZD4547 **B)** FGFR2 specific inhibitor Alofanib and viability was detected by CTG. "% ± NSEM" and n=3 for each condition

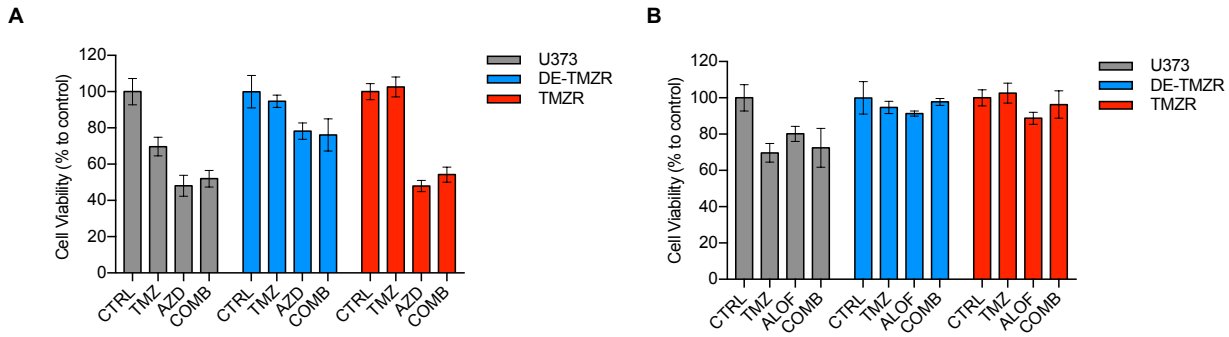

Figure 3.9 Combination of FGFR inhibitors with TMZ. Cells were serum starved for one day and treated with respective drug for 72 hours. TMZ 250 μM, AZD4547 7.5 μM and Alofanib 25 μM "% ± NSEM" and n=3 for each condition

3.1.3.3. The role of MGMT in TMZ resistance

According to our RNA-seq results, another highly elevated gene in TMZ-resistant cells was O^6-methylguanine-DNA methyltransferase (MGMT). Indeed, MGMT expression and activity is known to be a major regulator TMZ response in GBMs [64] . The expression of *MGMT* is regulated by *MGMT* promoter methylation, histone acetylation, transcription factors and microRNA expression [138], and its activity protects the cellular genome from the mutagenic effects of alkylating agents. To check basal levels of *MGMT* expression in our cells, we conducted qRT-PCR and noted that *MGMT* gene was not detectable in U373 parental cells. However, in consistency with RNA-seq experiments (**Figure 3.7B**), we revealed that *MGMT* is highly expressed in U373 derived TMZ resistant cell lines DE-TMZR and TMZR and in T98G cells that is defined as innately TMZ-resistant [148] (**Figure 3.10A**). qRT-PCR result was in accordance with Western Blot analysis of MGMT protein expression across these cells (**Figure 3.10B**). Taken together, these results show that MGMT was strongly upregulated in TMZ-resistant cell lines we generated.

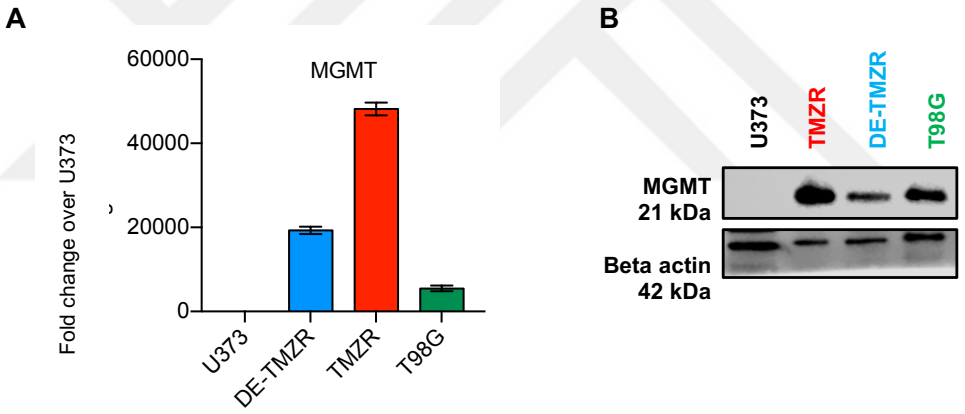

Figure 3.10. MGMT expression levels of TMZR cell lines. **A)** qRT-PCR results of MGMT expression normalized to U373 cell lines. **B)** Western Blot of MGMT protein levels.

As MGMT induction was a very significant event observed in TMZ-res cells, we aimed to understand its importance with functional experiments. First, in the gain-of-function approach, we tested whether MGMT induction was sufficient to establish TMZ resistance in parental U373 cells. To this end, we overexpressed MGMT in U373 cells by viral transduction and verified the overexpression by qRT-PCR (**Figure 3.11A**). Clonogenic

assays revealed that U373 cells that overexpress MGMT gain resistance markedly, up to the dosage that our TMZ-resistant cells can endure (**Figure 3.11B**).

Next, we wanted to see whether we can restore TMZ sensitivity in TMZ-resistant cells by loss-of-function approach. To this end, we established CRISPR/Cas9 mediated MGMT knockouts in established TMZ-resistant cell lines DE-TMZR, TMZR and innately TMZ-resistant T98G. We employed two different MGMT gRNAs and observed markedly low MGMT protein levels in all cell lines with MGMT gRNA2, compared to nontargeting gRNA (NT1) (**Figure 3.12**). Upon TMZ treatment, we observed a significant decrease of cell viability in all three TMZ-resistant cell lines with MGMT knockout (**Figure 3.12**), but not in control cells (cells with NT1). Thus, we validated the important role of MGMT in our models of TMZ resistance.

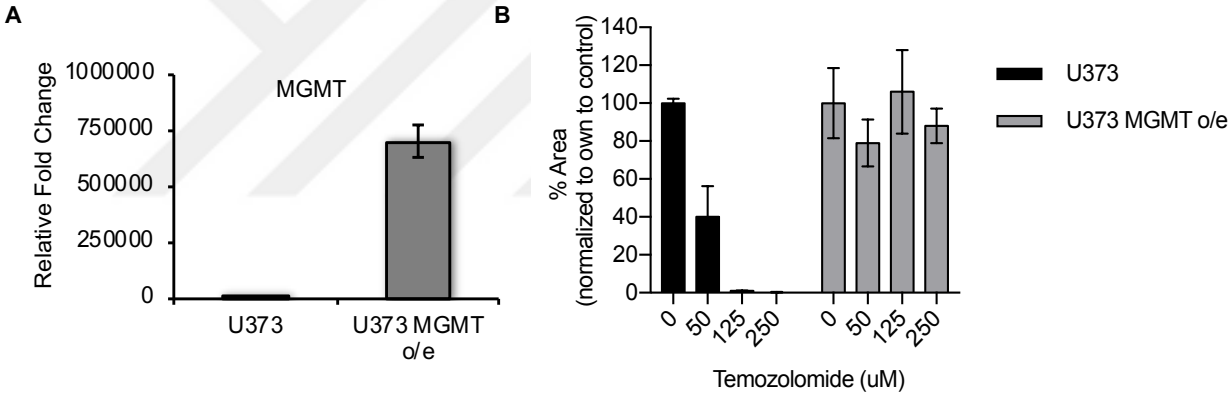

Figure 3.11. Overexpressing MGMT in U373 causes TMZ resistance. A) qRT-PCR detection of *MGMT* gene in U373 parental and MGMT overexpression plasmid transduced cell (denoted as U373 MGMT o/e). Normalization to GAPDH was performed for each sample. **B)** Clonogenic assay of TMZ treatment on MGMT overexpressed U373 cell line. "% ± NSTDEV" and n=3 for each condition.

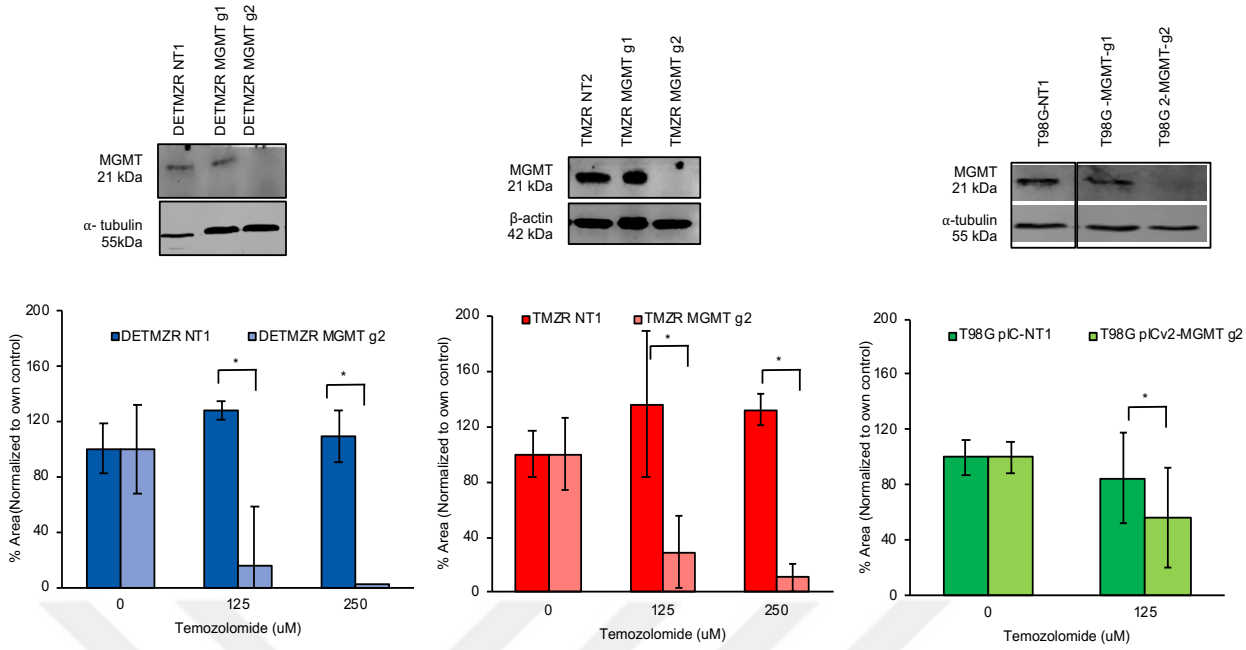

Figure 3.12. MGMT Knockout cells. Western blot of MGMT protein and respective clonogenic assay of MGMT knockout cells. * denotes $p<0.05$, t-test, "% ± NSTDEV" and n=3 for each condition. (*Western Blots are assisted by Duygu Uçku, a KUSOM undergraduate researcher).*

3.2. Identifying the epigenetic regulators of Temozolomide resistance in GBM

3.2.1. Epigenetic probes screens to identify epigenetic vulnerabilities of TMZ-resistant cell lines

Although MGMT silencing by promoter hypermethylation is the first, and still a highly important, prognostic indicator for GBM patients [157,158], there could be several other epigenetic alterations that contribute to TMZ response of GBMs that remains to be uncovered. Although the TMZ resistance in our established cell lines exhibit strong dependency on MGMT, there can still be additional genetic and epigenetic events accompanying MGMT activity in TMZ-resistant cells. Therefore, in order to explore the epigenetic vulnerabilities of our GBM cell lines and identify epigenetic sensitizers of TMZ response, we conducted several screens with chemical libraries of epigenetic probes targeting chromatin modifiers.

Our epigenetics probes library targets various histone modifying enzymes such as bromodomains, histone deacetylases, histone demethylases, histone methytransferases, kinases, etc (**Table 2.1**).

In the first screen with a library of 86 probes, the effects of the individual drugs alone or in combination with TMZ (500 μM) on U373 and T98G cells were explored with cell viability assays for 3 days (**Figure 3.13, Appendix C**). With 500 μM TMZ treatment, we observed 13% and 40% viability decrease in T98 and U373 cells, compared to their untreated controls. Hits were defined as drug + TMZ combination that can decrease cell viability to lower than 50% (**Table 3.1**). Accordingly, we obtained 21 hits or U373 screen and 11 hits for T98G screen.

When we look among hits for U373, they were distributed among kinase inhibitors, HDAC, histone demethylase inhibitors (HDACi, KDMi), PARP inhibitors, DNA methyltransferase inhibitor (DNMTi), bromodomain inhibitors and histone methyltransferase inhibitors (HMTi). For T98G, HDACi and KDMi were the majority of hits. In both screens HDACi was the major group of targets; 8 out of 21 for U373 and 6 out of 11 for T98G.

To test the effect of epigenetic probes on our established TMZ resistant models DE-TMZR and TMZR, we performed a second screen with an extended version of the chemical library containing 97 inhibitors (**Table 2.2**). U373, DE-TMZR and TMZR cells were treated with respective drugs with or without TMZ (250 μM for U373, 500 μM for DE-TMZR and TMZR) (**Figure 3.14**). All cell viability results are listed in Appendix III. Hits were defined as drug + TMZ combination that can decrease cell viability to 50% (**Table 3.2**). Coherent with the previous data, HDAC inhibitors (Belinostat, Mocenitostat, Ricolinostat, etc.) were the majority of the hits among screens.

Top hits of all screens are presented as heatmap in **Figure 3.15.** PARP inhibitors can block BER pathway and they are currently in clinical trials for GBM [159]. We observed that two independent PARP inhibitors, Rucaparib and Olaparib, can induce cell death combined with TMZ on U373, DE-TMZR and TMZR cell lines. In addition, for U373, DE-TMZR and TMZR, PARPi as single agents did not induce cell death, whereas they act only in combination with TMZ. Discovering PARPi as TMZ-sensitizing agents validate the effectiveness of our drug screen.

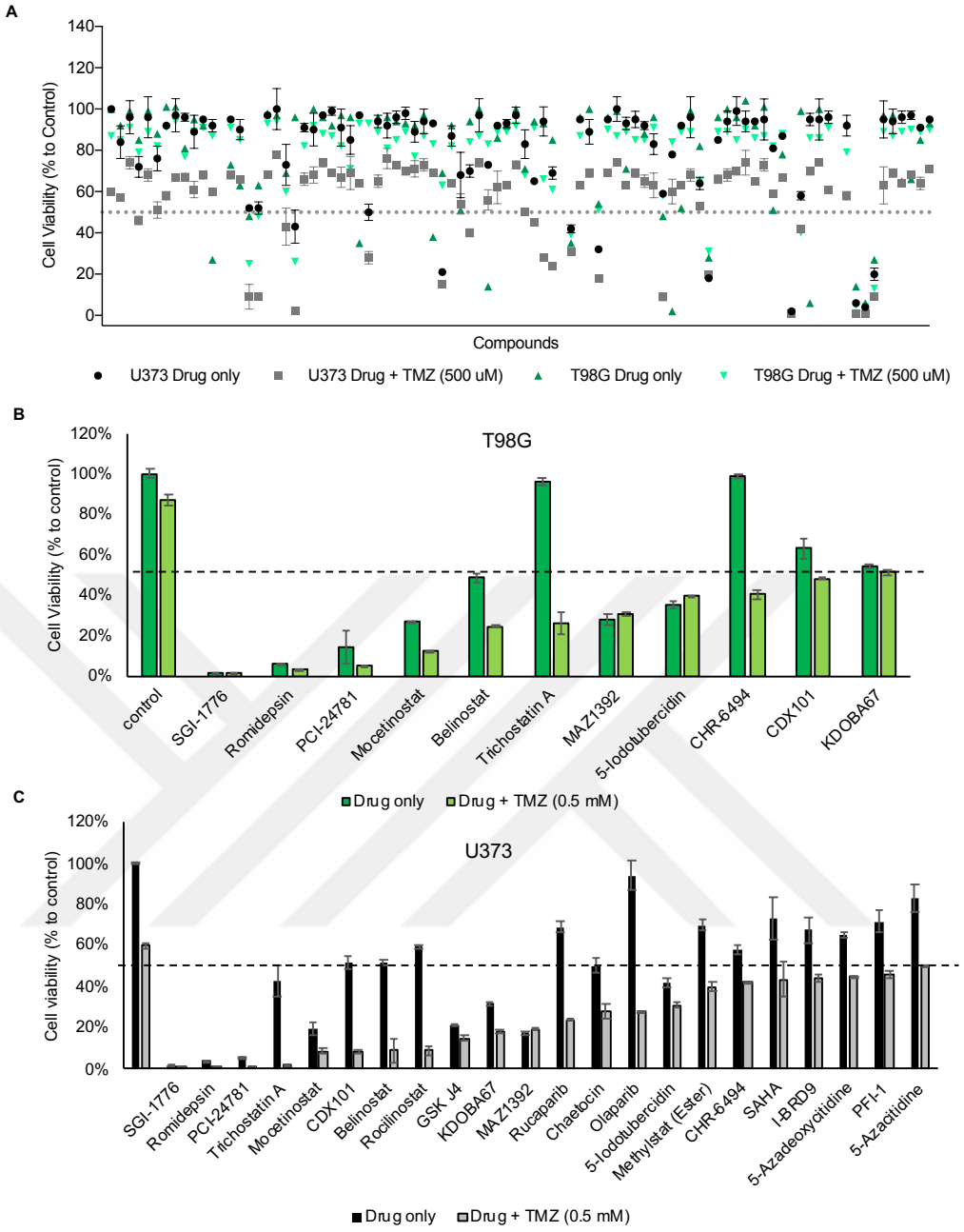

Figure 3.13. Epigenetic probe screen among U373 and T98G cells. A) U373 and T98G cells were treated with probe library alone or in combination with TMZ for 3 days. **B,C)** Top hits of both screens "% ± NSTDEV" and n=3 for each condition. Hits were determined as those decreased viability combined with TMZ below 50% threshold.

Table 3.1 Hits of T98G and U373 1st library. "%viability ± %error"

	T98G		U373		
Drug name	**Drug only (% to control)**	**Drug + TMZ (% to control)**	**Drug only (% to control)**	**Drug + TMZ (% to control)**	**Target**
Control	100 ± 1	87 ± 1	100 ± 1	60 ± 1	
DMSO	99 ± 2	85 ± 3	94 ± 1	66 ± 1	
CHR-6494	38 ± 3	40 ± 2	58 ± 2	42 ± 0	Kinase
5-Iodotubercidin	35 ± 1	39 ± 0	42 ± 2	31 ± 1	
SGI-1776	2 ± 0	1 ± 0	2 ± 1	1 ± 1	
Romidepsin	6 ± 0	4 ± 0	4 ± 0	1 ± 1	HDAC
PCI-24781	14 ± 8	5 ± 0	6 ± 0	1 ± 0	
Trichostatin A	52 ± 8	26 ± 5	43 ± 8	2 ± 0	
SAHA			73 ± 10	43 ± 9	
Mocenitostat	27 ± 0	13 ± 0	20 ± 3	9 ± 1	
CXD101	63 ± 5	48 ± 0	52 ± 3	9 ± 1	
Belinostat	48 ±2	25 ± 0	52 ± 1	9 ± 6	
Ricolinostat			59 ± 1	9 ± 2	
GSK-J4			21 ± 0	15 ± 1	KDM
Methylstat			70 ± 3	40 ± 2	
KDOBA67	54 ± 5	51 ± 1	32 ± 1	18 ± 1	
Rucaparib			69 ± 3	24 ± 0	PARP
Olaparib			94 ± 7	28 ± 0	
5-Azadeoxyctidine			65 ± 1	45 ± 0	DNMT
PFI-1			72 ± 5	46 ± 2	Bromodomain
I-BDR9			68 ± 6	44 ± 2	
Chaetocin			50 ± 4	28 ± 3	HMT
MAZ1392	28 ± 3	13 ± 0	18 ± 1	20 ± 0	tRNA synthethase

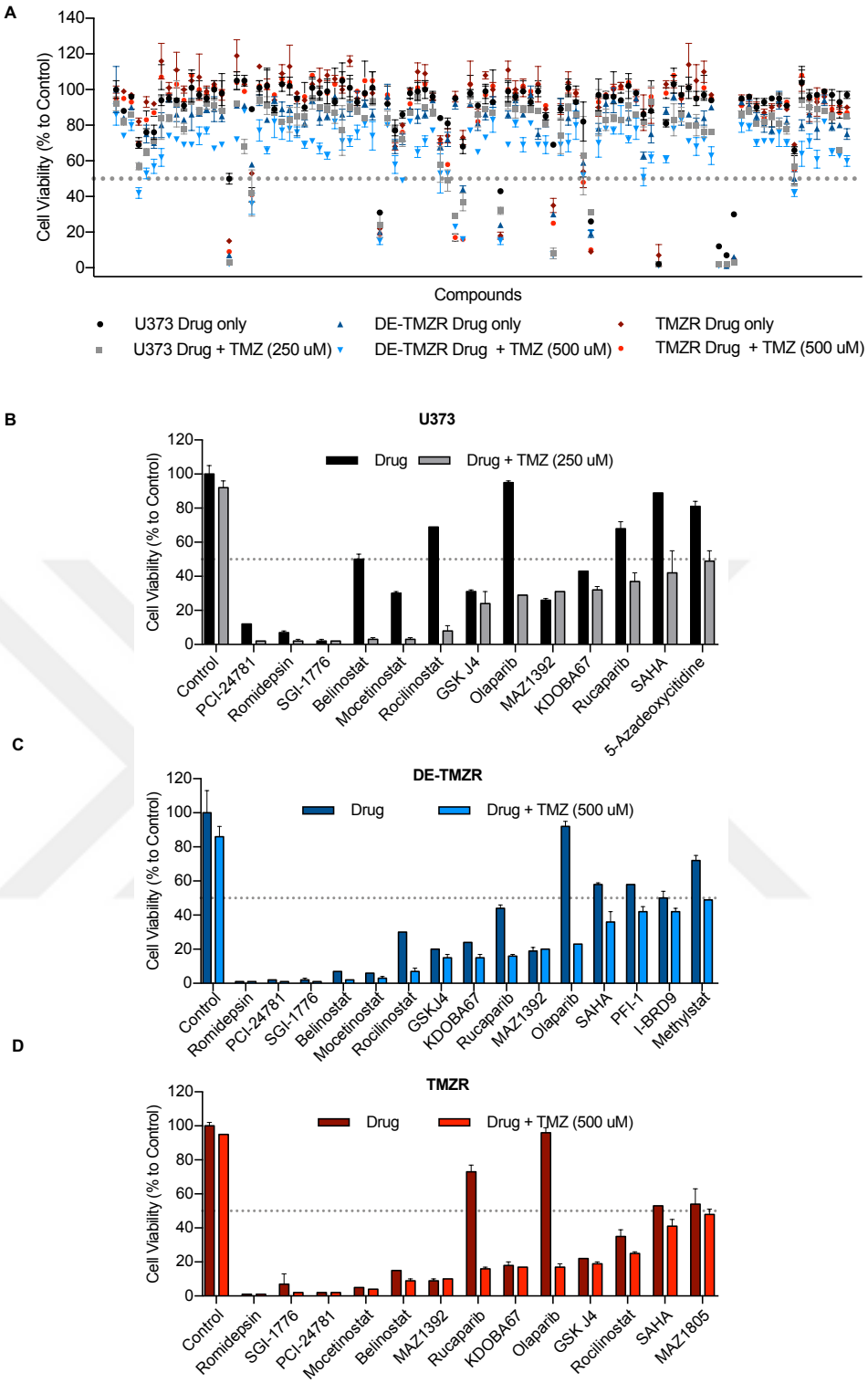

Figure 3.14. Epigenetic probe screen among U373 and T98G cells. A) U373, DE-TMZR and TMZR cells were treated with or without library combined with TMZ for 3 days. B,C,D) Hits defined as 50% threshold.

Table 3.2 Hits of U373 and established TMZ-Res cells with 2nd library. "%viability ± %error"

	U373		DE-TMZR		TMZR		
Drug name	**Drug only (% to control)**	**Drug + TMZ (% to control)**	**Drug only (% to control)**	**Drug + TMZ (% to control)**	**Drug only (% to control)**	**Drug + TMZ (% to control)**	**Target**
Control	100 ± 5	92 ± 4	100 ± 13	86 ± 6	100 ± 2	95 ± 0	
PCI-24781	12 ± 0	2 ± 0	2 ± 0	1 ± 0	2 ± 0	2 ± 0	HDAC
Romidepsin	7 ± 1	2 ± 1	1 ± 0	1 ± 0	1 ± 0	1 ± 0	HDAC
SGI-1776	2 ± 1	2 ± 0	2 ± 1	1 ± 0	7 ± 6	2 ± 0	Kinase
Belinostat	50 ± 3	3 ± 1	7 ± 0	2 ± 0	15 ± 0	9 ± 1	HDAC
Mocetinostat	30 ± 1	3 ± 1	6 ± 0	3 ± 1	5 ± 0	4 ± 0	HDAC
Ricolinostat	69 ± 0	8 ± 3	30 ± 0	7 ± 2	35 ± 4	25 ± 1	HDAC
GSK J4	31 ± 1	24 ± 7	20 ± 0	15 ± 0	22 ± 0	19 ± 1	KDM
Olaparib	95 ± 1	29 ± 0	92 ± 3	23 ± 0	96 ± 3	17 ± 2	PARP
MAZ1392	26 ± 1	31 ± 0	19 ± 2	20 ± 0	9 ± 1	10 ± 0	tRNA synth.
KDOBA67	43 ± 0	32 ± 2	24 ± 0	15 ± 2	18 ± 2	17 ± 0	KDM
Rucaparib	68 ± 4	37 ± 5	44 ± 2	16 ± 1	73 ± 4	16 ± 1	PARP
SAHA	89 ± 0	42 ± 13	58 ± 1	36 ± 6	53 ± 0	41 ± 4	HDAC
5-Azadeoxy.	81 ± 3	49 ± 6					DNMT
PFI-1			58 ± 0	42 ± 3			Bromodomain
I-BRD9			50 ± 4	42 ± 2			Bromodomain
Methylstat			72 ± 34	49 ± 0			KDM
MAZ1805					54 ± 9	48 ± 3	tRNA synth.

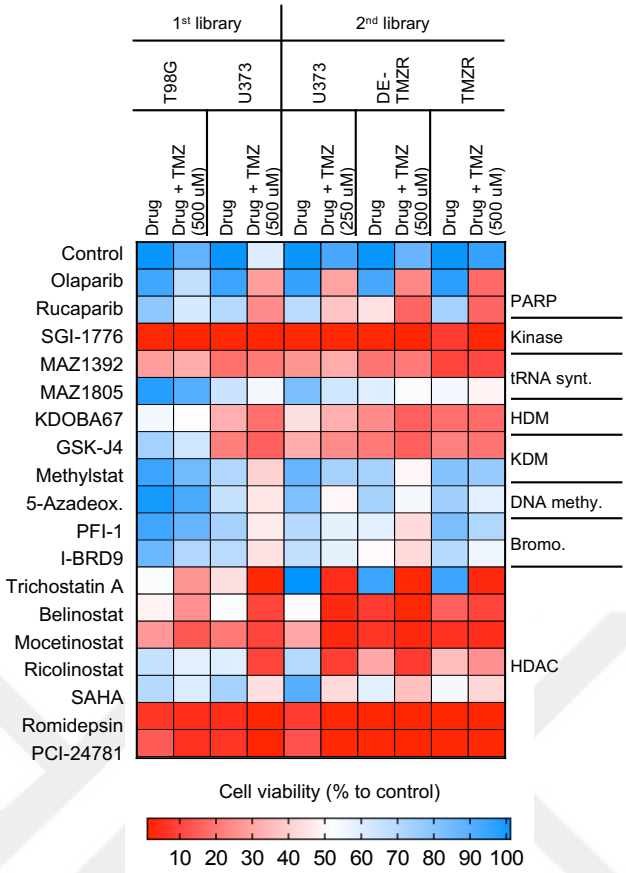

Figure 3.15. Heat map of top hits of epigenetic probes screen. Cell viability of top hits among screens is represented as heatmap. HDM: histone demethylase, KDM: lysine demethylase, HDAC: histone deacetlylase.

SGI-1776 is a Serine/threonine-protein kinase inhibitor, competing with Pim1 for ATP [160]. We have seen cell viability less than 10% in all across the screens with SGI-1776. MAZ1392 is halofuginone and MAZ1805 is the inactive halofuginol. Halofuginone is known to inhibit prolyl-tRNA synthetase thus initiating amino acid starvation response [161]. We observed that the active form MAZ1392 can enhance more cell death in all the cells regardless of TMZ induction compared to MAZ1805. Histone demethylase inhibitor KDOBA67, and Lysine demethylase (KDM) inhibitor GSK-J4 induced cell death more than 70% in U373, DE-TMZR and TMZR cell lines, whereas its toxicity effect was only around 30% in T98G.

3.2.2. HDACi is the major group of TMZ-sensitizers in the epigenetic screens

Among the top 18 hits, we detected 7 HDACi (namely, Trichostatin A, Belinostat, Mocetinostat, Ricolinostat, SAHA, Romidepsin and PCI-24781) could induce cell death significantly in all the screens either as single agents or in combination with TMZ.

HDAC expression has been found to be enhanced in many tumors including GBM [162]. Thus, we investigated the effect of all the HDACi in our probe library as single agents (**Figure 3.16**). Pan-HDAC inhibitor PCI-24781 and HDAC1/2 inhibitor Romidepsin and HDAC1/2/3 inhibitor Mocetinostat can induce more than 70% cell death in all of the tested cells as single agents. Other pan-HDACi included in the library, Trichostatin A and SAHA did not induce cell death as single agents, however their combination with TMZ could induce significant cell death (**Figure 3.15** and **Figure 3.16**). Despite some encouraging results from preclinical studies for pan-HDACi, early clinical trials showed only modest therapeutic benefits and pan-HDACi can induce undesired toxicity [109,163,164], thus it is more preferable to narrow down the target to inhibit. Ricolinostat, a selective HDAC6 inhibitor, caught our eye as it can induce significantly more cell death as a single agent in our established TMZ-resistant models DE-TMZR and TMZR than the parental cell line U373 or innately TMZ-resistant cell line T98G (**Figure 3.16**).

To validate our screens, we further studied Belinostat, Vorinostat and Ricolinostat in detail. In addition, we have included another selective HDAC6 inhibitor probe CAY10603 in our studies to look into the role of HDAC6i in our resistant models. In the drug screen, the working concentrations of the probes were 5 μM for Belinostat, 2.5 μM for SAHA (Vorinostat) and 10 μM for Ricolinostat. First, we investigated their effect on cell viability as single agents in a dose-dependent manner (**Figure 3.17**). We observed more cell death in DE-TMZR and TMZR cells compared to U373 with all 4 drugs. Hence, we hypothesized that our TMZ-resistant cells became more vulnerable to HDAC inhibition, especially HDAC6 inhibition.

A

Name	Target
SAHA (Vorinostat)	pan-HDAC
Trichostatin A	pan-HDAC
Belinostat (PXD101)	pan-HDAC
PCI-24781 (Abexinostat)	pan-HDAC
Romidepsin	HDAC1 and 2
Mocetinostat	HDAC1, 2 and 3
Entinostat (MS-275)	HDAC1 and 3
CI-994 (Tacedinaline)	HDAC1, 2, 3 and 8
Valproic acid	HDAC2
RGFP966	HDAC3
Santacruzamate	HDAC2
Tubastatin A	HDAC6 and 8
Ricolinostat (ACY-1215)	HDAC6
PCI-34051	HDAC8
TMP269	HDAC4, 5, 7 and 9
EX 527 (Selisistat)	SIRT1
SRT1720	SIRT1
AGK2	SIRT2

B

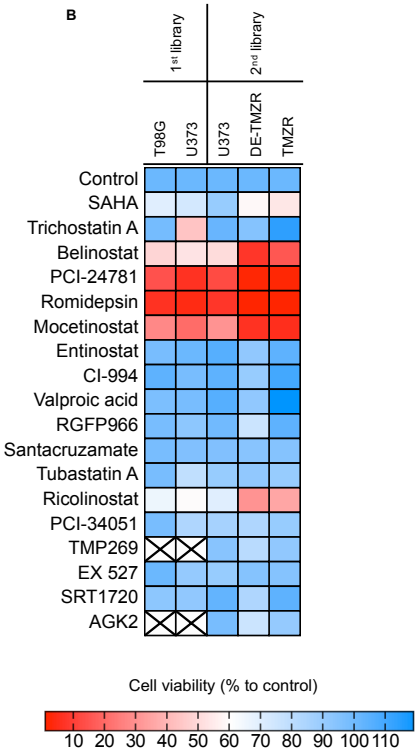

Figure 3.16. All HDACi in epigenetics probes library. A) Table of HDACi and their targets **B)** Heatmap of cell viability

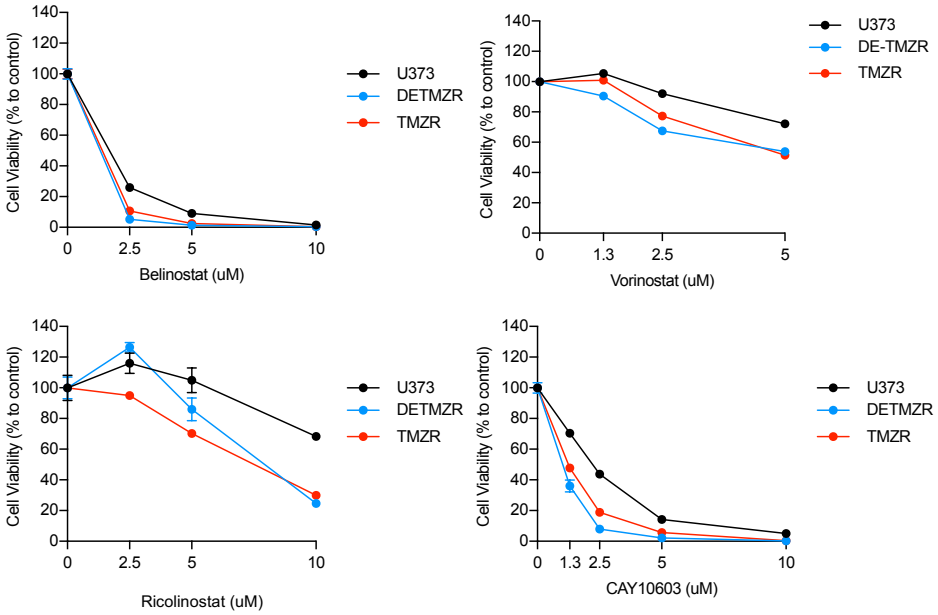

Figure 3.17. Cell viability of selected HDACi. Cells were treated for 72 hours and viability was detected by CTG. "% ± NSTDEV" and n=3 for each condition

3.2.3. The role of HDAC6 and its inhibition in TMZ-Resistant cells

3.2.3.1. Endogenous expression levels of HDACs

Since HDACs revealed to be potential targets in our TMZ resistant models, we investigated the endogenous HDAC gene expression levels of HDAC1-10 by qRT-PCR in U373, DE-TMZR and TMZR cells **(Figure 3.18).**

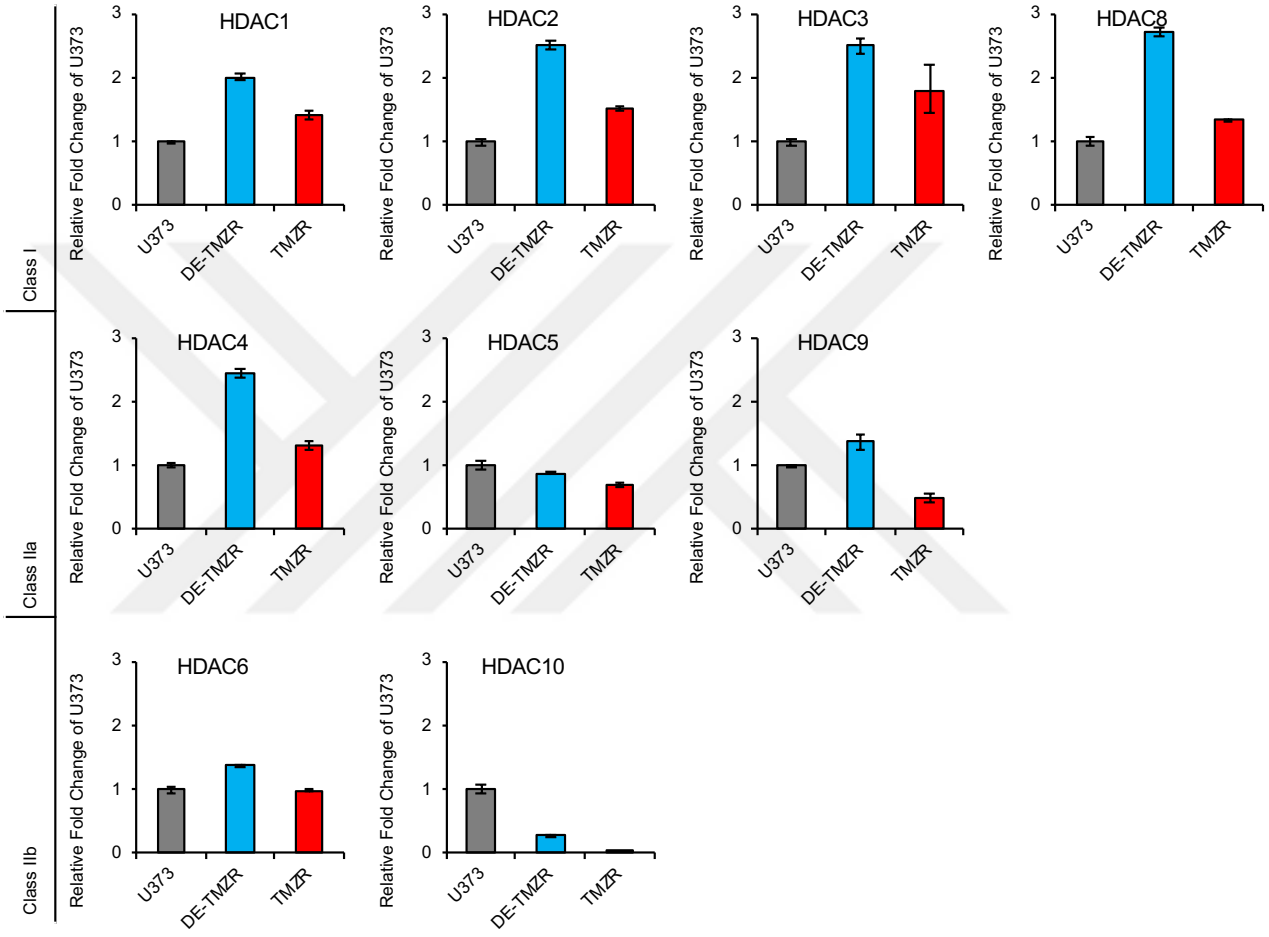

Figure 3.18. Endogenous HDAC expression. HDAC gene expression levels detected by qRT-PCR. Values were normalized to the level of housekeeping gene, GAPDH and expressed as fold change of U373 parental cell line. Error bars represent "± "mean and samples are in triplicate.

When we examined the endogenous expression levels of Class I HDAC (HDAC1, 2, 3 and 8), we observed DE-TMZR and TMZR express higher levels of some of these genes compared to U373. This might be one contributing mechanism to the selective vulnerability of DE-TMZR (Cell viability: 6%) and TMZR (Cell viability: 5%) compared to U373 (Cell viability: 30%) and T98G (Cell viability:27%) to HDACi (**Figure 3.16**). However, a class I HDAC inhibitor CI-994 did not induce cell death more than 20% across the screens. For class II HDAC, we only observed HDAC4 higher expression in DE-TMZR. TMP269 is a class II HDAC inhibitor, and when we inspected the viability results among all screens, we realized that TMP269 reduced cell viability to 93% in U373, 91% in TMZR and 80% in DE-TMZR. For Class IIb HDACs, we observed similar expression levels of HDAC6 and reduced levels in DE-TMZR and TMZR for HDAC10.

We further explored HDAC6 endogenous gene expression of our TMZ-resistant models by comparing to 2 other GBM cell lines and a normal brain sample. We observed that HDAC6 levels were innately high in U87MG and T98G cell lines (**Figure 3.19A**). Also, when we compared HDAC6 levels to normal brain sample, we observed a marked elevation of HDAC6 expression in all our cell lines compared to normal brain samples (**Figure 3.19B**)

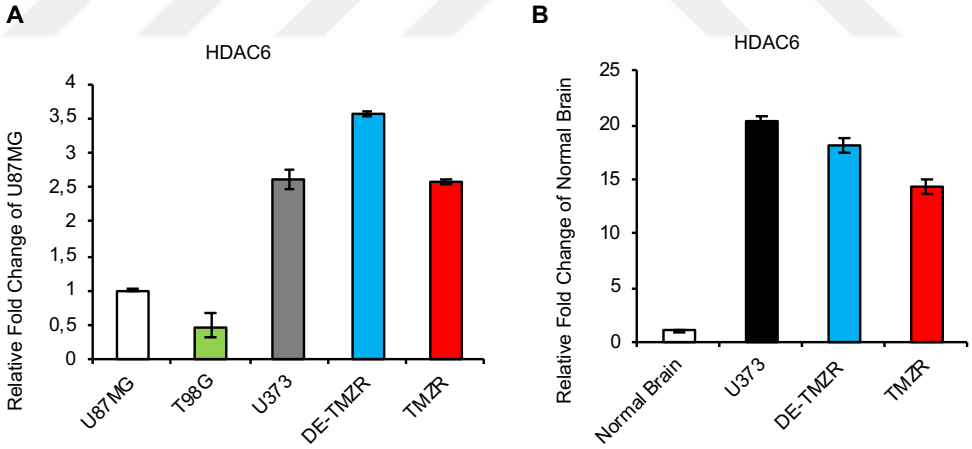

Figure 3.19. HDAC6 levels detected by qRT-PCR. A) Endogenous levels of U87MG, T98G, U373, DE-TMZR and TMZR cell lines. **B)** Endogenous levels of normal brain sample, U373, DE-TMZR and TMZR cell lines. Values were normalized to the level of housekeeping gene, GAPDH. Error bars represent "± "mean and samples are in triplicate. *This experiment was performed by Duygu Uçku.*

3.2.3.2. HDAC6 Inhibition by Chemical Inhibitors

DE-TMZR and TMZR cells were observed to have more vulnerability towards Ricolinostat compared to U373 cells. We validated this result with dose-dependent Ricolinostat treatments. A similar pattern was observed with another selected HDAC6i, CAY10603 **(Figure 3.37).**

To inspect the TMZ sensitization potential of HDAC6i, cells were cotreated with Ricolinostat/CAY10603 and TMZ for 5 days (**Figure 3.20**). Accordingly, for both drugs compared to TMZ alone, the combination induced significantly more cell death. Looking at the comparison between Ricolinostat or CAY10603 effect compared to the combination, we observed significance in U373 and TMZR but not in DE-TMZR cells.

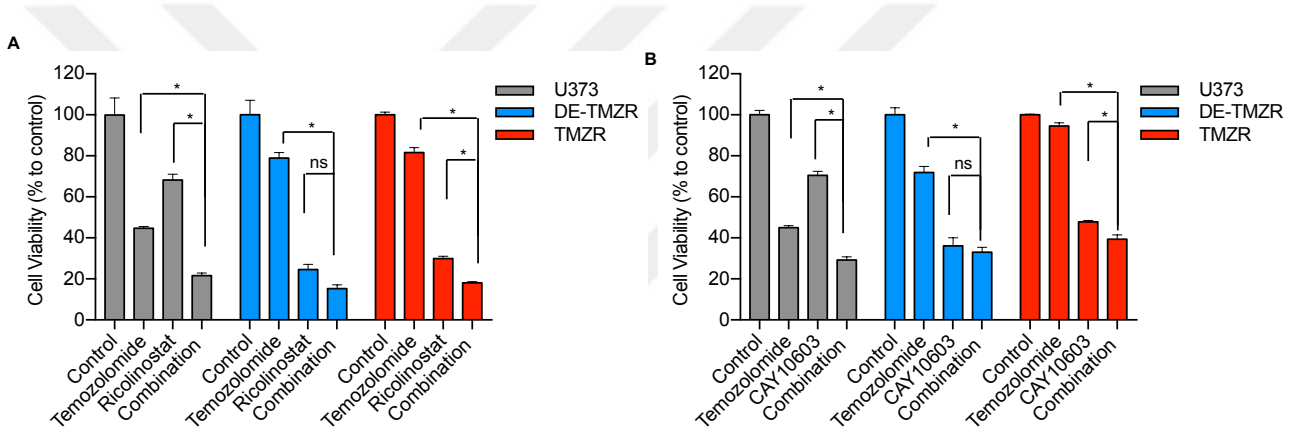

Figure 3.20 HDAC6i combined with TMZ. Cells were treated with Ricolinostat (10 μM) or CAY10603 (1.3 μM) combined with TMZ (50 μM for U373, 250 μM for DE-TMZR and TMZR) for 5 days. Cell viability was detected by CTG. * $p<0.05$, "ns" stands for non-significant. Two-way ANOVA, Tukey's multiple comparisons test. "% ± NSTDEV" and n=3 for each condition

3.2.3.3. HDAC6 Knockout cells by CRISPR/Cas9

To complement chemical approach, we established U373, DE-TMZR and TMZR HDAC6 knock-out cells by CRISPR/Cas9 method. The knockout efficiency was detected by Western Blot of HDAC6 and acetylated-alpha-tubulin, a known HDAC6 target (**Figure 3.21A**). We have chosen one HDAC6 gRNA for each cell line and tested the effect of TMZ response by CTG (**Figure 3.21B**). We have observed significantly increased response to TMZ at 125 μM, when HDAC6 was depleted.

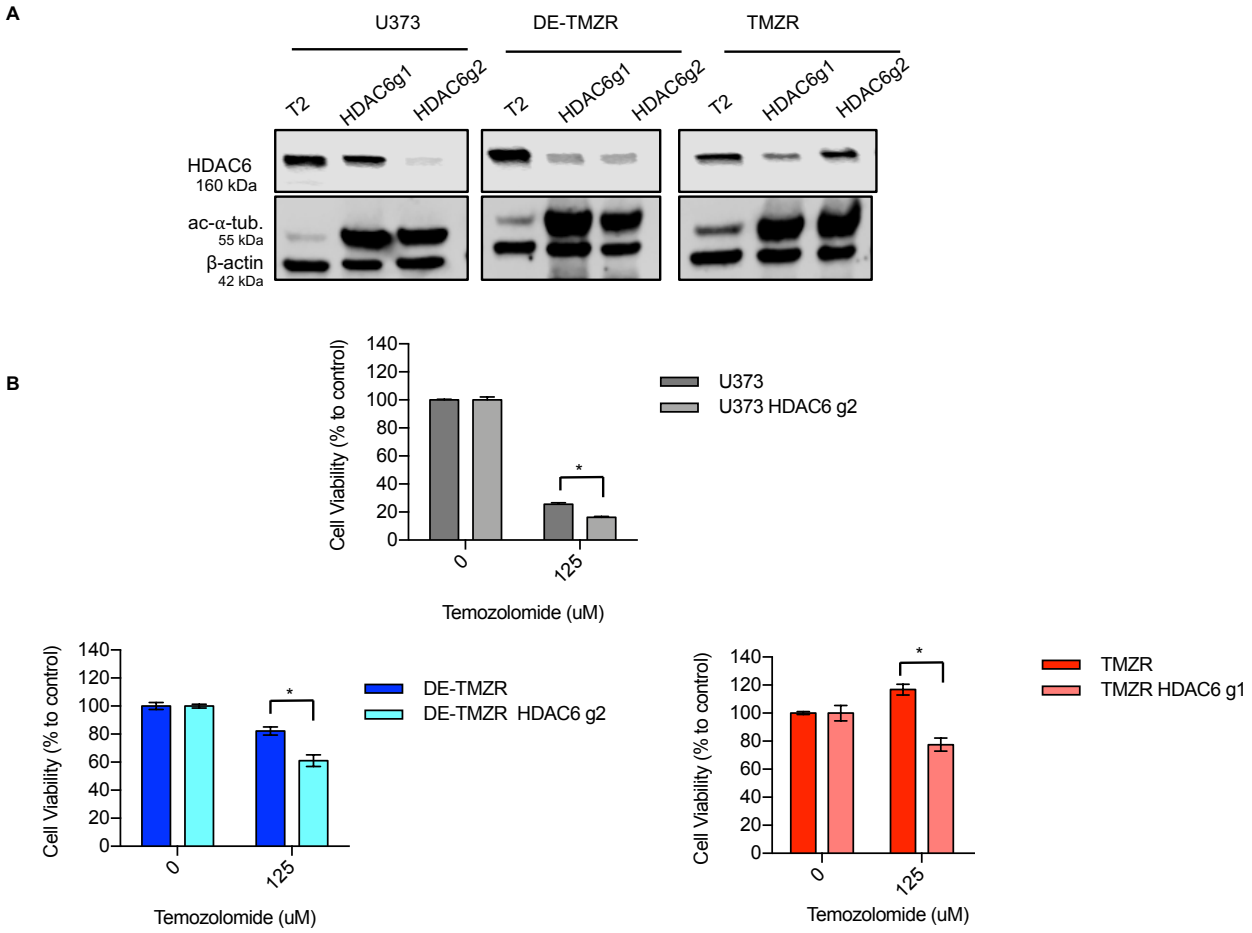

Figure 3.21. HDAC6 Knockout cells. A) Western Blot of HDAC6 and ac-α-tubulin to detect knockout levels. β-actin was used as a loading control. **B)** CTG assay of Temozolomide treated HDAC6 KO cells. * $p<0.05$, t-test "% ± NSTDEV" and n=3 for each condition.

To detect the effect of HDAC6 KO on cell growth, we performed a proliferation assay by seeding 500 cells in triplicates for each cell line to 6well plates and explored the proliferative capacities of cells for 14 days. When we normalized cells to day 0 seeding, we observed significant decrease in colony area for U373 and DE-TMZR cells, whereas we did not observe difference for TMZR (**Figure 3.22**).

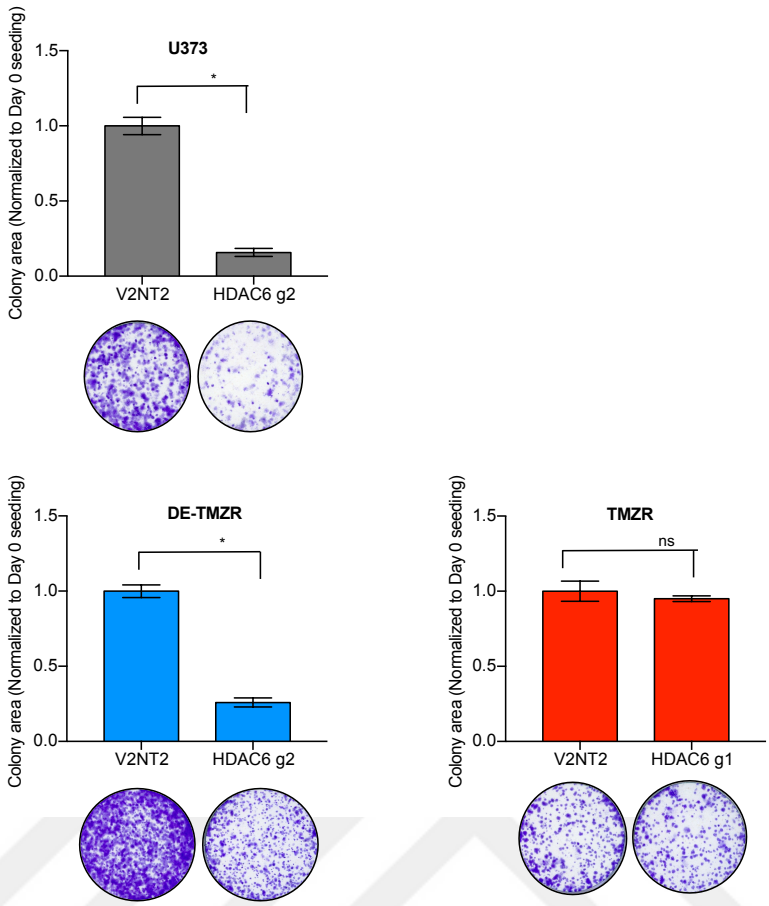

Figure 3.22. Proliferation assays of HDAC6 KO cells. 14 day proliferation by clonogenic assay. * $p<0.05$, t-test "% ± NSTDEV" and n=3 for each condition.

3.2.3.4. Histone alterations in HDAC6 inhibited cells

It is known that Ricolinostat can alter histone H3 acetylation levels, so we inspected acetylation levels after treatment for 36 hours (**Figure 3.23**). Since Ricolinostat is a histone deacetylase inhibitor, we observed increased acetylation levels of H3K9ac, H3K14ac, H3K18ac and H3K27ac upon treatment in all cells.

When endogenous histone acetylation levels were compared, we observed higher acetylation of some histone marks in our TMZ-resistant cells. DE-TMZR had significantly increased acetylation marks for H3K9ac, H3K14ac and H3K18ac. For H2K27ac, both DE-TMZR and TMZR had increased levels.

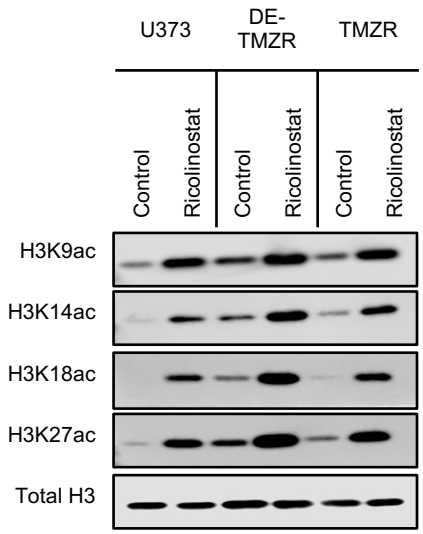

Figure 3.23. Acetylation marks of histone H3. Cells were treated with 10 μM Ricolinostat for 36 hours. Total H3 is used as a loading control.

3.2.3.5. Ricolinostat treatment induces apoptosis in TMZ-resistant cells

To investigate the mode of cell death upon Ricolinostat treatment, we investigated variety of apoptotic markers. PARP cleavage by caspases is an indicator of apoptosis, thus we detected the levels of cPARP protein by Western Blot. Cells were treated with TMZ and/or Ricolinostat for 36 hours (**Figure 3.24**). We observed significant cPARP levels in Ricolinostat treated DE-TMZR and TMZR cells, but not U373 cells. In addition, 250 μM TMZ treatment solely did not induce PARP cleavage, whereas combination with Ricolinostat produced cPARP in all 3 cell lines.

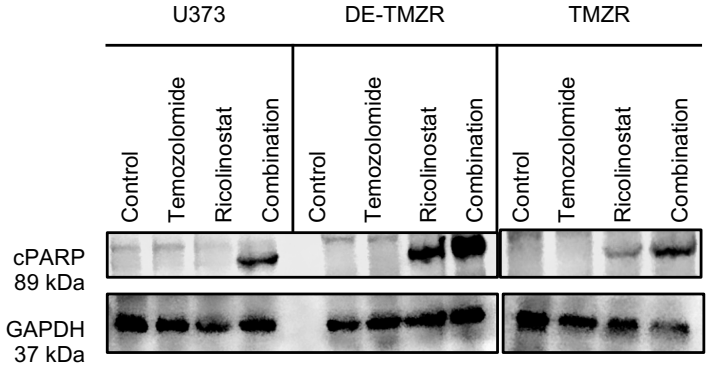

Figure 3.24. PARP cleavage upon TMZ and/or Ricolinostat treatment. Cells were treated with the respective drug for 36 hours. GAPDH was used as a loading control.

We also tested the executioner caspase activity via a luminescence-based assay, caspase glo 3/7. Cells were treated with the respective drug and after 40 hours, caspase-3/7 activities were detected by luminescence (**Figure 3.25**). Accordingly, we observed significant increase in only Ricolinostat treated or in combination treated cells, whereas TMZ alone did not induce caspase activity at 40-hour time point.

To investigate whether caspase inhibition would reverse cell death, we pre-treated our cells with general caspase inhibitor Z-VAD-FMK, and after a day co-treatment with Z-VAD-FMK and the respective drugs for 3 more days were performed. Significant recovery from cell death upon Ricolinostat treatment and the combination was observed (**Figure 3.26**). Hence, we concluded that, cell death upon Ricolinostat treatment relies on apoptosis. However, considering the levels of cell viability recovery, it is possible that apoptosis is not the solely responsible cell death mechanism upon Ricolinostat treatment.

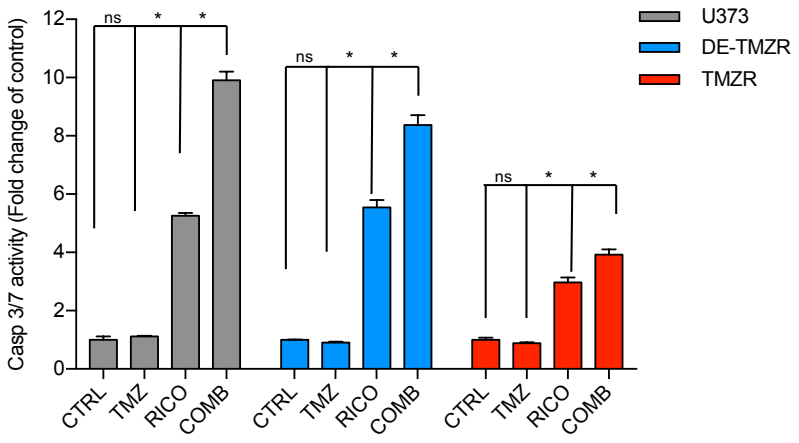

Figure 3.25. Caspase Glo 3/7 activity assay. 40 hours after treatment. n=3, * $p<0.05$, "ns" stands for non-significant. Two-Way ANOVA, Tukey's multiple comparisons test compared to control group.

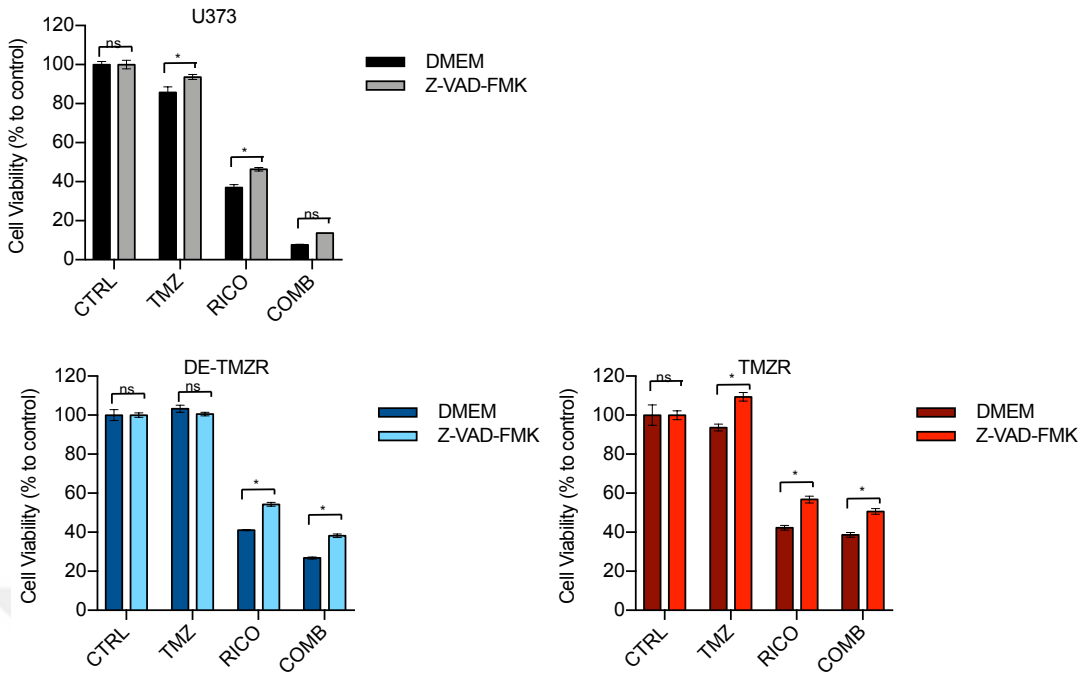

Figure 3.26. General caspase inhibitor recovers cell viability upon Ricolinostat treatment. n=3, * $p<0.05$, "ns" stands for non-significant, Two-Way ANOVA.

3.2.3.6. Transcriptome changes upon Ricolinostat treatment

To examine the mechanism of how our established TMZ-resistant cells are more vulnerable to Ricolinostat treatment, we conducted RNA sequencing (RNA-seq) to study the transcriptome changes. Cells were treated with Ricolinostat for 36 hours, the time point prior to the start of cell death. RNA-seq analysis was performed by Dr. Adam Cribbs in Oxford University, and further analyses were done with Genialis Tool [146]. Heatmap and PCA analysis among triplicates of our samples revealed consistency among replicates (**Figure 3.27**).

In all 3 cell lines more than 3500 genes were differently expressed upon Ricolinostat treatment (**Figure 3.28**). Considering the vast amount of changes upon treatment, we performed gene set enrichment analysis on "Control vs Ricolinostat" groups among REACTOME database. Top 10 altered gene sets are indicated in **Figure 3.29**. Ricolinostat treatment altered "Unwinding of DNA" and "G_1/S-Specific Transcription" pathways in all three cell lines. In addition, cell cycle related pathways were altered with Ricolinostat treatment.

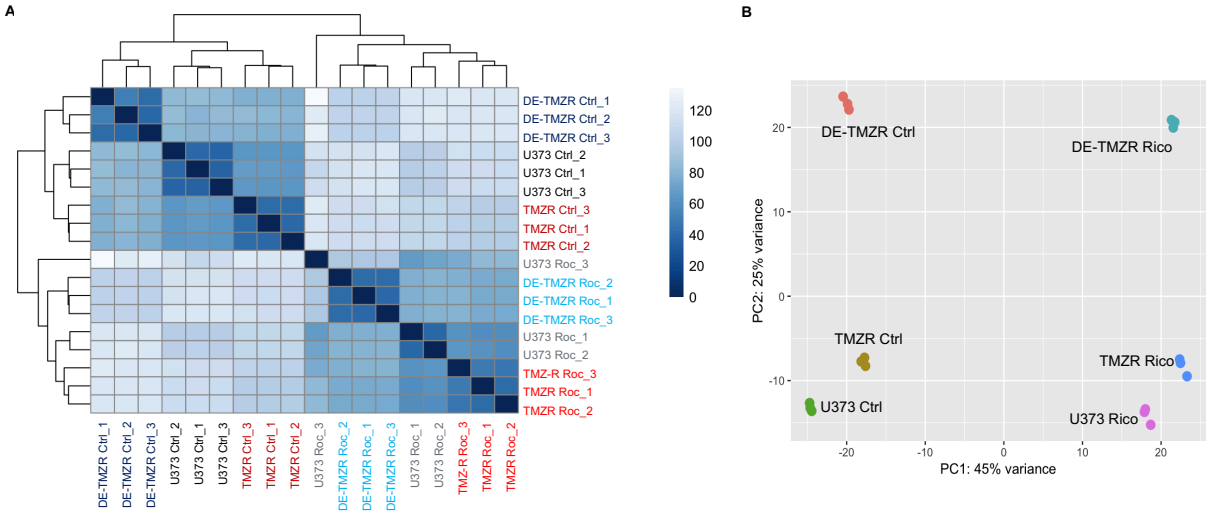

Figure 3.27 Heatmap and Principal Component Analysis for vehicle or Ricolinostat treated RNA-seq samples.

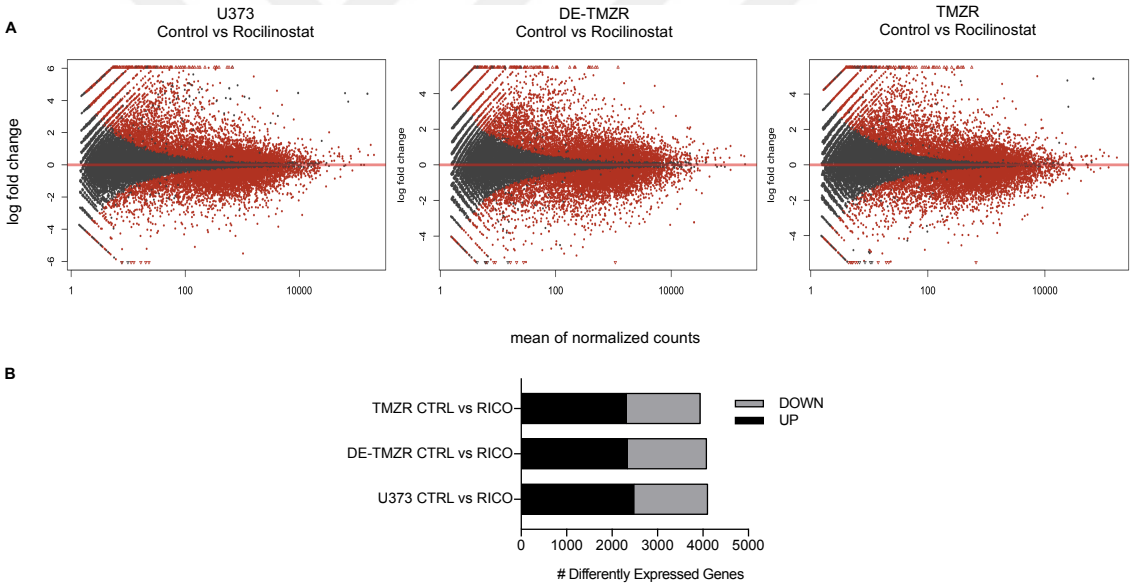

Figure 3.28. MA plots of Control vs Ricolinostat. A) MA plots indicating log2 fold changes attributable to a given variable over the mean of normalized counts for all the samples in the DESeq DataSet. Points was colored red if the adjusted p-value is less than 0.01. Points which fall out of the window are plotted as open triangles pointing either up or down. **B)** Bar graph of number of differently expressed genes.

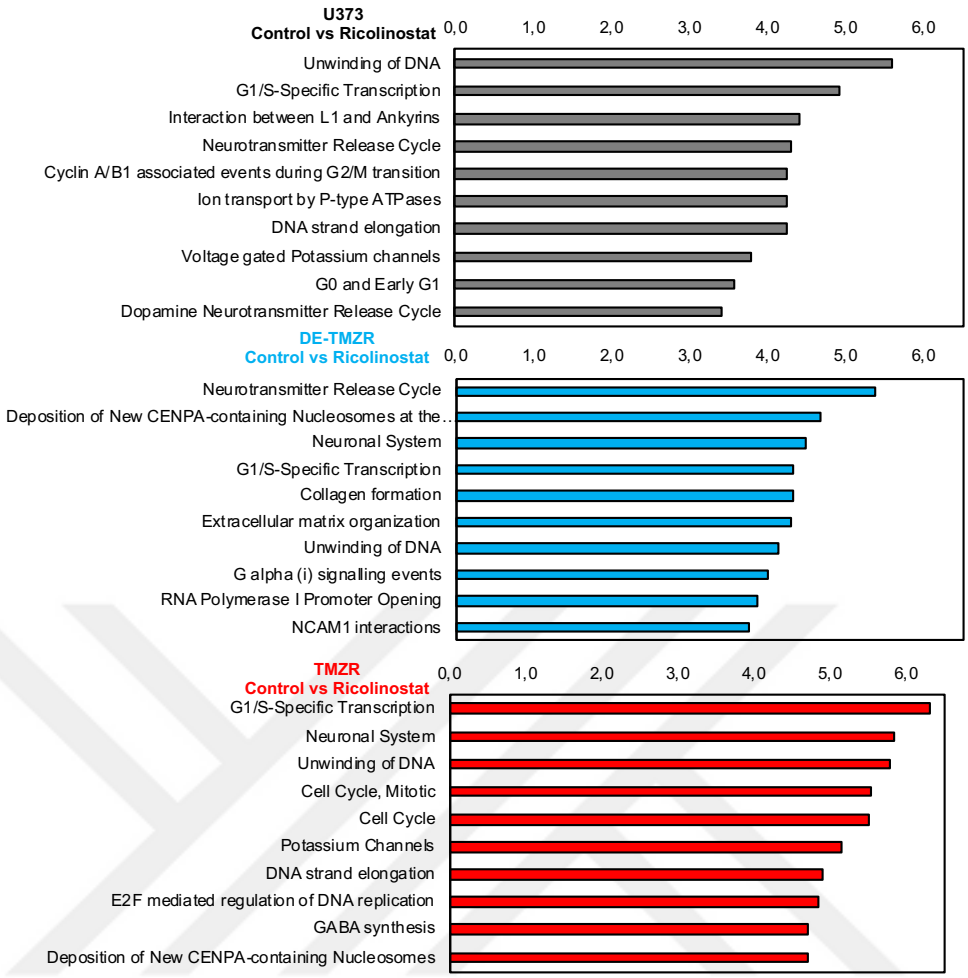

Figure 3.29. GSEA analysis among Ctrl vs Ricolinostat treated samples. Enrichment significance is shown as z-scores. GSEA performed among Reactome database by Genialis tool [146].

3.2.3.6.1. Cell cycle is altered with Ricolinostat treatment

We observed that upon Ricolinostat treatment, majority of the genes that are responsible for progression to S phase were downregulated. In **Figure 3.30**, a heatmap of genes of "G_1/S-Specific Transcription" Reactome dataset can be seen. The transition from G_1 phase of the cell cycle to S phase is vital for the control of cell proliferation, and its misregulation is commonly observed in cancer cells. "G_1/S-Specific Transcription" Reactome dataset includes genes that have role in G_1 to S transition such as *CCNA1 (Cyclin A1), CCNE1 (Cyclin E1), CDC25A, E2F1* and *CDK1*. Hence, we revealed that Ricolinostat treatment inhibits cell cycle related gene expression.

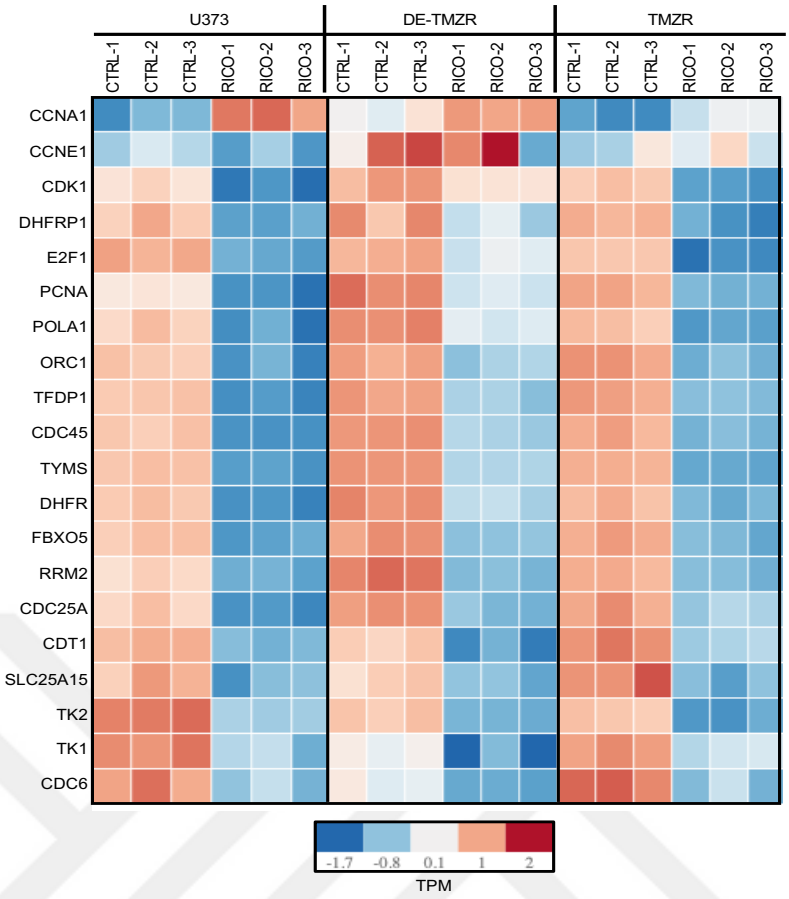

Figure 3.30 Heatmap of "G_1/S-Specific Transcription" Reactome dataset. Heatmap showing z-score of log2(x + 1) transformed gene expression of selected genes for samples.

Next, we studied the major cell cycle regulator genes in further detail (**Figure 3.31**). We observed that almost all of the genes were downregulated with Ricolinostat treatment, suggesting cell cycle inhibition that leads to apoptosis. In addition, we observed G_1/S and G_2/M transition blocker p21 (*CDKN1A*, Cyclin Dependent Kinase Inhibitor 1A) was highly upregulated upon Ricolinostat treatment. Validation of RNA-seq by qRT-PCR has shown that Ricolinostat treatment significantly increased p21 expression in all cells (**Figure 3.32**). In addition, we observed expression of p21 by Western blot on Ricolinostat treated samples (**Figure 3.33**).

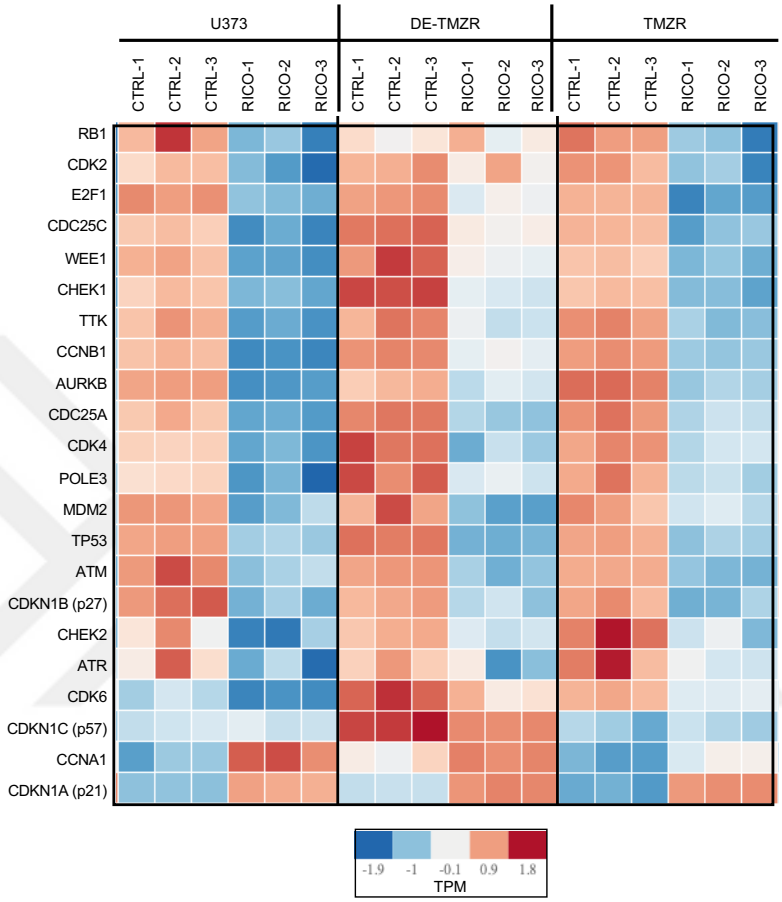

Figure 3.31 Major cell cycle regulators Showing row-wise scaled transformed expression using Z-score based on the z score of log2(x+1) values of selected genes for samples. Expression type prior to scaling is TPM. The color scale goes from -1.9 to 1.8.

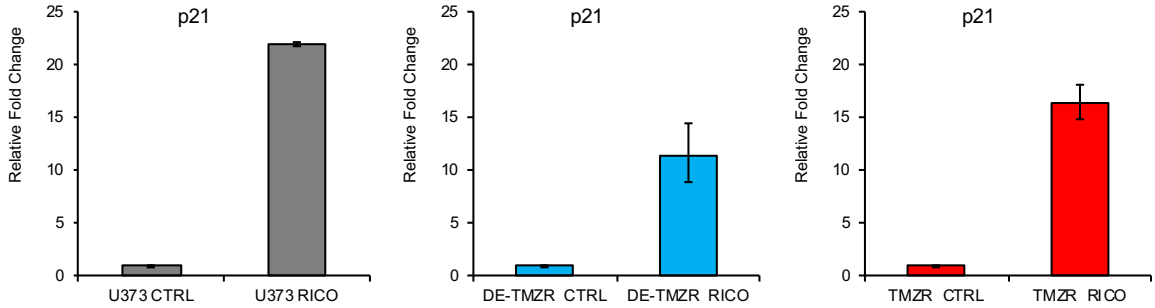

Figure 3.32 p21 gene expression levels of 36 hours Ricolinostat treated samples. qRT-PCR values were normalized to the level of housekeeping gene, GAPDH. Error bars represent "± "mean and samples are in triplicate.

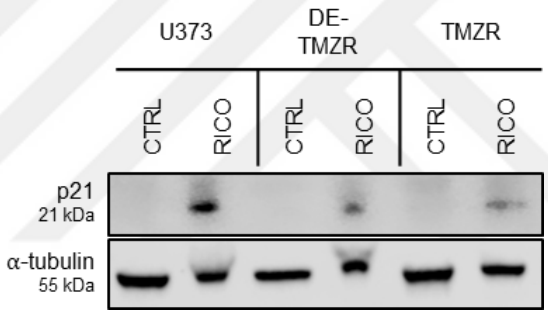

Figure 3.33 p21 Western Blot. Cells were treated for 16 hours. α-tubulin is used as a loading control.

Cell cycle alterations among cells upon Temozolomide or Ricolinostat treatment was studied by Propium Iodide assay, using flow cytometry. First, we examined the cell cycle differences among U373, DE-TMZR and TMZR over the course of 72 hours upon treatment with 250 μM TMZ. We observed decrease in G_0/G_1 cell cycle phase and increase in G_2/M phase in parental U373 cells (**Figure 3.34A**). We did not observe a significant shift in cell cycle phases upon TMZ treatment with DE-TMZR and TMZR cells (**Figure 3.34B, C**). Second, we treated cells with Ricolinostat. In 48 hours we observed a shift in G_0/G_1 phases in U373 and DE-TMZR cells, but not in TMZR. However, at 72 hours we observed similar fractions of apoptotic cells in all cells (**Figure 3.35**).

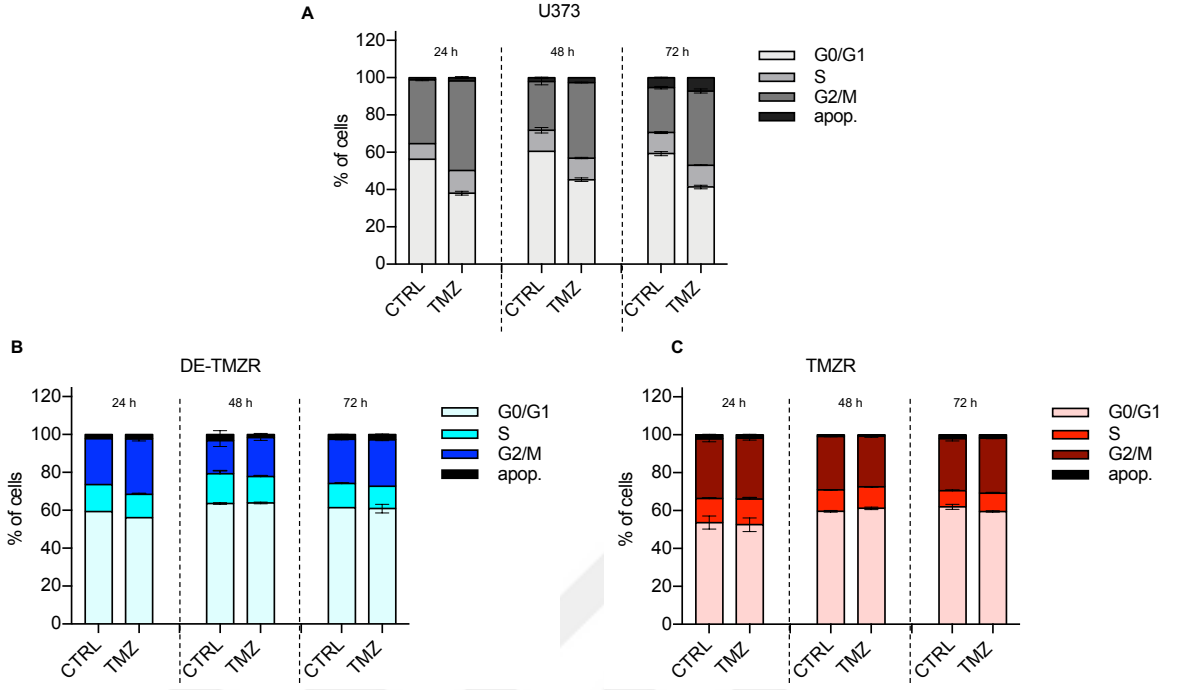

Figure 3.34. Cell cycle changes upon TMZ treatment. Cells were treated with 250 μM TMZ, collected at 24, 48 and 72 hours. Flow cytometry PI staining, samples are in duplicates.

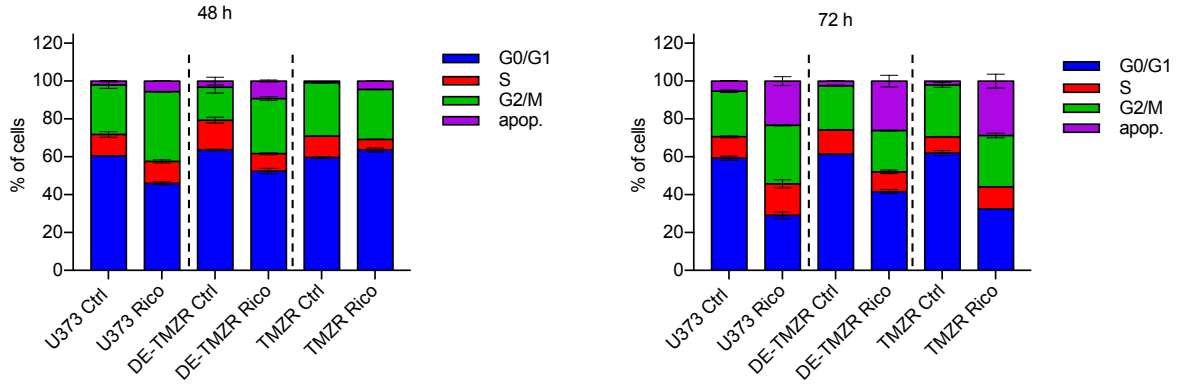

Figure 3.35. Cell cycle changes upon Ricolinostat treatment. Cells were treated with 10 μM Ricolinostat, collected at 48 and 72 hours. Flow cytometry PI staining. Samples were in duplicates.

3.2.3.6.2. DNA damage and repair related pathways are affected by Ricolinostat

As cell cycle regulation is tightly controlled by DNA repair pathways, we investigated the endogenous expression of DNA repair pathway components in TMZ resistant cell lines. We also examined their changes upon Ricolinostat treatment (**Figure 3.36)**. Similar patterns of decrease in DNA repair genes upon Ricolinostat treatment was observed throughout the samples. The Direct Repair gene MGMT, was highly upregulated in DE-TMZR and TMZR when compared to U373 (**Figure 3.10**). We noticed that MGMT was down regulated with Ricolinostat treatment. We validated this observation with qRT-PCR (**Figure 3.37**) and further explored the relationship between MGMT and HDAC6 inhibition.

We studied the effects of TMZ and/or Ricolinostat treatment on cells with varying MGMT expressions. In MGMT overexpressed U373 cell line, we observed increase in cell viability upon Ricolinostat and the combination. The opposite was observed when we treated MGMT Knockout cells; cell viability decreased in Ricolinostat and TMZ co-treated cells (**Figure 3.38**).

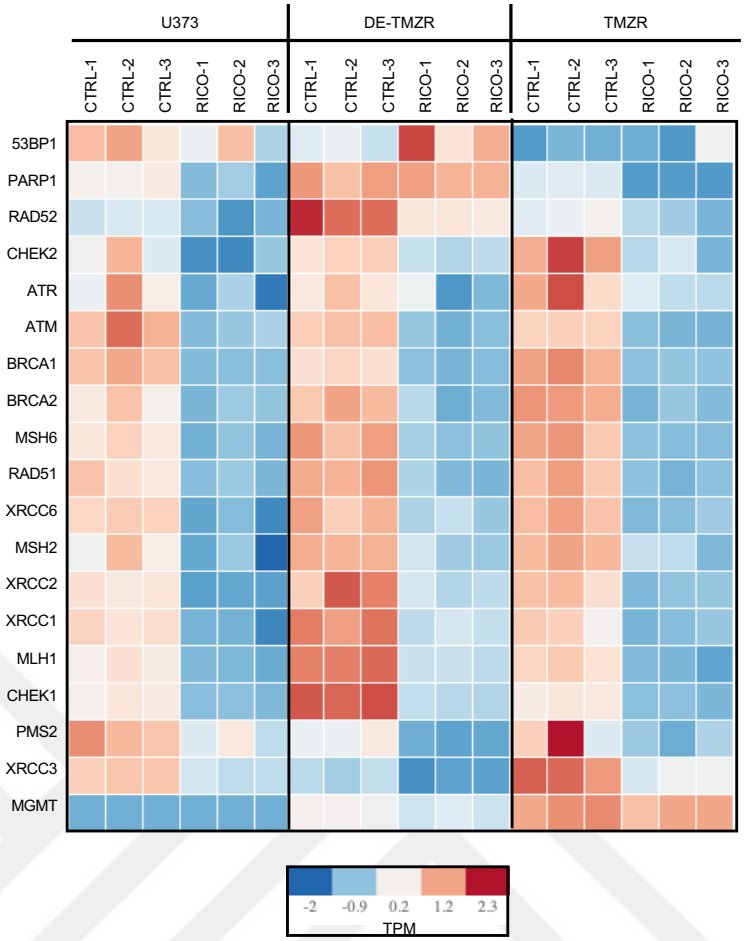

Figure 3.36. Heatmap of DNA Damage Repair Genes. Heatmap showing z-score of log2(x + 1) transformed gene expression of selected genes for samples.

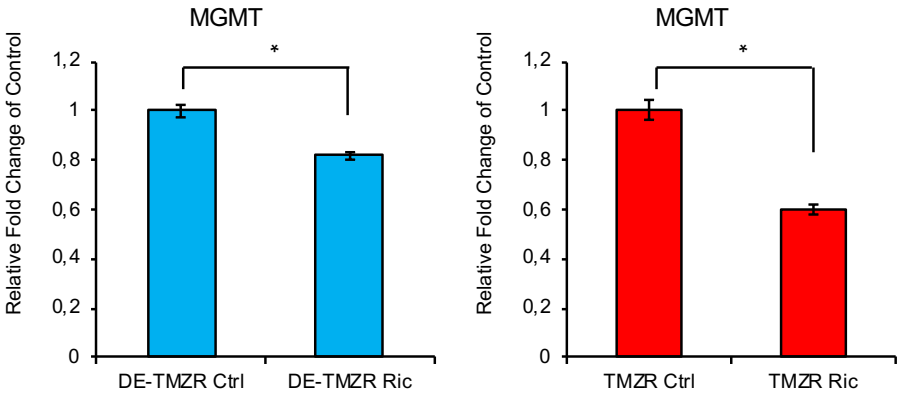

Figure 3.37. qRT-PCR results of MGMT gene expression levels of 36 hours Ricolinostat treated cells. *qRT-PCR is done by Duygu Uçku.*

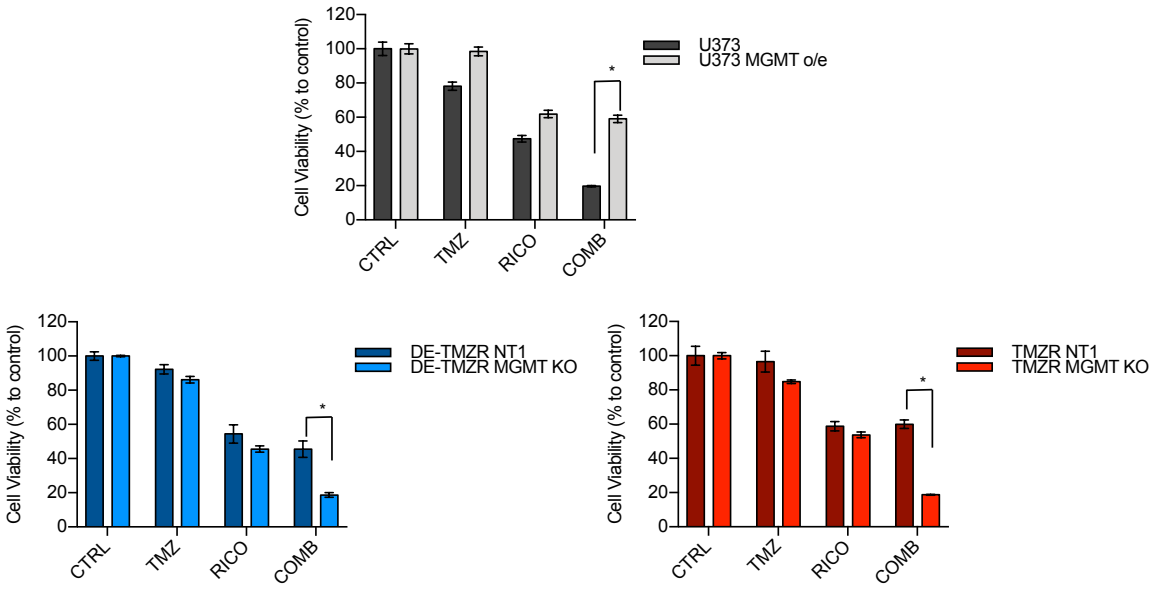

Figure 3.38. Additive effect of Ricolinostat on MGMT overexpression and knockout cells. Cells were treated for 5 days. * indicates $p < 0.05$, ANOVA

ATM and ATR are responsible for maintaining genomic stability in the face of constant exposure to DNA-damaging agents. They can activate a cascade of events that lead to various DNA repair mechanisms and effect cell cycle progression. We detected that ATM and ATR levels were downregulated with Ricolinostat treatment (**Figure 3.36**). We confirmed this finding by Western Blot (**Figure 3.39**). In addition, we observed that TMZR cells had upregulated levels of ATM and ATR compared to U373. Hence, we treated the cells with chemical inhibitors, KU55933 (ATMi) and AZD6738 (ATRi) (**Figure 3.40**). For both drugs, we observed a significant shift in cell viability of DE-TMZR and TMZR compared to U373. Lastly, we co-treated ATMi and ATRi with TMZ for 72 hours and observed an additive effect on U373 (**Figure 3.41**). Overall, our established resistant models were more vulnerable to ATM or ATR inhibition.

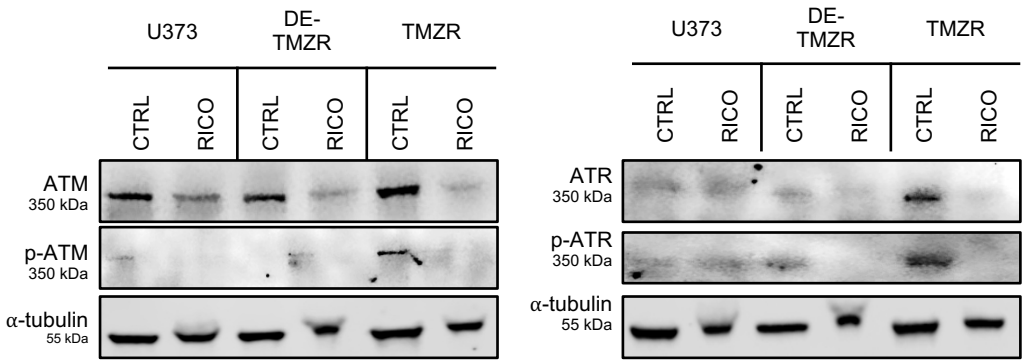

Figure 3.39 Western blot of ATM, p-ATM, ATR and p-ATR. Cells were treated for 36 hours. α-tubulin is used as a loading control.

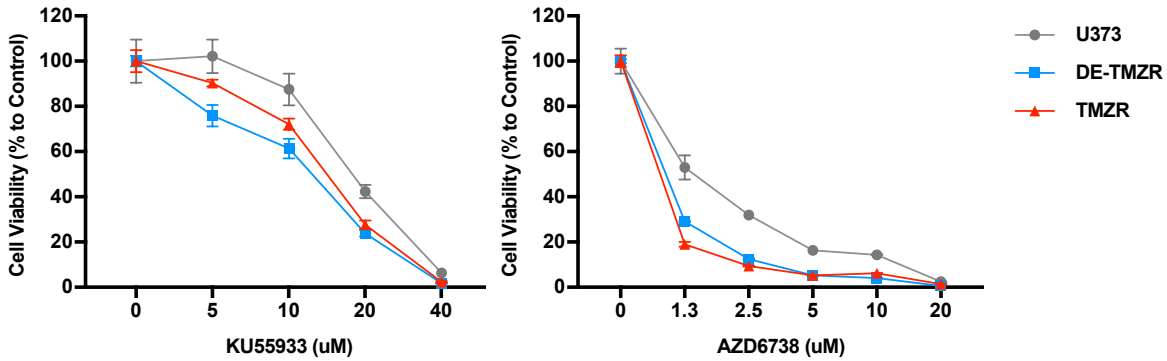

Figure 3.40 Cell viability of ATM or ATR inhibition. Cells were treated with the respective drug for 72 hours.

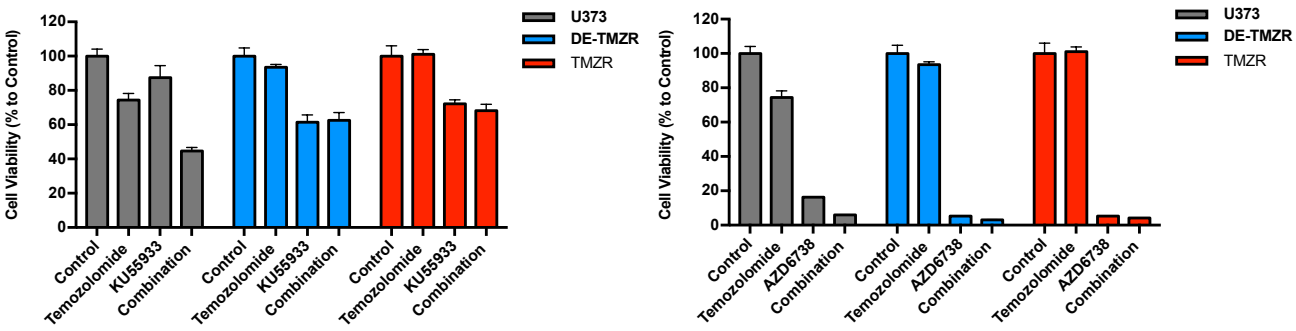

Figure 3.41 Cell viability of ATM or ATR inhibition combined with TMZ. Cells were treated with the respective drug for 72 hours. (KU55933 (10μM), AZD6738 (5μM), TMZ (250 μM))

3.2.4. Genome wide chromatin accessibility detection by ATAC-seq

3.2.4.1. Optimization for GBM cell lines

To investigate the chromosomal changes in our DE-TMZR and TMZR cell lines compared to U373 parental cell line, and how Ricolinostat treatment alters the resistant cell lines to be vulnerable to treatment, we performed ATAC-seq.

First, to optimize this delicate procedure, the DNA needed to be fragmented into 300-500 bp. Thus we optimized the composition of the lysis buffer and duration of the transposase reaction accordingly for U373 cells. In **Figure 3.42A** the DNA fragmentation peaks with the chosen lysis buffer is shown after transposition with Tn5 enzyme. In **Figure 3.42B** the DNA fragmentation analysis after PCR is shown.

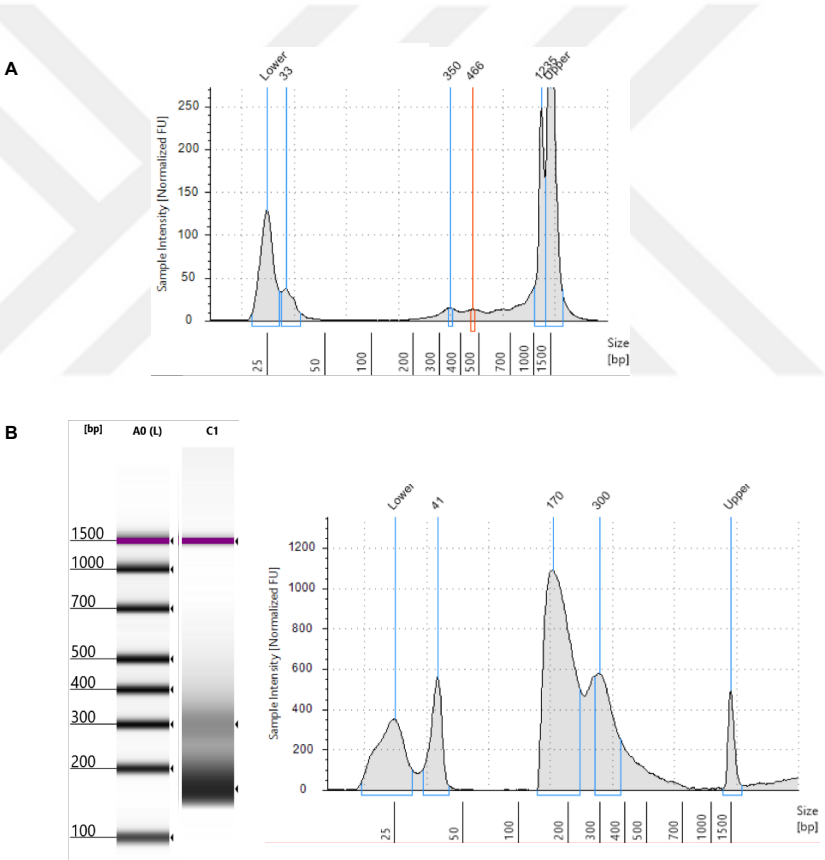

Figure 3.42. ATAC-seq A) Fragmentation optimization **B)** Peaks after PCR. TapeStation fragment analyzer

3.2.4.2. Chromatin accessibility among cell lines

For ATAC-seq we have treated U373, DE-TMZR and TMZR cells with DMSO or Ricolinostat for 36 hours. Samples were prepared for NGS as explained in materials & methods, NGS library preparation was performed with Dr. Martin Philpott in Oxford University. Bioinformatical analysis were done by Dr. Adam Cribbs (Oxford University).

The correlation between technical replicates were investigated via histogram (**Figure 3.43A**) and Principal Component Analysis (PCA) plot (**Figure 3.43B**). We observed great correlation between replicates of samples.

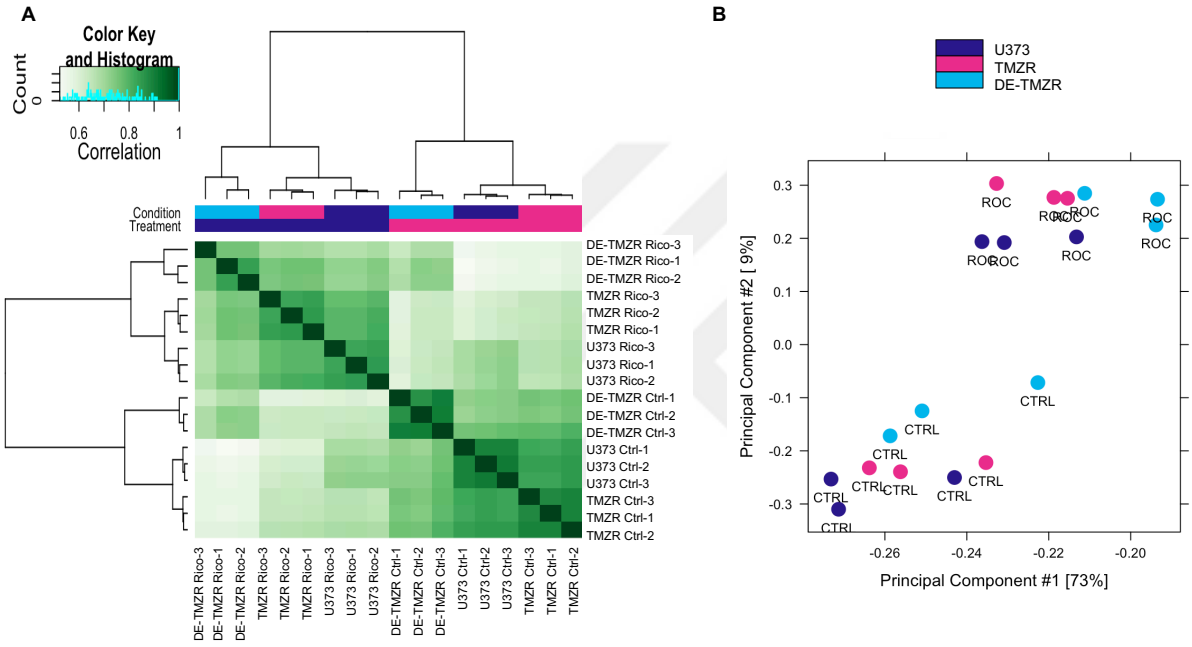

Figure 3.43. Correlation plots of ATAC-seq A) Heatmap among the samples that were analyzed by ATAC-seq **B)** PCA plot

Then, we investigated the chromatin accessibility changes among cell lines. DE-TMZR had 37,142 regions altered and TMZR had 17,975 regions altered compared to U373 (**Figure 3.44A, Figure 3.46A**).

In U373 vs DE-TMZR ATAC-seq comparison, we observed majority of the alterations were in distal intergenic regions (44%). Around 11% were promoter regions, and 3.1% composed of exons (**Figure 3.44B**). When we compared RNA-seq and ATAC-seq experiments, we found 246 genes overlapping (**Figure 3.44B**). When we checked the expression profiles of these genes in the RNA-seq dataset, we identified the top upregulated

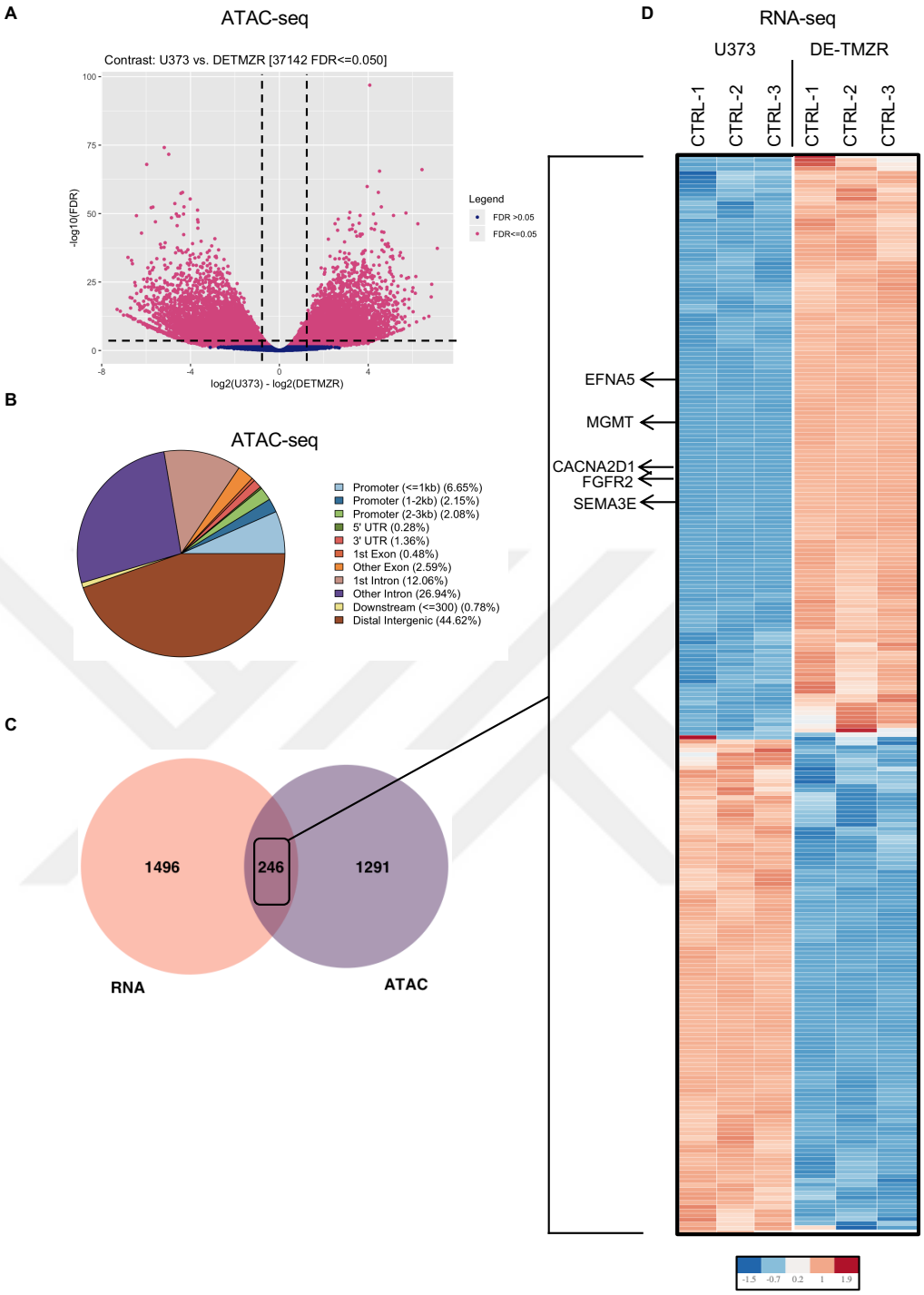

Figure 3.44 ATAC-seq results of U373 vs DE-TMZR. A) Volcano plot indicating the differential ATAC-seq peak analysis between among U373 vs DE-TMZR cells. **B)** Pie chart of distribution of annotated peaks of regions. **C)** Correlation analysis between RNA-seq and ATAC-seq. **D)** RNA-seq expression heatmap of common 246 genes.

genes among U373 vs DE-TMZR, namely, *EFNA5*, *MGMT*, *CACNA2D1*, *FGFR2* and *SEMA3E* (**Figure 3.7**, **Figure 3.44D**). We assessed MGMT gene regions of peak enrichment in U373 and DE-TMZR cells (**Figure 3.45A**) and observed peak enhancements near the exon2 and exon3 in DE-TMZR ATAC-seq samples. For RNA-seq, we detected expression only in DE-TMZR samples, but not U373. Next, we focused on the MGMT transcription start site region (TSS) of MGMT gene, which is located at chromosome 10: 131265454-131565783 (RefSeq, NM_002412) [165]. ATAC-seq data showed that DE-TMZR samples have enriched peaks compared to U373 around the TSS (**Figure 3.45B**).

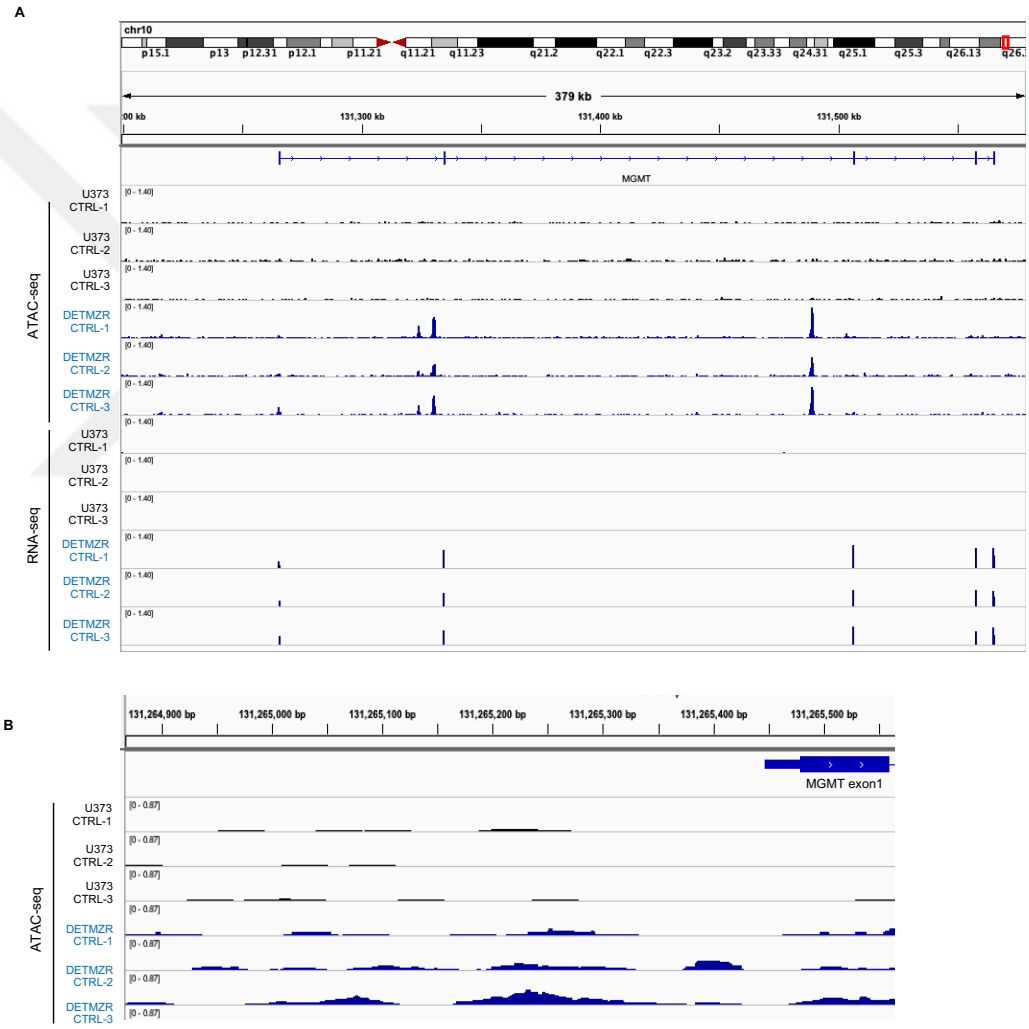

Figure 3.45. IGV plot of MGMT gene. Aligned to human hg19. **A)** ATAC-seq and RNA-seq samples B) Close up of ATAC-seq samples to TSS of MGMT.

For U373 vs TMZR cells ATAC-seq result, we observed majority of the alterations were in distal intergenic regions (46%). Around 10% were promoter regions, and 2.6% were in exons (**Figure 3.46B**). When we compared RNA-seq and ATAC-seq data, we found 77 genes overlapping (**Figure 3.46B**). When we examined their expression profiles in our RNA-seq experiment, we identified the top upregulated genes among U373 vs TMZR, namely, *EFNA5, CACNA2D1* and *FGFR2* (**Figure 3.7**, **Figure 3.46D**).

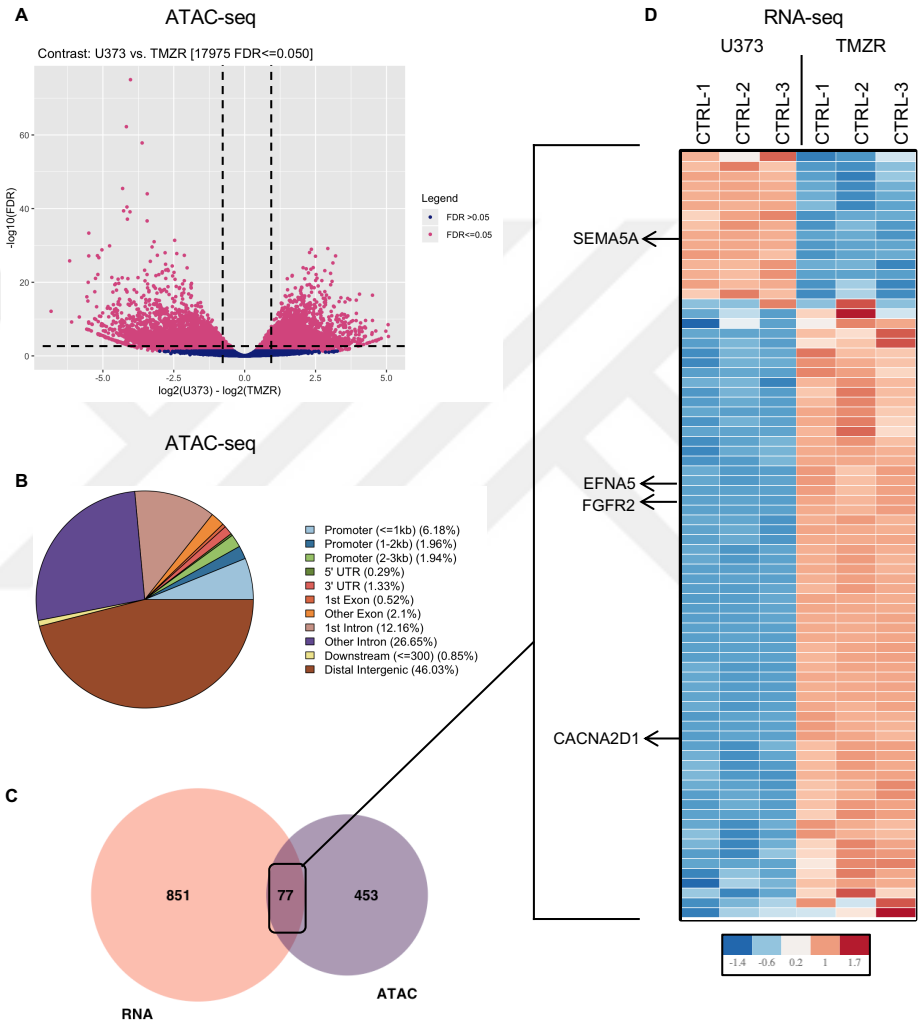

Figure 3.46 ATAC-seq results of U373 vs TMZR. A) Volcano plot indicating the differential ATAC-seq peak analysis between among U373 vs TMZR cells. **B)** Pie chart of distribution of annotated peaks of regions. **C)** Correlation analysis between RNA-seq and ATAC-seq. **D)** RNA-seq expression heatmap of common 77 genes.

Lastly, we focused on changes upon Ricolinostat treatment in our cell lines. Differential ATAC-seq peak analysis between Ctrl vs Rico treatment for all three cells revealed a massive amount of chromatin changes (**Figure 3.47A**). Thus, we focused on the genes that were also correlated in our RNA-seq experiment and performed gene set enrichment analysis among the common genes of U373, DE-TMZR and TMZR Ctrl vs Rico treated samples. GSEA among Reactome database revealed 6 genes (*BRIP1, FANCA, FANCD2, FEN1, TOPBP1* and *WEE1*) that had roles in Fanconi Anemia Pathway, G2/M DNA replication checkpoint and TP53 regulation of DNA Repair genes among others (**Figure 3.47B, Figure 3.47C**).

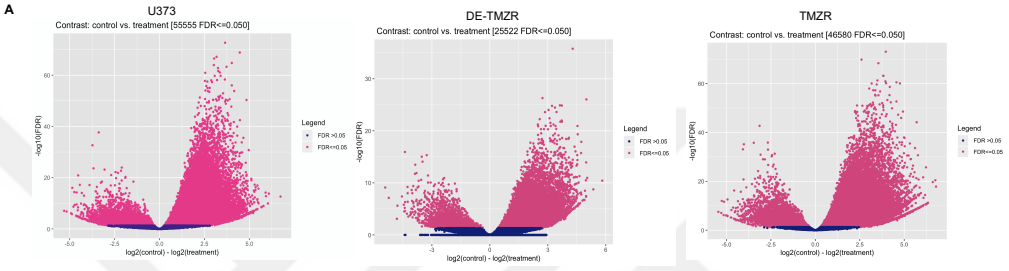

B

Name	P-value
Signal regulatory protein (SIRP) family interactions	0.002
Synthesis and interconversion of nucleotide di- and triphosphates	0.008
Metabolism of nucleotides	0.011
Oxidative Stress Induced Senescence	0.013
Fanconi Anemia Pathway	0.015
Cell surface interactions at the vascular wall	0.017
Transcriptional activation of mitochondrial biogenesis	0.019
Pre-NOTCH Transcription and Translation	0.020
FBXW7 Mutants and NOTCH1 in Cancer	0.026
G2/M DNA replication checkpoint	0.026
Loss of Function of FBXW7 in Cancer and NOTCH1 Signaling	0.026
Mitochondrial biogenesis	0.028
Pre-NOTCH Processing in the Endoplasmic Reticulum	0.032
Synthesis of 12-eicosatetraenoic acid derivatives	0.032
Synthesis of 15-eicosatetraenoic acid derivatives	0.032
Synthesis of 5-eicosatetraenoic acids	0.032
ECM proteoglycans	0.035
Regulation of gene expression in late stage pancreatic	0.037
Constitutive Signaling by NOTCH1 t(7;9)Translocation	0.037
Signaling by NOTCH1 t(7;9)Translocation Mutant	0.037
POLB-Dependent Long Patch Base Excision Repair	0.037
Pre-NOTCH Expression and Processing	0.037
Ligand-receptor interactions	0.042
Activation of PUMA and translocation to mitochondria	0.042
TP53 Regulates Transcription of DNA Repair Genes	0.042

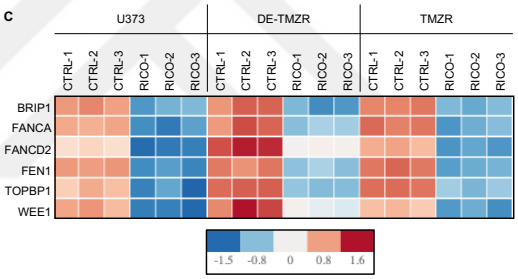

Figure 3.47 ATAC-seq results of Ricolinostat treated samples. A) Volcano plot indicating the differential ATAC-seq peak analysis between Ctrl vs Rico treatment for U373, DE-TMZR and TMZR cells. **B)** GSEA Reactome database among correlated genes of RNA-seq and ATAC-seq data, common of U373, DE-TMZR and TMZR. **C)** RNA-seq expression heatmap of selected Fanconi Anemia and G_2/M checkpoint pathways.

3.2.5. Testing the leads on established primary GBM cell lines

3.2.5.1. Establishing primary cell lines from GBM patient biopsies

Primary GBM cell line models were established from patient tumor biopsies in collaboration with Prof. İhsan Solaroğlu. Pathological analysis results of these tumors, as performed Koç University Hospital of four proliferating cell lines, KUGBM8, KUGBM12, KUGBM13 and Patient 22 are listed in **Table 3.3**. Serum based (labeled as -DMEM) and non-serum based (labeled as -EF) cell lines were established and their photos are indicated in **Figure 3.48**.

Table 3.3 List of GBM patient derived primary cell lines.

Pathology reports of patients after surgery. NA stands for not applicable.

Cell line name	Sex	Age	MGMT status	p53	IDH1	EGFR	PTEN	p16	VEGF
KUGBM8	M	41	methylated (80-100%)	positive (score 3)	negative	positive (score 3)	negative(score 32)	positive (score 4)	NA
KUGBM12	F	79	methylated (0-20%)	negative	negative	positive (score 1)	positive (score 3)	negative	positive (score 3)
KUGBM13	M	50	methylated (80-100%)	positive (score 1)	negative	positive (score 4)	negative(score 1)	positive (score 4)	positive (score 3)
Patient 22	M	78	methylated (80-100%)	positive (score 2)	negative	positive (score 4)	NA	negative	negative

KUGBM8 was derived from a 41-year-old male patient (**Figure 3.49**) with MGMT methylated promoter and EGFR amplification (**Table 3.3**). After cell line establishment, we tested KUGBM8 cells for their tumor forming capacities in SCID mice. Firefly Luciferase (Fluc) and mCherry expressing stable KUGBM8-DMEM and KUGBM8-EF cells were generated by viral transduction. Initially, mCherry expression was checked under the fluorescence microscopy and their Fluc activity was validated by utilizing *in vitro* luminescence assay (**Figure 3.50A**). Increasing number of Fluc-mCherry expressing cells (0-50.000/well) were seeded on 96-well black-bottom plate and treated with 1000 ug/ml D-Luciferin. Bioluminescence measurements were taken (**Figure 3.50B)**.

For tumor implantation, 4 mice for each condition were used and 120.000 cells per mouse were injected in 7 μl PBS stereotactically into the brain by Ahmet Cingöz. After injection, tumor cells were visualized with IVIS Lumina III equipment. Accordingly, Fluc activity of tumors was measured by injecting mice with 150 ug/g body weight of D-Luciferin intraperitoneally. We observed that KUGBM-EF-FMC cells have higher capacities

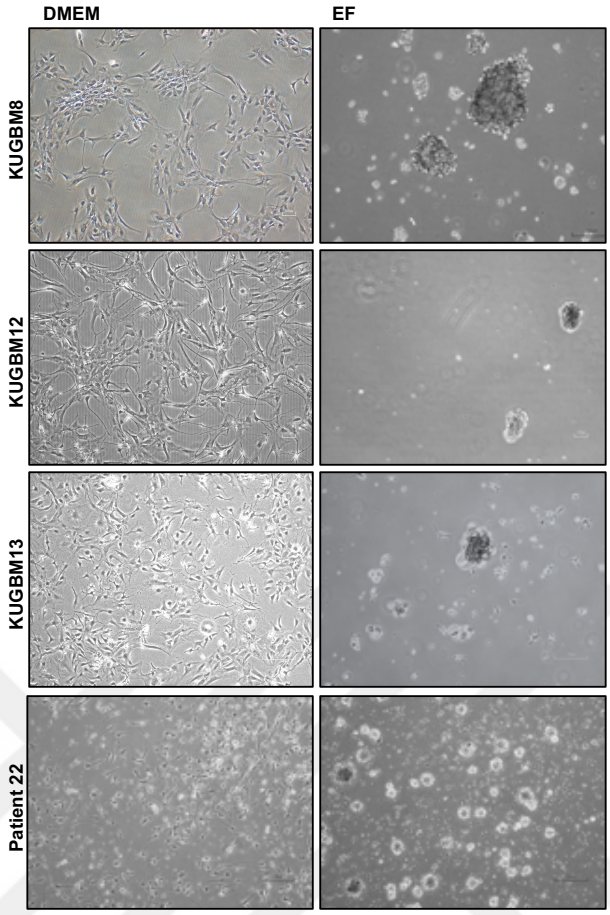

Figure 3.48. Representative photos of established cell lines.

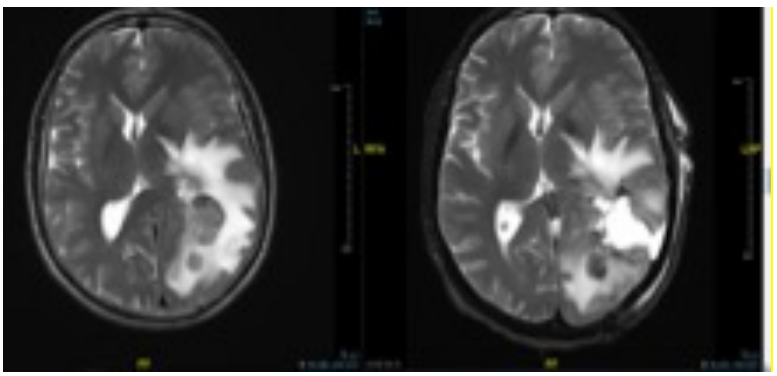

Figure 3.49 MRI of KUGBM8 patient prior to surgery. *Image courtesy of Dr. İhsan Solaroğlu*

of tumor formation in mice. As we were successful in establishing our own primary GBM cell line, we have continued our experiments with KUGBM8-EF cell line for validation of our findings in a clinically relevant model (**Figure 3.50C**).

When we treated KUGBM8-EF cell line with Temozolomide, we observed that its response to TMZ is similar with U373. 250 μM of TMZ reduced cell viability up to 20-30% (**Figure 3.51A**). In addition, we sought to study the dynamics of TMZ response of KUGBM8-EF *in vivo*. We treated mice with 2 mg/ml of TMZ [166] for 5 days. We observed significant shrinkage attenuation of tumor growth in TMZ treated mice compared to DMSO treated control group (**Figure 3.51C**).

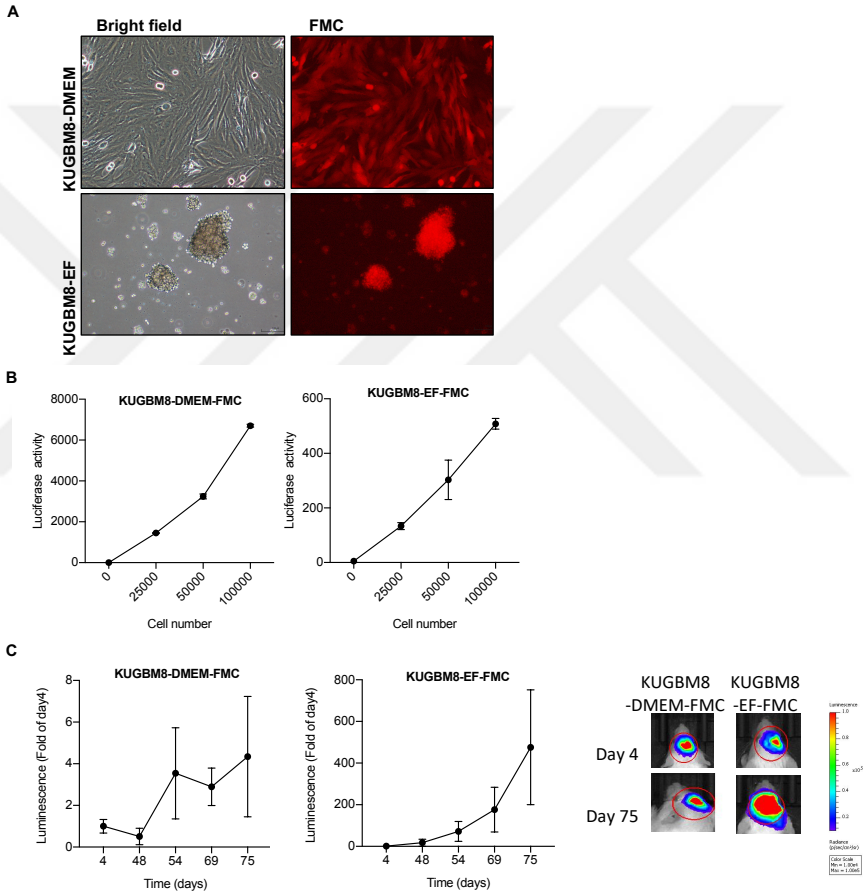

Figure 3.50 *In vivo* growth capacities of KUGBM8-DMEM and KUGBM8-EF cells. A) Photos taken in bright field and fluorescence B) Luciferase activity assay. C) Luminescence growth rate of KUGBM8-DMEM and KUGBM8-EF injected mice and their representative images. 4 mice for each condition were used and 120.000 cells per mouse were injected stereotactically into the brain. *Mice experiments were performed in collaboration with Ahmet Cingöz.*

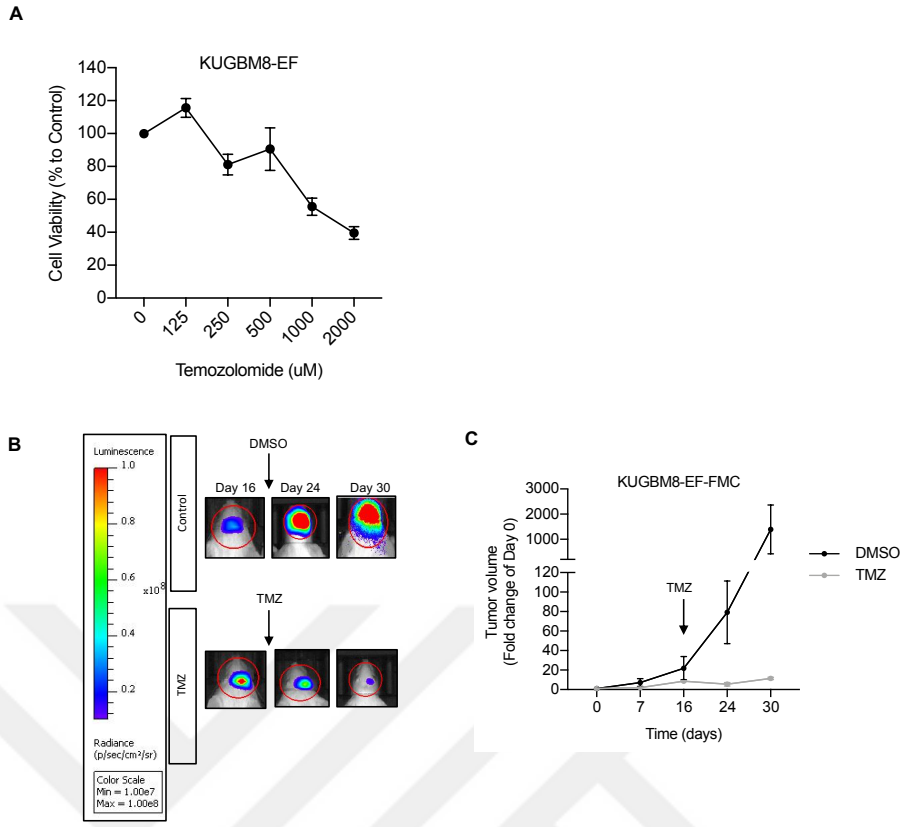

Figure 3.51 ***In vivo*** **TMZ experiments. A)** TMZ response of KUGBM8-EF cells *in vitro*. Cells were treated for 5 days. **B)** Representative images of luminescence of TMZ response of KUGBM8-EF-FMC cells *in vivo*. **C)** Tumor volume graphs of DMSO vs TMZ treated KUGBM8-EF-FMC injected mice. *Mice experiments were performed in collaboration with Ahmet Cingöz.*

3.2.5.2. Generation of KUGBM8-EF TMZ resistant cell line

Since U373 cannot grow in mice brain, we obtained a more sustainable *in vivo* model by generating TMZ resistant sublines from KUGBM8-EF cell line. Cells were treated with 250 μM TMZ for 10 days with drug renewal each day. Cells were passaged every 5th day. Remaining population was left to proliferate for 15 days. TMZ response was detected by CTG, after TMZ treatment for 5 days (**Figure 3.52A**). We observed significant increase in cell viability when compared to control group. We also studied the proliferative capacities of KUGBM8-EF TMZ-resistant cells by CTG and observed that Resistant cell lines tend to grow slower than control group (**Figure 3.52B**). In addition, we looked at the endogenous

levels of MGMT in KUGBM8-EF TMZ resistant lines and observed MGMT expression is elevated (**Figure 3.52C**).

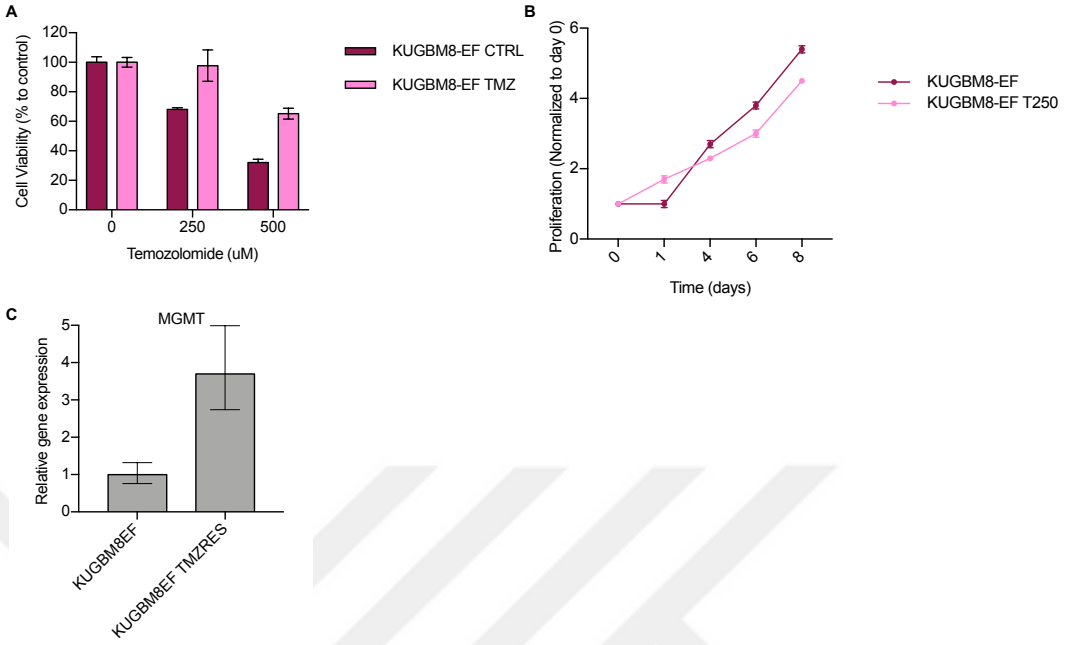

Figure 3.52 TMZ resistant cell line from KUGBM8-EF was established. A) TMZ response after 5 days of treatment was detected by CTG. **B)** Proliferative capacities of KUGBM8-EF and KUGBM8-EF T250 cell lines were studied by CTG

3.2.5.3. The role of HDAC6 inhibition on KUGBM8-EF cell line

One of the main aims of this thesis was to be able to translate findings to primary GBM models to mimic clinical response. For this reason, we studied the role of HDAC6 in KUGBM8-EF cell line. First, we treated the cells with Ricolinostat and TMZ and observed a similar result of enhanced combinatorial effect of Ricolinostat and TMZ (**Figure 3.53**).

Additionally, we knocked out HDAC6 via two different guide RNAs. For HDAC6-g1 we observed knockdown, whereas HDAC6 g2 significantly knocked out HDAC6 expression in KUGBM8-EF (**Figure 3.54A**). Afterwards we studied the proliferation rates of these knockdown/knockout cells and observed a significant decrease in HDAC6 knockdown (HDAC6 g1) cells (**Figure 3.54B**). Lastly, when we treated these cells with TMZ, significant sensitization towards TMZ response was observed in both sublines (**Figure 3.54C**).

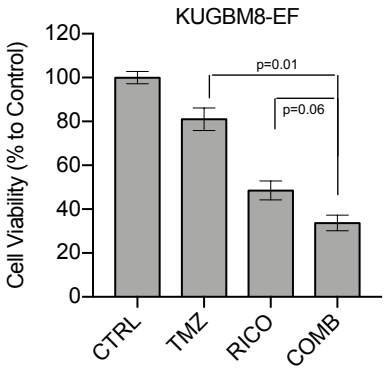

Figure 3.53 KUGBM8-EF cells were treated with 10 μM Ricolinostat and 250 μM TMZ for 5 days.

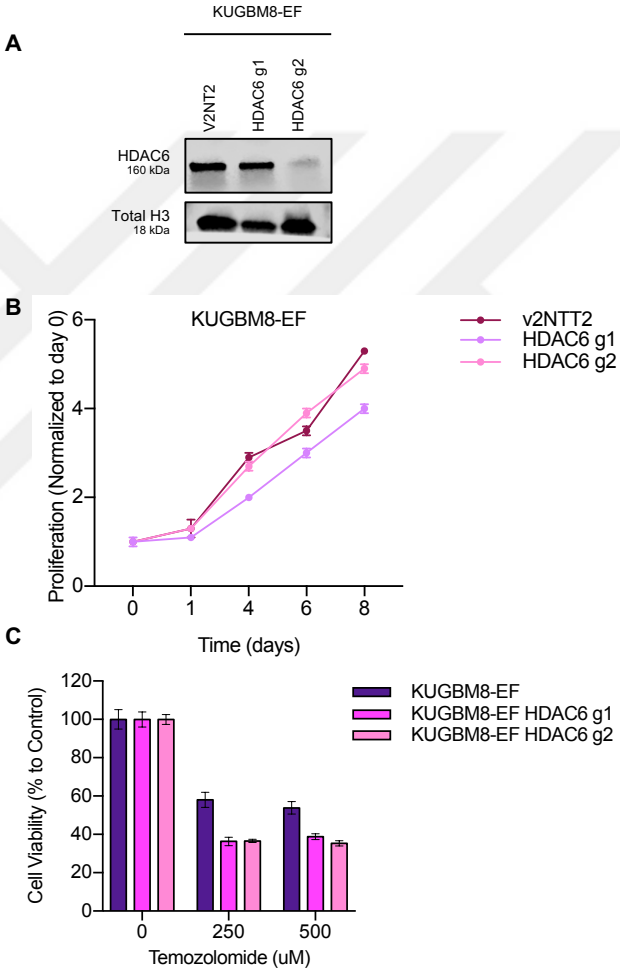

Figure 3.54 HDAC6 silenced KUGBM8-EF cell lines. A) Western blot of HDAC6 and loading control total H3. **B)** Proliferation rates determined by CTG assay. **C)** TMZ responses of 5 day treated cells.

4. DISCUSSION

Glioblastoma multiforme (GBM) is a malignant brain tumor, with median survival of around 16 months [153]. Standard of care for GBM has remained unchanged in the last 20 years, and it consists of surgery, irradiation and chemotherapy with Temozolomide (TMZ) [37,153]. GBM is a heterogenous tumor with extremely infiltrative capacities to the surrounding tissue, therefore surgery is inadequate to remove tumors entirely. In addition, blood brain barrier is a major obstacle, blocking efficient delivery of therapeutic agents to the tumor site. Therefore, recurrence is frequent among primary GBM patients (more than 90%), and therapy resistance is commonly observed in the recurrent tumors.

In this thesis, acquired Temozolomide resistance in GBM was investigated by establishment and characterization of TMZ-resistant cell line models. In addition, epigenetic vulnerabilities of these resistant cell lines were thoroughly examined.

Establishment and characterization of TMZ resistant models

In 1961, Dr. Frei and Dr. Freireich initiated a high-dose drug combination clinical trial for the treatment of pediatric leukemia [167]. This harsh regimen was unseen before; however, children began to respond to the treatment, and 11 out of 16 were detected as leukemia free. Unfortunately, this success story was short-lived; almost all patients relapsed, forming cancers that were not responsive to the previous treatment regimen. Dr. Frei commented on this failure: *"The children died one after the other-felled by virtue of the adaptation designed to protect them…it was a consequence of the body's defense system subverting cancer treatment*" [168]. After 60 years, recurrence of cancers with a more malignant and therapy resistant state is still the leading cause of cancer-related deaths.

Advancements in molecular biology and genetics resulted in success stories for some cancer types. Targeting selective mutations are possible for some types of leukemias, Hodgkin's lymphomas, testicular cancers, etc. For example, targeting the oncogenic fusion protein Bcr-Abl with Imatinib on patients with Philadelphia chromosome-positive chronic myeloid leukemia, was a major triumph against cancer [169]. Unfortunately, most malignant cancers such as GBMs are highly heterogeneous and pursuing targeted therapy for these patients is very complicated.

Resistance to treatment in cancer can be innate or acquired. Acquired drug resistance can develop during treatment of tumor cells that were initially sensitive. This is an adaptive response with accumulation of new mutations and epigenetic alterations that develop over time. Considering the heterogeneity of tumors, the resistance in the recurrent tumors is likely due to a combination of both innate resistance and acquired adaptation. Therefore, studying the mechanisms of resistance is crucial to have a better design of novel therapeutic approaches. To this end, establishing *in vitro* and *in vivo* models of resistance that mimic the clinical settings are extremely beneficial. In the literature, drug resistant cell lines are generally established by two main approaches. In the first one, tumor cells are subjected to escalating doses of therapeutic agents slowly and over a long period of time, allowing them to accumulate adaptive changes. In the second method, tumor cells are subjected a high dose of the therapeutic agent to give a competitive advantage to innately resistant cells, which are then clonally expanded. To model and study two modes of resistance in this thesis, we established two different TMZ-resistant models, derived from U373 GBM cell line. While investigating the TMZ resistance, both models were used throughout the study. Their characterizations of proliferative capacities and transcriptomic changes were studied extensively. In addition, epigenetic vulnerabilities of the TMZ-resistant models were examined in detail.

TMZ-resistant cells do not exhibit typical multi drug resistance characteristics

Many factors can add up to form drug resistant populations in cancers: Increased rates of drug efflux mechanisms [170], metabolic alterations, and mutations accumulated in signaling mechanisms that take part in senescence and cell death, epigenetic changes, etc. Cancer stem cells (CSCs); a subset of cells can give rise to a new tumor, are also considered to take part in therapy resistance.

Multidrug resistance (MDR) is defined as the resistance to one chemotherapeutic drug accompanied by resistance to other chemotherapeutic drugs that may have different structures and mechanism of action [66]. MDR is common in many cancers, including GBM. So, we have investigated whether DE-TMZR and TMZR have cross resistance to other alkylating agents Cisplatin, Carboplatin, Cyclophosphamide and Lomustine. Except for Lomustine, we did not observe cross resistance when compared to U373 cell line. Since

mechanism of action of Lomustine also includes the formation of O6-MeG, we were not surprised for this outcome. Drug efflux mechanisms, a reason for MDR, include ATP-binding cassette (ABC) transporter family[171]. When we examined their levels, we did not observe any significant difference among ABC transporters between U373, DE-TMZR and TMZR in our RNA-seq analysis. In addition, we did not observe any TMZ sensitization when we treated cells with Verapamil [172],a drug that can reverse multi drug resistance by blocking p-glycoproteins (data not shown). Thus, our resistance models are unlikely to be dependent on multidrug resistance.

Many drug resistance phenotypes are dependent on constant drug treatment, however recurrence with drug-resistant subpopulations occur when patients are not going through therapy. Thus, to investigate the stable changes responsible for TMZ resistance, TMZ-resistant cell lines with more than 2 months drug holidays were generated in our experiments. We have performed an RNA-seq experiment among the parental cell line (U373), drug induced TMZ-resistant cells (DE-TMZR^{T} & TMZR^{T}) and drug holiday stable TMZ-resistant cells (DE-TMZR & TMZR). Looking at the common significantly upregulated and downregulated genes among all groups, we observed 47 common altered genes.

The receptor tyrosine kinase FGFR2 was among the top 5 upregulated genes among TMZ-resistant cell lines and this upregulation was preserved in drug holiday sublines. It has been known that FGFR pathway has an important role in gliomagenesis. Recently, Furnari group has shown that ionizing irradiation induces PTEN phosphorylation by FGFR2 in GBM cells. This phosphorylated PTEN binds to the chromatin and recruits RAD51, a member of DSB repair pathway, to promote repair [88]. We treated our cells with general FGFR inhibitor AZD4547, and selective FGFR2 inhibitor Alofanib. FGFR2 inhibition did not cause cell death, whereas pan-FGFRi AZD4547 has shown to decrease cell viability. In addition, we did not observe any combinatorial effects of Temozolomide and FGFR inhibition. So, we might speculate that even though FGFR2 is highly upregulated in our TMZ resistant models, its inhibition is not sufficient to resensitize resistant cells.

DNA damage and repair signaling alterations in TMZ-resistant cells

With limited chemotherapeutic agents considered for GBM treatment, TMZ leads the frontline for the last 15 years. Alkylating agents such as TMZ induce damages in DNA by

methylation of purine bases. When damage is induced in DNA, the response is to repair the damage if possible, or undergo cell death if repair is not achievable. TMZ induced DNA methylation can be repaired by BER, MMR and DR enzyme MGMT [173]. GBM cells regularly override mechanisms regarding these repair pathways to resist induced DNA damage, and they proliferate uncontrollably. Thus, enhanced DNA damage repair is one of the major reasons of drug resistance.

In our work, we showed that U373 cells did not normally express MGMT [148], yet it was highly expressed in DE-TMZR and TMZR with RNA sequencing We verified this marked finding with additional qRT-PCR and Western Blots. In addition, when we silenced MGMT in DE-TMZR and TMZR with CRISPR/Cas9 system, we were able to recover TMZ sensitivity. We also performed the opposite; overexpression of MGMT in U373 parental cell line conferred resistance to TMZ. Therefore, we demonstrated that both of our established TMZ resistant models were MGMT-dependent. Considering the majority of GBM recurrent patients have elevated MGMT expression with TMZ resistance [81,158], we can conclude that our models are in parallel with clinic, and they can be beneficial for further understanding of the epigenetic regulations among TMZ-resistant cells.

A study performed by Zhang *et al*. in 2010, also utilized U373 cells for TMZ resistant cell line generation. They used dose escalation method for 6 months to establish their resistant model and observed MGMT induction. However, their model required selective pressure of TMZ to obtain and maintain MGMT levels [173]. This finding is partly in line with ours, however we observed that MGMT was still upregulated in TMZ-resistant lines even after 6 months of drug holiday.

A very recent paper by Chen *et al*. defined a novel enhancer located between the promoters of marker of proliferation Ki67 (MKI67) and MGMT genes (named as K-M enhancer) that was highly activated in TMZ-resistant patient-derived xenograft (PDX) lines and recurrent tumor samples. When this enhancer was deleted, a significant reduction of MGMT expression caused increased TMZ sensitivity [79]. In our work, we also examined the defined region of K-M enhancer in our U373, DE-TMZR and TMZR cells among our ATAC-seq results. Accordingly, we did not observe a significant chromatin alteration in this region. Hence, our MGMT upregulation in the resistant cell lines might be independent of this novel enhancer and involve other regulatory elements that remain elusive.

Previous studies linked mutational inactivation of MSH2 or MSH6 in the MMR pathway to tolerance of cytotoxic O6-MeG lesions, resulting in TMZ resistance in GBM patients [45,173]. For DE-TMZR and TMZR cells, we observed slight upregulation of key MMR genes MSH2, MSH6, MLH1 compared to U373. Thus, silenced MMR components observed in clinic in TMZ-resistant GBM does not seem to be occurring in our case.

In literature, it was also observed that when the BER enzyme PARP1 was silenced, the toxicity of TMZ was elevated [82,83,149]. In our analysis, PARP1 was upregulated in DE-TMZR, whereas downregulated in TMZR when compared to U373. On the other hand, PARPBP (PARP1 Binding Protein) was upregulated in both samples. When we treated cells with PARP inhibitors Rucaparib and Olaparib, we observed significant sensitization to TMZ. Therefore, PARP activity is a likely regulator of TMZ-resistance in our models.

When O6-MeG lesions persist, DSBs can be induced by TMZ due to replication fork collapse mediated by MMR induced single strand gaps formed at O6-MeG and Thymidine mispairs [174]. The repair of DSBs occur through homologous recombination (HR) or non-homologous end-joining (NHEJ). MRE11, a component of the Mre11/Rad50/Nbs1 (MRN complex) has a role in DNA damage detection and signaling. Mirzoeva *et al*. in 2006 have published that TMZ induced O6-MeG lesions, acted upon by the MMR, drive formation of the MRN complex. The MRN complex in turn contributes to the control of G_2 arrest and cytotoxicity. They have detected MRE11 deficient cells have less sensitivity to TMZ [175]. On the contrary, in 2010, Eich and colleagues reported that NBS1, another component of the MRN DSB signaling complex, mutants are more sensitive to TMZ than the wild-type cells [176]. Since MRN signaling is shared between NHEJ and HR pathways, these contradictory results may be upon the downstream effects of MRN complex. In our work, we detected that both of these genes were upregulated in DE-TMZR cells, whereas NBS1 was upregulated only in TMZR cells. Considering that our drug holiday cell lines were in TMZ-free culture for more than 3 months at the time of RNAseq experiments, accumulated O6-MeG lesions might have caused these cells to have their DNA damage signaling complexes constantly activated. Yet, both DE-TMZR and TMZR overrode DSBs repair pathways to endure their damaged DNA.

In summary, our established TMZ- resistant models, DE-TMZR and TMZR were highly dependent on Direct Reversal enzyme MGMT activity. In addition, key elements of

BER and DSB repair pathways were upregulated in these cell lines to preserve survival against TMZ induced damage.

Cell cycle alterations in TMZ-resistant cells

Cell cycle arrest is the expected outcome upon TMZ treatment, but our established TMZ-resistant cells bypassed this phenotype and they could be expanded in the culture. So, we sought to investigate the proliferative capacities and the cell cycle states of the established cell lines. First, proliferation curves of U373, DE-TMZR and TMZR cells were detected by luminescence-based assay. We observed that TMZR cells tended to proliferate more than U373, whereas DE-TMZR cells proliferated less. This finding was also consistent with the long term (10-15 days) clonogenic assay results. We also investigated cell cycle phases upon TMZ exposure with PI staining. As expected, with TMZ-sensitive U373 cells, majority of the cell population were halted at G_2/M phase after 24 hours of TMZ treatment and apoptotic cells were observed around 72 hours. Nevertheless, there was no significant difference in the cell cycle phases of DE-TMZR and TMZR upon TMZ treatment. When we investigated the 132 genes (KEGG Cell cycle) that have roles in cell cycle regulation by Gene set enrichment analysis. Among U373 vs DE-TMZR and U373 vs TMZR cells, we observed many cell cycle-related genes upregulated in TMZ-resistant cell lines, especially DE-TMZR. Proliferating cell nuclear antigen (PCNA) is a key factor in DNA replication and cell cycle regulation, and it was markedly upregulated in both TMZ-resistant cell lines. Thus, DE-TMZR and TMZR have modified their machinery of cell cycle, partly contributing to their resistance to TMZ.

HDAC6 inhibition can induce cell death in TMZ-resistant cell lines

To determine the epigenetic factors regulating TMZ response in our models, we performed an unbiased epigenetic probe screen on U373, T98G, DE-TMZR and TMZR cells.

Top hits of all the screens revealed histone deacetylase inhibitors (HDACi) as a major regulator of TMZ response. HDACs have a variety of roles in the cell, they deacetylate histone lysine residues and non-histone proteins, such as hormone receptors, transcription factors, DNA repair enzymes, inflammation mediators, chaperone proteins and cytoskeleton proteins [100,101]. HDAC inhibitors (Vorinostat, Panobinostat, Belinostat, etc) have been

approved for clinical use by the FDA for many cancer types including GBM [109,110]. It is known that with HDACi treatment, diverse pathways can be triggered in tumor cells, resulting in cell cycle arrest, senescence, differentiation, autophagy and apoptosis.

Vorinostat (SAHA) was found to induce G_2 cell cycle arrest in glioma cells while upregulating p21 (CDKN1A) levels, with enhanced expression of antiproliferative genes p21WAF1, p27KIP1, DR5 and TNFα *in vitro* [117]. In our screen, we observed that Vorinostat as a single agent can reduce cell viability in U373 and T98 cells. However, the reduction in the viability of DE-TMZR and TMZR cells were significantly more with the same dose of Vorinostat or other HDACis. Similarly, DE-TMZR and TMZR were more affected by TMZ and Vorinostat combination compared to U373. Since our TMZ-resistant cells can bypass G_2 cell cycle arrest upon TMZ exposure, we thought that Vorinostat could overcome this bypass of G_2 cell cycle arrest.

Pan-HDAC inhibition induced unwanted cytotoxicity in clinical trials [163], hence we pursued more selective HDAC inhibitors. Ricolinostat (Rocilinostat, ACY-1215) was the first selective HDAC6 inhibitor, found to have antineoplastic activities. We observed that as a single agent, it reduced cell viability to 60-70% in U373 and T98G, whereas to 30-35% in DE-TMZR and TMZR cells. With further studies, we observed a selective vulnerability for Ricolinostat treatment in our established TMZ-resistant models. When we look at the endogenous expression of acetylation levels of H3 via western blot, we observed that DE-TMZR and TMZR expressed H3K9ac, H3K14ac and H3K18ac marks higher than U373, suggesting a hyperacetylated chromatin state at the resistant cells. Also, in all samples, Ricolinostat was found to have additive effect on cell death when combined with Temozolomide.

HDAC6 is a member of class II HDAC, and works in both the nucleus and the cytoplasm, controlling epigenetic and non-epigenetic mechanisms. Known targets of HDAC6 include cortactin, Hsp90 and α-tubulin [122]. Additionally, recent studies have shown links of HDAC6 with EGFR, MAPK, AKT and p53 signaling pathways [107,177–180]. Ricolinostat binds to HDAC6 and disturbs the Hsp90 protein chaperone system through hyperacetylation of Hsp90, thus aggresomal protein degradation is blocked. This primes to accumulation of unfolded and misfolded ubiquitinated proteins and inhibit cell growth and induce apoptosis [181,182]. For GBM cells, Li and colleagues investigated TMZ induced ER-stress tolerance

(ERST) in a panel of cell lines including A172, U373, U87MG and U251. They observed that ERST occurs in TMZ-resistant glioma cells, and HDAC6 inhibition can overcome ERST via HSP70 and HSP90 [128]. There are a few studies linking HDAC6 inhibition in GBM cells to decreased growth, through SMAD2 phosphorylation inhibition and expression of p21 [124]. In addition, HDAC6 overexpression increases proliferation in GBM. When HDAC6 was knockdown or inhibited by HDAC6i, TMZ sensitization is observed via decrease of EGFR protein levels and impaired activation of the EGFR pathway [125]. However, these studies are at preclinical level at the moment and detailed research including *in vivo* experiments are required. In our models, dissecting the nuclear and nonnuclear mechanisms of HDAC6 inhibition in relation to TMZ response will be very important.

We investigated the effects of HDAC6 inhibition, by chemicals (Ricolinostat and another selective HDAC6i CAY10603) and knockout experiments via CRISPR/Cas9 system. We observed that HDAC6 knockout cells grew slower than their controls. In addition, when we combined Ricolinostat with TMZ, we observed additive effect on cell viability. The mode of cell death involved apoptosis, as we demonstrated with PARP cleavage and Caspase-3/7 activation. We showed that Ricolinostat induced cell death required caspases, however considering the recovery rates with caspase inhibitors, it is possible that other cell death mechanisms are also involved.

The results from RNA-seq experiments performed on all three cell lines with and without Ricolinostat treatment revealed marked alterations in cell cycle and DNA repair networks. Similar to Li *et al*. [124], we observed decrease in *EGFR* genes with Ricolinostat treatment among our samples. In concordance with the literature, we observed cell cycle genes were altered in Ricolinostat treated cells, in favor of cell cycle arrest. p21 gene was highly upregulated when cells were treated with Ricolinostat. It is known that binding of p21 to PCNA can inhibit DNA replication [183]. In this line, PCNA was highly upregulated in our TMZ-resistant models and was downregulated with Ricolinostat treatment. Cell cycle phases shifted towards G_2/M and G_0/G_1 in DE-TMZ and TMZR cells, respectively, upon treatment. Furthermore, our correlation studies of ATAC-seq and RNA-seq among Ricolinostat treated samples revealed "G_2/M DNA replication checkpoint" genes altered in our samples. *WEE1* (G_2 Checkpoint Kinase), which acts as a negative regulator of G_2 to M transition by blocking activated cyclin B1-CDK1, was among the altered genes. Inhibition of WEE1 was correlated

with sensitization to DNA damaging agents in p53 inactive GBM cells. With WEE1 inhibition, p53 inactive cells cannot rebalance CDK activities and ultimately and undergo apoptosis [184,185]. TMZR endogenously expressed more WEE1 compared to U373. With Ricolinostat treatment, *WEE1* expression was downregulated in all samples. Hence inhibition of WEE1 might have a role in TMZ sensitization in our models.

DNA damage pathways were collectively downregulated in Ricolinostat treated celld. Hence, we studied the effect of Ricolinostat on MGMT gene levels and observed that MGMT was significantly decreased upon Ricolinostat treatment. To further investigate the relationship between MGMT and HDAC6 and their response to TMZ, we treated MGMT overexpressed U373 and MGMT knockout DE-TMZR, TMZR cells with Ricolinostat and TMZ. We observed that, the effect of Ricolinostat is lessened in MGMT overexpressing cells. In MGMT knockdown, Ricolinostat has shown enhanced cell death in combination to TMZ. To our knowledge, direct relationship between MGMT and HDAC6 has not been studied so far and ours is the first study to put this relation forward.

Another important gene that was altered was *FANCD2,* a member of the Fanconi anemia complementation group (FANC). *FANCD2* was highly upregulated in DE-TMZR and TMZR cell lines and was downregulated with Ricolinostat treatment based on the RNA-seq and ATAC-seq results. ATM in response to DNA damage calls out MRN complex, resulting in its localization of FANCD2 to nuclear foci with BRCA1 and BRCA2, starting DNA repair [186]. Collis group in 2014 published the inhibition of FANCD2 resulted in sensitization to TMZ and Carmustine [187]. Thus, FANCD2 inhibition with Ricolinostat might have a role in resensitization to Temozolomide and/or inhibiting DNA repair to induce cell death.

In sum, our TMZ-resistant GBM cell line models have enhanced MGMT expression and altered DNA repair capacities. In addition, these cell models fail to undergo G_2/M cell cycle arrest upon TMZ treatment. With Ricolinostat treatment, DNA repair pathways decrease, and cell cycle arrest is induced. We suggest that upregulation of p21 has a role in this cell cycle blockage, which needs to be followed up with comprehensive studies. Thus, with HDAC6 inhibition, cell cycle progress and DNA repair are inhibited, leading to apoptosis (**Figure 4.1**).

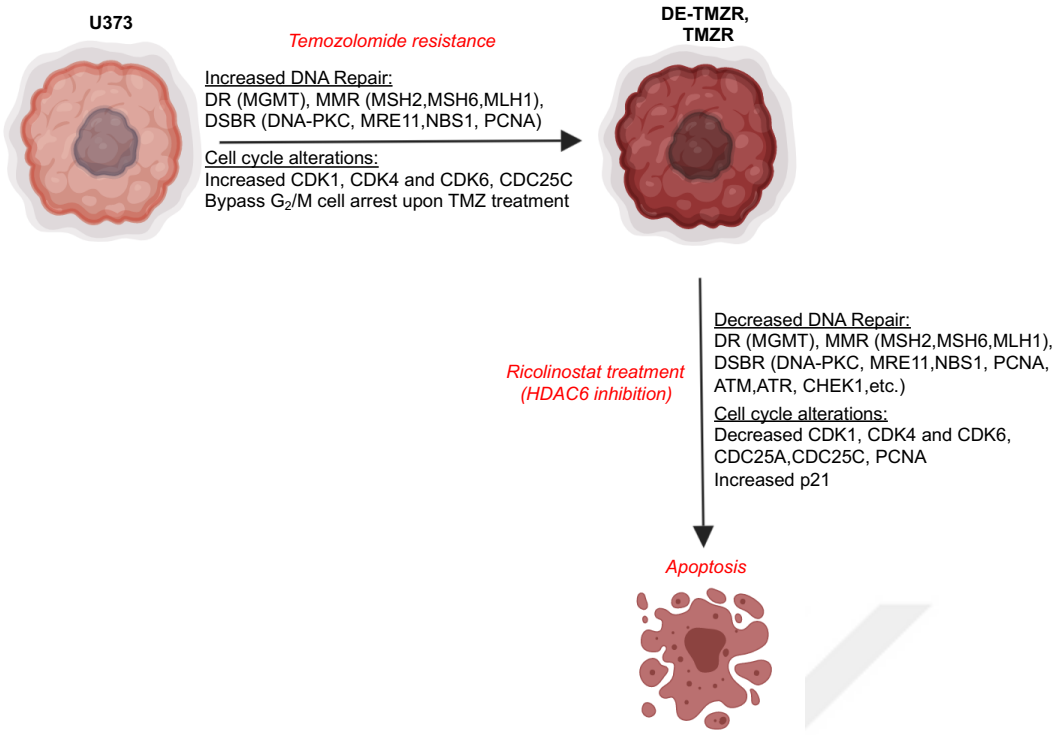

Figure 4.1 Proposed model for TMZ resistant cell lines and changes upon Ricolinostat treatment. DR: Direct Repair, MMR: Mismatch Repair, DSBR: Double Strand Break Repair

Generation of primary GBM cell lines

Standard cell line-based models are the most commonly utilized tools to study cancer [132]. However, the serum-containing medium alters the genomes and transcriptomes of cells and causes depletion of stem cell-like tumor cells. Prolonged cell culture changes the genetic and morphological characteristics of cancers. For example, GBM cell lines lack EGFR amplification, whereas more than 40% of primary GBM tumor specimens contain this mutation[134]. Thus, serum-based monolayer cultures are not the best option to investigate therapeutic effects of a novel finding in GBM. It has been shown that culturing GBM cells in serum free condition media as suspension-based cultures improved the overall recapitulation of GBM biology in culture. For this purpose, to investigate the therapeutic approaches, we established several primary GBM cell lines from patient samples.

To address TMZ resistance in GBM, we established primary GBM cell lines that are serum based and non-serum based and investigated the capacity of tumor formation in *in vivo*

xenografts. Considering the *in vivo* growth capacities, non-serum based KUGBM8-EF was chosen for further studies.

We showed that KUGBM8-EF were moderately sensitive to TMZ and then established TMZ-resistant KUGBM8-EF sublines with pulsed high dosage treatment (referred to as KUGBM8-EF TMZRes). In these cells as well, we have observed MGMT upregulation, greatly supporting our previous findings.

This primary cell line model was also useful to validate effect of HDAC6 inhibition on TMZ response. Similar to U373, DE-TMZR and TMZR, Ricolinostat was able to enhance the effect on cell death in combination to TMZ in KUGBM8-EF. In addition, we observed altered proliferation rates and enhanced TMZ response upon HDAC6 knockout. Hence, we validated that our findings regarding HDAC6 inhibition in serum-based cell lines were consistent in our own primary GBM cell line.

In the future, this primary GBM cell line model along others established during this project will be utilized for further studies as clinically relevant models for GBM.

Clinical implications

For GBM patients several completed and ongoing clinical trials are performed with general HDAC inhibitors: Currently, the most studied in GBM is Vorinostat (https://clinicaltrials.gov, June 2019). However, some of the trials have been withdrawn and/or prematurely terminated, and others did not show improved prognosis compared to Stupp regimen [101,120].

Unfortunately, pan-HDAC inhibition resulted in undesired side effects such as Thrombocytopenia, neutropenia, and anemia, arrhythmias, liver toxicities, etc. Thus, to decrease the undesired effects of HDAC inhibition, more selective HDACi therapies should be considered in patients. For this reason, we investigated all the HDACi in our epigenetics probes library and focused on more selective HDACi. Romidepsin (HDAC1 and 2 inhibitor), Mocetinostat (HDAC 1, 2 and 3 inhibitor) as single agents decreased cell viability less than 20% across all screens. Romidepsin (FK228) is a class I HDAC inhibitor and is FDA-approved for the treatment of refractory Cutaneous T-Cell Lymphoma and Peripheral T-Cell Lymphoma. It was found to induce apoptosis and inhibits proliferation and metastasis of GBM cells [188]. In 2004, Romidepsin was studied in a phase I/ II trial on patients with recurrent

high-grade gliomas in a small size patient group, but at the standard dose and schedule, it was ineffective for patients with recurrent GBM [189].

Ricolinostat, a selective HDAC6 inhibitor was extensively studied throughout this project, however there are no clinical trials with this drug on GBM patients. Our preclinical findings suggest that Ricolinostat treatment alone can induce significant cell death in Temozolomide resistant cell lines, hence we suggest clinical trials with HDAC6 inhibition on TMZ-resistant recurrent GBM patient populations might be beneficial.

HDAC6 was found to be upregulated in GBM patients [107,124,126]. In addition, a study performed on HDAC6 knockout mice reported that HDAC6-deficient mice are viable, fertile with normal lymphoid development and have moderately affected immune response [109]. Thus, inhibition of HDAC6 might be clinically tolerated and might overcome undesired side effects of pan-HDACi.

Considering the cytototoxic effect of HDAC inhibition alone in TMZ-resistant cells, applying HDAC inhibitors after TMZ-resistant recurrence can be a powerful therapeutic strategy. This might allow for decreasing of tumor burden with a single agent. Upon elimination of HDACi-vulnerable resistant tumor population, standard regimen and/or other combinatorial treatments can be followed.

.

5. BIBLIOGRAPHY

1. Ferlay, J. *et al*. Cancer incidence and mortality worldwide: sources, methods and major patterns in GLOBOCAN 2012. *Int. J. cancer* **136**, E359-86 (2015).
2. Sağlık Bakanlığı, T. C. Türkiye Kanser İstatistikleri. 18–25 (2017). Available at: https://hsgm.saglik.gov.tr/depo/birimler/kanser-db/istatistik/2014-RAPOR._uzuuun.pdf. (Accessed: 20th May 2019)
3. Pavon, L. F. *et al*. In vitro analysis of neurospheres derived from glioblastoma primary culture: A novel methodology paradigm. *Front. Neurol*. **4 JAN**, 1–9 (2014).
4. Hanif, F., Muzaffar, K., Perveen, K., Malhi, S. M. & Simjee, S. U. Glioblastoma Multiforme: A Review of its Epidemiology and Pathogenesis through Clinical Presentation and Treatment. *Asian Pac. J. Cancer Prev*. **18**, 3–9 (2017).
5. Ohgaki, H. & Kleihues, P. Population-based studies on incidence, survival rates, and genetic alterations in astrocytic and oligodendroglial gliomas. *J. Neuropathol. Exp. Neurol*. **64**, 479–489 (2005).
6. Ramirez, Y., Weatherbee, J., Wheelhouse, R. & Ross, A. Glioblastoma Multiforme Therapy and Mechanisms of Resistance. *Pharmaceuticals* **6**, 1475–1506 (2013).
7. Tamimi, A. F. & Juweid, M. Epidemiology and Outcome of Glioblastoma. *Glioblastoma* (2017). doi:10.15586/CODON.GLIOBLASTOMA.2017.CH8
8. Ostrom, Q. T. *et al*. CBTRUS statistical report: Primary brain and other central nervous system tumors diagnosed in the United States in 2009-2013. *Neuro. Oncol*. **18**, v1–v75 (2016).
9. Krex, D. *et al*. Long-term survival with glioblastoma multiforme. *Brain* (2007). doi:10.1093/brain/awm204
10. Stupp, R. *et al*. Radiotherapy plus concomitant and adjuvant temozolomide for glioblastoma. *N. Engl. J. Med*. **352**, 987–96 (2005).
11. Ostrom, Q. T. *et al*. CBTRUS Statistical Report: Primary Brain and Central Nervous System Tumors Diagnosed in the United States in 2008-2012. *Neuro. Oncol*. **17 Suppl 4**, iv1–iv62 (2015).
12. Mansouri, A. & Karamchandani. Molecular Genetics of Secondary Glioblastoma. in *Glioblastoma* (2017). doi:10.15586/codon.glioblastoma.2017.ch2
13. Furnari, F. B. *et al*. Malignant astrocytic glioma: genetics, biology, and paths to treatment. *Genes Dev*. **21**, 2683–2710 (2007).
14. The Cancer Genome Atlas Research Network. Comprehensive genomic characterization defines human glioblastoma genes and core pathways. *Nature* **455**, 1061–1068 (2008).
15. Ohgaki, H. & Kleihues, P. Genetic pathways to primary and secondary glioblastoma. *Am. J. Pathol*. **170**, 1445–53 (2007).
16. Brennan, C. W. W. *et al*. The somatic genomic landscape of glioblastoma. *Cell* **155**, 462–477 (2013).
17. Yan, H. IDH1 and IDH2 mutations in gliomas. *N. Engl. J. Med*. **360**, 765–773 (2009).
18. Prensner, J. R. & Chinnaiyan, A. M. Metabolism unhinged: IDH mutations in cancer. *Nat. Med*. **17**, 291–293 (2011).

19. Ranjit, M., Motomura, K., Ohka, F., Wakabayashi, T. & Natsume, A. Applicable advances in the molecular pathology of glioblastoma. *Brain Tumor Pathol*. **32**, 153–162 (2015).
20. Lombardi, M. Y. & Assem, M. Glioblastoma Genomics: A Very Complicated Story. in *Glioblastoma* (2017). doi:10.15586/codon.glioblastoma.2017.ch1
21. Cancer, T., Atlas, G. & McLendon, R, Friedman, A, Bigner, D, Van Meir, EG, Brat, DJ, Mastrogianakis, GM, Olson, JJ, et al. Comprehensive genomic characterization defines human glioblastoma genes and core pathways. *Nature* **455**, 1061–8 (2008).
22. Cloughesy, T. F., Cavenee, W. K. & Mischel, P. S. Glioblastoma: From Molecular Pathology to Targeted Treatment. *Annu. Rev. Pathol. Mech. Dis*. **9**, 1–25 (2014).
23. Sugawa, N., Ekstrand, A. J., Jamest, C. D. & Collins, V. P. *Identical splicing of aberrant epidermal growth factor receptor transcripts from amplified rearranged genes in human glioblastomas (oncogenes/central nervous system tumors/gene deletion). Proc. Nati. Acad. Sci. USA* (1990).
24. Lee, J. C. *et al*. Epidermal growth factor receptor activation in glioblastoma through novel missense mutations in the extracellular domain. *PLoS Med*. **3**, 2264–2273 (2006).
25. Sonoda, Y. *et al*. Akt pathway activation converts anaplastic astrocytoma to glioblastoma multiforme in a human astrocyte model of glioma. *Cancer Res*. **61**, 6674–8 (2001).
26. Benitez, J. A. *et al*. PTEN regulates glioblastoma oncogenesis through chromatin-associated complexes of DAXX and histone H3.3. *Nat. Commun*. **8**, 15223 (2017).
27. Li, Y., Jenkins, C. W., Nichols, M. A. & Xiong, Y. Cell cycle expression and p53 regulation of the cyclin-dependent kinase inhibitor p21. *Oncogene* **9**, 2261–8 (1994).
28. Burton, E. C. *et al*. Aberrant p53, mdm2, and proliferation differ in glioblastomas from long-term compared with typical survivors. *Clin. Cancer Res*. **8**, 180–187 (2002).
29. Ringshausen, I., O'Shea, C. C., Finch, A. J., Swigart, L. B. & Evan, G. I. Mdm2 is critically and continuously required to suppress lethal p53 activity in vivo. *Cancer Cell* **10**, 501–514 (2006).
30. Giacinti, C. & Giordano, A. RB and cell cycle progression. *Oncogene* **25**, 5220–5227 (2006).
31. Sherr, C. J. Cancer Cell Cycles. *Science (80-.)*. **274**, 1672–1677 (1996).
32. Dick, F. A. & Rubin, S. M. Molecular mechanisms underlying RB protein function. *Nat. Rev. Mol. Cell Biol*. **14**, 297–306 (2013).
33. Narita, M. *et al*. Rb-mediated heterochromatin formation and silencing of E2F target genes during cellular senescence. *Cell* (2003).
34. Brown, J. S., O'Carrigan, B., Jackson, S. P. & Yap, T. A. Targeting DNA repair in cancer: Beyond PARP inhibitors. *Cancer Discov*. **7**, 20–37 (2017).
35. Sancar, A., Lindsey-Boltz, L. A., Unsal-Kaçmaz, K. & Linn, S. Molecular mechanisms of mammalian DNA repair and the DNA damage checkpoints. *Annu. Rev. Biochem*. **73**, 39–85 (2004).
36. Wang, J., Su, H., Zhao, H., Chen, Z. & To, S. T. Progress in the application of molecular biomarkers in gliomas. *Biochem. Biophys. Res. Commun*. **465**, 1–4 (2015).
37. Stummer, W. *et al*. Radiotherapy plus concomitant and adjuvant temozolomide for glioblastoma. *Neuropathology* **10**, S26–S29 (2005).

38. Stupp, R. *et al*. Effects of radiotherapy with concomitant and adjuvant temozolomide versus radiotherapy alone on survival in glioblastoma in a randomised phase III study: 5-year analysis of the EORTC-NCIC trial. *Lancet Oncol*. **10**, 459–466 (2009).
39. Messaoudi, K., Clavreul, A. & Lagarce, F. Toward an effective strategy in glioblastoma treatment. Part I: resistance mechanisms and strategies to overcome resistance of glioblastoma to temozolomide. *Drug Discov. Today* **20**, 899–905 (2015).
40. Erasimus, H., Gobin, M., Niclou, S. & Van Dyck, E. DNA repair mechanisms and their clinical impact in glioblastoma. *Mutat. Res. - Rev. Mutat. Res.* **769**, 19–35 (2016).
41. Kelley, K., Knisely, J., Symons, M. & Ruggieri, R. Radioresistance of Brain Tumors. *Cancers (Basel)*. **8**, (2016).
42. Sulli, G., Di Micco, R. & di Fagagna, F. d'Adda. Crosstalk between chromatin state and DNA damage response in cellular senescence and cancer. *Nat. Rev. Cancer* **12**, 709–720 (2012).
43. Mangoni, M. *et al*. Basic Knowledge of Glioblastoma Radiobiology. *Curr. Clin. Pathol*. (2016). doi:10.1007/978-3-319-28305-0_9
44. Damia, G. & D'Incalci, M. Targeting DNA repair as a promising approach in cancer therapy. *Eur. J. Cancer* **43**, 1791–1801 (2007).
45. Zhang, J., Stevens, M. F. G. & Bradshaw, T. D. Temozolomide: mechanisms of action, repair and resistance. *Curr. Mol. Pharmacol*. **5**, 102–14 (2012).
46. Shen, W., Hu, J.-A. & Zheng, J.-S. Mechanism of temozolomide-induced antitumour effects on glioma cells. *J. Int. Med. Res*. **42**, 164–72 (2014).
47. Arora, A. & Somasundaram, K. Glioblastoma vs temozolomide: can the red queen race be won? *Cancer Biol. Ther*. **0**, 1–8 (2019).
48. Weller, M., Cloughesy, T., Perry, J. R. & Wick, W. Standards of care for treatment of recurrent glioblastoma--are we there yet? *Neuro. Oncol*. **15**, 4–27 (2013).
49. Fernandes, C. *et al*. Current Standard of Care in Glioblastoma Therapy. in *Glioblastoma* (2017).
50. Van Den Bent, M. J. *et al*. Randomized phase II trial of erlotinib versus temozolomide or carmustine in recurrent glioblastoma: EORTC brain tumor group study 26034. *J. Clin. Oncol*. **27**, 1268–1274 (2009).
51. Papait, R., Magrassi, L., Rigamonti, D. & Cattaneo, E. Temozolomide and carmustine cause large-scale heterochromatin reorganization in glioma cells. *Biochem. Biophys. Res. Commun*. **379**, 434–439 (2009).
52. Thomas, A. *et al*. Temozolomide in the Era of Precision Medicine. *Cancer Res*. 1–4 (2017). doi:10.1158/0008-5472.CAN-16-2983
53. Herrlinger, U. *et al*. Lomustine-temozolomide combination therapy versus standard temozolomide therapy in patients with newly diagnosed glioblastoma with methylated MGMT promoter (CeTeG/NOA-09): a randomised, open-label, phase 3 trial. *Lancet (London, England)* **393**, 678–688 (2019).
54. Hottinger, A. F., Pacheco, P. & Stupp, R. Tumor treating fields: a novel treatment modality and its use in brain tumors. *Neuro. Oncol*. **18**, 1338–1349 (2016).
55. Kirson, E. D. *et al*. Disruption of Cancer Cell Replication by Alternating Electric Fields. *Cancer Res*. **64**, 3288–3295 (2004).
56. Stupp, R. *et al*. Effect of Tumor-Treating Fields Plus Maintenance Temozolomide vs

Maintenance Temozolomide Alone on Survival in Patients With Glioblastoma. *JAMA* **318**, 2306 (2017).
57. Westphal, M., Maire, C. L. & Lamszus, K. EGFR as a Target for Glioblastoma Treatment: An Unfulfilled Promise. *CNS Drugs* **31**, (2017).
58. Ellingson, B. M. *et al*. Quantitative volumetric analysis of conventional MRI response in recurrent glioblastoma treated with bevacizumab. *Neuro. Oncol*. (2011). doi:10.1093/neuonc/noq206
59. Patel, M. A., Kim, J. E., Ruzevick, J., Li, G. & Lim, M. The future of glioblastoma therapy: synergism of standard of care and immunotherapy. *Cancers (Basel)*. **6**, 1953–85 (2014).
60. Wang, E. *et al*. The role of Factor Inhibiting HIF (FIH-1) in inhibiting HIF-1 transcriptional activity in glioblastoma multiforme. *PLoS One* **9**, (2014).
61. Shiao-Pei Weathers, M. J. de G. M. VEGF Manipulation in Glioblastoma. (2015).
62. Pearson, J. R. D. & Regad, T. Targeting cellular pathways in glioblastoma multiforme. *Signal Transduct. Target. Ther*. **2**, 17040 (2017).
63. Nikiforova, M. N. *et al*. Targeted next-generation sequencing panel (GlioSeq) provides comprehensive genetic profiling of central nervous system tumors. *Neuro. Oncol*. **18**, 379–387 (2016).
64. Hegi, M. E. *et al*. MGMT Gene Silencing and Benefit from Temozolomide in Glioblastoma. *N. Engl. J. Med*. **352**, 997–1003 (2005).
65. Franceschi, E. *et al*. Gefitinib in patients with progressive high-grade gliomas: a multicentre phase II study by Gruppo Italiano Cooperativo di Neuro-Oncologia (GICNO). *Br. J. Cancer* **96**, 1047–51 (2007).
66. Wu, Q., Yang, Z., Nie, Y., Shi, Y. & Fan, D. Multi-drug resistance in cancer chemotherapeutics: Mechanisms and lab approaches. *Cancer Lett*. **347**, 159–166 (2014).
67. Zahreddine, H. & Borden, K. L. B. Mechanisms and insights into drug resistance in cancer. *Front. Pharmacol*. **4 MAR**, 1–8 (2013).
68. Gottesman, M. M. Mechanisms of Cancer Drug Resistance. *Annu. Rev. Med*. **53**, 615–627 (2002).
69. Ostrom, Q. T. *et al*. CBTRUS Statistical Report: Primary Brain and Central Nervous System Tumors Diagnosed in the United States in 2007-2011. *Neuro. Oncol*. **16**, iv1–iv63 (2014).
70. Herst, P. M. Is inhibiting the DNA damage response the answer to treatment resistance in glioma stem cells? *Transl. Cancer Res*. **5**, S815–S822 (2016).
71. Brown, R., Curry, E., Magnani, L., Wilhelm-Benartzi, C. S. & Borley, J. Poised epigenetic states and acquired drug resistance in cancer. *Nat. Rev. Cancer* **14**, 747–753 (2014).
72. NAIDU, M. D., MASON, J. M., PICA, R. V., FUNG, H. & PEÑA, L. A. Radiation Resistance in Glioma Cells Determined by DNA Damage Repair Activity of Ape1/Ref-1. *J. Radiat. Res*. **51**, 393–404 (2010).
73. Bao, S. *et al*. Glioma stem cells promote radioresistance by preferential activation of the DNA damage response. *Nature* **444**, 756–60 (2006).
74. Schaich, M. *et al*. A MDR1 (ABCB1) gene single nucleotide polymorphism predicts outcome of temozolomide treatment in glioblastoma patients. *Ann. Oncol*. (2009). doi:10.1093/annonc/mdn548

75. Everhard, S. *et al*. Identification of regions correlating MGMT promoter methylation and gene expression in glioblastomas. *Neuro. Oncol*. **11**, 348–56 (2009).
76. van Nifterik, K. A. *et al*. Absence of the MGMT protein as well as methylation of the MGMT promoter predict the sensitivity for temozolomide. *Br. J. Cancer* **103**, 29–35 (2010).
77. Villalva, C. *et al*. O6-Methylguanine-methyltransferase (MGMT) promoter methylation status in glioma stem-like cells is correlated to temozolomide sensitivity under differentiation-promoting conditions. *Int. J. Mol. Sci*. **13**, 6983–94 (2012).
78. Kohsaka, S. & Tanak, S. Chemotherapeutic Agent for Glioma. in *Clinical Management and Evolving Novel Therapeutic Strategies for Patients with Brain Tumors* (InTech, 2013). doi:10.5772/54353
79. Chen, X. *et al*. A novel enhancer regulates MGMT expression and promotes temozolomide resistance in glioblastoma. *Nat. Commun*. / **9**, 2949 (2018).
80. McFaline-Figueroa, J. L. *et al*. Minor changes in expression of the mismatch repair protein MSH2 exert a major impact on glioblastoma response to temozolomide. *Cancer Res*. **75**, 3127–3138 (2015).
81. Verbeek, B., Southgate, T. D., Gilham, D. E. & Margison, G. P. O6-Methylguanine-DNA methyltransferase inactivation and chemotherapy. *British Medical Bulletin* **85**, 17–33 (2008).
82. Fu, D., Calvo, J. A. & Samson, L. D. Balancing repair and tolerance of DNA damage caused by alkylating agents. *Nat. Rev. Cancer* **12**, 104–20 (2012).
83. Perazzoli, G. *et al*. Temozolomide resistance in glioblastoma cell lines: Implication of MGMT, MMR, P-glycoprotein and CD133 expression. *PLoS One* **10**, 1–23 (2015).
84. Liu, X. *et al*. Potentiation of temozolomide cytotoxicity by poly(ADP)ribose polymerase inhibitor ABT-888 requires a conversion of single-stranded DNA damages to double-stranded DNA breaks. *Mol. Cancer Res*. **6**, 1621–1629 (2008).
85. Gomez-Manzano, C. *et al*. Characterization of p53 and p21 Functional Interactions in Glioma Cells en Route to Apoptosis. *JNCI J. Natl. Cancer Inst*. **89**, 1036–1044 (1997).
86. Zhu, J.-X. *et al*. Treatment of recurrent malignant gliomas by surgery combined with recombinant adenovirus-p53. *Chinese J. Cancer Prev. Treat*. **17**, 126–128 (2010).
87. Benitez, J. A. *et al*. PTEN regulates glioblastoma oncogenesis through chromatin-associated complexes of DAXX and histone H3.3. *Nat. Commun*. **9**, (2018).
88. Ma, J. *et al*. Inhibition of Nuclear PTEN Tyrosine Phosphorylation Enhances Glioma Radiation Sensitivity through Attenuated DNA Repair. *Cancer Cell* 1–15 (2019). doi:10.1016/J.CCELL.2019.01.020
89. Tanaka, M. *et al*. MMAC1/PTEN inhibits cell growth and induces chemosensitivity to doxorubicin in human bladder cancer cells. *Oncogene* **19**, 5406–12 (2000).
90. Allis, C. D. & Jenuwein, T. The molecular hallmarks of epigenetic control. *Nat. Rev. Genet*. **17**, 487–500 (2016).
91. Dawson, M. A. & Kouzarides, T. Cancer Epigenetics: From Mechanism to Therapy. *Cell* **150**, 12–27 (2012).
92. Lund, A. H. & van Lohuizen, M. Epigenetics and cancer. *Genes Dev*. **18**, 2315–35 (2004).
93. Ellis, L., Atadja, P. W. & Johnstone, R. W. Epigenetics in cancer: targeting

chromatin modifications. *Mol. Cancer Ther.* **8**, 1409–20 (2009).
94. Wang, Y. *et al.* Beyond the double helix: writing and reading the histone code. *Novartis Found. Symp.* **259**, 3–17; discussion 17-21, 163–9 (2004).
95. Rodríguez-Paredes, M. & Esteller, M. Cancer epigenetics reaches mainstream oncology. *Nat. Med.* **17**, 330–9 (2011).
96. Feinberg, A. P. & Tycko, B. The history of cancer epigenetics. *Nat. Rev. Cancer* **4**, 143–153 (2004).
97. Esteller, M. Cancer epigenomics: DNA methylomes and histone-modification maps. *Nat. Rev. Genet.* **8**, 286–298 (2007).
98. Allfrey, V. G., Faulkner, R. & Mirsky, A. E. Acetylation and Methylation of Histones and their possible role Iin the regulation of RNA synthesis. *Proc. Natl. Acad. Sci. U. S. A.* (1964).
99. Falkenberg, K. J. & Johnstone, R. W. Histone deacetylases and their inhibitors in cancer, neurological diseases and immune disorders. *Nat. Rev. Drug Discov.* **13**, 673–691 (2014).
100. Szyf, M. Epigenetics, DNA methylation, and chromatin modifying drugs. *Annu. Rev. Pharmacol. Toxicol.* **49**, 243–63 (2009).
101. Burbano, R. R. *et al.* An update on the epigenetics of glioblastomas. *Epigenomics* **8**, 1289–1305 (2016).
102. Roos, W. P. & Krumm, A. The multifaceted influence of histone deacetylases on DNA damage signalling and DNA repair. *Nucleic Acids Res.* **44**, 10017–10030 (2016).
103. Ropero, S. & Esteller, M. The role of histone deacetylases (HDACs) in human cancer. *Molecular Oncology* (2007). doi:10.1016/j.molonc.2007.01.001
104. Chen, C.-S., Weng, S.-C., Tseng, P.-H., Lin, H.-P. & Chen, C.-S. Histone Acetylation-independent Effect of Histone Deacetylase Inhibitors on Akt through the Reshuffling of Protein Phosphatase 1 Complexes *. (2005). doi:10.1074/jbc.M505733200
105. Krumm, A. *et al.* Enhanced histone deacetylase activity in malignant melanoma provokes RAD51 and FANCD2-triggered drug resistance. *Cancer Res.* (2016). doi:10.1158/0008-5472.CAN-15-2680
106. Choi, E. J. *et al.* Enhanced cytotoxic effect of radiation and temozolomide in malignant glioma cells: Targeting PI3K-AKT-mTOR signaling, HSP90 and histone deacetylases. *BMC Cancer* **14**, 17 (2014).
107. Marampon, F. *et al.* HDAC4 and HDAC6 sustain DNA double strand break repair and stem-like phenotype by promoting radioresistance in glioblastoma cells. *Cancer Lett.* **397**, 1–11 (2017).
108. Lian, H. *et al.* HDAC6 promotes cell proliferation and confers resistance to temozolomide in glioblastoma. *Cancer Lett.* **379**, 134–142 (2016).
109. Lee, D. H., Ryu, H.-W., Won, H.-R. & Kwon, S. H. Advances in epigenetic glioblastoma therapy. *Oncotarget* **8**, 18577–18589 (2017).
110. Robert, C. & Rassool, F. V. HDAC Inhibitors. in *Advances in cancer research* **116**, 87–129 (2012).
111. Lee, J.-H., Choy, M. L., Ngo, L., Foster, S. S. & Marks, P. A. Histone deacetylase inhibitor induces DNA damage, which normal but not transformed cells can repair. *Proc. Natl. Acad. Sci.* **107**, 14639–14644 (2010).

112. Adamopoulou E and Naumann U. HDAC inhibitors and their potential applications to glioblastoma therapy. *Oncoimmunology* (2013). doi:10.4161/onci.25219
113. Yelton, C. J. & Ray, S. K. Histone deacetylase enzymes and selective histone deacetylase inhibitors for antitumor effects and enhancement of antitumor immunity in glioblastoma. *Neuroimmunol. Neuroinflammation* **5**, 46 (2018).
114. Rasmussen, R. D., Gajjar, M. K., Jensen, K. E. & Hamerlik, P. Enhanced efficacy of combined HDAC and PARP targeting in glioblastoma. *Mol. Oncol.* **10**, 751–763 (2016).
115. Hrgovic, I. *et al*. The histone deacetylase inhibitor trichostatin a decreases lymphangiogenesis by inducing apoptosis and cell cycle arrest via p21-dependent pathways. *BMC Bioinformatics* **13**, 1–15 (2012).
116. Newbold, A., Falkenberg, K. J., Prince, H. M. & Johnstone, R. W. How do tumor cells respond to HDAC inhibition? *FEBS J.* **283**, 4032–4046 (2016).
117. Xu, J. *et al*. Vorinostat modulates cell cycle regulatory proteins in glioma cells and human glioma slice cultures. *J. Neurooncol.* (2011). doi:10.1007/s11060-011-0604-7
118. Singh, M. M. *et al*. Preclinical activity of combined HDAC and KDM1A inhibition in glioblastoma. *Neuro. Oncol.* **17**, 1463–1473 (2015).
119. Rajendran, P., Ho, E., Williams, D. E. & Dashwood, R. H. Dietary phytochemicals, HDAC inhibition, and DNA damage/repair defects in cancer cells. *Clin. Epigenetics* **3**, 4 (2011).
120. Bagci-Onder, T. *et al*. Real-time imaging of the dynamics of death receptors and therapeutics that overcome TRAIL resistance in tumors. *Oncogene* (2013). doi:10.1038/onc.2012.304
121. Vorinostat in Treating Patients With Progressive or Recurrent Glioblastoma Multiforme - ClinicalTrials.gov. Available at: https://clinicaltrials.gov/ct2/show/NCT00238303?term=NCT00238303&rank=1. (Accessed: 31st May 2019)
122. Sakamoto, K. M. & Aldana-Masangkay, G. I. The role of HDAC6 in cancer. *J. Biomed. Biotechnol.* **2011**, (2011).
123. Safa, A. R. Role of histone deacetylases 6 (HDAC6) in cancers. *J. Pharmacol. Ther. Res.* **1**,
124. Li, S., Liu, X., Chen, X., Zhang, L. & Wang, X. Histone deacetylase 6 promotes growth of glioblastoma through inhibition of SMAD2 signaling. *Tumor Biol.* **36**, 9661–9665 (2015).
125. Zhang, Y. *et al*. Mice lacking histone deacetylase 6 have hyperacetylated tubulin but are viable and develop normally. *Mol. Cell. Biol.* **28**, 1688–701 (2008).
126. HDAC6 Expression in Sun Brain. Available at: https://www.oncomine.org/resource/main.html#cso%3AsizeSmallLarge%3Bcv%3Adetail%3Bd%3A111290077%3Bdso%3ApvalueOverex%3Bdt%3Adataset%3Bec%3A%5B2%5D%3Bepv%3A2937%3Bet%3Aover%3Bf%3A542637%3Bg%3A10013%3Bgt%3Aboxplot%3Bp%3A200010739%3Bpg%3A1%3Bpvf%3A2947%2C1441. (Accessed: 30th May 2019)
127. Avril, T., Vauléon, E. & Chevet, E. Endoplasmic reticulum stress signaling and chemotherapy resistance in solid cancers. *Oncogenesis* **6**, e373 (2017).
128. Li, Z. yang *et al*. A novel HDAC6 inhibitor Tubastatin A: Controls HDAC6-p97/VCP-mediated ubiquitination-autophagy turnover and reverses Temozolomide-

induced ER stress-tolerance in GBM cells. *Cancer Lett*. **391**, 89–99 (2017).
129. Lin, T.-W. *et al*. TDP-43/HDAC6 axis promoted tumor progression and regulated nutrient deprivation-induced autophagy in glioblastoma. *Oncotarget* **8**, 56612–56625 (2017).
130. Yin, C. & Li, P. Growth suppression of glioma cells using HDAC6 inhibitor, tubacin. *Open Med*. **13**, 221–226 (2018).
131. Liu, J. R., Yu, C. W., Hung, P. Y., Hsin, L. W. & Chern, J. W. High-selective HDAC6 inhibitor promotes HDAC6 degradation following autophagy modulation and enhanced antitumor immunity in glioblastoma. *Biochem. Pharmacol*. **163**, 458–471 (2019).
132. Sui, A. *et al*. Histone demethylase KDM6B regulates 1,25-dihydroxyvitamin D3-induced senescence in glioma cells. *J. Cell. Physiol*. (2019). doi:10.1002/jcp.28431
133. Huszthy, P. C. *et al*. In vivo models of primary brain tumors: Pitfalls and perspectives. *Neuro. Oncol*. **14**, 979–993 (2012).
134. Xie, Y. *et al*. The Human Glioblastoma Cell Culture Resource: Validated Cell Models Representing All Molecular Subtypes. *EBioMedicine* **2**, 1351–1363 (2015).
135. Carlson, B. L., Pokorny, J. L., Schroeder, M. a & Sarkaria, J. N. *Establishment, maintenance and in vitro and in vivo applications of primary human glioblastoma multiforme (GBM) xenograft models for translational biology studies and drug discovery. Current protocols in pharmacology / editorial board, S.J. Enna (editor-in-chief) ... [et al.]* **Chapter 14**, (2011).
136. Xiao, W., Sohrabi, A. & Seidlits, S. K. Integrating the glioblastoma microenvironment into engineered experimental models. *Futur. Sci. OA* **3**, FSO189 (2017).
137. Bagci-Onder, T., Wakimoto, H., Anderegg, M., Cameron, C. & Shah, K. A Dual PI3K/mTOR Inhibitor, PI-103, Cooperates with Stem Cell-Delivered TRAIL in Experimental Glioma Models. *Cancer Res*. **71**, 154–163 (2011).
138. Nie, E. *et al*. MiR-198 enhances temozolomide sensitivity in glioblastoma by targeting MGMT. *J. Neurooncol*. **133**, 59–68 (2017).
139. Guzmán, C., Bagga, M., Kaur, A., Westermarck, J. & Abankwa, D. ColonyArea: An ImageJ Plugin to Automatically Quantify Colony Formation in Clonogenic Assays. *PLoS One* **9**, e92444 (2014).
140. Banelli, B. *et al*. The histone demethylase KDM5A is a key factor for the resistance to temozolomide in glioblastoma. *Cell Cycle* **14**, 3418–3429 (2015).
141. Tiek, D. M. *et al*. Alterations in Cell Motility, Proliferation, and Metabolism in Novel Models of Acquired Temozolomide Resistant Glioblastoma. *Sci. Rep*. **8**, 1–11 (2018).
142. Picelli, S. *et al*. Tn5 transposase and tagmentation procedures for massively scaled sequencing projects. *Genome Res*. (2014). doi:10.1101/gr.177881.114
143. Buenrostro, J. D., Giresi, P. G., Zaba, L. C., Chang, H. Y. & Greenleaf, W. J. Transposition of native chromatin for fast and sensitive epigenomic profiling of open chromatin, DNA-binding proteins and nucleosome position. *Nat. Methods* **10**, 1213–1218 (2013).
144. Buenrostro, J. D., Wu, B., Chang, H. Y. & Greenleaf, W. J. ATAC-seq: A method for assaying chromatin accessibility genome-wide. *Curr. Protoc. Mol. Biol*. **2015**, 21.29.1-21.29.9 (2015).

145. Cribbs, A. *et al*. Inhibition of histone H3K27 demethylases selectively modulates inflammatory phenotypes of natural killer cells. *J. Biol. Chem.* **293**, 2422–2437 (2018).
146. Genialis.
147. Hsu, P. D. *et al*. Genome-Scale CRISPR-Cas9 Knockout Screening in Human Cells. *Nat. Biotechnol.* **31**, 827–32 (2013).
148. Lee, S. Y. Temozolomide resistance in glioblastoma multiforme. *Genes Dis.* **3**, 198–210 (2016).
149. Montaldi, A. P., Godoy, P. R. D. V. D. V & Sakamoto-Hojo, E. T. APE1/REF-1 down-regulation enhances the cytotoxic effects of temozolomide in a resistant glioblastoma cell line. *Mutat. Res. - Genet. Toxicol. Environ. Mutagen.* **793**, 19–29 (2015).
150. Baer, J. C. *et al*. Depletion of O6-alkylguanine-DNA alkyltransferase correlates with potentiation of temozolomide and CCNU toxicity in human tumour cells. *Br. J. Cancer* **67**, 1299–1302 (1993).
151. Ho, G. Y., Woodward, N. & Coward, J. I. G. Cisplatin versus carboplatin: comparative review of therapeutic management in solid malignancies. *Crit. Rev. Oncol. Hematol.* **102**, 37–46 (2016).
152. Emadi, A., Jones, R. J. & Brodsky, R. A. Cyclophosphamide and cancer: golden anniversary. *Nat. Rev. Clin. Oncol.* **6**, 638–647 (2009).
153. Stupp, R., Lukas, R. V & Hegi, M. E. Improving survival in molecularly selected glioblastoma. *Lancet* **393**, 615–617 (2019).
154. Chae, Y. K. *et al*. Inhibition of the fibroblast growth factor receptor (FGFR) pathway: the current landscape and barriers to clinical application. *Oncotarget* **8**, 16052 (2017).
155. Gavine, P. R. *et al*. AZD4547: An orally bioavailable, potent, and selective inhibitor of the fibroblast growth factor receptor tyrosine kinase family. *Cancer Res.* (2012). doi:10.1158/0008-5472.CAN-11-3034
156. Tyulyandina, A. *et al*. Alofanib, an allosteric FGFR2 inhibitor, has potent effects on ovarian cancer growth in preclinical studies. *Invest. New Drugs* (2017). doi:10.1007/s10637-016-0404-1
157. Chahal, M. *et al*. O(6)-Methylguanine-DNA Methyltransferase Is a Novel Negative Effector of Invasion in Glioblastoma Multiforme. *Mol. Cancer Ther.* **11**, 2440–2450 (2012).
158. Kitange, G. J. *et al*. Induction of MGMT expression is associated with temozolomide resistance in glioblastoma xenografts. *Neuro. Oncol.* **11**, 281–91 (2009).
159. Ciechomska, I. A., Marciniak, M. P., Jackl, J. & Kaminska, B. Pre-treatment or Post-treatment of Human Glioma Cells With BIX01294, the Inhibitor of Histone Methyltransferase G9a, Sensitizes Cells to Temozolomide. *Front. Pharmacol.* **9**, 1271 (2018).
160. Batra, V. *et al*. Initial Testing (Stage 1) of SGI-1776, a PIM1 Kinase Inhibitor, by the Pediatric Preclinical Testing Program. *Pediatr. Blood Cancer* **59**, 749 (2012).
161. Pines, M. Halofuginone for fibrosis, regeneration and cancer in the gastrointestinal tract. *World J. Gastroenterol.* **20**, 14778–86 (2014).
162. Romani, M., Pistillo, M. P. & Banelli, B. Epigenetic Targeting of Glioblastoma. *Front. Oncol.* **8**, 1–9 (2018).

163. Gryder, B. E., Sodji, Q. H. & Oyelere, A. K. Targeted cancer therapy: Giving histone deacetylase inhibitors all they need to succeed. *Future Medicinal Chemistry* **4**, 505–524 (2012).
164. Ceccacci, E. & Minucci, S. Inhibition of histone deacetylases in cancer therapy: lessons from leukaemia. *Br. J. Cancer* **114**, 605–11 (2016).
165. Iatsyshyna, A. P. Mgmt expression: Insights into its regulation. *Biopolym. Cell* **29**, 99–106 (2013).
166. Azzalin, A. *et al*. Inhibitors of GLUT/SLC2A Enhance the Action of BCNU and Temozolomide against High-Grade Gliomas. *Neoplasia (United States)* **19**, 364–373 (2017).
167. Freireich, E. J., Gehan, E. A., Sulman, D., Boggs, D. R. & Frei, E. The effect of chemotherapy on acute leukemia in the human. *J. Chronic Dis*. (1961). doi:10.1016/0021-9681(61)90118-7
168. Mukherjee, S. *The Emperor of All Maladies: A Biography of Cancer*. *Journal of Postgraduate Medicine Education and Research* (2011).
169. Iqbal, N. & Iqbal, N. Imatinib: a breakthrough of targeted therapy in cancer. *Chemother. Res. Pract.* **2014**, 357027 (2014).
170. Cisternino, S., Mercier, C., Bourasset, F., Roux, F. & Scherrmann, J. M. Expression, Up-Regulation, and Transport Activity of the Multidrug-Resistance Protein Abcg2 at the Mouse Blood-Brain Barrier. *Cancer Res.* **641. Ciste**, 3296–3301 (2004).
171. Haar, C. P. *et al*. Drug Resistance in Glioblastoma: A Mini Review. doi:10.1007/s11064-011-0701-1
172. Yusa, K. & Tsuruo, T. Reversal mechanism of multidrug resistance by verapamil: direct binding of verapamil to P-glycoprotein on specific sites and transport of verapamil outward across the plasma membrane of K562/ADM cells. *Cancer Res.* **49**, 5002–6 (1989).
173. Zhang, J., Stevens, M. F. G. G., Laughton, C. A., Madhusudan, S. & Bradshaw, T. D. Acquired resistance to temozolomide in glioma cell lines: Molecular mechanisms and potential translational applications. *Oncology* **78**, 103–114 (2010).
174. Yoshimoto, K. *et al*. Complex DNA repair pathways as possible therapeutic targets to overcome temozolomide resistance in glioblastoma. *Front. Oncol.* **2**, 186 (2012).
175. Mirzoeva, O. K., Kawaguchi, T. & Pieper, R. O. The Mre11/Rad50/Nbs1 complex interacts with the mismatch repair system and contributes to temozolomide-induced G_2 arrest and cytotoxicity. *Mol. Cancer Ther.* **5**, 2757–2766 (2006).
176. Eich, M., Roos, W. P., Dianov, G. L., Digweed, M. & Kaina, B. Nijmegen breakage syndrome protein (NBN) causes resistance to methylating anticancer drugs such as temozolomide. *Mol. Pharmacol.* **78**, 943–51 (2010).
177. Batchu, S. N., Brijmohan, A. S. & Advani, A. The therapeutic hope for HDAC6 inhibitors in malignancy and chronic disease. *Clin. Sci.* **130**, 987–1003 (2016).
178. Amengual, J. E. *et al*. Mechanisms of acquired drug resistance to the HDAC6 selective inhibitor ricolinostat reveals rational drug-drug combination with ibrutinib. *Clin. Cancer Res.* **23**, 3084–3096 (2017).
179. Cosenza, M., Civallero, M., Marcheselli, L., Sacchi, S. & Pozzi, S. Ricolinostat, a selective HDAC6 inhibitor, shows anti-lymphoma cell activity alone and in combination with bendamustine. *Apoptosis* **22**, 827–840 (2017).
180. Ding, G. *et al*. HDAC6 promotes hepatocellular carcinoma progression by inhibiting

P53 transcriptional activity. *FEBS Lett*. **587**, 880–886 (2013).
181. Kovacs, J. J. *et al*. HDAC6 Regulates Hsp90 Acetylation and Chaperone-Dependent Activation of Glucocorticoid Receptor. *Mol. Cell* **18**, 601–607 (2005).
182. Bali, P. *et al*. Inhibition of histone deacetylase 6 acetylates and disrupts the chaperone function of heat shock protein 90: a novel basis for antileukemia activity of histone deacetylase inhibitors. *J. Biol. Chem*. **280**, 26729–34 (2005).
183. Podust, V. N., Podust, L. M., Goubin, F., Ducommun, B. & Hübscher, U. Mechanism of inhibition of proliferating cell nuclear antigen-dependent DNA synthesis by the cyclin-dependent kinase inhibitor p21. *Biochemistry* **34**, 8869–75 (1995).
184. Pappano, W. N., Zhang, Q., Tucker, L. A., Tse, C. & Wang, J. Genetic inhibition of the atypical kinase Wee1 selectively drives apoptosis of p53 inactive tumor cells. *BMC Cancer* **14**, 430 (2014).
185. Wu, S. *et al*. Activation of WEE1 confers resistance to PI3K inhibition in glioblastoma. *Neuro. Oncol*. **20**, 78–91 (2018).
186. Núñez, F. J. *et al*. IDH1R132H acts as a tumor suppressor in glioma via epigenetic upregulation of the DNA damage response. *bioRxiv* 389817 (2018). doi:10.1101/389817
187. Patil, A. A. *et al*. FANCD2 re-expression is associated with glioma grade and chemical inhibition of the Fanconi Anaemia pathway sensitises gliomas to chemotherapeutic agents. *Oncotarget* **5**, 6414–24 (2014).
188. Sawa, H. *et al*. Histone deacetylase inhibitor, FK228, induces apoptosis and suppresses cell proliferation of human glioblastoma cells in vitro and in vivo. *Acta Neuropathol*. (2004). doi:10.1007/s00401-004-0841-3
189. Iwamoto, F. M. *et al*. A phase I/II trial of the histone deacetylase inhibitor romidepsin for adults with recurrent malignant glioma: North American Brain Tumor Consortium Study 03-03. *Neuro. Oncol*. **13**, 509–516 (2011).
190. Yang, W., Liu, Y., Gao, R., Yu, H. & Sun, T. HDAC6 inhibition induces glioma stem cells differentiation and enhances cellular radiation sensitivity through the SHH/Gli1 signaling pathway. *Cancer Lett*. **415**, 164–176 (2018).
191. Park, S. Y., Park, J. W. & Chun, Y. S. Jumonji histone demethylases as emerging therapeutic targets. *Pharmacol. Res*. **105**, 146–151 (2016).
192. Schwartzentruber, J. *et al*. Driver mutations in histone H3.3 and chromatin remodelling genes in paediatric glioblastoma. *Nature* **482**, 226–231 (2012).
193. Price, B. D. KDM5A demethylase: Erasing histone modifications to promote repair of DNA breaks. *J. Cell Biol*. **216**, 1871–1873 (2017).
194. Plch, J., Hrabeta, J. & Eckschlager, T. KDM5 demethylases and their role in cancer cell chemoresistance. *Int. J. Cancer* **144**, 221–231 (2019).
195. Rasmussen, P. B. & Staller, P. The KDM5 family of histone demethylases as targets in oncology drug discovery. *Epigenomics* **6**, 277–286 (2014).
196. Banelli, B. *et al*. Small molecules targeting histone demethylase genes (KDMs) inhibit growth of Temozolomide-resistant glioblastoma cells. *Oncotarget* (2017). doi:10.18632/oncotarget.16820
197. KDM5A Expression in Sun Brain. Available at: https://www.oncomine.org/resource/main.html#a%3A1968%3Bac%3A1968%3Bd%3A16585726%3Bdso%3AfoldChangeOverex%3Bdt%3ApredefinedClass%3Bec%3

A%5B%5D%3Bet%3Aover%3Bf%3A1925233%3Bg%3A5927%3Bgt%3Aboxplot%3Bp%3A200001352%3Bpg%3A1%3Bpvf%3A2947%2C194403%3Bscr%3Adatase. (Accessed: 31st May 2019)

198. Dai, B. *et al*. Histone demethylase KDM5A inhibits glioma cells migration and invasion by down regulating ZEB1. *Biomed. Pharmacother.* **99**, 72–80 (2018).
199. Wilting, R. H. & Dannenberg, J. H. Epigenetic mechanisms in tumorigenesis, tumor cell heterogeneity and drug resistance. *Drug Resist. Updat.* **15**, 21–38 (2012).
200. Mullighan, C. G. *et al*. CREBBP mutations in relapsed acute lymphoblastic leukaemia. *Nature* (2011). doi:10.1038/nature09727
201. Bryan, E. J. *et al*. Mutation analysis of EP300 in colon, breast and ovarian carcinomas. *Int. J. Cancer* (2002). doi:10.1002/ijc.10682
202. Gui, Y. *et al*. Frequent mutations of chromatin remodeling genes in transitional cell carcinoma of the bladder. *Nat. Genet.* (2011). doi:10.1038/ng.907
203. Seligson, D. B. *et al*. Global histone modification patterns predict risk of prostate cancer recurrence. *Nature* (2005). doi:10.1038/nature03672
204. Tzao, C. *et al*. Prognostic significance of global histone modifications in resected squamous cell carcinoma of the esophagus. *Mod. Pathol.* (2009). doi:10.1038/modpathol.2008.172
205. Liu, B. L. *et al*. Global histone modification patterns as prognostic markers to classify glioma patients. *Cancer Epidemiol. Biomarkers Prev.* (2010). doi:10.1158/1055-9965.EPI-10-0454
206. Stemmer, M., Thumberger, T., Del Sol Keyer, M., Wittbrodt, J. & Mateo, J. L. CCTop: An Intuitive, Flexible and Reliable CRISPR/Cas9 Target Prediction Tool. *PLoS One* (2015). doi:10.1371/journal.pone.0124633
207. Shalem, O. *et al*. Genome - scale CRISPR - Cas9 knockout screening in human cells. *Science (80-.).* **343**, 84–87 (2014).
208. Onder, T. T. *et al*. Chromatin-modifying enzymes as modulators of reprogramming. *Nature* **483**, 598–602 (2012).
209. Shalem, O., Sanjana, N. E. & Zhang, F. High-throughput functional genomics using CRISPR-Cas9. *Nat. Rev. Genet.* **16**, 299–311 (2015).
210. Banelli, B. *et al*. Small molecules targeting histone demethylase genes (KDMs) inhibit growth of Temozolomide-resistant glioblastoma cells. *Oncotarget* **5**, (2017).
211. Vinogradova, M. *et al*. An inhibitor of KDM5 demethylases reduces survival of drug-tolerant cancer cells. *Nat. Chem. Biol.* **12**, 531–538 (2016).
212. Hammitzsch, A. *et al*. CBP30, a selective CBP/p300 bromodomain inhibitor, suppresses human Th17 responses. *Proc. Natl. Acad. Sci.* (2015). doi:10.1073/pnas.1501956112
213. Kitange, G. J. *et al*. Retinoblastoma Binding Protein 4 Modulates Temozolomide Sensitivity in Glioblastoma by Regulating DNA Repair Proteins. *Cell Rep.* **14**, 2587–98 (2016).
214. Cha, Y. *et al*. Drug repurposing from the perspective of pharmaceutical companies. *Br. J. Pharmacol.* **175**, 168–180 (2018).
215. Fry, D. W. *et al*. A specific inhibitor of the epidermal growth factor receptor tyrosine kinase. *Science* **265**, 1093–5 (1994).

6. APPENDIX A - EPIKOL SCREEN

6.1. Introduction

To investigate the chromatin modifiers altering Temozolomide response in GBM cells, we screened a CRISPR/Cas9 based library (EPIKOL) with TMZ treatment on U373 and TMZR cell lines.

EPIKOL (**Epi**genetic **K**nock-**O**ut **L**ibrary) was designed in Koç University as a collaborative effort of Dr. Tamer Önder, Dr. Tuğba Bağcı-Önder, Dr. Nathan Lack and their graduate students Can Aztekin, Fidan Şeker and Ezgi Özyerli-Göknar. The library is composed of 247 different chromatin modifiers that target domain exons of various chromatin remodelers (**Table 6.1**)

Table 6.1 Contents of EPIKOL

Target Molecule	
Chromatin	24
Histone	201
DNA	20

Function	
Chromatin remodelling	43
Eraser	42
Writer	104
Reader	39
DNA modification	8
Histone chaperone	3

Modification	
DNA methylation	3
DNA hydroxymethylation	3
DNA demethylation	1
Histone acetylation	34
Histone deacetylation	14
Histone methylation	61
Histone demethylation	20
Histone ubiquitination	17
Histone deubiquitination	3
Histone phosphorylation	1
Histone citrullination	1

6.1.1. Histone methylation/demethylation in GBM

Histone methylation is catalyzed by the histone-lysine methyltransferases (HMTs), and is reversed by the histone-lysine demethylases (KDMs). Methylation of the histone controls the regulation of gene expression; trimethylation of H3K4, H3K36, and H3K79 is a representative marker for active transcription. In contrast, mono-methylation of H4K20, di-/tri-methylation of H3K9, and tri-methylation of H3K27 indicate heterochromatin, hence the related gene being turned off [190].

Currently, little is known about the mechanisms that deregulate histone methylation in GBM. In pediatric gliomas, frequent mutations in the gene H3F3a, which encodes replication-independent histone 3 variant H3.3, are seen. Patients with H3F3A G34 mutation are characterized by high rates of mutation in *TP53*, *ATRX* and *DAXX*

genes, high levels of alternative lengthening of telomeres activity and DNA hypomethylation, thus enhancing gliomagenesis [191].

Drug resistance is indicated to be linked to histone methylation and demethylation status. KDMs are a complex class of proteins, subdivided into amine oxidase and the Jumonji domain-containing protein families (JmjC)[101,192].

6.1.1.1. KDM5A

KDM5A (JARID1A) is a member of JmjC protein family and regulates lysine 4 of histone H3. It is involved in the regulation of p53 activity, and thus indirectly targets p21 activity [193].

KDM5A is highly expressed in lung cancer, hematopoietic cancer, gastric cancer, hepatocellular carcinoma and GBM (**Figure 6.1**) [191,194]. In addition, in 2015, Banelli and colleagues published an article on the role of KDM5A and TMZ resistance in GBM. They showed that KDM5A is transiently expressed at high levels in their established TMZ resistant cell line model derived from a human GBM cell line and also in GSC primary cultures derived from human tumors. When they overexpress KDM5A they obtained significant rises of TMZ resistance and decrease level of apoptosis [195]. In their follow up paper on 2017, they inhibited KDMs with small molecule inhibitors, JIB-04 and CPI-455 and seen preferential inhibition proliferation of TMZ-resistant GBM cells [196]. Thus, the role of KDM5A in GBM and TMZ resistance is interesting to study.

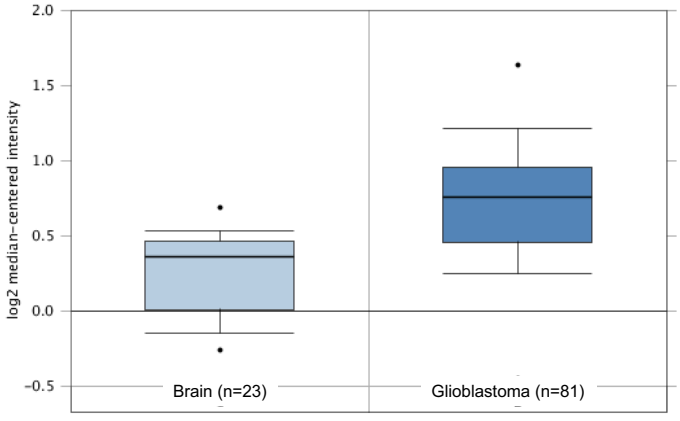

Figure 6.1 KDM5A Expression in Sun Brain Glioblastoma cohort vs. Normal Brain, p-value 1.01E-8, fold change 1.4. Data obtained from Oncomine [197].

Another article published in 2018, compared the levels of KDM5A in primary glioma with metastatic glioma and detected metastatic glioma had decreased KDM5A. Lower levels of KDM5A was also linked to poor survival and increase in invasive abilities [198].

Thus, the role of KDM5A can be controversial in GBM cell proliferation, migration and drug response, so further studies are necessary.

6.1.1.2. CREBBP/P300

Acetylation of lysine residues at histone tails is catalyzed by histone acetyl transferases (HATs). Acetyl groups neutralize the positive charge of lysines, resulting in a loose DNA-nucleosome association that increases DNA accessibility for transcription factors, thus related with activation. CREBBP (KAT3A) and EP300 (KAT3B) the function of TP53, RB, E2F and MYB proteins, which play important roles in tumorigenesis [199].

CREBBP and EP300 loss-of-function mutations were identified in various human cancers such as leukemia [200], colon, breast and ovarian cancers [201]. Inactivation of CREBBP and KAT3A was linked to tumorigenesis and drug resistance in acute lymphoblastic leukemia [202].

H3K18 hypoacetylation is associated with an increased risk of tumor recurrence in patients with low-grade prostate cancer [203], and this histone modification was suggested to be involved in acquired drug resistance. In contrast, studies in esophageal squamous cell carcinoma [204] and glioblastoma [205] patients correlated H3K18 hypoacetylation with better prognosis, suggesting that H3K18ac status may affect tumorigenesis or drug sensitivity in a cell-type-dependent manner.

6.2. Materials & methods

6.2.1. Generation of EPIKOL library and screen strategy

Briefly gRNAs were designed to target DNA sequences encoding the catalytic or critical domains of 247 chromatin modifiers. For this, DNA sequences of protein domains from NCBI Unigene software and used CCTop to design gRNAs [206]. In cases where no gRNA with these criteria were found, gRNA sequences from GeCKO library that target 5' first coding exon of genes were taken [207]. For each gene, 5-10 gRNAs were designed and 80 non-targeting gRNAs from GeCKO Library was added to the library. The list of gRNAs is indicated in **Table 6.5.** The library was cloned into LentiCrisprV2 vector [147] which contains both gRNA and Cas9 enzyme. Library preparation and cloning was performed by Dr. Tamer Önder.

The library was packaged by standard virus packaging techniques [208]. Briefly 293T HEK cells was transfected by Fugene transfection agent (Promega) with EPIKOL plasmid, pMD2.D (VSV-G) and pCMV-dR8.2 (gag/pol/rev). After 36 hours virus supernatant was collected for 2 days, filtered and stored at -80°C.

In positive selection screens, a strong selective pressure is introduced that only cells with survival-enhancing perturbation remains after selection [209]. Thus, for TMZ EPIKOL screen a dosage/treatment that kills more than >90% of the control groups was selected. After selection most gRNAs will be depleted due to treatment, and only a small number of cells that contains gRNA providing the protective mutation survived and proliferated.

U373 and TMZR cells were transduced with low multiplicity of infection (MOI= 0.4) to ensure single gRNA per cell. To preserve the variability of all gRNA in EPIKOL (n=1718 gRNAs) each set consisted of at least 687’200 cells. Non-infected cells were selected by puromycin (2 ug/ml) for 3 days. Afterwards cells are grown in culture for 18 days for Cas9 activity. Previously, time needed for Cas9 activity expression in U373 was detected by Ezgi Özyerli and Fidan Şeker. After 18 days, for TMZ screen cells are divided into two groups. One group is treated with TMZ (250 μM) for 15 days, which kills the cell population up to 90%. DMSO vehicle control was given alongside. Remaining population and the vehicle control were expanded for 40 days for U373, counted and pellets was collected folds of 687,200 cells. For TMZR collection cells were treated with 250 μM TMZ for 30 days and pellets were collected at this time point (**Figure 6.2**).

Genomic DNA (gDNA) isolation was performed with NucleoSpin® Tissue (Macherey-Nagel) according to manufacturer's instructions. For NGS preparation of the samples nested PCR was performed.

The nested PCR assay included two consecutive PCR amplifications. Briefly, first round of amplification contained outer primer pair (V2-adaptor-F and V2-adaptor-R). 2 μl of the first amplification product was directly transferred to the second-round reaction mixture containing a stagger mix of primers and a different individual index primer for different samples. 100 µl external and internal PCR reactions were prepared by mixing 2 µl dNTP (10 mM), 1 µl Phusion Polymerase, 20 µl 6X GC Buffer, 5 µl Forward Primer (10 μM), 5 µl Reverse Primer (10 μM), 1 µg gDNA (to ensure at least 100x library coverage) and filled with nuclease free water. For internal PCR reaction, primers were changed accordingly, and 2 µl external PCR product without clean-up directly was added instead of 1 µg gDNA. Thermal cycler condition for PCR is: 3 minutes at 95°C for initial denaturation, 30 seconds 95°C, 20 seconds 65°C, 15 seconds 72°C (17x cycle (external PCR) 23x cycle (internal PCR)) for amplification, and 3 minutes at 72°C for final extension. List of primers are indicated in **Table 6.2**

Amplification product was then visualized on 1% agarose gel, and the desired PCR product size (~330 bp) was isolated by NucleoSpin® Gel and PCR Clean-up (Macherey-Nagel) according to manufacturer's instructions. Samples were sequenced at BGI Hong Kong and biostatistical analysis was performed by Tunç Morova.

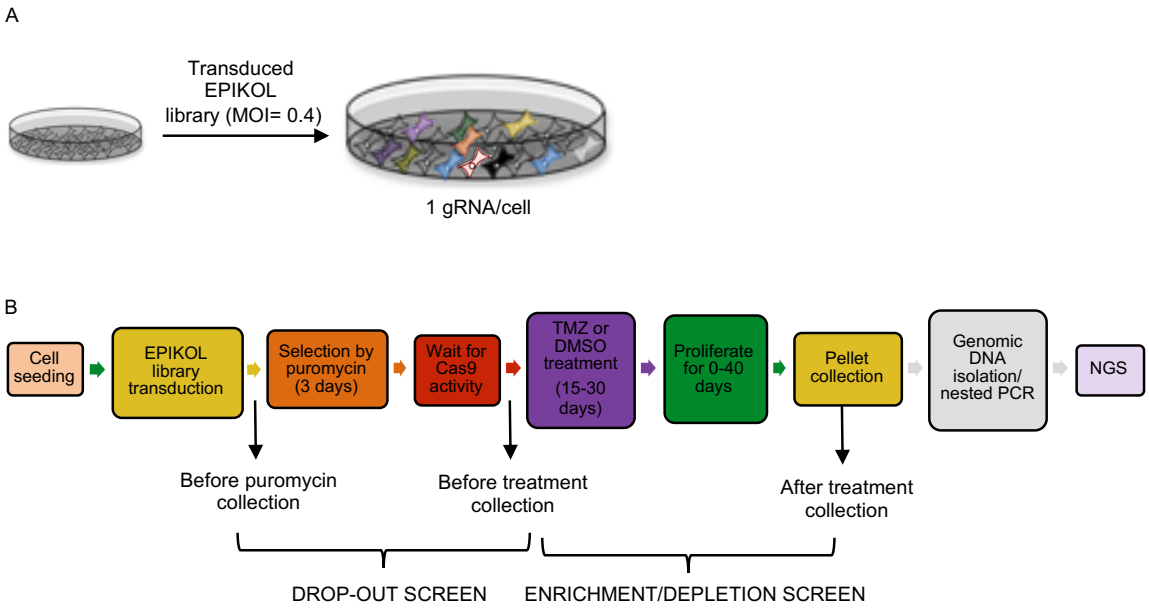

Figure 6.2 Schematics of EPIKOL screen

Table 6.2 Primers used in nested PCR

Primer	Sequence
External Forward Primer	AATGGACTATCATATGCTTACCGTAACTTGAAAGTATTTCG
External Reverse Primer	TCTACTATTCTTTCCCCTGCACTGTTGTGGGCGATGTGCGCTCTG
Forward_stagger1	AATGATACGGCGACCACCGAGATCTACACTCTTTCCCTACACGACGCTCTTCCGATCTATCTTGTGGAAAGGACGAAACACCG
Forward_stagger2	AATGATACGGCGACCACCGAGATCTACACTCTTTCCCTACACGACGCTCTTCCGATCTCTTCTTGTGGAAAGGACGAAACACCG
Forward_stagger3	AATGATACGGCGACCACCGAGATCTACACTCTTTCCCTACACGACGCTCTTCCGATCTGACTCTTGTGGAAAGGACGAAACACCG
Forward_stagger4	AATGATACGGCGACCACCGAGATCTACACTCTTTCCCTACACGACGCTCTTCCGATCTTCGATCTTGTGGAAAGGACGAAACACCG
Forward_stagger5	AATGATACGGCGACCACCGAGATCTACACTCTTTCCCTACACGACGCTCTTCCGATCTATCGCTCTTGTGGAAAGGACGAAACACCG
Forward_stagger6	AATGATACGGCGACCACCGAGATCTACACTCTTTCCCTACACGACGCTCTTCCGATCTGTCAGATCTTGTGGAAAGGACGAAACACCG
Forward_stagger7	AATGATACGGCGACCACCGAGATCTACACTCTTTCCCTACACGACGCTCTTCCGATCTTGCATCGTCTTGTGGAAAGGACGAAACACCG
Forward_stagger8	AATGATACGGCGACCACCGAGATCTACACTCTTTCCCTACACGACGCTCTTCCGATCTCTACGTGATCTTGTGGAAAGGACGAAACACCG
Forward_stagger9	AATGATACGGCGACCACCGAGATCTACACTCTTTCCCTACACGACGCTCTTCCGATCTACTCGTGATTCTTGTGGAAAGGACGAAACACCG
Reverse_index5	CAAGCAGAAGACGGCATACGAGATCACTGTGTGACTGGAGTTCAGACGTGTGCTCTTCCGATCTTCTACTATTCTTTCCCCTGCACTGT
Reverse_index6	CAAGCAGAAGACGGCATACGAGATATTGGCGTGACTGGAGTTCAGACGTGTGCTCTTCCGATCTTCTACTATTCTTTCCCCTGCACTGT
Reverse_index7	CAAGCAGAAGACGGCATACGAGATGATCTGGTGACTGGAGTTCAGACGTGTGCTCTTCCGATCTTCTACTATTCTTTCCCCTGCACTGT
Reverse_index8	CAAGCAGAAGACGGCATACGAGATTCAAGTGTGACTGGAGTTCAGACGTGTGCTCTTCCGATCTTCTACTATTCTTTCCCCTGCACTGT
Reverse_index9	CAAGCAGAAGACGGCATACGAGATCTGATCGTGACTGGAGTTCAGACGTGTGCTCTTCCGATCTTCTACTATTCTTTCCCCTGCACTGT
Reverse_index10	CAAGCAGAAGACGGCATACGAGATAAGCTAGTGACTGGAGTTCAGACGTGTGCTCTTCCGATCTTCTACTATTCTTTCCCCTGCACTGT
Reverse_index11	CAAGCAGAAGACGGCATACGAGATGTAGCCGTGACTGGAGTTCAGACGTGTGCTCTTCCGATCTTCTACTATTCTTTCCCCTGCACTGT
Reverse_index12	CAAGCAGAAGACGGCATACGAGATTACAAGGTGACTGGAGTTCAGACGTGTGCTCTTCCGATCTTCTACTATTCTTTCCCCTGCACTGT
Reverse_index25	CAAGCAGAAGACGGCATACGAGATATCAGT GTGACTGGAGTTCAGACGTGTGCTCTTCCGATCTTCTACTATTCTTTCCCCTGCACTGT
Reverse_index26	CAAGCAGAAGACGGCATACGAGATGCTCATGTGACTGGAGTTCAGACGTGTGCTCTTCCGATCTTCTACTATTCTTTCCCCTGCACTGT
Reverse_index27	CAAGCAGAAGACGGCATACGAGATAGGAATGTGACTGGAGTTCAGACGTGTGCTCTTCCGATCTTCTACTATTCTTTCCCCTGCACTGT
Reverse_index28	CAAGCAGAAGACGGCATACGAGATCTTTTGGTGACTGGAGTTCAGACGTGTGCTCTTCCGATCTTCTACTATTCTTTCCCCTGCACTGT
Reverse_index29	CAAGCAGAAGACGGCATACGAGATAGTTGGTGACTGGAGTTCAGACGTGTGCTCTTCCGATCTTCTACTATTCTTTCCCCTGCACTGT
Reverse_index30	CAAGCAGAAGACGGCATACGAGATCCGGTGGTGACTGGAGTTCAGACGTGTGCTCTTCCGATCTTCTACTATTCTTTCCCCTGCACTGT
Reverse_index31	CAAGCAGAAGACGGCATACGAGATATCGTGGTGACTGGAGTTCAGACGTGTGCTCTTCCGATCTTCTACTATTCTTTCCCCTGCACTGT
Reverse_index32	CAAGCAGAAGACGGCATACGAGATTGAGTGGTGACTGGAGTTCAGACGTGTGCTCTTCCGATCTTCTACTATTCTTTCCCCTGCACTGT

6.2.2. Cloning of KDM5A, CREBBP and EP300 into plentiCRISPRv2 plasmid

Genes indicating in **Table 6.3** targeting gRNAs and cloned into plentiCRISPRv2 backbone according to Zhang Lab's protocol [147] .

Briefly, lentiCRISPRv2 vector was digested with BsmBI Restriction Enzyme and gel purified with MN PCR-Clean Up Kit. Extracted plasmids were treated with Antartic Phosphotase (AP). 1 µl of each oligo (100 μM) was annealed with T4 Polynucleotide Kinase and T4 DNA Ligase Buffer in 10 µl reaction in a thermal cycler with the following settings: 37°C for 30 min, 95°C for 4 min and then ramp down to 25°C at 5°C/min. Oligos were diluted to 1:200 were used as inserts for cloning. 20 µl ligation reactions were prepared with 50 ng BsmBI-digested, AP-treated vectors, 1 µl of inserts and T4 DNA Ligase (NEB) in 10X T4 DNA Ligase buffer (NEB), respectively. Ligation reaction were incubated for 3 hours at room temperature. 50 µl Stbl3 bacteria was mixed with 5 µl of the ligation reaction for 15 minutes on ice. Heat shock was applied at 42°C for 30 seconds. Later, 250 µl Luria-Bertani (LB) broth was supplemented and cultured in 37°C at 225 rpm in a shaker for an hour. The reaction was spread on Carbenicillin resistant plates and incubated overnight at 37°C. Next day colonies were picked individually, grown in LB and plasmid DNA was extracted by MN Nucleospin Plasmid Kit. To confirm the inserts, samples were sent to sequencing to Macrogen Europe with U6 promoter sequencing (Forward sequencing primer for U6 promoter ACTATCATATGCTTACCGTAAC).

Packaging of plasmids were done by HEK 293T cells. Cells were transfected with the envelope protein (VSVG) and Gag-Pol (8.2 dVPR) utilizing FuGENE Transfection Reagent (Promega) in the afternoon. Next morning fresh medium was added. Viruses were collected after 48 and 72 hours of transfection.

6.2.3. T7 Endonuclease assay

Genomic DNA was isolated with MN Nucleospin Tissue Kit. Primers were designed to amplify the cleavage sequence introduced by CRISPR-Cas9 infections from genomic DNA (**Table 6.3**). 800 ng PCR product was used to form heteroduplex by incubation of 5 minutes 95°C; ramp down to 85°C at -2C/s; ramp down to 25°C at -0.1°C /s; hold at 4°C. T7 Endonuclease (NEB) was added to the reaction and incubated at 37 °C for 2 hours. Product cleavage was observed on 1.5% agarose gel.

Table 6.3 Oligos and T7 primers

Name	Sequence	Notes
KDM5A-g1	CACCGCCATGCTCCATTAGCACGTT	epikol_00530 (JARID1A_JMJC_1)
KDM5A-g2	CACCGCTGATGTGCCCAAAGGAGAC	epikol_00538 (JARID1A_PHD_4)
KDM5A-g3	CACCGCCACTACCTGATGTGCCCAA	epikol_00535 (JARID1A_PHD_1)
KDM5A-g4	CACCGACGACTGACCCAAGTGTCAT	GenScipt KDM5A CRISPR Guide RNA 4
KDM5A-g5	CACCGACCTCCCTTCTCTGCTATA	GenScipt KDM5A CRISPR Guide RNA 6
EP300 424 (Bromo)	CACCGCCTTCCCTTTCGTCAACCTG	
EP300 426	CACCGCTGTAATAAGTGGCATCACG	
EP300 428	CACCGCCACAGACACTGTGTTGCTA	
CBP-1	CACCGGCCGGAAAGGTAATGACTCT	
CBP-2	CACCGTGCCGGAAAGGTAATGACTC	
CBP-3	CACCGACAAAAACCTCCCCGGCTTC	
T7_EP300_426&428_F	TCACCTGTGGGTGCAGATTC	
T7_EP300_426&428_R	GCAAACAAAGGCAGAAGGCA	
T7_CBP_g1&g2_F	AAAAGTGACACAAGGCCCCA	
T7_CBP_g1&g2_R	GATGTCACAGCAGCCAGGAT	
T7_CBP_g3_F	CATCCACGCCGTCAATTTCC	
T7_CBP_g3_R	AAACTTCATTCGTGCACCGC	

6.2.4. shRNA cloning of KDM5A

shKDM5A were kind gifts from Dr. Tamer Önder (Koç University). Briefly, Synthetic 97-mer oligonucleotides (Macrogen) were cloned into pSMP plasmid. As a control shRNA, a firefly luciferase targeting shRNA plasmid, pSMP-Luc (shFF, Addgene # 36394) was used. pSMP-Luc (shFF) vector was cut with EcoRI (NEB) and XhoI (NEB) enzymes and treated with AP enzyme. shRNA oligos were amplified with shCloning primers (Forward:5'-GATGGCTGCTCGAGAAGGTATATTGCTGTTGACAGTGAGCG-3', Reverse: 5'-GTCTAGAGGAATTCCGAGGCAGTAGGCA-3') and PCR products were cut with

EcoRI (NEB) and XhoI (NEB) enzymes. After digestion, PCR products were run on a 2% agarose gel. 110bp bands were cut out and purified (Gel extraction kit, MN). Extracted oligos were ligated (Quick Ligase, NEB) into pSMP backbone. Ligation product was transformed into *Stbl3* competent bacteria. All vectors were confirmed by Sanger sequencing using MSCV-fwd primer (5'-CCCTTGAACCTCCTCGTTCGACCT-3').

For retroviral packaging, 293T cells were seeded as $0.3x10^6$ per 6 well plates and next day transfected with shRNA, VSV-G and pUMVC plasmids with Fugene transfection reagent (Promega, USA). The virus containing media was collected for two days, combined, filtered through 0.45 μm filters (Millipore, USA), aliquoted and stored at -80 °C. U87MG or U373 cells were seeded as 0.3x106 per well into 6-well plates. Next day, the cells were infected with 300 μl of viral supernatants and 300 μl complete medium with Protamine Sulfate (10 μg/mL). 2 days later, fresh media with Puromycin (1 μg/mL) was added and the cells were selected for 3 days. Knockdown validations were performed by qRT-PCR.

Table 6.4 List of KDM5A oligos and qRT-PCR primers

Name	Sequence
KDM5A-1 (128)	TGCTGTTGACAGTGAGCGACCTGATCTTCTGCATCAGTTATAGTGAAGCCACAGATGTATAACTGATGCAGAAGATCAGGCTGCCTACTGCCTCGGA
KDM5A-2 (129)	TGCTGTTGACAGTGAGCGCGGACCGCATAGAAGAAGTAAATAGTGAAGCCACAGATGTATTTACTTCTTCTATGCGGTCCATGCCTACTGCCTCGGA
KDM5A-3 (130)	TGCTGTTGACAGTGAGCGACGGACGTTTCTTAAGAAGAATTAGTGAAGCCACAGATGTAATTCTTCTTAAGAAACGTCCGCTGCCTACTGCCTCGGA
KDM5A-qRTPCR-Forward	CCGTCTTTGAGCCGAGTTG
KDM5A-qRTPCR-Reverse	GGACTCTTGGAGTGAAACGAAA

6.2.5. Chemical inhibitors

KDM5-C70 and JIB-O4 was kind gifts from Dr. Udo Oppermann, Oxford University.

6.3. Results & Discussion

To understand which chromatin modifying genes regulate TMZ response in GBM cells lines, U373 and TMZR cells was subjected to EPIKOL. To ensure single gRNA infection per cell infection with low multiplicity of infection (MOI= 0.4). To preserve the variability of all gRNA in EPIKOL (n=1718 gRNAs), as 400 cells per guide, each pellet set consisted of at least 687'200 cells.

Prior to EPIKOL-TMZ screen the TMZ dosage that will be used in screens was detected by trypan blue counting assay in the format of the screen. Cells were seeded in 687'200 cells to a 10 cm plate and DMSO or TMZ was added every day. Each 5th day cells were trypsinized, counted and re-seeded with treatment. 250 μM TMZ was the dosage applied in all the screens, and cells were treated for 15 days with drug renewal each day. Every 5th day cells were trypsinized and re-seeded. At the end of 15 days, U373 cells were viable <10% compared to DMSO treated controls. They were expanded for 40 days. For TMZR screen, cells were treated for 25 days, and experiment was terminated at day 30. Pellets were collected before puromycin selection, before treatment (after Cas9 activity) and after treatment.

Following gDNA isolation from the collected pellets, samples were prepared for Illumina Next Gen sequencing (NGS) with nested-PCR. After second PCR, PCR product was run on 1.5% agarose gel. Representative image can be seen in **Figure 6.3** Gel extraction was performed on the desired PCR product. All these procedures were followed for both screens and samples were sent to BGI Hong Kong for sequencing. Bioinformatical analysis were done by Tunç Morova. Bioinformatic analysis were done between end of experiment, DMSO vehicle vs TMZ treated samples.

In **Figure 6.4** read count distribution values for screen time points is plotted across all samples and their two sets. We can see a gaussian distribution across samples. When we focus on the end point of DMSO vs TMZ treated samples, we observed that (**Figure 6.5**) log2 gRNA counts among DMSO vs TMZ treatments are not drastically differentiated. Hence normalized counts of depleted and enriched guideRNAs among DMSO vs TMZ groups were studied.

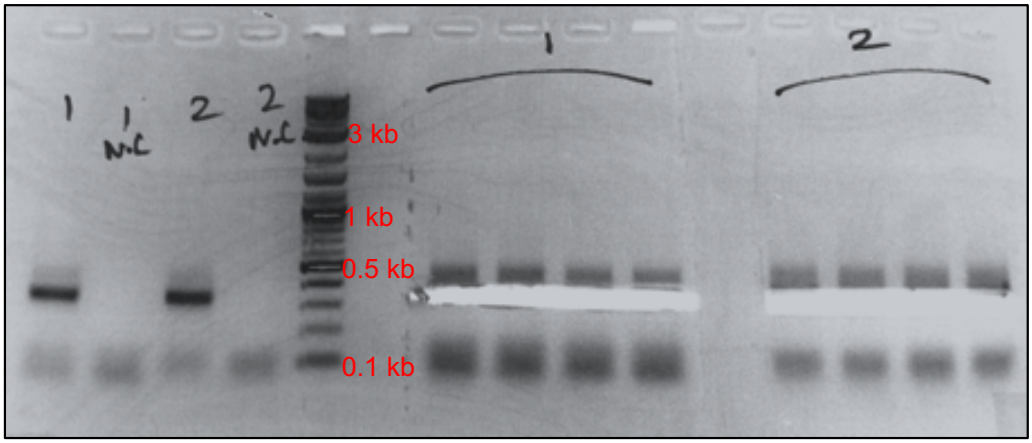

Figure 6.3 Representative gel image of EPIKOL sample preparation for NGS. Right panel, 1 and 2 represent U373 before puro samples with index 1 and 2 respectively. N.C. stands for negative control which do not contain gDNA. Left panel, the desired PCR product size (around 333bp) was cut from the gel and DNA was purified.

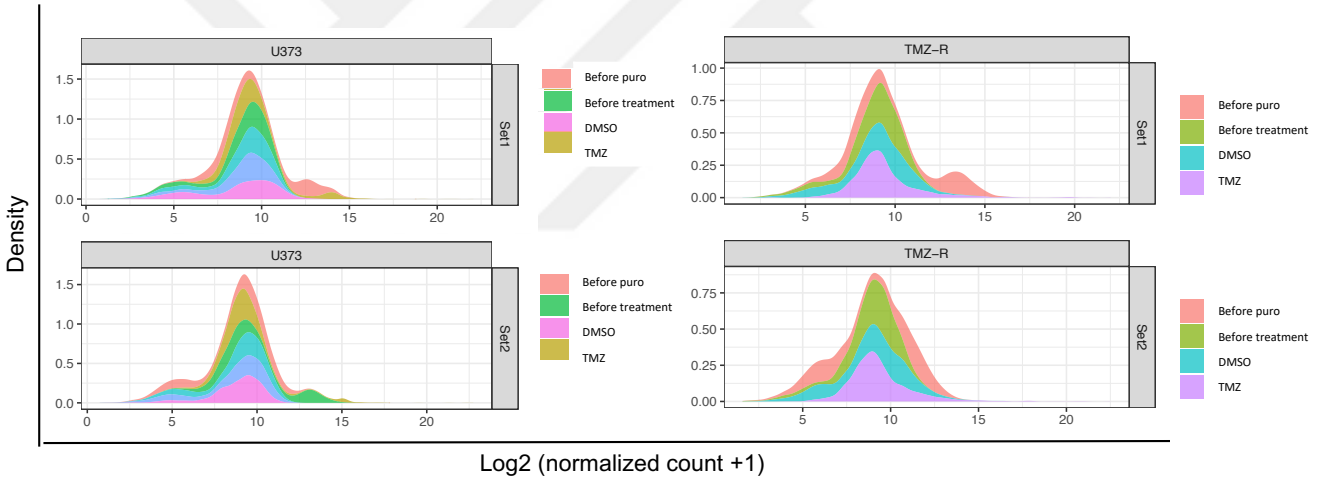

Figure 6.4 Read count distribution for screen time points are plotted.

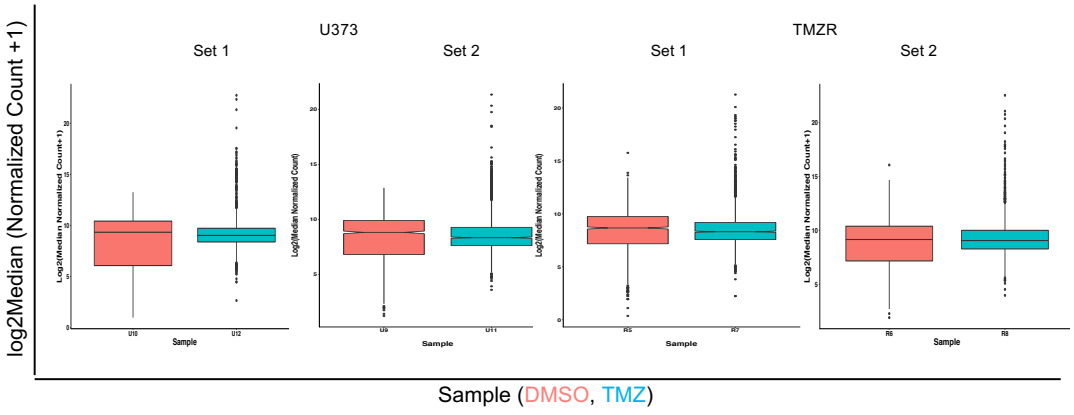

Figure 6.5 Box plot of log2 gRNA counts among DMSO and TMZ treated samples

6.3.1. KDM5A silencing increases TMZ induced cell death

When we look at the U373 EPIKOL screen, we observe that JARID1A (KDM5A) was among the top depleted genes in our TMZ treated samples in both sets when compared to the DMSO vehicle (**Figure 6.6**). KDM5A was found to be depleted in one of the sets of TMZR EPIKOL screen too. Thus, we believe that KDM5A expression can be a potential barrier in TMZ sensitivity in GBM cells.

Recent literature by Banelli *et al*. [140,210] also indicated KDM5A is elevated in their established TMZ resistant A172 cell line and knockdown of KDM5A enhances cell death in GBM cells. However, the mechanism behind this phenomenon is not known. Hence KDM5A is a promising target to study.

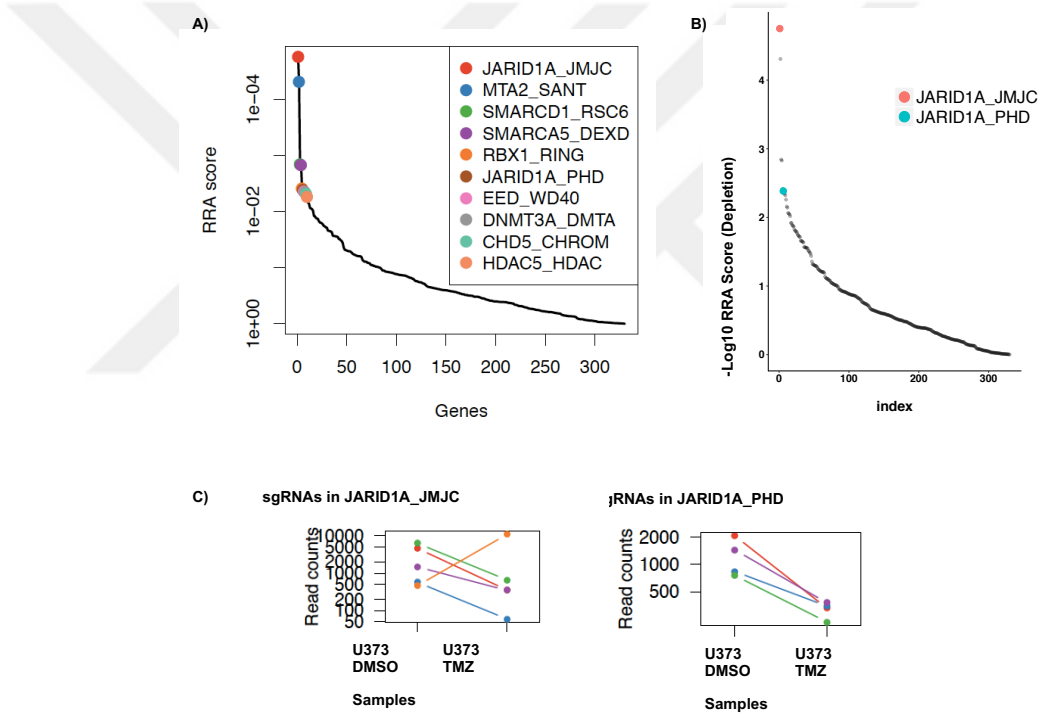

Figure 6.6 KDM5A is among top hits of U373 depletion screen A) Distribution of depleted RRA scores in set 1 of U373 TMZ treated vs U373 DMSO day 55. **B)** JARID1A (KDM5A) was a top hit in U373 depletion screen. **C)** gRNA distribution of JMJC and PHD targeting guides.

We have chosen 3 best working guide RNAs from EPIKOL library (1 targeting JMJC domain, 2 targeting PHD), and 2 more from Genscript. U373 cells were transduced with these KDM5A targeting guideRNA containing plentiCRISPRv2 plasmids and after Cas9 activation, the effect on TMZ response was detected. We have seen significant sensitization to TMZ at 125 μM for U373 cells (**Figure 6.7**).

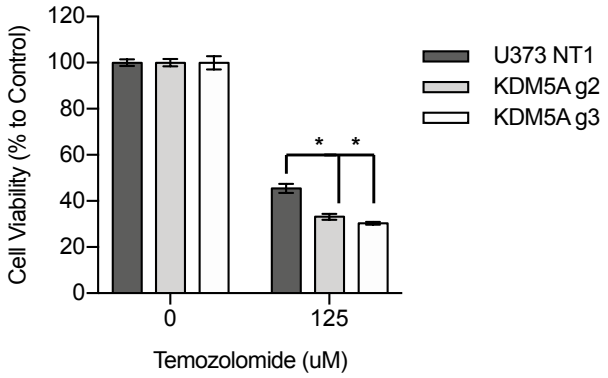

Figure 6.7 KDM5A silencing induces TMZ sensitivity on U373 cells. Viability was detected by CTG after 5 days of treatment. T-test to TMZ treated non-targeting control (NT1) was performed. * denotes $p<0.05$.

In parallel, KDM5A was also knockdown in U373 by 3 different shRNAs. We have checked TMZ response via clonogenic assay; and seen sh128 and U373 sh130, when compared to shControl, at 10 and 25 μM of TMZ, colony area was detected to significantly decrease (**Figure 6.8**).

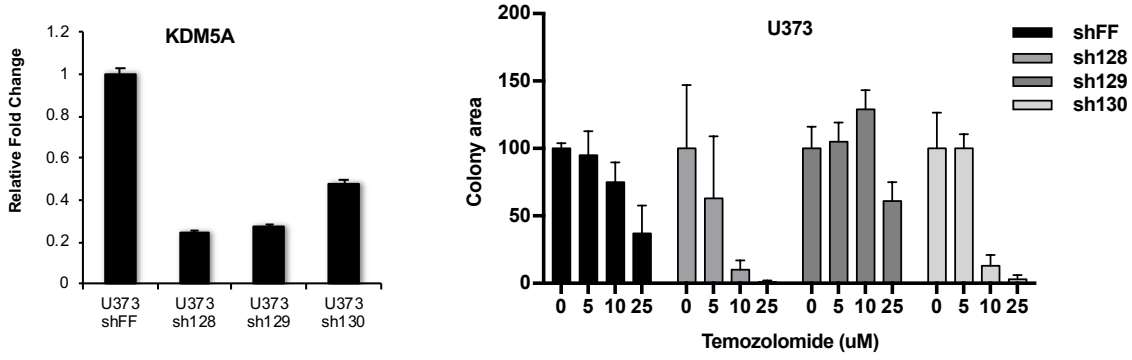

Figure 6.8 U373 KDM5A knockdown cells (sh128, sh129 and sh130) was generated and validated by qRT-PCR. Colony formation assay of TMZ treated U373 KDM5A KD cells.

Lastly, we have inhibited KDM5 with a selective chemical inhibitor KDM5-C70 [211] on U373, DE-TMZR and TMZR cell lines. However, we did not observe significant cell death even at 10 μM. JIB-O4 [210,211] is a pan-Jumonji histone demethylase inhibitor with lower IC_{50} tendency towards KDM5A. It also targets JMJD2E, JMJD2B, JMJD2A, JMJD3 and JMJD2C. When we treated our cells with JIB-O4 we have seen 40% decrease in cell viability at 10 μM for U373, and 70% for DE-TMZR and TMZR (**Figure 6.9**).

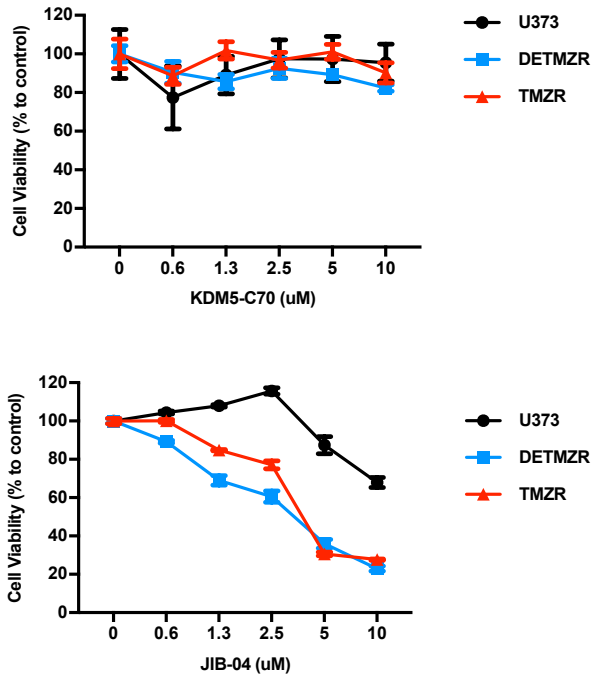

Figure 6.9 Cell viability results of KDM inhibition. Cells were treated with KDM5-C70 or JIB-O4 for 3 days.

Our preliminary work on KDM5A is consistent with literature regarding TMZ sensitization capacities. We have seen for U373 cells, silencing of KDM5A by CRISPR or shRNAs increased cell death upon TMZ treatment. However, further studies are necessary regarding the role of KDM5A in our established resistant models.

1.1.1. EP300 has a role in TMZ resistance

To define TMZ resistance causing genes, we have performed an enrichment screen on TMZR cells. Looking at guide distribution scores of TMZR screen set 1, EP300 bromodomain targeting gRNAs and EP300 RING domain targeting gRNAs scored at the top, alongside CREBBP Bromodomain targeting gRNAs (**Figure 6.10**).

To investigate the role of CREBBP (CBP) and EP300 on TMZ response, we have knocked out CBP or EP300 genes in U373 parental cell line. T7 endonuclease assay shows the DNA cleavages (**Figure 6.11A,B**). We then performed a clonogenic assay on U373 with TMZ treatment and observed increase in colony area with CBP or EP300 knockout cells (**Figure 6.11C**).

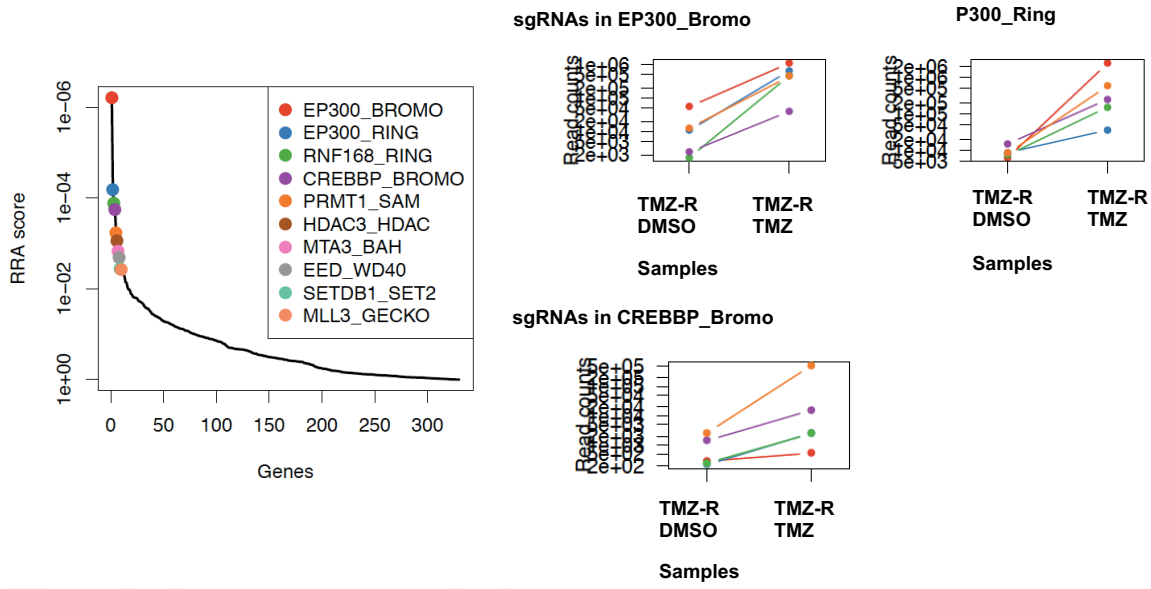

Figure 6.10 Distribution of enriched RRA scores in TMZ-R TMZ treated vs TMZ-R DMSO day 30.

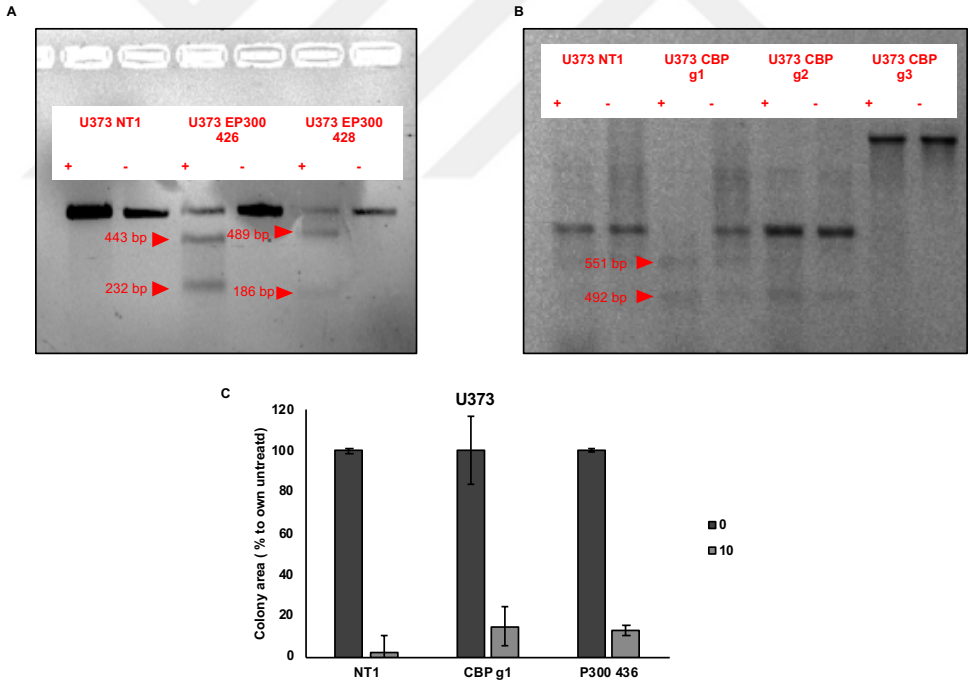

Figure 6.11 Silencing of CBP or EP300 enhances TMZ resistance. A, B) T7 Endonuclease assay + indicates the presence of T7 endonuclease enzyme whereas – indicates absence. **C)** Clonogenic assay performed on CBP and P300 knockout U373 cells.

Lastly, to investigate the inhibition of CREBBP and EP300, we treated U373 and TMZR cells with SGC-CBP30 [212], a Bromodomains inhibitor targeting both CREBBP,

EP300. Long term proliferation assay by clonogenic assay has shown that with SGC-CBP30 treatment colony area increases (**Figure 6.12**).

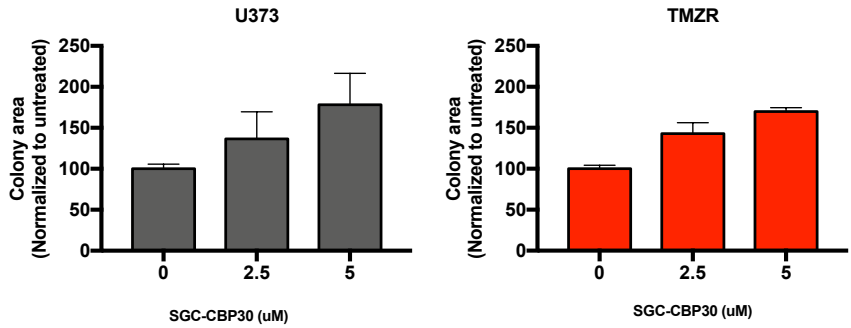

Figure 6.12 Clonogenic assay of cells treated with SGC-CBP30, a CREBBP/EP300-selective chemical probe.

In sum, we have preliminary data on the role of CREBBP/EP300 and TMZ resistance in GBM cell lines. Our work has shown that H3K18ac is elevated in DE-TMZR and TMZR cells compared to U373 (**Figure 3.23**), which is suggested to have a role in drug resistance in GBM. In addition, a paper published in 2016, have linked RBBP4 as a modulator of TMZ sensitivity through regulation of MGMT and RAD51 DNA repair proteins. They have shown that RBBP4 interacts with CREBBP/EP300 to form a chromatin-modifying complex that binds within the promoter of MGMT and RAD51 [213]. Thus, targeting these epigenetic regulator genes for TMZ sensitization might be a good target for therapy strategies.

Table 6.5 List of EPIKOL gRNAs

ID	Gene.ID	Sequence
epikol_00001	ACAT1_AT_1	GCTTGGTTCCATTGCAATTC
epikol_00002	ACAT1_AT_2	AGTGCTACAAGAACACCCAT
epikol_00003	ACAT1_AT_3	TGCAATGGAACCAAGCTTAG
epikol_00004	ACAT1_AT_4	ATGGAACCAAGCTTAGTGGC
epikol_00005	ACAT1_AT_5	CTGCCTAAAAAAGATCCAAT
epikol_00006	ACTL6B_1	TCAGTCCGCGCTGGGTACGC
epikol_00007	ACTL6B_2	CAGTCCGCGCTGGGTACGCT
epikol_00008	ACTL6B_3	GGCTCCTTCTCAGTCCGCGC
epikol_00009	ACTL6B_4	GCTCCTTCTCAGTCCGCGCT
epikol_00010	ACTL6B_5	AGTCCGCGCTGGGTACGCTG
epikol_00011	ACTR_PAS_1	TGTCTGGTAATAAAGCTCTC
epikol_00012	ACTR_PAS_2	GCTTTGAAGATATAATCCGA
epikol_00013	ACTR_PAS_3	CGGATTATATCTTCAAAGCC
epikol_00014	ACTR_PAS_4	TTCTTGATAGTGACGTTTCT
epikol_00015	ACTR_PAS_5	GTCTAAATGATGGGCAGTCA
epikol_00016	ASH1_BROMO_1	CTTTGAAGATCTGGGCTAGG
epikol_00017	ASH1_BROMO_2	TTTCTTTGAAGATCTGGGCT
epikol_00018	ASH1_BROMO_3	CACAAATTTCTTTGAAGATC
epikol_00019	ASH1_BROMO_4	ACAAATTTCTTTGAAGATCT
epikol_00020	ASH1_BROMO_5	TTTGAAGATCTGGGCTAGGC
epikol_00021	ASH1_SET_1	TCTAGAACGATTTCGAGCTG

epikol_00022	ASH1_SET_2	AGGGGAGGTCGTCAGTGAAC
epikol_00023	ASH1_SET_3	GTTCACTGACGACCTCCCCT
epikol_00024	ASH1_SET_4	CATCATTGAATACCTAGGGG
epikol_00025	ASH1_SET_5	GTTCATCATTGAATACCTAG
epikol_00026	ASH2L_PHD_1	TGGTTCACGGCTGACACATT
epikol_00027	ASH2L_PHD_2	GAAGAGAATGGCCGACAGTT
epikol_00028	ASH2L_PHD_3	TGAAGAGAATGGCCGACAGT
epikol_00029	ASH2L_PHD_4	GAATGGCCGACAGTTGGGTG
epikol_00030	ASH2L_PHD_5	GCTCTACCTCACCCAACTGT
epikol_00031	ASH2L_SPRY_1	GCCTCTCATGGAGTACGGAA
epikol_00032	ASH2L_SPRY_2	CCCAGTCTGGCAGCGGTATC
epikol_00033	ASH2L_SPRY_3	ACCTTTCCGTACTCCATGAG
epikol_00034	ASH2L_SPRY_4	CTCAGATGACCGGCTGACTG
epikol_00035	ASH2L_SPRY_5	AGTCTGGCAGCGGTATCTGG
epikol_00036	ASXL1_PHD_1	CTTTCAGGCTGCACGCACAC
epikol_00037	ASXL1_PHD_2	TTCTGTCACGATGACTGTAT
epikol_00038	ASXL1_PHD_3	GTTCACTGACAGCAGCACGG
epikol_00039	ASXL1_PHD_4	GACAGAACGCACCGCAGCCT
epikol_00040	ASXL1_PHD_5	AAAGCCATGATCATGTGCCA
epikol_00041	ASXL2_PHD_1	TCTTCGGAGAACGCCTGAAC
epikol_00042	ASXL2_PHD_2	ACGCCTGAACAGGAATGGTC
epikol_00043	ASXL2_PHD_3	AGGGGCCGATGCAATCATCA
epikol_00044	ASXL2_PHD_4	GCAGGAGACGCACAGTTTGG
epikol_00045	ASXL2_PHD_5	AAGCGGCAGTAACATTTCGA
epikol_00046	ASXL3_PHD_1	AAGGACCTATGCAGTCGTCA
epikol_00047	ASXL3_PHD_2	TTCTGCCATGACGACTGCAT
epikol_00048	ASXL3_PHD_3	CTGTCGGCAAAGTTCTGAAC
epikol_00049	ASXL3_PHD_4	TATGCAGTCGTCATGGCAGA
epikol_00050	ASXL3_PHD_5	AATCCTGCCACAGGCTTGTC
epikol_00051	ATAD2_BROMO_1	CAACAGGCTTAGTAAACACT
epikol_00052	ATAD2_BROMO_2	TCTTAAGAAATGTTACACAT
epikol_00053	ATAD2_BROMO_3	TACAATCCAGATAGAGATCC
epikol_00054	ATAD2_BROMO_4	ATTACAGATGAAAGGTCCAT
epikol_00055	ATAD2_BROMO_5	TCTATCTGGATTGTATTCTA
epikol_00056	ATAD2B_BROMO_1	TAACATCTTCAGCAAACCGG
epikol_00057	ATAD2B_BROMO_2	GAGAGTTGCGGTTGTTTCTC
epikol_00058	ATAD2B_BROMO_3	TTCTCAGGGATGTAACCAAG
epikol_00059	ATAD2B_BROMO_4	CAGGGATGTAACCAAGAGGC
epikol_00060	ATAD2B_BROMO_5	GATGTTAAAGCGTTTATCTG
epikol_00061	ATRX_HELIC_1	TGAAATTCTTCGAATGGCAG
epikol_00062	ATRX_HELIC_2	TTCGAATGGCAGAGGAAATT
epikol_00063	ATRX_HELIC_3	CTTCGAATGGCAGAGGAAAT
epikol_00064	ATRX_HELIC_4	TCTCTTTGAAATTCTTCGAA
epikol_00065	ATRX_HELIC_5	TCGAATGGCAGAGGAAATTG
epikol_00066	BAZ1A_BROMO_1	CGAAGGAGTTCTGGCCGACA
epikol_00067	BAZ1A_BROMO_2	TGGTACGACATGATGACAGC
epikol_00068	BAZ1A_BROMO_3	AGGAGTTCTGGCCGACAGGG
epikol_00069	BAZ1A_BROMO_4	ATTCATGAACTCCTCCCTGT
epikol_00070	BAZ1A_BROMO_5	TGAACAACTTGTTGTAGAAT
epikol_00071	BAZ1A_PHD_1	GAGCTTTGGTCGAACACAGT
epikol_00072	BAZ1A_PHD_2	TGCAAGATATGTCGAAAGAA
epikol_00073	BAZ1A_PHD_3	CTTTGTGATGGCTGTGATAG
epikol_00074	BAZ1A_PHD_4	TTCTTTGTGATGGCTGTGAT
epikol_00075	BAZ1A_PHD_5	GAAAACATGGTTCTTTGTGA
epikol_00076	BAZ1B_BROMO_1	AGCGGTACTTCACGATCTTG
epikol_00077	BAZ1B_BROMO_2	TCGTGAAGTACCGCTTCAGC
epikol_00078	BAZ1B_BROMO_3	GGTACTTCACGATCTTGTGG
epikol_00079	BAZ1B_BROMO_4	GCTGAGGTTTACAACTGCCG
epikol_00080	BAZ1B_BROMO_5	TGATGTGATCACGCACCCCA
epikol_00081	BAZ2A_BROMO_1	CTCACCAAACGTGGGTTCAC
epikol_00082	BAZ2A_BROMO_2	CGGTACCCACTCACCAAACG
epikol_00083	BAZ2A_BROMO_3	TGAACCCACGTTTGGTGAGT
epikol_00084	BAZ2A_BROMO_4	GGTACCCACTCACCAAACGT
epikol_00085	BAZ2A_BROMO_5	GTGAACCCACGTTTGGTGAG
epikol_00086	BAZ2A_MBD_1	CCTGGTATTATGGCCCCTGT
epikol_00087	BAZ2A_MBD_2	CCCACAGGGGCCATAATACC
epikol_00088	BAZ2A_MBD_3	AGGTCTCCCCCTGCCATCGG
epikol_00089	BAZ2A_MBD_4	GAGAGAGGTGCGCATCAAGA
epikol_00090	BAZ2A_MBD_5	GAAGGGCAGCCACCGATGGC
epikol_00091	BAZ2B_BROMO_1	GTAAACTTGAAACTTGTTCC

epikol_00092	BAZ2B_BROMO_2	TGGAAACTCATGAGGATGCA
epikol_00093	BAZ2B_BROMO_3	GGAACAAGTTTCAAGTTTAC
epikol_00094	BAZ2B_BROMO_4	CTAATTGTGGAAAAATCCAT
epikol_00095	BAZ2B_BROMO_5	ACTTAGTTTCTCTCTAATTG
epikol_00096	BAZ2B_HMBD_1	AACTTTGGAGGGCGCCTTCA
epikol_00097	BAZ2B_HMBD_2	GTAGCATATTATGCTCCATG
epikol_00098	BAZ2B_HMBD_3	AATATGCTACTTCTCCTTGA
epikol_00099	BAZ2B_HMBD_4	CTCCATGTGGAAAGAAACTT
epikol_00100	BAZ2B_HMBD_5	TGCCTAAGTTTCTTTCCACA
epikol_00101	BMI_RING_1	TAGACATTCTATTATGGTTG
epikol_00102	BMI_RING_2	GGAATGTAGACATTCTATTA
epikol_00103	BMI_RING_3	AACGTGTATTGTTCGTTACC
epikol_00104	BMI_RING_4	GACAATACTTGCTGGTCTCC
epikol_00105	BMI_RING_5	ACAAATAGGACAATACTTGC
epikol_00106	BPTF_BROMO_1	GGATTATGAGGGGTTGAAGA
epikol_00107	BPTF_BROMO_2	AGGATTATGAGGGGTTGAAG
epikol_00108	BPTF_BROMO_3	GGTGCATCATTAGGGTCTAC
epikol_00109	BPTF_BROMO_4	CATTAGGGTCTACTGGTTCA
epikol_00110	BPTF_BROMO_5	GAAAGGCCAGGCCATCTTAT
epikol_00111	BPTF_GECKO_3	GTTCCGCAGTACCTCGTAAA
epikol_00112	BPTF_GECKO_4	ACGCTATCTTTCAGATCAGC
epikol_00113	BPTF_GECKO_5	ACCATTAGCTGCCGCCAGAA
epikol_00114	BPTF_PHD_1	TGGTACCATGGGCGCTGCGT
epikol_00115	BPTF_PHD_2	AGATGCCAACGCAGCGCCCA
epikol_00116	BRD1_BROMO_1	GCTGCGCAAATATCCTGGCG
epikol_00117	BRD1_BROMO_2	TGCGCAGCCCGTGAGTCTGA
epikol_00118	BRD1_BROMO_3	GGGCTGCGCAAATATCCTGG
epikol_00119	BRD1_BROMO_4	TGCAAGACAAGGACCCCGCC
epikol_00120	BRD1_BROMO_5	GAGCGCAGCAGCACCGTCAG
epikol_00121	BRD1_PHD_1	AAAAGACAGATGACGACCGC
epikol_00122	BRD1_PHD_2	GTGTTCATCGAGCCCATCGA
epikol_00123	BRD1_PHD_3	GGGCTCGATGAACACCGTGT
epikol_00124	BRD1_PHD_4	AAAGACAGATGACGACCGCT
epikol_00125	BRD1_PHD_5	TGTTCATCGAGCCCATCGAT
epikol_00126	BRD2_BROMO_1	ATCAGTTCGCATGGCCATTC
epikol_00127	BRD2_BROMO_2	TGTGGAAACATCAGTTCGCA
epikol_00128	BRD2_BROMO_3	CCTTGTGTAGGTATTGCAGC
epikol_00129	BRD2_BROMO_4	GCCTGTGGATGCTGTCAAAC
epikol_00130	BRD2_BROMO_5	CCTGTGGATGCTGTCAAACT
epikol_00131	BRD3_BROMO_1	ATTTGATTGCGTCCACGGGC
epikol_00132	BRD3_BROMO_2	TTCAATTTGATTGCGTCCAC
epikol_00133	BRD3_BROMO_3	GTTCAATTTGATTGCGTCCA
epikol_00134	BRD3_BROMO_4	TCTGGAAACACCAGTTCGCC
epikol_00135	BRD3_BROMO_5	TGCGTCCACGGGCTGGTAGA
epikol_00136	BRD4_BROMO_1	TTCAGCTTGACGGCATCCAC
epikol_00137	BRD4_BROMO_2	GAGTGGTGCTCAAGACACTA
epikol_00138	BRD4_BROMO_3	GCTGGAAAGGCCATGCAAAC
epikol_00139	BRD4_BROMO_4	CTCTGAGCAGGTATTGCAGT
epikol_00140	BRD4_BROMO_5	GAGCAGGTATTGCAGTTGGT
epikol_00141	BRD7_GECKO_1	AACTGATGAGACAATTGCAG
epikol_00142	BRD7_GECKO_2	GTTATTCCAACCTTCTTGTT
epikol_00143	BRD7_GECKO_3	AGCTCTTTAGCCAAACAAGA
epikol_00144	BRD7_GECKO_4	AGTTACCTTTAGTTCTTCTA
epikol_00145	BRD7_GECKO_5	GTTGATTCAAAGCTTCTTGA
epikol_00146	BRD8_BROMO_1	AGCTCTCCATACAAGCATGA
epikol_00147	BRD8_BROMO_2	GTTACAGATGACATAGCACC
epikol_00148	BRD8_BROMO_3	GGTGCTATGTCATCTGTAAC
epikol_00149	BRD8_BROMO_4	TGTCATCTGTAACAGGCTGC
epikol_00150	BRD8_BROMO_5	TGCACAATGCTGTGGTAGCC
epikol_00151	BRD9_BROMO_1	GCTGGCGGAGGAAGTGTTCC
epikol_00152	BRD9_BROMO_2	TGTTCCAGGAGTTGCTGAAT
epikol_00153	BRD9_BROMO_3	GGAGCAATTGCATCCGTGAC
epikol_00154	BRD9_BROMO_4	GTCACGGATGCAATTGCTCC
epikol_00155	BRD9_BROMO_5	TTCATGGTGCCAAAATCCAT
epikol_00156	BRDT_BROMO_1	ATGGCCCTTTCAACGTCCTG
epikol_00157	BRDT_BROMO_2	GCATCCACAGGACGTTGAAA
epikol_00158	BRDT_BROMO_3	AGCATCCACAGGACGTTGAA
epikol_00159	BRDT_BROMO_4	TGTAGTTTCACAGCATCCAC
epikol_00160	BRDT_BROMO_5	AAGTTGTCCTAAAGGATTTA
epikol_00161	BRPF1_BROMO_1	CTGCCTCAAGTATAACGCCA

epikol_00162	BRPF1_BROMO_2	TCTGTCTGAGGTAACCGAAT
epikol_00163	BRPF1_BROMO_3	TTGATGTGGTCTAGGTAGTC
epikol_00164	BRPF1_BROMO_4	AGGCAACATCTTCAGCGAGC
epikol_00165	BRPF1_BROMO_5	CATCCTCCTTCGCAAAACCT
epikol_00166	BRPF1_PHD_1	AGCAGACAGATGACGGGCGC
epikol_00167	BRPF1_PHD_2	GCAGACAGATGACGGGCGCT
epikol_00168	BRPF1_PHD_3	ACCGCCCTTGTTGGGGCACA
epikol_00169	BRPF1_PHD_4	TTTGCAAACAACGGGGCTCA
epikol_00170	BRPF1_PHD_5	ATTTGCAAACAACGGGGCTC
epikol_00171	BRPF3_BROMO_1	TGTTCTGTTGAGGACAACAC
epikol_00172	BRPF3_BROMO_2	GACAACACTGGACCTGCTGC
epikol_00173	BRPF3_BROMO_3	GTCCTCAACAGAACATTGAA
epikol_00174	BRPF3_BROMO_4	CAGGATCCTTCTCCTGCAGC
epikol_00175	BRPF3_BROMO_5	ACTGGACCTGCTGCAGGAGA
epikol_00176	BRPF3_PHD_1	TTGAGGCTGGTTTCGCGCAT
epikol_00177	BRPF3_PHD_2	ATTGAGGCTGGTTTCGCGCA
epikol_00178	BRPF3_PHD_3	TTGAAGGCGCCACCCTTATT
epikol_00179	BRPF3_PHD_4	ACAATATCCCGCCTGCCCGC
epikol_00180	BRPF3_PHD_5	CGCCACCCTTATTGGGGCAA
epikol_00181	BRWD1_BROMO_1	GGATATTCAACCAAATCAAC
epikol_00182	BRWD1_BROMO_2	ATTTAGACAACCTGTTGATT
epikol_00183	BRWD1_BROMO_3	AAATCAACAGGTTGTCTAAA
epikol_00184	BRWD1_BROMO_4	CAACTGGAAGAAACAGTGTA
epikol_00185	BRWD1_BROMO_5	GTAAGGGAAACTCTAGATGC
epikol_00186	BRWD3_BROMO_1	AGAATGTGAACGGGTTATTC
epikol_00187	BRWD3_BROMO_2	CCGTTCACATTCTTCGTCTC
epikol_00188	BRWD3_BROMO_3	GAATGTGAACGGGTTATTCA
epikol_00189	BRWD3_BROMO_4	CAGAGACGAAGAATGTGAAC
epikol_00190	BRWD3_BROMO_5	CAAACCCCAGGAAGGAGAGT
epikol_00191	CARM1_MTA_1	AGCACGGAAAATCTACGCGG
epikol_00192	CARM1_MTA_2	ACGGAAAATCTACGCGGTGG
epikol_00193	CARM1_MTA_3	CTTGGGCGGCAAAAAACGAC
epikol_00194	CARM1_MTA_4	TGGAGCACGGAAAATCTACG
epikol_00195	CARM1_MTA_5	TGACCACGATGCGGTCCGTC
epikol_00196	CBX1_GECKO_1	GGCCGACTCACCATTTCATC
epikol_00197	CBX1_GECKO_2	AAAAGTTCTCGACCGTCGAG
epikol_00198	CBX1_GECKO_3	CTTTGCCCTTTACCACTCGA
epikol_00199	CBX1_GECKO_4	CTGCAGGAAAAACTCTGATG
epikol_00200	CBX1_GECKO_5	TTACAGTCAGAAAAGCCACG
epikol_00201	CBX2_CHROM_1	ACCTGGTCAAGTGGCGCGGC
epikol_00202	CBX2_CHROM_2	GAGTACCTGGTCAAGTGGCG
epikol_00203	CBX2_CHROM_3	ACCAGCCGCGCCACTTGACC
epikol_00204	CBX2_CHROM_4	GGAAGGCCAGGAGCAGCCTC
epikol_00205	CBX2_CHROM_5	TGGAAGGCCAGGAGCAGCCT
epikol_00206	CBX3_GECKO_1	AACACAGTGCTGACAATACT
epikol_00207	CBX3_GECKO_2	AGACTTGGTGCTGGCGAAAG
epikol_00208	CBX3_GECKO_3	AAACAGGCTGACAAACCAAG
epikol_00209	CBX3_GECKO_4	AGAAACGCTTCAATCAATTC
epikol_00210	CBX3_GECKO_5	AAACAGGAAAGATTCAGATG
epikol_00211	CBX4_CHROM_1	GAGTATCTGGTGAAATGGAG
epikol_00212	CBX4_CHROM_2	ATCTGGTGAAATGGAGAGGC
epikol_00213	CBX4_CHROM_3	TGCTGATCGCCTTCCAGAAC
epikol_00214	CBX4_CHROM_4	TGGAAGGCGATCAGCAGCCT
epikol_00215	CBX4_CHROM_5	GGAAGGCGATCAGCAGCCTG
epikol_00216	CBX5_CHROM_1	CTAGACAGGCGCGTGGTTAA
epikol_00217	CBX5_CHROM_2	GCTAGACAGGCGCGTGGTTA
epikol_00218	CBX5_CHROM_3	GAAGGTGCTAGACAGGCGCG
epikol_00219	CBX5_CHROM_4	GCGCGTGGTTAAGGGACAAG
epikol_00220	CBX5_CHROM_5	AAGTGGAATATCTACTGAAG
epikol_00221	CBX6_CHROM_1	TCGGATCCGCCGTTTGATGA
epikol_00222	CBX6_CHROM_2	CCGCCGTTTGATGATGGATT
epikol_00223	CBX6_CHROM_3	CCGAATCCATCATCAAACGG
epikol_00224	CBX6_CHROM_4	CGGCCGAATCCATCATCAAA
epikol_00225	CBX6_CHROM_5	GCATCGAGTACCTGGTGAAA
epikol_00226	CBX7_CHROM_1	GCATCCGGAAGAAGCGCGTG
epikol_00227	CBX7_CHROM_2	AAGTCGAGTATCTGGTGAAG
epikol_00228	CBX7_CHROM_3	ATCTGGTGAAGTGGAAAGGA
epikol_00229	CBX7_CHROM_4	TCGTAGGCCATGACGAGGCG
epikol_00230	CBX7_CHROM_5	TCTCCTCGTAGGCCATGACG
epikol_00231	CBX8_CHROM_1	CCCTCCTGAAGCGGCGCATA

epikol_00232	CBX8_CHROM_2	TCCGTATGCGCCGCTTCAGG
epikol_00233	CBX8_CHROM_3	CCGTATGCGCCGCTTCAGGA
epikol_00234	CBX8_CHROM_4	CGGCCGAAGCCCTCCTGAAG
epikol_00235	CBX8_CHROM_5	GCGCCGCTTCAGGAGGGCTT
epikol_00236	CDY1_GECKO_1	TTAACATGGATTCTATCCCT
epikol_00237	CDY1_GECKO_2	GTCTTTCCTCATGGCTTCCC
epikol_00238	CDY1_GECKO_3	CTGATCATTCTGTGTCTTTC
epikol_00239	CDY1_GECKO_4	ATATCCTAGAATACCTCTGT
epikol_00240	CDY1_GECKO_5	CTCTGTCCAAAGGTCGTATA
epikol_00241	CDY1L_CHROM_1	GTGGAAAGGCTATGACAGCG
epikol_00242	CDY1L_CHROM_2	ACAGCACCTCGTGAACTGTG
epikol_00243	CDY1L_CHROM_3	CGAGGACGACACTTGGGAGC
epikol_00244	CDYL_GECKO_4	AAAGCCGGTCGGAGCTTTAT
epikol_00245	CDYL_GECKO_5	TACGACGTCTGACAGATGAC
epikol_00246	CHAF1A_1	TCTTCCACCAGCTCGCCCGA
epikol_00247	CHAF1A_2	CTTCCACCAGCTCGCCCGAG
epikol_00248	CHAF1A_3	CTCTTCCACCAGCTCGCCCG
epikol_00249	CHAF1A_4	TGAGTACAGAGTCTTCTTCG
epikol_00250	CHAF1A_5	AGGCGGCCCCTCGGGCGAGC
epikol_00251	CHAF1B_1	ACACATCGAGGGTCTTCGCC
epikol_00252	CHAF1B_2	CCTGAGGGGGAGTCGTGCCG
epikol_00253	CHAF1B_3	AGGGGTTCCCTCTACCGGTC
epikol_00254	CHAF1B_4	GGGGTTCCCTCTACCGGTCT
epikol_00255	CHAF1B_5	GCCTGAGGGGGAGTCGTGCC
epikol_00256	CHD1_CHROM_1	GGTCCCATATCCACAACACT
epikol_00257	CHD1_CHROM_2	CTCCCAAGTGTTGTGGATAT
epikol_00258	CHD1_CHROM_3	CTCAAGCAGCAGAATGTTAG
epikol_00259	CHD1_CHROM_4	GTCCCATATCCACAACACTT
epikol_00260	CHD1_CHROM_5	TCTAACATTCTGCTGCTTGA
epikol_00261	CHD1_HELIC_1	AGGCTAGAGCCCATCGAATT
epikol_00262	CHD1_HELIC_2	TTGTTATATTTGATTCCGAT
epikol_00263	CHD1_HELIC_3	ACAGAATGATCTTCAGGCAC
epikol_00264	CHD1_HELIC_4	CCCTAGACCTCCAGCTCTTG
epikol_00265	CHD1_HELIC_5	GATCAATAAAAGGAGAACTG
epikol_00266	CHD1L_HELIC_1	ATGCTAGTAGCTTATCCAGC
epikol_00267	CHD1L_HELIC_2	CTACTAGCATTCCTGTATTC
epikol_00268	CHD1L_HELIC_3	TACTAGCATTCCTGTATTCT
epikol_00269	CHD1L_HELIC_4	CTTGGAGAATATCCAACATC
epikol_00270	CHD1L_HELIC_5	TATCCAACATCTGGGTCATT
epikol_00271	CHD2_CHROM_1	GAAGCTAATGGCGACCCTAG
epikol_00272	CHD2_CHROM_2	CCTTCCACTTGATGAGGTAC
epikol_00273	CHD2_CHROM_3	GTATATGCGATTGAAGCTAA
epikol_00274	CHD2_CHROM_4	ACCAACCCTTCCACTTGATG
epikol_00275	CHD2_CHROM_5	CAGTGTCAAAGTCACCACTA
epikol_00276	CHD2_HELIC_1	GGTGAGAATGTTGGATATCC
epikol_00277	CHD2_HELIC_2	GTTGACAAGACTTCGAGAAA
epikol_00278	CHD2_HELIC_3	TAATAGTTAGGTATTCAGCC
epikol_00279	CHD2_HELIC_4	TTGACAAGACTTCGAGAAAG
epikol_00280	CHD2_HELIC_5	TGACAAGACTTCGAGAAAGG
epikol_00281	CHD3_CHROM_1	TACCATATGACCAGTCCACG
epikol_00282	CHD3_CHROM_2	ACCATATGACCAGTCCACGT
epikol_00283	CHD3_CHROM_3	TCCCACGTGGACTGGTCATA
epikol_00284	CHD3_CHROM_4	ATATGACCAGTCCACGTGGG
epikol_00285	CHD3_CHROM_5	CATCTTCCTCCCACGTGGAC
epikol_00286	CHD3_HELIC_1	TCAGCTTTCGCAGCATCTTC
epikol_00287	CHD3_HELIC_2	GAAGATGCTGCGAAAGCTGA
epikol_00288	CHD3_HELIC_3	CTGCGAAAGCTGAAGGAGCA
epikol_00289	CHD3_HELIC_4	TACAAGTATGAGCGCATCGA
epikol_00290	CHD3_HELIC_5	GCGCATCGATGGTGGTATCA
epikol_00291	CHD4_PHD_1	GGATGATCTCACCGCCTTGC
epikol_00292	CHD4_PHD_2	CACGGGGACAGGTATCACAC
epikol_00293	CHD4_PHD_3	CCTTCTCCATGTCGGGATCC
epikol_00294	CHD4_PHD_4	CGACATGGAGAAGGCTCCCG
epikol_00295	CHD4_PHD_5	CAGACCATGTGGTAAGCACG
epikol_00296	CHD5_CHROM_1	GTCGATGTCATCGATCTCCC
epikol_00297	CHD5_CHROM_2	TGCTTGAGGTTGTCGTAGTA
epikol_00298	CHD5_CHROM_3	TCCCAGGTGCACTGGTCGTA
epikol_00299	CHD5_CHROM_4	CTACTACGACAACCTCAAGC
epikol_00300	CHD5_CHROM_5	AGGTGCACTGGTCGTAGGGC
epikol_00301	CHD5_PHD_1	GGCCTACCATCTCGTATGCC

epikol_00302	CHD5_PHD_2	ATACGAGATGGTAGGCCCTC
epikol_00303	CHD5_PHD_3	CCCTCGGGCAGGTGTCGCAC
epikol_00304	CHD5_PHD_4	CCTGTGCGACACCTGCCCGA
epikol_00305	CHD5_PHD_5	GTCCAGGCATACGAGATGGT
epikol_00306	CHD6_CHROM_1	CTTGGAGGTGGCCCACACCA
epikol_00307	CHD6_CHROM_2	CTGTTTCTGCATCCTTGGTG
epikol_00308	CHD6_CHROM_3	TGTTTCTGCATCCTTGGTGT
epikol_00309	CHD6_CHROM_4	CACACCAAGGATGCAGAAAC
epikol_00310	CHD6_CHROM_5	ACACCAAGGATGCAGAAACA
epikol_00311	CHD6_HELIC_1	GGTAATCTTCTAGGATGTCG
epikol_00312	CHD6_HELIC_2	CTACTCCCTAAGCTGATTGC
epikol_00313	CHD6_HELIC_3	TGGCCACCTGCAATCAGCTT
epikol_00314	CHD6_HELIC_4	CTCCCTAAGCTGATTGCAGG
epikol_00315	CHD6_HELIC_5	GGCCACCTGCAATCAGCTTA
epikol_00316	CHD7_CHROM_1	GCACGTAGCACAGATGACCG
epikol_00317	CHD7_CHROM_2	TACGTGCAAAGTCCATTATC
epikol_00318	CHD7_CHROM_3	TGCACGTAGCACAGATGACC
epikol_00319	CHD7_CHROM_4	TTGCACGTAGCACAGATGAC
epikol_00320	CHD7_CHROM_5	CATAGATCAAGCAAAGATCG
epikol_00321	CHD7_HELIC_1	GGTGCGCTGCTTGGACATAC
epikol_00322	CHD7_HELIC_2	TTCCCAGATGGTGCGCTGCT
epikol_00323	CHD7_HELIC_3	AGGATCGACGGCCGAGTAAG
epikol_00324	CHD7_HELIC_4	CAAGCTGCTGCCAAAACTGA
epikol_00325	CHD7_HELIC_5	CTGCTGCCAAAACTGAAGGC
epikol_00326	CHD8_CHROM_1	GCTTCAGTATATTGTCCAGA
epikol_00327	CHD8_CHROM_2	CTTCAGTATATTGTCCAGAA
epikol_00328	CHD8_CHROM_3	TACTATCTCCCAACTAGAGA
epikol_00329	CHD8_CHROM_4	AGCCCATTCACAATGCAGAT
epikol_00330	CHD8_CHROM_5	CCTCTTATCCTTCTCTAGTT
epikol_00331	CHD8_HELIC_1	GGTTCGTTCAGCCGGCAAAC
epikol_00332	CHD8_HELIC_2	TGGCCACCAGCTTTAAGCTT
epikol_00333	CHD8_HELIC_3	GTCAATAAGAACCAGTTTGC
epikol_00334	CHD8_HELIC_4	AATAATCCTCTAGGATGTCT
epikol_00335	CHD8_HELIC_5	TTGCTTCCAAAGCTTAAAGC
epikol_00336	CHD9_GECKO_1	TATCTAAAGCAAGAAGTTAT
epikol_00337	CHD9_GECKO_2	CTCTATATCATCTTTAAAGA
epikol_00338	CHD9_CHROM_3	GGCCCACTCACAGTGAAGAT
epikol_00339	CHD9_CHROM_5	TTTCAAAAGCTGCTCTTCTG
epikol_00340	CHD9_GECKO_4	CATCTTTAAAGATGATATAG
epikol_00341	CHD9_HELIC_1	GGTTCGTTGCCTTGACATTC
epikol_00342	CHD9_HELIC_2	CTTCCCAAAATGAAAGCCGG
epikol_00343	CHD9_HELIC_3	GATGAGCACTTTATGACCTC
epikol_00344	CHD9_HELIC_4	ATGACCTCCGGCTTTCATTT
epikol_00345	CHD9_HELIC_5	GATAGTCCTCCAGAATGTCA
epikol_00346	CLOCK_PAS_1	CATCTAGACATAGTTTAGAA
epikol_00347	CLOCK_PAS_2	GGCAAATACCCTATTATGGG
epikol_00348	CLOCK_PAS_3	AGGCTATGATTACTATCATG
epikol_00349	CLOCK_PAS_4	AATGGCAAATACCCTATTAT
epikol_00350	CLOCK_PAS_5	AAATGGCAAATACCCTATTA
epikol_00351	CREBBP_BROMO_1	CCTAGAAGCACTGTATCGAC
epikol_00352	CREBBP_BROMO_2	AGGGCCTGGCGTAACTCCTC
epikol_00353	CREBBP_BROMO_3	GCCGGAAAGGTAATGACTCT
epikol_00354	CREBBP_BROMO_4	TGCCGGAAAGGTAATGACTC
epikol_00355	CREBBP_BROMO_5	CTGTCGATACAGTGCTTCTA
epikol_00356	CREBBP_KAT_1	CTCCACCGTCTTGTCTGAGC
epikol_00357	CREBBP_KAT_2	CAAAAACCTCCCCGGCTTCA
epikol_00358	CREBBP_KAT_3	CCCCGGCTTCAGGGTGATTC
epikol_00359	CREBBP_KAT_4	GAATCACCCTGAAGCCGGGG
epikol_00360	CREBBP_KAT_5	ACAAAAACCTCCCCGGCTTC
epikol_00361	CXXC1_PHD_1	AGCAGTTGATGTCCGGTTTG
epikol_00362	CXXC1_PHD_2	CCGACAGTACCACTCCCGGA
epikol_00363	CXXC1_PHD_3	CATCCGGGAGTGGTACTGTC
epikol_00364	CXXC1_PHD_4	GTACCACTCCCGGATGGCCT
epikol_00365	CXXC1_PHD_5	CCATCCGGGAGTGGTACTGT
epikol_00366	DMAP1_DMTA_1	GCAGCGGCGCACGGAACGCA
epikol_00367	DMAP1_DMTA_2	ACAGGAGCTGCGCAAGATTG
epikol_00368	DMAP1_DMTA_3	CACTGCAGAGCAGCGGCGCA
epikol_00369	DMAP1_DMTA_4	TCTTGCGCAGCTCCTGTAGC
epikol_00370	DMAP1_DMTA_5	CGTGCGCCGCTGCTCTGCAG
epikol_00371	DNMT1_DMTA_1	GCAGCCAGAAAACACATCCA

epikol_00372	DNMT1_DMTA_2	TTCTGGCTGCGGGGGGTTGT
epikol_00373	DNMT1_DMTA_3	GGCTGCGGGGGGTTGTCGGA
epikol_00374	DNMT1_DMTA_4	AGTAGGTGCGCGAATTGAAG
epikol_00375	DNMT1_DMTA_5	CGCAGCCAGAAAACACATCC
epikol_00376	DNMT3A_DMTA_1	AAGAGAGACAGCACCCGGAT
epikol_00377	DNMT3A_DMTA_2	AAAGAGAGACAGCACCCGGA
epikol_00378	DNMT3A_DMTA_3	CGGGTGCTGTCTCTCTTTGA
epikol_00379	DNMT3A_DMTA_4	GGGGAAGATCATGTACGTCG
epikol_00380	DNMT3A_DMTA_5	GGACCGCTACATTGCCTCGG
epikol_00381	DNMT3B_DMTA_1	AACAATGACAGGACTCGAAT
epikol_00382	DNMT3B_DMTA_2	CGATGCCATCAAACAATGAC
epikol_00383	DNMT3B_DMTA_3	CGAGTCCTGTCATTGTTTGA
epikol_00384	DNMT3B_DMTA_4	AAACAATGACAGGACTCGAA
epikol_00385	DNMT3B_DMTA_5	TCAAATACGTGAACGACGTG
epikol_00386	DNMT3L_1	CATCTGCTGCGGAAGTCTCC
epikol_00387	DNMT3L_2	AGATCCCTCCCTCAAACAGA
epikol_00388	DNMT3L_3	ACACAGCACCCTCTGTTTGA
epikol_00389	DNMT3L_4	AGCACCCTCTGTTTGAGGGA
epikol_00390	DNMT3L_5	CAGATCCCTCCCTCAAACAG
epikol_00391	DOT1L_MTA_1	AGACATCCCGGCCAAGTATG
epikol_00392	DOT1L_MTA_2	CAGCAACCTGGAGCACGACC
epikol_00393	DOT1L_MTA_3	CGTCGAGAAAGCAGACATCC
epikol_00394	DOT1L_MTA_4	TGTGGGCCAGGTCGTGCTCC
epikol_00395	DOT1L_MTA_5	GCCATAGTGATGTTTGCAGT
epikol_00396	DTX3L_RING_1	CATGGCTTTGTTGATACAAG
epikol_00397	DTX3L_RING_2	GACATGGCTTTGTTGATACA
epikol_00398	DTX3L_RING_3	GTCTGGCATGTGGGACAGAT
epikol_00399	DTX3L_RING_4	ACATGGCTTTGTTGATACAA
epikol_00400	DTX3L_RING_5	CAGAATTCATGCTTGCACTT
epikol_00401	EED_WD40_1	TTTAACTGGCACAGTAAAGA
epikol_00402	EED_WD40_2	CCGGTTGTTGCAATCTTACG
epikol_00403	EED_WD40_3	CCACGTAAGATTGCAACAAC
epikol_00404	EED_WD40_4	ATGGCTCGTATTGCTATCAT
epikol_00405	EED_WD40_5	CAATACGAGCCATCCTCTGC
epikol_00406	EHMT1_SET_1	CTCTACCGGACGCGGGACAT
epikol_00407	EHMT1_SET_2	GCTCTACCGGACGCGGGACA
epikol_00408	EHMT1_SET_3	GCTGCAGCTCTACCGGACGC
epikol_00409	EHMT1_SET_4	GGCTGCAGCTCTACCGGACG
epikol_00410	EHMT1_SET_5	CCCAGCCCATGTCCCGCGTC
epikol_00411	EHMT2_SET_1	CGCAGATGAAGGTCCCCTGT
epikol_00412	EHMT2_SET_2	CTCTACCGAACAGCCAAGAT
epikol_00413	EHMT2_SET_3	GCTCTACCGAACAGCCAAGA
epikol_00414	EHMT2_SET_4	CCGAACAGCCAAGATGGGCT
epikol_00415	EHMT2_SET_5	TCGCAGATGAAGGTCCCCTG
epikol_00416	ELP3_1	ATCAAGACCTTGCGATACTG
epikol_00417	ELP3_2	GCAATGATATCCACCAGGCG
epikol_00418	ELP3_3	CGGCAGCAATGATATCCACC
epikol_00419	ELP3_4	ATGGGTTTCGCCTTTAACTT
epikol_00420	ELP3_5	TGATATCCACCAGGCGGGGC
epikol_00421	EP300_BROMO_1	TTTGGAGGCACTTTACCGTC
epikol_00422	EP300_BROMO_2	GGGTCCACAGGTTGACGAAA
epikol_00423	EP300_BROMO_3	AGGGTCCACAGGTTGACGAA
epikol_00424	EP300_BROMO_4	CCTTCCCTTTCGTCAACCTG
epikol_00425	EP300_BROMO_5	CCTAAAAGCTGAGGGTCCAC
epikol_00426	EP300_RING_1	CTGTAATAAGTGGCATCACG
epikol_00427	EP300_RING_2	CCGTAGCAACACAGTGTCTG
epikol_00428	EP300_RING_3	CCACAGACACTGTGTTGCTA
epikol_00429	EP300_RING_4	GTTCTGGTAACTGTAATAAG
epikol_00430	EP300_RING_5	CCAAAGAAACGCTCTCCCCT
epikol_00431	EP400_HELIC_1	CATCGATTCTTACATAGGTG
epikol_00432	EP400_HELIC_2	ATTGAAATCTGAAGGACGTC
epikol_00433	EP400_HELIC_3	AGGAGTGGTGCGATAGGATC
epikol_00434	EP400_HELIC_4	AATTGAAATCTGAAGGACGT
epikol_00435	EP400_HELIC_5	TTCTTACATAGGTGAGGTAA
epikol_00436	ERCC6_HELIC_1	TTGGGTACTGGAAACGTTCT
epikol_00437	ERCC6_HELIC_2	GTTGAAAATATGGCACAAGC
epikol_00438	ERCC6_HELIC_3	TTGAAAATATGGCACAAGCA
epikol_00439	ERCC6_HELIC_4	TCATTGTATCTCGTAATCAG
epikol_00440	ERCC6_HELIC_5	TTGAGTCTTTGTTGAAAATA
epikol_00441	EZH1_SET_1	CGGATGGGGCACCTTCATAA

epikol_00442	EZH1_SET_2	CCCCTCTGATGTGGCCGGAT
epikol_00443	EZH1_SET_3	CCCCCTCTGATGTGGCCGGA
epikol_00444	EZH1_SET_4	CTTTATGAAGGTGCCCCATC
epikol_00445	EZH1_SET_5	GCCCCATCCGGCCACATCAG
epikol_00446	EZH2_SET_1	CTGGCACCATCTGACGTGGC
epikol_00447	EZH2_SET_2	CACCATCTGACGTGGCAGGC
epikol_00448	EZH2_SET_3	ACCATCTGACGTGGCAGGCT
epikol_00449	EZH2_SET_4	CCCCAGCCTGCCACGTCAGA
epikol_00450	EZH2_SET_5	CATCTGACGTGGCAGGCTGG
epikol_00451	GCN5_HELIC_1	AACAGAGTATGGAGGTTATC
epikol_00452	GCN5_HELIC_2	TGGGGAGGTAACAAAGATAT
epikol_00453	GCN5_HELIC_3	ACAGAGTATGGAGGTTATCA
epikol_00454	GCN5_HELIC_4	CAAATTCAAACAGAGTATGG
epikol_00455	GCN5_HELIC_5	TATGGAGGTTATCAGGGCTT
epikol_00456	GCN5_NAT_1	CCAGACAGACCACCAAAGTC
epikol_00457	GCN5_NAT_2	GCTGTTCACCCAGATTATCA
epikol_00458	GCN5_NAT_3	CCAGACTTTGGTGGTCTGTC
epikol_00459	GCN5_NAT_4	CTGTTCACCCAGATTATCAA
epikol_00460	GCN5_NAT_5	GACTTTGGTGGTCTGTCTGG
epikol_00461	GTF3C4_1	CCGAGGTGCGGTGGATAACC
epikol_00462	GTF3C4_2	CATCTGCGACGTGCACAACC
epikol_00463	GTF3C4_3	ATCTGCGACGTGCACAACCC
epikol_00464	GTF3C4_4	TGCGGTGGATAACCAGGTCC
epikol_00465	GTF3C4_5	CGACGTGCACAACCCGGGCC
epikol_00466	H2AFY2_1	GTTCAAGTACCGGATCAGCG
epikol_00467	H2AFY2_2	TTCAAGTACCGGATCAGCGT
epikol_00468	H2AFY2_3	CAAGCTGTCCCGTTCAGCTA
epikol_00469	H2AFY2_4	GGCGGCAGTCATTGAGTACC
epikol_00470	H2AFY2_5	CAGGGGCGCCCACGCTGATC
epikol_00471	H2AFZ_1	CTTATCAAGGCTACCATAGC
epikol_00472	H2AFZ_2	TTATCAAGGCTACCATAGCT
epikol_00473	H2AFZ_GECKO_1	ACCCATTTACCTCTGCGGTG
epikol_00474	H2AFZ_GECKO_2	CGCGCCGCAGGCTGGCGGTA
epikol_00475	H2AFZ_GECKO_3	TTCATCGACACCTAAAATCT
epikol_00476	HAT1_1	AAGAGTTGATGGGTATACTC
epikol_00477	HAT1_2	GAGTATACCCATCAACTCTT
epikol_00478	HAT1_3	GTATACCCATCAACTCTTTG
epikol_00479	HAT1_4	GTATGAAGTAAGGTTCCGAA
epikol_00480	HAT1_5	CAACACGGAACATTGTTGAC
epikol_00481	HBO1_1	ACCAGGTATCAAGCTCATAG
epikol_00482	HBO1_2	AGGATATGGAGAATGATACC
epikol_00483	HBO1_3	CGATATATCTCATCACCAGG
epikol_00484	HBO1_4	CTGCCAAAACCTGTGCCTGT
epikol_00485	HBO1_5	CTTGAAAATTATGCAGGTAG
epikol_00486	HCFC1_1	GGGACTCGCCTCCTGGTGTT
epikol_00487	HCFC1_2	CTCGCCTCCTGGTGTTTGGT
epikol_00488	HCFC1_3	ACTCGCCTCCTGGTGTTTGG
epikol_00489	HCFC1_4	TTGGTGGGATGGTGGAGTAT
epikol_00490	HCFC1_5	CCTCCTGGTGTTTGGTGGGA
epikol_00491	HDAC1_HDAC_1	AGTAGTAACAGACTTTCCTC
epikol_00492	HDAC1_HDAC_2	TGAGTCATGCGGATTCGGTG
epikol_00493	HDAC1_HDAC_3	CTATGGTCTCTACCGAAAAA
epikol_00494	HDAC1_HDAC_4	TTCGGTGAGGCTTCATTGGG
epikol_00495	HDAC1_HDAC_5	GGATTCGGTGAGGCTTCATT
epikol_00496	HDAC10_HDAC_1	AGGACGCTCGATCTCGCACT
epikol_00497	HDAC10_HDAC_2	TCTGCGGTTGTCAGCCCGCG
epikol_00498	HDAC10_HDAC_3	GGACGCTCGATCTCGCACTC
epikol_00499	HDAC10_HDAC_4	GTTGTCAGCCCGCGAGGCCT
epikol_00500	HDAC10_HDAC_5	CGCGCTGCCGCAGGCGATCC
epikol_00501	HDAC11_HDAC_1	AGGCCCCTTCGGACCCAGAC
epikol_00502	HDAC11_HDAC_2	TTCCTCCTGTCTGGGTCCGA
epikol_00503	HDAC11_HDAC_3	ATCCCTTTGATGCCGGAAAA
epikol_00504	HDAC11_HDAC_4	CCCTTTGATGCCGGAAAATG
epikol_00505	HDAC11_HDAC_5	TCCCTTTGATGCCGGAAAAT
epikol_00506	HDAC2_HDAC_1	TGGGTCATGCGGATTCTATG
epikol_00507	HDAC2_HDAC_2	GCGGATTCTATGAGGCTTCA
epikol_00508	HDAC2_HDAC_3	ACAGCAAGTTATGGGTCATG
epikol_00509	HDAC2_HDAC_4	CATAACTTGCTGTTAAATTA
epikol_00510	HDAC2_HDAC_5	CATAATTTAACAGCAAGTTA
epikol_00511	HDAC3_HDAC_1	TATTTCTACGACCCCGACGT

epikol_00512	HDAC3_HDAC_2	CTATTTCTACGACCCCGACG
epikol_00513	HDAC3_HDAC_3	CACGTCGGGGTCGTAGAAAT
epikol_00514	HDAC3_HDAC_4	AGTGGAAGTTGCCCACGTCG
epikol_00515	HDAC3_HDAC_5	TAGTGGAAGTTGCCCACGTC
epikol_00516	HDAC4_HDAC_1	GCATCAGCGTGTCATACACG
epikol_00517	HDAC4_HDAC_2	TGGATCCTCCCGGCGTGCTC
epikol_00518	HDAC4_HDAC_3	TCCTCCCGGCGTGCTCGGGG
epikol_00519	HDAC4_HDAC_4	CTGCAGGAGACGGGCCTCCG
epikol_00520	HDAC4_HDAC_5	TGCTACTCCCGCAGGTGCAC
epikol_00521	HDAC5_HDAC_1	GTGTGTTCCCGCACATGCAC
epikol_00522	HDAC5_HDAC_2	TGGATCCGGCCAGCATGCTC
epikol_00523	HDAC5_HDAC_3	GGATCCGGCCAGCATGCTCA
epikol_00524	HDAC5_HDAC_4	TAAAGCACCAGTGCATGTGC
epikol_00525	HDAC5_HDAC_5	CACGTGCACCCTGAGCATGC
epikol_00526	Ino80_HELIC_3	GCTTTGTCTGCCCTAAGCGG
epikol_00527	Ino80_HELIC_4	TGGACAGGGCCCACCGCTTA
epikol_00528	Ino80_HELIC_5	CTTTGTCTGCCCTAAGCGGT
epikol_00529	Jarid1a_GECKO_5	ACGACTGACCCAAGTGTCAT
epikol_00530	Jarid1a_JMJC_1	CCATGCTCCATTAGCACGTT
epikol_00531	Jarid1a_JMJC_2	CATGCTCCATTAGCACGTTG
epikol_00532	Jarid1a_JMJC_3	TAGCACGTTGGGGTTCATGA
epikol_00533	Jarid1a_JMJC_4	GGCTGGGATTCAAATAACTC
epikol_00534	Jarid1a_JMJC_5	TTTCCTCGTGCCTATCACTC
epikol_00535	Jarid1a_PHD_1	CCACTACCTGATGTGCCCAA
epikol_00536	Jarid1a_PHD_2	CCTTTGGGCACATCAGGTAG
epikol_00537	Jarid1a_PHD_3	TTGGGCACATCAGGTAGTGG
epikol_00538	Jarid1a_PHD_4	CTGATGTGCCCAAAGGAGAC
epikol_00539	Jarid1b_JMJC_1	ATACCCTGGGACTCCATACC
epikol_00540	Jarid1b_JMJC_2	CCCCAGCACACTGATTAGTT
epikol_00541	Jarid1b_JMJC_3	CCTCAGCAAAATTAAAACCC
epikol_00542	Jarid1b_JMJC_4	TACCGAACTAATCAGTGTGC
epikol_00543	Jarid1b_JMJC_5	TTTCCAAGAGCCTACCACAG
epikol_00544	Jarid1b_PHD_1	GACCGGCTACTGTTGTGTGA
epikol_00545	Jarid1b_PHD_2	AGCCATCACACAACAGTAGC
epikol_00546	Jarid1b_PHD_3	CCTCTCCATGATGTTCCCAA
epikol_00547	Jarid1b_PHD_4	CCCTTGGGAACATCATGGAG
epikol_00548	Jarid1b_PHD_5	AGTCTCCCTTGGGAACATCA
epikol_00549	Jarid1c_JMJC_1	ACTCCATTAACTACCTCCAC
epikol_00550	Jarid1c_JMJC_2	GTGAGCCGAAGACCTGGTAT
epikol_00551	Jarid1c_JMJC_3	AAGTGAGGGCACCCCATACC
epikol_00552	Jarid1c_JMJC_4	CCATGGGACATGAGGGTGTT
epikol_00553	Jarid1c_JMJC_5	AGCCGCTGTGGTAAGCACGG
epikol_00554	Jarid1c_PHD_1	GGCACCGCCAGACACCCTTG
epikol_00555	Jarid1c_PHD_2	GATGTGTTCTCGAGGGGATG
epikol_00556	Jarid1c_PHD_3	TCTGCCGGATGTGTTCTCGA
epikol_00557	Jarid1c_PHD_4	CATCCCCTCGAGAACACATC
epikol_00558	Jarid1c_PHD_5	CTGAGATCCCCAAGGGTGTC
epikol_00559	Jarid1d_JMJC_1	ACTCTATTAACTATCTGCAT
epikol_00560	Jarid1d_JMJC_2	CTGGTATGGTGTACCCTCCC
epikol_00561	Jarid1d_JMJC_3	CCCAACACTTTGATGTCCCA
epikol_00562	Jarid1d_JMJC_4	TCCGCACAAACCAGTGTGCA
epikol_00563	Jarid1d_JMJC_5	GGCTGGCTATCAAACAGCTC
epikol_00564	Jarid1d_PHD_1	CATCCCCACGGGAGCATACT
epikol_00565	Jarid1d_PHD_2	TTGCCAAGTATGCTCCCGTG
epikol_00566	Jarid1d_PHD_3	ATTTGCCAAGTATGCTCCCG
epikol_00567	Jarid1d_PHD_4	TTTGCCAAGTATGCTCCCGT
epikol_00568	Jarid1d_PHD_5	CTGAAATCCCCAGAGGCATC
epikol_00569	Jarid2_JMJC_1	TACATTGACTACTTACACAC
epikol_00570	Jarid2_JMJC_2	GTGTGTAAGTAGTCAATGTA
epikol_00571	Jarid2_JMJC_3	AAGAGGGGATCAAGGTGCAC
epikol_00572	Jarid2_JMJC_4	CCGGGAAGCAGACGACAAAC
epikol_00573	Jarid2_JMJC_5	CTCTTTGCACAGCACCTCCG
epikol_00574	Jarid2_JMJCN_1	CATCGAGTCGGTCCGCGCTC
epikol_00575	Jarid2_JMJCN_2	TCCGCTCATCTACATCGAGT
epikol_00576	Jarid2_JMJCN_3	CGGATCGTGGAACTCCTTGG
epikol_00577	Jarid2_JMJCN_4	ATCGTGGAACTCCTTGGCGG
epikol_00578	Jarid2_JMJCN_5	GGGTGATCCCCCCTCCGGAC
epikol_00579	Jhdm1d_JMJC_1	ACTTCGGTGGAACTTCAGTC
epikol_00580	Jhdm1d_JMJC_2	ATTTGGCACGTTATGAATCT
epikol_00581	Jhdm1d_JMJC_3	CTCCAAAGAACACCTCACTC

epikol_00582	Jhdm1d_JMJC_4	CCATGCTGTGCTCACTTCTC
epikol_00583	Jhdm1d_JMJC_5	CCTGAGAAGTGAGCACAGCA
epikol_00584	Jmjd1a_JMJC_1	GCCATCTCGCCTTGTGTACT
epikol_00585	Jmjd1a_JMJC_2	CGCCTTGTGTACTCGGGCAG
epikol_00586	Jmjd1a_JMJC_3	CCCGAGTACACAAGGCGAGA
epikol_00587	Jmjd1a_JMJC_4	GTTCCATATTTCCGATCTTC
epikol_00588	Jmjd1a_JMJC_5	GCTAATGTCATGGTCTATGT
epikol_00589	Jmjd1b_JMJC_1	ATTGAGCCTGCCATCTCGTT
epikol_00590	Jmjd1b_JMJC_2	GGCTACCTAGCTACTTTGTA
epikol_00591	Jmjd1b_JMJC_3	CTACTTTGTAAGGCCTGATC
epikol_00592	Jmjd1b_JMJC_4	AATATACCAAACGAGATGGC
epikol_00593	Jmjd1b_JMJC_5	CCATCTCGTTTGGTATATTC
epikol_00594	Jmjd1b_JMJCSF_1	ACGAAGCAGAGGATTCATGA
epikol_00595	Jmjd1b_JMJCSF_2	CCTCATAGAGTCGCTTACGG
epikol_00596	Jmjd1b_JMJCSF_3	CTCATAGAGTCGCTTACGGA
epikol_00597	Jmjd1b_JMJCSF_4	ACTCCTCATAGAGTCGCTTA
epikol_00598	Jmjd1b_JMJCSF_5	CCTCCGTAAGCGACTCTATG
epikol_00599	Jmjd1c_JMJCSF_1	TGAACAAAAAGCTCCGTCAA
epikol_00600	Jmjd1c_JMJCSF_2	TCACGTATTGGATCATGTTC
epikol_00601	Jmjd1c_JMJCSF_3	CATGTTCTGGTAGAACTTCA
epikol_00602	Jmjd1c_JMJCSF_4	ATCCAATACGTGACCAAAGT
epikol_00603	Jmjd1c_JMJCSF_5	AAGGAACTGAATAAGAGTAC
epikol_00604	Jmjd2a_JMJC_1	TACTCTGTTCCACCTGAGCA
epikol_00605	Jmjd2a_JMJC_2	CAGCATTAACGGGGAAATCA
epikol_00606	Jmjd2a_JMJC_3	ATATTTCTTCAGCATTAACG
epikol_00607	Jmjd2a_JMJC_4	AGCCGGCATGGTAACCATAA
epikol_00608	Jmjd2a_JMJC_5	ACTCCGCACAGTTAAAACCA
epikol_00609	Jmjd2a_JMJCN_1	TCCCAAGGAGCTCATCGGGC
epikol_00610	Jmjd2a_JMJCN_2	TCATCGGGCAGGGCTAGCCA
epikol_00611	Jmjd2a_JMJCN_3	TTGAATCCCAAGGAGCTCAT
epikol_00612	Jmjd2a_JMJCN_4	GCCCTGCCCGATGAGCTCCT
epikol_00613	Jmjd2a_JMJCN_5	TTTCGGAACTCTTCCATAGT
epikol_00614	Jmjd2b_JMJC_1	ACCAGAGCACGGCAAGCGCC
epikol_00615	Jmjd2b_JMJC_2	TACGCCATCCCACCAGAGCA
epikol_00616	Jmjd2b_JMJC_3	AGGGGATCCCGTACTTCTTC
epikol_00617	Jmjd2b_JMJC_4	CGCAGCCCTGCGAGCTCCCG
epikol_00618	Jmjd2b_JMJC_5	ACCACGCCGGCTTCAATCAC
epikol_00619	Jmjd2b_JMJCN_1	CGTGGCCTACATAGAGTCGC
epikol_00620	Jmjd2b_JMJCN_2	GTGGCCTACATAGAGTCGCA
epikol_00621	Jmjd2b_JMJCN_3	GGCTCCCTGCGACTCTATGT
epikol_00622	Jmjd2b_JMJCN_4	CTTGGCCAGGCCCGCCCGGT
epikol_00623	Jmjd2b_JMJCN_5	GGGAGCCCACCGGGCGGGCC
epikol_00624	Jmjd2c_JMJC_1	GGAGATAATTAATGCTATAG
epikol_00625	Jmjd2c_JMJC_2	AGCATTAATTATCTCCACTT
epikol_00626	Jmjd2c_JMJC_3	TATGCTATACCTCCGGAGCA
epikol_00627	Jmjd2c_JMJC_4	AACCAGCATGGTAGCCATAT
epikol_00628	Jmjd2c_JMJC_5	TCATGAATTCTCCAGCCTCC
epikol_00629	Jmjd2c_JMJCN_1	CCTTTGCAAGACCCGCACGA
epikol_00630	Jmjd2c_JMJCN_2	CCATCGTGCGGGTCTTGCAA
epikol_00631	Jmjd2c_JMJCN_3	TCTAAAGGAGCCCATCGTGC
epikol_00632	Jmjd2c_JMJCN_4	CTTTAGACTCCATGTATGCA
epikol_00633	Jmjd2c_JMJCN_5	CAAGGTATTTGTTGAACTCC
epikol_00634	JMJD2D_GECKO_1	AACCTGAACGCTATGACCTG
epikol_00635	JMJD2D_GECKO_2	GCTCCAAATCTTCGAAATTC
epikol_00636	JMJD2D_GECKO_3	CAGATTATCCACCCGTCAAA
epikol_00637	Jmjd2d_JMJC_1	TGGCCAGGCGTTCCAGGCGC
epikol_00638	Jmjd2d_JMJC_2	CCATGGTTTCAACTGCGCAG
epikol_00639	Jmjd2d_JMJC_3	CCACAACCCCGGGAACTGCC
epikol_00640	Jmjd2d_JMJC_4	CCTCTGCGCAGTTGAAACCA
epikol_00641	Jmjd2d_JMJCN_1	AGCCAGCTCTGTGTGCACCT
epikol_00642	Jmjd2d_JMJCN_2	TCATTAAACTCTTCTTTGGT
epikol_00643	Jmjd2d_JMJCN_3	AGGTGCACACAGAGCTGGCT
epikol_00644	JmjD3_JMJC_1	GCGAACCACTCGCAGTCGCC
epikol_00645	JmjD3_JMJC_2	TCGCGGTGCACGAGCACTAC
epikol_00646	JmjD3_JMJC_3	CGCGGTGCACGAGCACTACT
epikol_00647	JmjD3_JMJC_4	TGCTCCGTCAACATCAACAT
epikol_00648	JmjD3_JMJC_5	ACCTCGTGTGGATTAATGCG
epikol_00649	Jmjd4_JMJC_1	TGGACCCCACAGTTTGCAAC
epikol_00650	Jmjd4_JMJC_2	TCAGAGACTACATCACCTAC
epikol_00651	Jmjd4_JMJC_3	AGGCGGGCTACTCCTCTCCC

epikol_00652	Jmjd4_JMJC_4	GCTGTCTCTACCTCAAAGAC
epikol_00653	Jmjd4_JMJC_5	AGTTGCAAACTGTGGGGTCC
epikol_00654	Jmjd5_CUPIN_1	AGTGGTCAGCCACGCCTTTC
epikol_00655	Jmjd5_CUPIN_2	GCCACGCCTTTCAGGATCAC
epikol_00656	Jmjd5_CUPIN_3	ACTGGCCGTGCATGCAGAAG
epikol_00657	Jmjd5_CUPIN_4	GAACTCGTTGACCGTCATGA
epikol_00658	Jmjd5_CUPIN_5	CGTTGACCGTCATGAGGGTC
epikol_00659	Jmjd6_JMJC_1	ATCAAAGTGACCCGAGACGA
epikol_00660	Jmjd6_JMJC_2	GGGCCACCACGCTCCGGAAC
epikol_00661	Jmjd6_JMJC_3	TGGGATTCACATCGACCCTC
epikol_00662	Jmjd6_JMJC_4	TAGTTCAGGGCCACAAGCGC
epikol_00663	Jmjd6_JMJC_5	AAAGTGACCCGAGACGAAGG
epikol_00664	Jmjd7_CUPIN_1	GCGGATAATGCACGGCCTGT
epikol_00665	Jmjd7_CUPIN_2	CGGATAATGCACGGCCTGTT
epikol_00666	Jmjd7_CUPIN_3	AGAGCGTTGCGGATAATGCA
epikol_00667	Jmjd7_CUPIN_4	CGCTCCACTTCTACCGGGAC
epikol_00668	Jmjd7_CUPIN_5	GGATAATGCACGGCCTGTTG
epikol_00669	Jmjd8_JMJC_1	CAGGATGACGGGCCTGACGA
epikol_00670	Jmjd8_JMJC_2	CGTCAGGCCCGTCATCCTGC
epikol_00671	Jmjd8_JMJC_3	GCAACCTGTCGCGGGAGCAC
epikol_00672	Jmjd8_JMJC_4	CGAAGCCAGCAACCTGTCGC
epikol_00673	Jmjd8_JMJC_5	GGGCCCTGTGCTCCCGCGAC
epikol_00674	Kat2a_BROMO_1	GATGACCTCGTAGTAGTCAG
epikol_00675	Kat2a_BROMO_2	GCGGCAGTACTCGCTGTCCG
epikol_00676	Kat2a_BROMO_3	CTGTCGCGAGTACAACCCCC
epikol_00677	Kat2a_BROMO_4	GAAGCCGCTACTACGTGACC
epikol_00678	Kat2a_BROMO_5	CGGCAGTACTCGCTGTCCGG
epikol_00679	Kat2a_NAT_1	GACAATCTCCGTGAAGCCCT
epikol_00680	Kat2a_NAT_2	GGCCTTGATCAAGGATGGGC
epikol_00681	Kat2a_NAT_3	GCTTGATGTGATACTCCTTC
epikol_00682	Kat2a_NAT_4	TGATGTGATACTCCTTCAGG
epikol_00683	Kat2a_NAT_5	CCTTCAGGTGGTTCATCAGG
epikol_00684	Kat2b_BROMO_1	TGAAGGGCCAAGCGCTTTGA
epikol_00685	Kat2b_BROMO_2	CAGGATATTATGAAGTTATA
epikol_00686	Kat2b_BROMO_3	ATTCTTGAGGCGTTCACTCA
epikol_00687	Kat2b_BROMO_4	ACACGTAGTACCTATTCTTG
epikol_00688	Kat2b_BROMO_5	GGGGTTGTACTCTTTGCAAT
epikol_00689	Kat2b_NAT_1	ATTAAAGATGGCCGTGTTAT
epikol_00690	Kat2b_NAT_2	AAAGATGGCCGTGTTATTGG
epikol_00691	Kat2b_NAT_3	TCTCTGTGAATCCTTGAGAT
epikol_00692	Kat2b_NAT_4	TTCCGTATGTTCCCATCTCA
epikol_00693	Kat2b_NAT_5	AACAGATACCACCAATAACA
epikol_00694	Kat5_CHROM_1	ATGGGTGACGCATGAGCGGC
epikol_00695	Kat5_CHROM_2	ATGAATGGGTGACGCATGAG
epikol_00696	Kat5_CHROM_3	GTCCTTCACGCTCAGGATCT
epikol_00697	Kat5_CHROM_4	GGCCGAGATCCTGAGCGTGA
epikol_00698	Kat5_CHROM_5	GCGTGAAGGACATCAGTGGC
epikol_00699	Kat5_NAT_1	ATCAACGGAAGACTACAATG
epikol_00700	Kat5_NAT_2	GCTTGCCGTAGCCCCGGCGC
epikol_00701	Kat5_NAT_3	CTGCCTCCCTACCAGCGCCG
epikol_00702	Kat5_NAT_4	TCAGCAGCTTGCCGTAGCCC
epikol_00703	Kat5_NAT_5	GCCGTAGCCCCGGCGCTGGT
epikol_00704	L3mbtl1_MBT_1	AGTACATGGACGGGTGTTGA
epikol_00705	L3mbtl1_MBT_2	AAGTACATGGACGGGTGTTG
epikol_00706	L3mbtl1_MBT_3	GCAGTCACTCACAACAAGAA
epikol_00707	L3mbtl1_MBT_4	CATGTACTTCATCCTCACCG
epikol_00708	L3mbtl1_MBT_5	TCTTGTTGTGAGTGACTGCC
epikol_00709	LSD2_AMOX_1	CAACGGTGGATTAAACTGAA
epikol_00710	LSD2_AMOX_2	TCAATTATCACCGAGTACCC
epikol_00711	LSD2_AMOX_3	TTCAATTATCACCGAGTACC
epikol_00712	LSD2_AMOX_4	TCTGCTAACTCCCGGGTACT
epikol_00713	LSD2_AMOX_5	GAGTGTGGTCACCAGCAAAC
epikol_00714	Mbd1_MEC_1	CGCGAAGTCTTTCGCAAGTC
epikol_00715	Mbd1_MEC_2	ATAGGTGTCTGAGCGTCCAC
epikol_00716	Mbd1_MEC_3	CTTCGCGGCGCTTCCAGCCA
epikol_00717	Mbd1_MEC_4	GTTGAGCTGACTCGATACCT
epikol_00718	Mbd1_MEC_5	GCCTTGTTTGAAGTCGAAGA
epikol_00719	Mbd2_MEC_1	CCTTCTTCCATCCGGGGGGG
epikol_00720	Mbd2_MEC_2	GAGGAAGTGATCCGAAAATC
epikol_00721	Mbd2_MEC_3	CCTCCCCCCCGGATGGAAGA

epikol_00722	Mbd2_MEC_4	AGGAAGTGATCCGAAAATCT
epikol_00723	Mbd2_MEC_5	CCCCCCCGGATGGAAGAAGG
epikol_00724	Mbd3_MEC_1	GCCGACAGCCCCGACCTTCT
epikol_00725	Mbd3_MEC_2	CGGGGCTGTCGGCCGGCCAC
epikol_00726	Mbd3_MEC_3	GGCCGACAGCCCCGACCTTC
epikol_00727	Mbd3_MEC_4	GGAGTGCCCGGCGCTCCCGC
epikol_00728	Mbd3_MEC_5	AGAAGGTCGGGGCTGTCGGC
epikol_00729	Mbd4_MEC_1	GATCTGAACTTCAGTCCTTG
epikol_00730	Mbd4_MEC_2	GTTGTGAAGCAAAGGTTATT
epikol_00731	Mbd4_MEC_3	GCTAATTATCTTCACAAAAA
epikol_00732	Mbd4_MEC_4	TTTACTGTACTTTCTAAAAG
epikol_00733	Mbd4_MEC_5	ACAGTAAAATCAAAATCTTC
epikol_00734	Mecp2_MEC_1	GGACACGGAAGCTTAAGCAA
epikol_00735	Mecp2_MEC_2	TCCGTGTCCAGCCTTCAGGC
epikol_00736	Mecp2_MEC_3	GACTTCACGGTAACTGGGAG
epikol_00737	Mecp2_MEC_4	ATTGCGTACTTCGAAAAGGT
epikol_00738	Mecp2_MEC_5	AAAAGCCTTTCGCTCTAAAG
epikol_00739	MgeA5_NAG_1	GCGAGAGATGTATTCAGTGG
epikol_00740	MgeA5_NAG_2	GGTGTGGATAGCAACGTAGT
epikol_00741	MgeA5_NAG_3	ACCTCTTCGATGGACTCTAC
epikol_00742	MgeA5_NAG_4	CTATGCGATCTCACCTGGAT
epikol_00743	MgeA5_NAG_5	TATGTGTGCAGCAGACAAAG
epikol_00744	Mina_CUPIN_1	AATGTCTGCCGGTGTGTCAA
epikol_00745	Mina_CUPIN_2	CTCTTCCATAGTACATCCCC
epikol_00746	Mina_CUPIN_3	CTGCACTGGCCACATACTAT
epikol_00747	Mina_CUPIN_4	AATGTGTACATAACTCCCGC
epikol_00748	Mina_CUPIN_5	CATCATCATAATGGGGCGGC
epikol_00749	Mll1_BROMO_1	CCGGTAGCGTAGCAAATGGC
epikol_00750	Mll1_BROMO_2	TCTGTCTCGGGATTTAAGTC
epikol_00751	Mll1_BROMO_3	GTCTCGGGATTTAAGTCTGG
epikol_00752	Mll1_BROMO_4	AGGTCCTTCGGGGGAGCTGC
epikol_00753	Mll1_BROMO_5	CAGCAGCCTTTAGATCTAGA
epikol_00754	Mll1_PHD_1	GGAAGGGCTCACAACAGACT
epikol_00755	Mll1_PHD_2	TGGAGGACCAGCTGGAAAAT
epikol_00756	Mll1_PHD_3	AGAGGAGAACGAGCGCCCTC
epikol_00757	Mll1_PHD_4	TCTCCTCTAAACAAAACTTG
epikol_00758	Mll1_PHD_5	CTCTAAACAAAACTTGTGGA
epikol_00759	MLL2_PHD_1	GCACTGAGAGCACTGCGAAC
epikol_00760	MLL2_PHD_2	GAGAGCACTGCGAACAGGCA
epikol_00761	MLL2_PHD_3	TGGTATGTGGCAGCTTTGGC
epikol_00762	MLL2_PHD_4	ACTGCGAACAGGCAAGGAGG
epikol_00763	MLL2_PHD_5	ACCAAGGTGATGCTGCTCAA
epikol_00764	MLL2_SET_1	ATTGATGCTACGTTGACCGG
epikol_00765	MLL2_SET_2	CACCATCATTCGGAACGAGG
epikol_00766	MLL2_SET_3	CTGGCTCGCTCCCGTATCCA
epikol_00767	MLL2_SET_4	CCTTGGCTGCATAGAGCCCC
epikol_00768	MLL2_SET_5	GTGATTGATGCTACGTTGAC
epikol_00769	MLL3_GECKO_1	GACACAGATCGCTGAAGAGT
epikol_00770	MLL3_GECKO_2	AAACCAACCTTCTAACAAGA
epikol_00771	MLL3_GECKO_3	TCTTCAGCGATCTGTGTCTG
epikol_00772	MLL3_GECKO_4	CTCCATGGCAAGATAAATCC
epikol_00773	MLL3_GECKO_5	CTTGATCATCTGAAGCTGTC
epikol_00774	MLL3_SET_1	CAATGTCTCGAGCAGCATAC
epikol_00775	MLL3_SET_2	GTGATTGACGCGACGCTCAC
epikol_00776	MLL3_SET_3	TGAGCGTCGCGTCAATCACA
epikol_00777	MLL3_SET_4	TTGACGCGACGCTCACAGGA
epikol_00778	MLL3_SET_5	ATTGACGCGACGCTCACAGG
epikol_00779	MLL4_PHD_1	TGCCCCAGCATCACGACACC
epikol_00780	MLL4_PHD_2	AGGTGTCGTGATGCTGGGGC
epikol_00781	MLL4_PHD_3	AGCACCAGGTGTCGTGATGC
epikol_00782	MLL4_PHD_4	GCACCAGGTGTCGTGATGCT
epikol_00783	MLL4_PHD_5	CACCAGGTGTCGTGATGCTG
epikol_00784	MLL4_SET_1	AGCGGGAGAAGTTCTACGAT
epikol_00785	MLL4_SET_2	CGATGTTGCGCTTACAGAAC
epikol_00786	MLL4_SET_3	AGATCAGCCATCCACGGGCG
epikol_00787	MLL4_SET_4	CAACATCGACGCGGGGGAGA
epikol_00788	MLL4_SET_5	AAGCGGGAGAAGTTCTACGA
epikol_00789	MLL5_PHD_1	CGTTCACATAGATATGTATC
epikol_00790	MLL5_PHD_2	TTGACTGCATGGGGATTGAT
epikol_00791	MLL5_PHD_3	GGCAACATATTGACTGCATG

epikol_00792	MLL5_PHD_4	TGGCAACATATTGACTGCAT
epikol_00793	MLL5_PHD_5	TTGGCAACATATTGACTGCA
epikol_00794	MLL5_SET_1	TATTCAATGATAAGTGCATC
epikol_00795	MLL5_SET_2	TCAATGATAAGTGCATCAGG
epikol_00796	MLL5_SET_3	GGAATGAGGCTCGATTCATC
epikol_00797	MLL5_SET_4	ATGAGGCTCGATTCATCAGG
epikol_00798	MLL5_SET_5	GGAATGAGGCTCGATTCATC
epikol_00799	MMP8_GECKO_1	ATTCCATTGGGTCCATCAAA
epikol_00800	MMP8_GECKO_2	TGCAACACTCCAGAGTTCAA
epikol_00801	MMP8_GECKO_3	CTATACCCCACAGCTGTCAG
epikol_00802	MMP8_GECKO_4	AACGCACTAACTTGACCTAC
epikol_00803	MMP8_GECKO_5	GCAACCAGTATCAGTCTACA
epikol_00804	MORF4L1_GECKO_1	GCCTCTTCTTTATGAAGCAA
epikol_00805	MORF4L1_GECKO_2	ACATATTACCAAATAATCTC
epikol_00806	MORF4L1_GECKO_3	ACCTTTGCTTCATAAAGAAG
epikol_00807	MORF4L1_GECKO_4	CCACATCTCCTGAGATTATT
epikol_00808	MORF4L1_GECKO_5	CATGCATTTACCTAGAGGTC
epikol_00809	MORF4L1_GECKO_6	TGTACTGAGGGAGCTCCTTC
epikol_00810	MORF4L1_TUDOR_1	CTCCTTCAGGAACAGGAAAA
epikol_00811	MORF4L1_TUDOR_2	GAGGGAGCTCCTTCAGGAAC
epikol_00812	MORF4L1_TUDOR_3	AGGAGGGGGTGGTGTACTGA
epikol_00813	MORF4L1_TUDOR_4	CAGGAGGGGGTGGTGTACTG
epikol_00814	MSL3_GECKO_1	GTTCAATTAGCTGGGATAGA
epikol_00815	MSL3_GECKO_2	TCGTAGATTACAGCGTAAAT
epikol_00816	MSL3_GECKO_3	GTGCCTGACAATTACCCCCC
epikol_00817	MSL3_GECKO_4	TGAGCAAATGAGCGCGAGCG
epikol_00818	MSL3_GECKO_5	ATCGTACAGCACTCGCGCCT
epikol_00819	MTA1_BAH_1	ATACCTGATCCGGAGAATCG
epikol_00820	MTA1_BAH_2	CGATTCTCCGGATCAGGTAT
epikol_00821	MTA1_BAH_3	TCGATTCTCCGGATCAGGTA
epikol_00822	MTA1_BAH_4	CCAAAGTGGTGTGCTTCTAC
epikol_00823	MTA1_BAH_5	CTATAAGGCCGGACCGGGGG
epikol_00824	MTA1_SANT_1	GAGGAAGCCCTGGAAAAATA
epikol_00825	MTA1_SANT_2	CAGGGCTTCCTCGAAAAGGT
epikol_00826	MTA1_SANT_3	TCATTGAGTACTACTACATG
epikol_00827	MTA1_SANT_4	GTAGTAGTACTCAATGATGC
epikol_00828	MTA1_SANT_5	ATGCTGGTCAGCGACTTCCA
epikol_00829	MTA2_BAH_1	TTACCTGGTTAGACGGATTG
epikol_00830	MTA2_BAH_2	TCTAACCAGGTAAGGATTGC
epikol_00831	MTA2_BAH_3	GCAATCCTTACCTGGTTAGA
epikol_00832	MTA2_BAH_4	GTTCCCGGTGCTTCAGTTGA
epikol_00833	MTA2_BAH_5	AGATATCTTGAGCCAGTACC
epikol_00834	MTA2_SANT_1	GGACTTCAATGATATTCGCC
epikol_00835	MTA2_SANT_2	TAGGGCCTCCTCAAATAGCA
epikol_00836	MTA2_SANT_3	CTCAGAGGCCATGCTATTTG
epikol_00837	MTA2_SANT_4	GGCCCTAGAGAAGTATGGGA
epikol_00838	MTA2_SANT_5	AGAGGCCATGCTATTTGAGG
epikol_00839	MTA3_BAH_1	TCTTATTAGGTATGGGTTGC
epikol_00840	MTA3_BAH_2	GCAACCCATACCTAATAAGA
epikol_00841	MTA3_BAH_3	TCTATCCTTCTTATTAGGTA
epikol_00842	MTA3_BAH_4	AGTATTGTCATATCTTGATA
epikol_00843	MTA3_BAH_5	TGATTCTGTCTCATTCAGAA
epikol_00844	MTA3_GECKO_1	GCAACCCATACCTAATAAGA
epikol_00845	MTA3_GECKO_2	AAAACACTATTAGCTGACAA
epikol_00846	MTA3_GECKO_3	GTTCTTCTATCCTTCTTATT
epikol_00847	MTA3_GECKO_4	TCAATCTGTCGATCCGTAAG
epikol_00848	MTA3_GECKO_5	ACCGTGCTACAACTAAAAAC
epikol_00849	MYST1_CHROM_1	GGAATTCTATGTACACTACG
epikol_00850	MYST1_CHROM_2	CCTGGTCGTTCACTCGAGAC
epikol_00851	MYST1_CHROM_3	GAATTCTATGTACACTACGT
epikol_00852	MYST1_CHROM_4	GTGGGTAGACAAGAACCGGC
epikol_00853	MYST1_CHROM_5	TACAGCATCCTTCACTGTCT
epikol_00854	MYST1_HAT_1	CAATTTCGTAGTTCCCGATG
epikol_00855	MYST1_HAT_2	CACCATTCCCCGAAGACTAT
epikol_00856	MYST1_HAT_3	TCACCATTCCCCGAAGACTA
epikol_00857	MYST1_HAT_4	GGGGAATGGTGAGAAATACC
epikol_00858	MYST1_HAT_5	TTCCCATAGTCTTCGGGGAA
epikol_00859	MYST2_GECKO_1	GGGTGACTCGAGCAGATCGT
epikol_00860	MYST2_GECKO_2	GACAACTCACCATGTGCCGG
epikol_00861	MYST2_GECKO_3	TTCAATCTCTGTGTTTGAAG

epikol_00862	MYST2_GECKO_4	CTCGAGATCTGTAGAAAAAT
epikol_00863	MYST2_GECKO_5	TCTTGCAGGCCAAATGTGTG
epikol_00864	MYST3_HAT_1	TGGCTCCACATCGTAATAGA
epikol_00865	MYST3_HAT_2	ATGGCTCCACATCGTAATAG
epikol_00866	MYST3_HAT_3	TCTTCCTCAATACCAGCGTA
epikol_00867	MYST3_HAT_4	CTAACACAGAATGATGTCAA
epikol_00868	MYST3_HAT_5	TAGCCCTTACGCTGGTATTG
epikol_00869	MYST3_PHD_1	ACTGTTGCCACAGTCGGCAC
epikol_00870	MYST3_PHD_2	CAGAAACTACAGATGGGGAT
epikol_00871	MYST3_PHD_3	TTCACTCGAACCGTTAGTTC
epikol_00872	MYST3_PHD_4	TCACTCGAACCGTTAGTTCA
epikol_00873	MYST3_PHD_5	CACTCGAACCGTTAGTTCAG
epikol_00874	MYST4_HAT_1	CAGCAAATGAAATTTACCGA
epikol_00875	MYST4_HAT_2	CTTCGGTAAATTTCATTTGC
epikol_00876	MYST4_HAT_3	TGATGAAAAGGGCTGTCATC
epikol_00877	MYST4_HAT_4	ACCGTCCAAATCCTTGCCTT
epikol_00878	MYST4_HAT_5	ACCAAAGGCAAGGATTTGGA
epikol_00879	MYST4_PHD_1	CCCAAACAGAAGCTACATAT
epikol_00880	MYST4_PHD_2	ACAGAAGCTACATATTGGAA
epikol_00881	MYST4_PHD_3	GCACAAGAGAGGAGTTCTTC
epikol_00882	MYST4_PHD_4	TGCCACAATCTGCACAAGAG
epikol_00883	MYST4_PHD_5	TCCAATATGTAGCTTCTGTT
epikol_00884	NAP1L1_GECKO_1	CATTCACATTCTTCTTCCGT
epikol_00885	NAP1L1_GECKO_2	TACCTTTCAATGTATCCTGT
epikol_00886	NAP1L1_GECKO_3	TAATGCAATTTATGAACCTA
epikol_00887	NAP1L1_GECKO_4	CTATCAGCCTCTATTTGATA
epikol_00888	NAP1L1_GECKO_5	CACCAACAGGATACATTGAA
epikol_00889	NAP1L2_NAP_1	CGCAGTTCCCCTATAGGGAT
epikol_00890	NAP1L2_NAP_2	CTCAATCGCAGTTCCCCTAT
epikol_00891	NAP1L2_NAP_3	TATGATCCCCATCCCTATAG
epikol_00892	NAP1L2_NAP_4	ACTGCGATTGAGTATTCCAC
epikol_00893	NAP1L2_NAP_5	TTATGATCCCCATCCCTATA
epikol_00894	NAP1L3_NAP_1	CAGTAGCAGTTGTGCGACTC
epikol_00895	NAP1L3_NAP_2	CAGAGTCGCACAACTGCTAC
epikol_00896	NAP1L3_NAP_3	TGAAACCGCCTATCATACAG
epikol_00897	NAP1L3_NAP_4	AGATCCTAAAGAAGTCCCCC
epikol_00898	NAP1L3_NAP_5	GATTCCTATGATTGGGAAGC
epikol_00899	NAT10_HELIC_1	ACAGAGTATGGAGGTTATCA
epikol_00900	NAT10_HELIC_2	GGGCGTATCGGATTGACTCC
epikol_00901	NAT10_HELIC_3	ATGCCATGAAAACAAGGTAG
epikol_00902	NAT10_HELIC_4	CGTGGTCTTATTCTCAGCAG
epikol_00903	NAT10_HELIC_5	TTAGCTTGAGGGACAGTGAC
epikol_00904	NAT10_NAT_1	CCAGACAGACCACCAAAGTC
epikol_00905	NAT10_NAT_2	GCTGTTCACCCAGATTATCA
epikol_00906	NAT10_NAT_3	CCAGACTTTGGTGGTCTGTC
epikol_00907	NAT10_NAT_4	CTGTTCACCCAGATTATCAA
epikol_00908	NAT10_NAT_5	GACTTTGGTGGTCTGTCTGG
epikol_00909	NCOA1_PAS_1	CGTCTACAGCATACTGCACG
epikol_00910	NCOA1_PAS_2	CAGCTACTTAGGTTACAATC
epikol_00911	NCOA1_PAS_3	GAGAATGTAACCAGCTACTT
epikol_00912	NCOA1_PAS_4	GCATCCTGCAGTTAAAGGTA
epikol_00913	NCOA1_PAS_5	TTTCGTCGTGTTGCCTCTTG
epikol_00914	NCOA1_SRC_1	TCTACACCGGCTCTTACAGG
epikol_00915	NCOA1_SRC_2	CAACTGCCGAACAGCAGTTA
epikol_00916	NCOA1_SRC_3	GCCTCTGCTAACTCTTCAGG
epikol_00917	NCOA1_SRC_4	ACAAAGTGGTGATATCTGAG
epikol_00918	NCOA1_SRC_5	TCTGCCTCTGCTAACTCTTC
epikol_00919	NCOA2_PAS_1	AAGGTATGGCTGTTCCGCCT
epikol_00920	NCOA2_PAS_2	CTTGGTCTGGCGAACCTCCG
epikol_00921	NCOA2_PAS_3	GTATGGCTGTTCCGCCTCGG
epikol_00922	NCOA2_PAS_4	TACCTTCAATTGTCGGATGC
epikol_00923	NCOA2_PAS_5	GCATCCGACAATTGAAGGTA
epikol_00924	NCOA2_SRC_1	GTTTGTATCCGACAAAGAGC
epikol_00925	NCOA2_SRC_2	TACACATGGAACCTCGCTCA
epikol_00926	NCOA2_SRC_3	GGGCTCCATCTGATCAGATT
epikol_00927	NCOA2_SRC_4	GTTAACTTGGCCAAGTCCAC
epikol_00928	NCOA2_SRC_5	GACCACCAAATCTGATCAGA
epikol_00929	NCOA3_PAS_1	CGTCTCGATTCACCACAAAT
epikol_00930	NCOA3_PAS_2	CTATTTGTGGTGAATCGAGA
epikol_00931	NCOA3_PAS_3	GCAATATAAGCAAGAGGACC

epikol_00932	NCOA3_PAS_4	GGTCCTCTTGCTTATATTGC
epikol_00933	NCOA3_PAS_5	TGTAAACACTTGTGTTAACC
epikol_00934	NCOA3_SRC_1	ACCTGTTCTTCTGATGACCG
epikol_00935	NCOA3_SRC_2	CCTCTACATCCAATATGCAT
epikol_00936	NCOA3_SRC_3	TAACAGTGACCCATGCATAT
epikol_00937	NCOA3_SRC_4	ACCCCGGTCATCAGAAGAAC
epikol_00938	NCOA3_SRC_5	CCCATGCATATTGGATGTAG
epikol_00939	NO66_CUPIN_1	TCGTCCGTTGATGTAGCGAG
epikol_00940	NO66_CUPIN_2	GACGCCGCTCGCTACATCAA
epikol_00941	NO66_CUPIN_3	CCCCCACTACGACGACATCG
epikol_00942	NO66_CUPIN_4	GCCTCGATGTCGTCGTAGTG
epikol_00943	NO66_CUPIN_5	TCCATGAAAGCGGTTCTTCG
epikol_00944	NSD1_PHD_1	CAGTCAATCCAAGGCACTCC
epikol_00945	NSD1_PHD_2	TTGGCATCTCAGTCAATCCA
epikol_00946	NSD1_PHD_3	GCTTTCCACCTGGAGTGCCT
epikol_00947	NSD1_PHD_4	GGGTGAGCTGCTGTTATGTG
epikol_00948	NSD1_PHD_5	TATGTGAGGCTCAGTGCTGT
epikol_00949	NSD1_SET_1	CCGCACATTACAGCGGGGTT
epikol_00950	NSD1_SET_2	CCCAACCCCGCTGTAATGTG
epikol_00951	NSD1_SET_3	ACACAGAAGTGGTCTGTGAA
epikol_00952	NSD1_SET_4	GTGAATGGAGATACCCGTGT
epikol_00953	NSD1_SET_5	TAGTGCAAAAAGGCCTACAC
epikol_00954	NSD2_PHD_1	AGGTGGAAAGCTCCGCAGCA
epikol_00955	NSD2_PHD_2	CTGCAGGTGAACCTCCCTTC
epikol_00956	NSD2_PHD_3	GGCTTTCCCGGAGGCCAGAA
epikol_00957	NSD2_PHD_4	CCTGCCTTGGGCTTTCCCGG
epikol_00958	NSD2_PHD_5	GGGCTTTCCCGGAGGCCAGA
epikol_00959	NSD2_SET_1	TGATGTCCCTCTTGGCGACC
epikol_00960	NSD2_SET_2	GAATTTGTTAACGAGTACGT
epikol_00961	NSD2_SET_3	ATTTGTTAACGAGTACGTTG
epikol_00962	NSD2_SET_4	AATTTGTTAACGAGTACGTT
epikol_00963	NSD2_SET_5	TGGGGCCAGCGTCTATTATA
epikol_00964	NSD3_PHD_1	ATGCAGATGAACTTGCTATC
epikol_00965	NSD3_PHD_2	ATGCCAATCCCAGGCACTCC
epikol_00966	NSD3_PHD_3	CAGGAAGTGATGCCAATCCC
epikol_00967	NSD3_PHD_4	GTGCTGCAAACACTTTCACC
epikol_00968	NSD3_PHD_5	GACTCTCTGATTCCTTGTGA
epikol_00969	NSD3_SET_1	CAAAACGGAGCGGAGAGGCT
epikol_00970	NSD3_SET_2	ATTAGTTACACTGTTCTCGT
epikol_00971	NSD3_SET_3	ATAATTGATGCCGGCCCAAA
epikol_00972	NSD3_SET_4	TAATTATAACCTAGATTGTC
epikol_00973	NSD3_SET_5	TTGGGCCGGCATCAATTATA
epikol_00974	PADI4_PAD_1	CACGCGTACACCTCCTGCGG
epikol_00975	PADI4_PAD_2	TGTGGTGTTCCAAGACAGCG
epikol_00976	PADI4_PAD_3	CTTGGAACACCACAGCCTCG
epikol_00977	PADI4_PAD_4	GGGAGGCCCTGCTGTTCGAA
epikol_00978	PADI4_PAD_5	CAGGGGCAAGGAATACCCGC
epikol_00979	PARP1_PARP_1	CGCATACTCCATCCTCAGTG
epikol_00980	PARP1_PARP_2	CCCAAAGTCGTGGGGGATCA
epikol_00981	PARP1_PARP_3	ATCTTTAAGATAGAGCGTGA
epikol_00982	PARP1_PARP_4	CTAATGTTAGCTGAAGGATC
epikol_00983	PARP1_PARP_5	TCCAGACTAATGTTAGCTGA
epikol_00984	PAXIP1_BRCT_1	GGGCTTTGGTTACGTTCTAT
epikol_00985	PAXIP1_BRCT_2	ATTTCTTATTGAGGGTTAGC
epikol_00986	PAXIP1_BRCT_3	GGCTTTGGTTACGTTCTATG
epikol_00987	PAXIP1_BRCT_4	AGAACGTAACCAAAGCCCAC
epikol_00988	PAXIP1_BRCT_5	TTTGATTGTTCCAGAGCCAA
epikol_00989	PBRM1_BAH_1	GGCCTGGTGCGTCCTCGTGT
epikol_00990	PBRM1_BAH_2	TCTTCTGGGTGAATGAAGAT
epikol_00991	PBRM1_BAH_3	TGGTATTTCAGTTGGCCTGC
epikol_00992	PBRM1_BAH_4	GTGTGCTGTGTTGTCATTCA
epikol_00993	PBRM1_BAH_5	GAAAAAGTATGGGTTCGAGA
epikol_00994	PBRM1_BROMO_1	TAATACCATCCGAGACTATA
epikol_00995	PBRM1_BROMO_2	CCGAGACTATAAGGATGAAC
epikol_00996	PBRM1_BROMO_3	TCTCTGTGAGCTCTTCATTA
epikol_00997	PBRM1_BROMO_4	ATTATAGAGTTCATGGCACA
epikol_00998	PBRM1_BROMO_5	CAAACTCATTTCTTGTTCGA
epikol_00999	PCAF_BROMO_1	TGAAGGGCCAAGCGCTTTGA
epikol_01000	PCAF_BROMO_2	CAGGATATTATGAAGTTATA
epikol_01001	PCAF_BROMO_3	ATTCTTGAGGCGTTCACTCA

epikol_01002	PCAF_BROMO_4	ACACGTAGTACCTATTCTTG
epikol_01003	PCAF_BROMO_5	GGGGTTGTACTCTTTGCAAT
epikol_01004	PCAF_NAT_1	ATTAAAGATGGCCGTGTTAT
epikol_01005	PCAF_NAT_2	TCTCTGTGAATCCTTGAGAT
epikol_01006	PCAF_NAT_3	TTCCGTATGTTCCCATCTCA
epikol_01007	PCAF_NAT_4	AACAGATACCACCAATAACA
epikol_01008	PCAF_NAT_5	ATCTCTGTGAATCCTTGAGA
epikol_01009	PCGF2_GECKO_1	CTGCCCCATGTGTGACGTGC
epikol_01010	PCGF2_GECKO_2	TCAAGACATTGTCTACAAAT
epikol_01011	PCGF2_GECKO_3	CGATGAAGTACCCCCCGCAG
epikol_01012	PCGF2_GECKO_4	CATCGACGCCACCACTATCG
epikol_01013	PCGF2_GECKO_5	AACCTGCATCGTGCGCTACC
epikol_01014	PCGF2_RING_1	CATCGACGCCACCACTATCG
epikol_01015	PCGF2_RING_2	CGATGAAGTACCCCCCGCAG
epikol_01016	PCGF2_RING_3	CAGGCACTCCACGATAGTGG
epikol_01017	PCGF2_RING_4	AACCTGCATCGTGCGCTACC
epikol_01018	PCGF2_RING_5	GGCAGTATTTGTTGGTCTCC
epikol_01019	PHF1_PHD_1	CAGCTGACCAGCCGGTTCCC
epikol_01020	PHF1_PHD_2	ACTTCTCACAGCTGACCAGC
epikol_01021	PHF1_PHD_3	CGCTCTGAGACTGTGGTCCC
epikol_01022	PHF1_PHD_4	TGTCTGTCGCTCTGAGACTG
epikol_01023	PHF1_PHD_5	GCTCTGAGACTGTGGTCCCT
epikol_01024	PHF1_TUDOR_1	GACTGATGGGCTGCTATACT
epikol_01025	PHF1_TUDOR_2	TGCTGGCCAGATGGACTGAT
epikol_01026	PHF1_TUDOR_3	GTGCTGGCCAGATGGACTGA
epikol_01027	PHF1_TUDOR_4	GTCAAGATGTGCTGGCCAGA
epikol_01028	PHF1_TUDOR_5	ATTCGCAGTTTCTGGTTCTA
epikol_01029	PHF2_GECKO_1	GACGTCACTGACATAGAACG
epikol_01030	PHF2_GECKO_2	CCAAACTGTGAGAAAACCCA
epikol_01031	PHF2_JMJC_1	TGTCATGGGTAGAAAACTAC
epikol_01032	PHF2_JMJC_2	AGTTTCTTTACAATGTCAGG
epikol_01033	PHF2_JMJC_3	GTACTGCCTAATCTGCGTGA
epikol_01034	PHF2_JMJC_4	AACTGTCCTTCACGCAGATT
epikol_01035	PHF2_JMJC_5	CACGCAGATTAGGCAGTACT
epikol_01036	PHF2_PHD_1	TGAAGCGGGTAACGTCGTAG
epikol_01037	PHF2_PHD_2	GATCGAGTGCGACGCCTGCA
epikol_01038	PHF2_PHD_3	AGTGCGACGCCTGCAAGGAC
epikol_01039	PHF8_JMJC_1	AGCTATCTCGCACACTCATG
epikol_01040	PHF8_JMJC_2	GACAGCTTTCGAACAATCTT
epikol_01041	PHF8_JMJC_3	GATTGTTCGAAAGCTGTCAT
epikol_01042	PHF8_JMJC_4	CAATCTTCGGTGTCTCCACA
epikol_01043	PHF8_JMJC_5	TGTCATGGGTCGAAAACTTG
epikol_01044	PHF8_PHD_1	GGGTCACATCGTAAGGCAGC
epikol_01045	PHF8_PHD_2	GATCGAGTGTGACATGTGCC
epikol_01046	PHF8_PHD_3	CATCGTAAGGCAGCCGGCAG
epikol_01047	PHF8_PHD_4	ATGTGCCAGGACTGGTTTCA
epikol_01048	PHF8_PHD_5	TGTTGGTGTTGAAGAGGAGA
epikol_01049	PPHLN1_1	TGCTATTGCTTTAGAGCGAG
epikol_01050	PPHLN1_2	CTGTGAAACTTTCGGGATGG
epikol_01051	PPHLN1_3	AGACTGTGAAACTTTCGGGA
epikol_01052	PPHLN1_4	CGAAAGTTTCACAGTCTTGT
epikol_01053	PPHLN1_5	GACAAGACTGTGAAACTTTC
epikol_01054	PRDM1_SET_1	CAGTTCCTAAGAACGCCAAC
epikol_01055	PRDM1_SET_2	CATTAAAGCCGTCAATGAAG
epikol_01056	PRDM1_SET_3	GGTCCAAAACGTGTGCCCTT
epikol_01057	PRDM1_SET_4	GGTGTAGATTTCACCTATTA
epikol_01058	PRDM1_SET_5	TGGTGTAGATTTCACCTATT
epikol_01059	PRDM10_SET_1	GCGCTTGGGGATGCGCCGCT
epikol_01060	PRDM10_SET_2	GGGGCCAAACTGGGTGCGCT
epikol_01061	PRDM10_SET_3	GGCCATACTGGTAAGCCACC
epikol_01062	PRDM10_SET_4	AATACACATGGTGGCCATAC
epikol_01063	PRDM10_SET_5	GGGATTTACATGAAGACCTA
epikol_01064	PRDM11_SET_1	CACATCTTCGGCCCCTATGA
epikol_01065	PRDM11_SET_2	TGTAAACGAGGTCATCCCCA
epikol_01066	PRDM11_SET_3	GGTGGAGATCTGCCCCTCAT
epikol_01067	PRDM11_SET_4	GGGCCGAAGATGTGGCCCTT
epikol_01068	PRDM11_SET_5	GCCAGCTGATTTGTCCTGGG
epikol_01069	PRDM12_SET_1	CGTGCTCCGGGGCGATCACG
epikol_01070	PRDM12_SET_2	CACCGGCCGCGTGATCGCCC
epikol_01071	PRDM12_SET_3	CTCCGGGGCGATCACGCGGC

epikol_01072	PRDM12_SET_4	TCCCGCCTTGATCCACGTCT
epikol_01073	PRDM12_SET_5	GATCAAGGCGGGAACCGAGA
epikol_01074	PRDM13_SET_1	GGCCGGCTTGCGCCTCGGAC
epikol_01075	PRDM13_SET_2	TTGCGCCTCGGACCGGTGCC
epikol_01076	PRDM13_SET_3	CACCGGTCCGAGGCGCAAGC
epikol_01077	PRDM13_SET_4	CAAGTACCTGTCAGACCGCA
epikol_01078	PRDM13_SET_5	GCTGGACGTCTCGCAATGCT
epikol_01079	PRDM14_SET_1	CATCACAGAATTGTCTCCGT
epikol_01080	PRDM14_SET_2	TCCGTAGGTCTTCACTTCAC
epikol_01081	PRDM14_SET_3	GAAGCGGGCACAGTTGACAT
epikol_01082	PRDM14_SET_4	GGGCCCAAACCTGACTCCTT
epikol_01083	PRDM14_SET_5	TCGCCAAAGGAGTCAGGTTT
epikol_01084	PRDM15_SET_1	GTCCAGGAGGGTCGCCAAAT
epikol_01085	PRDM15_SET_2	AGTCCAGGAGGGTCGCCAAA
epikol_01086	PRDM15_SET_3	TTCCCATTTGGCGACCCTCC
epikol_01087	PRDM15_SET_4	CCGCTTGACGAGCTGAGTGA
epikol_01088	PRDM15_SET_5	CGACTGGAAGATGGAGCCGA
epikol_01089	PRDM16_SET_1	AAAGGAGACAGACTTCGGAT
epikol_01090	PRDM16_SET_2	GTGGAAGTGTCGCCCCAGGA
epikol_01091	PRDM16_SET_3	GCGTGGATGCAAATCAGGCG
epikol_01092	PRDM16_SET_4	GTTCTGCGTGGATGCAAATC
epikol_01093	PRDM16_SET_5	GTCATTAAGGACATTGAGCC
epikol_01094	PRDM2_SET_1	TATGTGAATTGGGCTTGCTC
epikol_01095	PRDM2_SET_2	GGGTCTTGTCAACAGCAGAA
epikol_01096	PRDM2_SET_3	AAAAAATTTGGGCCATTTGT
epikol_01097	PRDM2_SET_4	ACTGGCTGCGATATGTGAAT
epikol_01098	PRDM2_SET_5	CTGGCTGCGATATGTGAATT
epikol_01099	PRDM3_SET_1	GAAAGACCCCAGTTATGGAT
epikol_01100	PRDM3_SET_2	GTCAACCAGATGTTGGAAGC
epikol_01101	PRDM3_SET_3	GATGCCAGTCAACCAGATGT
epikol_01102	PRDM3_SET_4	CTCAAGTACATTAGATTCGC
epikol_01103	PRDM3_SET_5	GTAGTTGCAGACATTGCGCC
epikol_01104	PRDM4_SET_1	GGTCCAAAGCAAGTCCGCAC
epikol_01105	PRDM4_SET_2	ATTCCTGTGCGGACTTGCTT
epikol_01106	PRDM4_SET_3	ACTTGCTTTGGACCTCTAAT
epikol_01107	PRDM4_SET_4	ACAAGGCAGTTAACCATATC
epikol_01108	PRDM4_SET_5	TGACTCTGCTGGCCAATTAG
epikol_01109	PRDM5_SET_1	TGGATGAAAATATGGATTAC
epikol_01110	PRDM5_SET_2	GAAGCCAGTTGGAGTGCCGT
epikol_01111	PRDM5_SET_3	CTGGCTTCGCTTCGTTCATG
epikol_01112	PRDM5_SET_4	ATGAACGAAGCGAAGCCAGT
epikol_01113	PRDM5_SET_5	ACAGACACGGAGCTTCTGAT
epikol_01114	PRDM6_SET_1	GTCCAATCCAGGTGCCTTGC
epikol_01115	PRDM6_SET_2	ACCTGGATTGGACCTTTCCA
epikol_01116	PRDM6_SET_3	GGGAACCTAGTAAGTCGAGC
epikol_01117	PRDM6_SET_4	CTAGTAAGTCGAGCTGGATG
epikol_01118	PRDM6_SET_5	CTACAGCACTTTATTGATGG
epikol_01119	PRDM8_SET_1	AGCATTCTCAGGGATGTCGC
epikol_01120	PRDM8_SET_2	GAACAGTACCGTATATCTTT
epikol_01121	PRDM8_SET_3	CATATAGGGAAGTATGGCTC
epikol_01122	PRDM8_SET_4	TGTTCTACCGCTCTCTCCGC
epikol_01123	PRDM8_SET_5	AACTAGTAACTCCTCGTCTT
epikol_01124	PRDM9_GECKO_1	CAGAAGATTCTGATGAAGAA
epikol_01125	PRDM9_GECKO_2	GTTCTCTCTGTGTCTTCTTC
epikol_01126	PRDM9_GECKO_3	TCCCTCTTACCTTGCTGCCT
epikol_01127	PRDM9_SET_1	CAGCCAGGAGTATCCATTGT
epikol_01128	PRDM9_SET_2	TGGATGGAAAAGATAAATCC
epikol_01129	PRMT1_SAM_1	CCGGGGCCCGCAAGGTCATC
epikol_01130	PRMT1_SAM_2	CCCGATGACCTTGCGGGCCC
epikol_01131	PRMT1_SAM_3	TGCTCTATGCCCGGGACAAG
epikol_01132	PRMT1_SAM_4	CTTGTCCCGGGCATAGAGCA
epikol_01133	PRMT1_SAM_5	CAACACCGTGCTCTATGCCC
epikol_01134	PRMT2_SAM_1	TCTTCTGTGCACACTATGCG
epikol_01135	PRMT2_SAM_2	TGTCAGCAAAGCCGTTCTGC
epikol_01136	PRMT2_SAM_3	GCCCGAGAAGGTGGACGTGC
epikol_01137	PRMT2_SAM_4	CGAGTCCATCCTGTATGCCC
epikol_01138	PRMT2_SAM_5	TGAAGGAGGACGGGGTCATT
epikol_01139	PRMT5_SAM_1	ATACAGCTTTATCCGCCGGT
epikol_01140	PRMT5_SAM_2	CAGCATACAGCTTTATCCGC
epikol_01141	PRMT5_SAM_3	CCGCAGGGAAGCGTTCACCA

epikol_01142	PRMT5_SAM_4	CTGATGAGACTACGGTCACT
epikol_01143	PRMT5_SAM_5	CGTAGTCTCATCAGACATGA
epikol_01144	PRMT6_SAM_1	TCAGCCACTTGGTTCGCGCG
epikol_01145	PRMT6_SAM_2	CTCTACCGCGTACACGCGCC
epikol_01146	PRMT6_SAM_3	CCGGCGCGTGTACGCGGTAG
epikol_01147	PRMT6_SAM_4	CCTCTACCGCGTACACGCGC
epikol_01148	PRMT6_SAM_5	GGTGGTGCGGTTCAACGGGC
epikol_01149	PRMT7_SAM_1	CACGGGACTCTTGTCAATGA
epikol_01150	PRMT7_SAM_2	CTCGATGGCATAGCAGAAGT
epikol_01151	PRMT7_SAM_3	TGGCTTTAGTGATAAGATTA
epikol_01152	PRMT7_SAM_4	TTCACAGCAGCATCAGCCAT
epikol_01153	PRMT7_SAM_5	TCAATGATGGCGGTCACAGC
epikol_01154	PRMT8_SAM_1	CCTTTCCATGTTCGCTGCCA
epikol_01155	PRMT8_SAM_2	CCCTGCCTTGGCAGCGAACA
epikol_01156	PRMT8_SAM_3	CCATGTTCGCTGCCAAGGCA
epikol_01157	PRMT8_SAM_4	TCAACACGGTGATCTTTGCC
epikol_01158	PRMT8_SAM_5	GATCATTAAGGCCAACCACT
epikol_01159	RBBP4_GECKO_1	CTACTCCATGAGTCTCTGTT
epikol_01160	RBBP4_GECKO_2	AGTAAGTGCCCACTGAGATT
epikol_01161	RBBP4_GECKO_3	AACCCAGACTTGCGTCTCCG
epikol_01162	RBBP4_GECKO_4	GACCTTGTCAGCTGATCCTG
epikol_01163	RBBP4_GECKO_5	CATTTAAGACCATCTGCCTG
epikol_01164	RBBP5_WD40_1	ATGATGGCCGAATTGTCATC
epikol_01165	RBBP5_WD40_2	TTTCAGGCGACTGTGACCAG
epikol_01166	RBBP5_WD40_3	AAATCGGAGTCATCGTCCAC
epikol_01167	RBBP5_WD40_4	GTCAATTGAGTTTGCCCGGA
epikol_01168	RBBP5_WD40_5	GATGGGGAATACATCGTGGC
epikol_01169	RBX1_RING_1	CTTCTGAAGTAGCGGACGCC
epikol_01170	RBX1_RING_2	AGAAGAGTGTACTGTCGCAT
epikol_01171	RBX1_RING_3	TCGCTGGCTCAAAACACGAC
epikol_01172	RBX1_RING_4	AGTACACTCTTCTGAAGTAG
epikol_01173	RBX1_RING_5	ACTTCCACTGCATCTCTCGC
epikol_01174	RNF168_RING_1	TCGACGGTCGACTGGAAGCA
epikol_01175	RNF168_RING_2	CTTCCAGTCGACCGTCGAAA
epikol_01176	RNF168_RING_3	CAGCGTGTGGTTACACGGGA
epikol_01177	RNF168_RING_4	AGCACGGTTTACACAGCGTG
epikol_01178	RNF168_RING_5	GATCTGCATGGAAATCCTCG
epikol_01179	RNF2_GECKO_2	AATTCACTGTGTAGACTTCG
epikol_01180	RNF2_GECKO_3	ATTATTGTGCTTGTTGATCC
epikol_01181	RNF2_GECKO_4	TTTCAACATACCCACTTCTA
epikol_01182	RNF2_GECKO_5	TGAGTTACAACGAACACCTC
epikol_01183	RNF2_RING_1	TCATCACAGCCCTTAGAAGT
epikol_01184	RNF20_RING_1	ACGCATGTTACAGCACGGAC
epikol_01185	RNF20_RING_2	TACACTTGGGACATTTGCGC
epikol_01186	RNF20_RING_3	CTTGGGACATTTGCGCTGGC
epikol_01187	RNF20_RING_4	GTGCTGTAACATGCGTAAAA
epikol_01188	RNF20_RING_5	ACTTGGGACATTTGCGCTGG
epikol_01189	RNF8_RING_1	AGAATGCCCCATTTGTCGGA
epikol_01190	RNF8_RING_2	GCTCCTACTGTATCAATGAA
epikol_01191	RNF8_RING_3	GAAACTGTGGGCACAGTTCA
epikol_01192	RNF8_RING_4	ACAGTAGGAGCAGAAACTGT
epikol_01193	RNF8_RING_5	AGATAGAATGCCCCATTTGT
epikol_01194	SATB1_1	GCAATGCCATTTCGATCAGC
epikol_01195	SATB1_2	CGCCATTGAATATGATTGCA
epikol_01196	SATB1_3	GGAGCATGCAGAATTTGTGC
epikol_01197	SATB1_4	TGTTCCACCACACAGAAAAC
epikol_01198	SATB1_5	AGAATTTGTGCTGGTGAGAA
epikol_01199	SETD1A_SET_1	CCGGAGCCGGATCCACGAGT
epikol_01200	SETD1A_SET_2	GGATCCGGCTCCGGCCAAAT
epikol_01201	SETD1A_SET_3	TGTCGTGGTCCACCCGGAAC
epikol_01202	SETD1A_SET_4	GCGGGAGAAGCGCTACGTGC
epikol_01203	SETD1A_SET_5	ATCTCCTCGTCCACGCCAAT
epikol_01204	SETD2_SET_1	GTCATACTCACAGAAAAGAA
epikol_01205	SETD2_SET_2	AGAGTTTAAAGCTCGAGTGA
epikol_01206	SETD2_SET_3	ACCTTTGTCCTAGAATATTG
epikol_01207	SETD2_SET_4	GGACTGTGAACGGACAACTG
epikol_01208	SETD2_SET_5	AACGTTAACTCTGAGCCTGA
epikol_01209	SETD3_SET1_1	GGCCAGTGCGATGTTTCCCA
epikol_01210	SETD3_SET1_2	AGCCATGGGAAACATCGCAC
epikol_01211	SETD3_SET1_3	GACCGAATCCTTCAAGCCAT

epikol_01212	SETD3_SET1_4	CGATGTTTCCCATGGCTTGA
epikol_01213	SETD3_SET1_5	GAGCCAGCCCTAACTCCTTC
epikol_01214	SETD3_SET2_1	GAAGGATTCTTTCACTTACG
epikol_01215	SETD3_SET2_2	TGCCAACAAACTACCCTTGA
epikol_01216	SETD3_SET2_3	GGATGGTTCCCGCGTGACCC
epikol_01217	SETD3_SET2_4	CAGTCTCTTCTGTTATGACG
epikol_01218	SETD3_SET2_5	ACGCGGGAACCATCCTCTGT
epikol_01219	SETD4_SET_1	CTGTGCACTCGCTCCGTACC
epikol_01220	SETD4_SET_2	GGGCCTCAGGTACACGGCTC
epikol_01221	SETD4_SET_3	GAAAGGCATTCCCGCTGCCT
epikol_01222	SETD4_SET_4	AAATTAGAACGACTTCACGT
epikol_01223	SETD4_SET_5	GAAGAGGTATTCATCTGTTA
epikol_01224	SETD6_SET_1	GTTCTAGGGAGCGAACCCTG
epikol_01225	SETD6_SET_2	TGAAGGGCAGCACGATGGAC
epikol_01226	SETD6_SET_3	TTCTAGATTGGCGTTGTGAT
epikol_01227	SETD6_SET_4	GGCACCATCACGGGGGAGTT
epikol_01228	SETD6_SET_5	ATCTCATGGCCTTTAGGAAT
epikol_01229	SETD7_SET_1	GATACGTGGTTATAGGGCTC
epikol_01230	SETD7_SET_2	AGGCACAGTACTTGGATACG
epikol_01231	SETD7_SET_3	TCCCAAGGAGGCACAGTACT
epikol_01232	SETD7_SET_4	CATTTGATGGGCCCAAAACG
epikol_01233	SETD7_SET_5	GAAGAGCTCACCGTTGCCTA
epikol_01234	SETD8_GECKO_1	TGGGCAAATACCTCTAGCCA
epikol_01235	SETD8_GECKO_2	AGGTACCAGGGGACCTTTCC
epikol_01236	SETD8_GECKO_3	TAACTGAGTTCTCTTCCTGA
epikol_01237	SETD8_GECKO_4	ACGGAGCGCCATGAAGTCCG
epikol_01238	SETD8_GECKO_5	GCCTGCTTACCCCGTCGGTG
epikol_01239	SETDB1_SET1_1	GGGCTGGGGTATCCGCTGCT
epikol_01240	SETDB1_SET1_2	TGCTTGGATGACATTGCCAA
epikol_01241	SETDB1_SET1_3	TCTGGACCATATCGAGAGCG
epikol_01242	SETDB1_SET1_4	AGTTCTCCACGCTCTCGATA
epikol_01243	SETDB1_SET1_5	CTTTGCAGACAAGGAGGGTC
epikol_01244	SETDB1_SET2_1	ATCATTGATGCCAAGCTTGA
epikol_01245	SETDB1_SET2_2	GGGTATCCACGAAGACATTC
epikol_01246	SETDB1_SET2_3	GTTTGTCCAGAATGTCTTCG
epikol_01247	SETDB1_SET2_4	GGGCTGGGACAGAACTTACT
epikol_01248	SETDB1_SET2_5	GCCAAGCTTGAAGGCAACCT
epikol_01249	SETDB2_SET1_1	TGTCTAGATGACATTGACAG
epikol_01250	SETDB2_SET1_2	GGTGTTCAAAACTGAGCAGA
epikol_01251	SETDB2_SET1_3	CTTATGGTATTGATGAAAAC
epikol_01252	SETDB2_SET1_4	AAAACTGAGCAGAAGGGATG
epikol_01253	SETDB2_SET1_5	GCTAACACTGAAAAATCTTA
epikol_01254	SETDB2_SET2_1	TTATTGGATGCCACAAAAGA
epikol_01255	SETDB2_SET2_2	TTGGTGAAGAATGCCACCAA
epikol_01256	SETDB2_SET2_3	ACATTCTGTACCAAGAGATT
epikol_01257	SETDB2_SET2_4	AAGCAAGAACAGAGCTAACA
epikol_01258	SETDB2_SET2_5	ACAGAGCTAACATGGGATTA
epikol_01259	SETMAR_SET_1	ACCATTGAGTCAATTCGGAC
epikol_01260	SETMAR_SET_2	AGGCTGGGGACTTCGTACCT
epikol_01261	SETMAR_SET_3	TGACTCAATGGTACCTAAGT
epikol_01262	SETMAR_SET_4	GCGTCTTGAACACTTGGAAG
epikol_01263	SETMAR_SET_5	CCAATTACATTATAGCCATC
epikol_01264	SFMBT1_1	GGTCCACAGCAGTTCCCTAT
epikol_01265	SFMBT1_2	CTCACAGGTAGTGATAACGG
epikol_01266	SFMBT1_3	CATAGCCATCATAGCGGAGA
epikol_01267	SFMBT1_4	AGGCTGATCTCTACCCCATT
epikol_01268	SFMBT1_5	GTGGACACACGTTTGCAAAA
epikol_01269	SFMBT2_1	TCTGCGCTACTGCGGTTACG
epikol_01270	SFMBT2_2	CTGGTGTGACGTAGTCATCG
epikol_01271	SFMBT2_3	CCCGCACGTGGTAATGATCG
epikol_01272	SFMBT2_4	CATCGCGGATTTGCACCCCG
epikol_01273	SFMBT2_5	GAACAACCCGGACACGTACT
epikol_01274	SHPRH_H15_1	GATACGATGTTCAACGGAAC
epikol_01275	SHPRH_H15_2	GGTCTCGTGAAACAGATCAA
epikol_01276	SHPRH_H15_3	AGAACTGACATACTTATAGA
epikol_01277	SHPRH_H15_4	ATACTTATAGATGGAAAGGA
epikol_01278	SHPRH_H15_5	GTGAAACAGATCAAAGGCCA
epikol_01279	SHPRH_HELIC_1	CGTTGAGAAAACGAGTGCTT
epikol_01280	SHPRH_HELIC_2	AGCTCTTACTGACAACAACA
epikol_01281	SHPRH_HELIC_3	ATAGGGAGGGTGCACCGAAT

epikol_01282	SHPRH_HELIC_4	TCATGGGCAGGGTTCAATAT
epikol_01283	SHPRH_HELIC_5	ATCCATTAGAACCTGTGTGC
epikol_01284	SIN3A_1	CTTTGGTAAGGCTCGATAGC
epikol_01285	SIN3A_2	AGGAGTCCGTCCTGTACACT
epikol_01286	SIN3A_3	TCTGGCAACAATCCGGGTTC
epikol_01287	SIN3A_4	AGACCAATCTGGCAACAATC
epikol_01288	SIN3A_5	CTGCTGGTAACTCTTTGGTA
epikol_01289	SIN3B_1	GCTGGATCCTATGCGCTTGC
epikol_01290	SIN3B_2	TTTGGGGAGTGCCCGGTAGC
epikol_01291	SIN3B_3	AATCGTCTGTCCACGAACCC
epikol_01292	SIN3B_4	TGGATTCCAGGATATAGTGC
epikol_01293	SIN3B_5	CTTCTTGGAGCTGACGAACG
epikol_01294	SIRT1_SIRT_1	TCAAACATCGCTTGAGGATC
epikol_01295	SIRT1_SIRT_2	CCATCCCTTGACCTGAAGTC
epikol_01296	SIRT1_SIRT_3	TACCCAGAACATAGACACGC
epikol_01297	SIRT1_SIRT_4	AACAGGTTGCGGGAATCCAA
epikol_01298	SIRT1_SIRT_5	ATAGCAAGCGGTTCATCAGC
epikol_01299	SIRT2_SIRT_1	TAGGTTGTCATAGAGGCCGG
epikol_01300	SIRT2_SIRT_2	TTCCTTGGCGAGGGCGAAGA
epikol_01301	SIRT2_SIRT_3	CTACTTCATGCGCCTGCTGA
epikol_01302	SIRT2_SIRT_4	CCAGCCCGGCTATTCGCTCC
epikol_01303	SIRT2_SIRT_5	GGCACGAATACCCGCTAAGC
epikol_01304	SIRT3_SIRT_1	GGTACGGGAGATCGTACTGC
epikol_01305	SIRT3_SIRT_2	CTCTACACGCAGAACATCGA
epikol_01306	SIRT3_SIRT_3	CAAAAATGGCCTCGGGGTAC
epikol_01307	SIRT3_SIRT_4	ATGAGCTTCAACCAGCTTTG
epikol_01308	SIRT3_SIRT_5	GGGTCTTTGGCAGACTGTGC
epikol_01309	SIRT4_SIRT_1	GTCTGGTATCCCCGATTCGG
epikol_01310	SIRT4_SIRT_2	AGTTTCTCGCCCAGTACCGC
epikol_01311	SIRT4_SIRT_3	TTTATGCCCGCACTGACCGC
epikol_01312	SIRT4_SIRT_4	TACTGGGCGAGAAACTTCGT
epikol_01313	SIRT4_SIRT_5	GTCCCAACCTGCGTTCAATG
epikol_01314	SIRT5_SIRT_1	AGTGGTGTTCCGACCTTCAG
epikol_01315	SIRT5_SIRT_2	GGGTGATGACCACGACTCGC
epikol_01316	SIRT5_SIRT_3	GTTCTACCACTACCGGCGGG
epikol_01317	SIRT5_SIRT_4	TATGGCGCGGTGCCCGGCGT
epikol_01318	SIRT5_SIRT_5	GGGAGTTCTACCACTACCGG
epikol_01319	SIRT6_SIRT_1	GTGGTGTTCCACACGGGTGC
epikol_01320	SIRT6_SIRT_2	CGTGGGCCGCGCGCTCTCAA
epikol_01321	SIRT6_SIRT_3	CTCAAAGGTGGTGTCGAACT
epikol_01322	SIRT6_SIRT_4	CATGGAGCCCGTCCACGTTC
epikol_01323	SIRT6_SIRT_5	CTTCCACAAACATGTTCCCG
epikol_01324	SIRT7_SIRT_1	GCGTCTATCCCAGACTACCG
epikol_01325	SIRT7_SIRT_2	GGGTTGGCTCGGCCTCGCTC
epikol_01326	SIRT7_SIRT_3	CAGACGGGTGATGCTCATGT
epikol_01327	SIRT7_SIRT_4	GTACATGTTCCCGTGGAGCT
epikol_01328	SIRT7_SIRT_5	AGCTCGGAGATGGCCGTGCG
epikol_01329	SMARCA1_DEXD_1	GAATATTTCGGTAGTGTTTC
epikol_01330	SMARCA1_DEXD_2	AAAGTTTCACTGGCGATACC
epikol_01331	SMARCA1_DEXD_3	ATTCGTGATGAAATGATGCC
epikol_01332	SMARCA1_DEXD_4	ACGCAAACATCCCACTCTCC
epikol_01333	SMARCA1_DEXD_5	ACTAACCGCTTGCTCCTAAC
epikol_01334	SMARCA1_HELIC_1	GGTAGTTCTGGATAAACTAT
epikol_01335	SMARCA1_HELIC_2	TGGTTATGAGTATTGTCGAC
epikol_01336	SMARCA1_HELIC_3	CAGCCAGATGACTCGCTTGC
epikol_01337	SMARCA1_HELIC_4	GAAGATTATTGCATGTGGCG
epikol_01338	SMARCA1_HELIC_5	TGGAGGTCTCGGAATTAACC
epikol_01339	SMARCA2_DEXD_1	CGGAATCTTAGCCGATGAAA
epikol_01340	SMARCA2_DEXD_2	GATGAGTGCAATGGTCTGTA
epikol_01341	SMARCA2_DEXD_3	TGACAAATGGGCTCCTTCTG
epikol_01342	SMARCA2_DEXD_4	ACAAGGGAGCGACGCATGGC
epikol_01343	SMARCA2_DEXD_5	TGAATTTGCCACTCCGTAGC
epikol_01344	SMARCA2_HELIC_1	GCTGAACTGTATCGGGCCTC
epikol_01345	SMARCA2_HELIC_2	AGCAGCACGATCTTCAGACT
epikol_01346	SMARCA2_HELIC_3	TGGCCTGGGCTTAAATCTTC
epikol_01347	SMARCA2_HELIC_4	CGATGCGGTGAGCTCGGTCT
epikol_01348	SMARCA2_HELIC_5	TTCTTGCTGAGCACAAGAGC
epikol_01349	SMARCA4_DEXD_1	GAGGTACGTGATGAGCGCGA
epikol_01350	SMARCA4_DEXD_2	GGCATCCTGGCCGACGAGAT
epikol_01351	SMARCA4_DEXD_3	GTCAAACTCGTACGCCCAGT

epikol_01352	SMARCA4_DEXD_4	TGACAAGTGGGCCCCCTCCG
epikol_01353	SMARCA4_DEXD_5	ACAAAGGCCCGTCTTGCTGC
epikol_01354	SMARCA4_HELIC_1	GAAGATTACTTTGCGTATCG
epikol_01355	SMARCA4_HELIC_2	ATCGCGGCTTTAAATACCTC
epikol_01356	SMARCA4_HELIC_3	GTGGTTGGTTGCTCGGAGTT
epikol_01357	SMARCA4_HELIC_4	CTCAGAGCCGGGCTCGTTGA
epikol_01358	SMARCA4_HELIC_5	ACCACGAAGGCGGAGGACCG
epikol_01359	SMARCA5_DEXD_1	ACCAAAACCATATGAGGCCC
epikol_01360	SMARCA5_DEXD_2	TAGTAATAGATGAAGCTCAC
epikol_01361	SMARCA5_DEXD_3	TTAGGAACCAAAACCATATG
epikol_01362	SMARCA5_DEXD_4	ACACATACATCCCATTCTCC
epikol_01363	SMARCA5_DEXD_5	GATGAGTGAATTCAAGAGAT
epikol_01364	SMARCA5_HELIC_1	ATGCATCTAGTAACCAACAG
epikol_01365	SMARCA5_HELIC_2	AAATTATGAGTACTGCAGGT
epikol_01366	SMARCA5_HELIC_3	CAGTCAAATGACAAGGGTAT
epikol_01367	SMARCA5_HELIC_4	TTCATGTTAAGCACGCGTGC
epikol_01368	SMARCA5_HELIC_5	TCTGCCCAATTCTATGTGCT
epikol_01369	SMARCAD1_DEXD_1	CTGGCATACCTCTATCAGGA
epikol_01370	SMARCAD1_DEXD_2	CATTATTACCCTCCTGATAG
epikol_01371	SMARCAD1_DEXD_3	TTTATGGTGCCCTACTTTGA
epikol_01372	SMARCAD1_DEXD_4	ATGACCGTAGTCTGTTTCGA
epikol_01373	SMARCAD1_DEXD_5	CATAAGGTGCTGGTAGCGAA
epikol_01374	SMARCAD1_HELIC_1	GAGTCTTTCCATCTAATCTG
epikol_01375	SMARCAD1_HELIC_2	TAGCCAATTTACCATGATGC
epikol_01376	SMARCAD1_HELIC_3	CCATAGAGTAGGCCAGACTA
epikol_01377	SMARCAD1_HELIC_4	TGATGAGTTTAATACCGATA
epikol_01378	SMARCAD1_HELIC_5	TCAACAAAAGCTGGTGGATT
epikol_01379	SMARCAL1_DEXD_1	CGGCCACTCCTTCCGGTAAA
epikol_01380	SMARCAL1_DEXD_2	CTCCCAGGTGAAGCGCACGG
epikol_01381	SMARCAL1_DEXD_3	CCCAGATTGCATCAACGTCG
epikol_01382	SMARCAL1_DEXD_4	TGCATCAACGTCGTGGTGAC
epikol_01383	SMARCAL1_DEXD_5	GGGAAGGACCGCCTGACAGC
epikol_01384	SMARCAL1_HELIC_1	GCTCTTGCGTAATTGCGTCC
epikol_01385	SMARCAL1_HELIC_2	TGCACACCATAAGGTGGTCC
epikol_01386	SMARCAL1_HELIC_3	GTGCAGCACATCCGCATCGA
epikol_01387	SMARCAL1_HELIC_4	TCCATCACCGCTGCCAATAT
epikol_01388	SMARCAL1_HELIC_5	AGCAGTTCCAACTGTCGGAG
epikol_01389	SMARCC2_CHROM_1	GGGTACGACCAGTCATGAAG
epikol_01390	SMARCC2_CHROM_2	ATAAGCAGGTTCTTCTGCAC
epikol_01391	SMARCC2_CHROM_3	GGTACGACCAGTCATGAAGA
epikol_01392	SMARCC2_CHROM_4	TGCTTATCCCTCTTCATGAC
epikol_01393	SMARCC2_CHROM_5	GATCCCAGCGAGTGAAATTG
epikol_01394	SMARCD1_RSC6_1	GATGGTTGTCTGGCCCATAC
epikol_01395	SMARCD1_RSC6_2	GTATGGGCCAGACAACCATC
epikol_01396	SMARCD1_RSC6_3	GGCCGGGAGACGTGAATGTA
epikol_01397	SMARCD1_RSC6_4	GCACAGGACCGCCACTACCC
epikol_01398	SMARCD1_RSC6_5	GTGTACTGTCCTACTGATGC
epikol_01399	SMARCD3_RSC6_1	TGCCTCCTGGGAGCTACGGG
epikol_01400	SMARCD3_RSC6_2	CAAGAGTTTGGTCATCGAGC
epikol_01401	SMARCD3_RSC6_3	GCATCGGACACCCACGACCC
epikol_01402	SMARCD3_RSC6_4	GAGCCGCTCAGCCATTGTCC
epikol_01403	SMARCD3_RSC6_5	GGCGGGGATCCAGTTTGAAC
epikol_01404	SMARCE1_GECKO_1	AAACTTACTGTTGCAGGAGC
epikol_01405	SMARCE1_GECKO_2	TTACCATCTGGATCTTCAGC
epikol_01406	SMARCE1_GECKO_3	GTGGGAGGTGGGGCATAAGA
epikol_01407	SMARCE1_GECKO_4	TCGACAGAGACAATCTCGCA
epikol_01408	SMARCE1_GECKO_5	AGACGACGAGAACATTCCGA
epikol_01409	SMYD1_SET_1	GCCAACAGTCATGGTTCACC
epikol_01410	SMYD1_SET_2	AGAATTGAGCTCCGGGCCCT
epikol_01411	SMYD1_SET_3	GCCCTAGGCAAGATCTCAGA
epikol_01412	SMYD1_SET_4	TACAGTTGGGCCAACAGTCA
epikol_01413	SMYD1_SET_5	CGTAGGCATCTTCCCCAACC
epikol_01414	SMYD2_SET_1	AGATGAAGAACTTTCTCATT
epikol_01415	SMYD2_SET_2	TGTGACCTACAAAGGGACCC
epikol_01416	SMYD2_SET_3	TTCTGCCAGGGTCCCTTTGT
epikol_01417	SMYD2_SET_4	GCTGTACAGGAAATCAAGCC
epikol_01418	SMYD2_SET_5	GGCAGAAGTCAGAGCTGTAC
epikol_01419	SMYD3_SET_1	GCTTCAAAAAGGTCAAAGGC
epikol_01420	SMYD3_SET_2	GCGAGCAGTCCGAGACATCG
epikol_01421	SMYD3_SET_3	GACTGCTCGCAGTAAGAGGT

epikol_01422	SMYD3_SET_4	TGAACACAATCGAACAGTTG
epikol_01423	SMYD3_SET_5	ATTGAACACAATCGAACAGT
epikol_01424	SMYD4_SET_1	ACAGCTTCAGTGTAACGCTC
epikol_01425	SMYD4_SET_2	TTCTAATCCGCTGTGACGCC
epikol_01426	SMYD4_SET_3	GGAGCATCGTTACCGACAGC
epikol_01427	SMYD4_SET_4	AATCCGCTGTGACGCCCGGA
epikol_01428	SMYD4_SET_5	AGTGCTAATGAAGGACACGC
epikol_01429	SMYD5_SET1_1	CAGGGGCCGTTCTACGAAGA
epikol_01430	SMYD5_SET1_2	GGGAGACCATCTTCGTAGAA
epikol_01431	SMYD5_SET1_3	TGCCACACAGCTCATCCGGA
epikol_01432	SMYD5_SET1_4	CATCTTCGTAGAACGGCCCC
epikol_01433	SMYD5_SET1_5	CGAAGATGGTCTCCCCCTTC
epikol_01434	SMYD5_SET2_1	TTTCTTAACTGTGAAGGATC
epikol_01435	SMYD5_SET2_2	GCTCTGGAGGATATTAAGCC
epikol_01436	SMYD5_SET2_3	CTGCATTGGGCACACAACTG
epikol_01437	SMYD5_SET2_4	GGAAAGGAGGTCTCTGCATT
epikol_01438	SMYD5_SET2_5	TGGAAAGGAGGTCTCTGCAT
epikol_01439	SP100_BROMO_1	AATCACAGTAGACCTTCAAG
epikol_01440	SP100_BROMO_2	CAGATGTACACCCGAGTAGA
epikol_01441	SP100_BROMO_3	CTGCACAAACCCTTCTACTC
epikol_01442	SP100_BROMO_4	TTAACCACATGGGCTTCTGT
epikol_01443	SP100_BROMO_5	TTGACTTTGTTTAACCACAT
epikol_01444	SRCAP_DEXD_1	CATCTCTCTGCTTGCCCACT
epikol_01445	SRCAP_DEXD_2	CAGTTCAACATCACGCTGGT
epikol_01446	SRCAP_DEXD_3	CCACCAGCGTGATGTTGAAC
epikol_01447	SRCAP_DEXD_4	GCGCCAGTTCTTGCGACGGA
epikol_01448	SRCAP_DEXD_5	GATAGCGCCAGTTCTTGCGA
epikol_01449	SRCAP_HELIC_1	CATCCAGCATTCGGGTCATC
epikol_01450	SRCAP_HELIC_2	TAGTAGATCCATCCAGGCGC
epikol_01451	SRCAP_HELIC_3	CACCCAGATGACCCGAATGC
epikol_01452	SRCAP_HELIC_4	CAGGACCGCTGTCACCGAAT
epikol_01453	SRCAP_HELIC_5	TCATCCTTTCAACTCGGAGT
epikol_01454	SSRP1_PHD1_1	CGAATGTCATAACGACCACG
epikol_01455	SSRP1_PHD1_2	GACGCAGTACTGTGGTGTAG
epikol_01456	SSRP1_PHD1_3	CTCGTGGTCGTTATGACATT
epikol_01457	SSRP1_PHD1_4	TCAGGAAGTGGTAGCGAGTT
epikol_01458	SSRP1_PHD1_5	CGAGTTTGGCCTTGCTTGAT
epikol_01459	SSRP1_PHD2_1	CTCAGGACTGCTCTACCCGC
epikol_01460	SSRP1_PHD2_2	TCATCGAAGCGGATGTGCAC
epikol_01461	SSRP1_PHD2_3	GTCAAAGGAACGAGTAGTAG
epikol_01462	SSRP1_PHD2_4	GACTGCTCTACCCGCTGGAG
epikol_01463	SSRP1_PHD2_5	TCCTTTGTCAACTTTGCTCG
epikol_01464	SUPT16H_1	GAAACTGGACCCGCTCAAAG
epikol_01465	SUPT16H_2	TACAGGAATGGCGTTGATCA
epikol_01466	SUPT16H_3	ATGGGGTCAAGAGAGGCTAC
epikol_01467	SUPT16H_4	CTCTTGACCCCATCAAGGAA
epikol_01468	SUPT16H_5	CGCTGGTAAATGCTACGGAA
epikol_01469	SUPT16H_FACT_1	TCCTTGACAAAAGTCGCTTC
epikol_01470	SUPT16H_FACT_2	GCATCAAATATTAAGGCACC
epikol_01471	SUPT16H_FACT_3	GGCTGGTACTGTCTGTTCTC
epikol_01472	SUPT16H_FACT_4	ATACCGAGCATCAAATATTA
epikol_01473	SUPT16H_FACT_5	GCTGGTACTGTCTGTTCTCC
epikol_01474	SUV39H1_CHROM_1	GGATCTTCTTGTAATCGCAC
epikol_01475	SUV39H1_CHROM_2	ACACACTTGAGATTCTGCCG
epikol_01476	SUV39H1_CHROM_3	TATTACCTGGTGAAATGGCG
epikol_01477	SUV39H1_CHROM_4	GATATCCACGCCATTTCACC
epikol_01478	SUV39H1_CHROM_5	GAGATTCTGCCGTGGCTCCC
epikol_01479	SUV39H1_SET_1	AGCTTCGTCATGGAGTACGT
epikol_01480	SUV39H1_SET_2	TTCCGCACGGATGATGGGCG
epikol_01481	SUV39H1_SET_3	CGTGGAGGACGTGTACACCG
epikol_01482	SUV39H1_SET_4	GGGCCAGATCTACGACCGTC
epikol_01483	SUV39H1_SET_5	CGCCCTGACGGTCGTAGATC
epikol_01484	SUV39H2_CHROM_1	GGAATACTTGTGTGACTACA
epikol_01485	SUV39H2_CHROM_2	GGCCAGATTCTACAAATACT
epikol_01486	SUV39H2_CHROM_3	ATCTTGTAAAATGGAAAGGA
epikol_01487	SUV39H2_CHROM_4	TGGAATATTATCTTGTAAAA
epikol_01488	SUV39H2_CHROM_5	TATTATCTTGTAAAATGGAA
epikol_01489	SUV39H2_SET_1	TTTCGAACTAGCAATGGACG
epikol_01490	SUV39H2_SET_2	AACTAGCAATGGACGTGGCT
epikol_01491	SUV39H2_SET_3	TGCATCTTTCGAACTAGCAA

epikol_01492	SUV39H2_SET_4	ACAGTGGATGCGGCTCGATA
epikol_01493	SUV39H2_SET_5	AATCACGTATCTCTTTGATC
epikol_01494	SUV420H1_SET_1	TCAGTGTCATGTACTCCACA
epikol_01495	SUV420H1_SET_2	GAGAACATGCTACTTAGACA
epikol_01496	SUV420H1_SET_3	AAACTGTGCTCAACTCTGGC
epikol_01497	SUV420H1_SET_4	GCTCTAAGAGACATTGAACC
epikol_01498	SUV420H1_SET_5	TCGAGATACAGCATGTGTGA
epikol_01499	SUV420H2_SET_1	TCATGTACTCAACCCGCAAG
epikol_01500	SUV420H2_SET_2	CAGCTGAGCACTCCGCTTGC
epikol_01501	SUV420H2_SET_3	GCAAGCGGAGTGCTCAGCTG
epikol_01502	SUV420H2_SET_4	GTGACATGCTTCTACGGCGA
epikol_01503	SUV420H2_SET_5	GTCCCGGAGCACCTTCACGC
epikol_01504	TAF1_BROMO_1	CAAAGTGATTGTCAATCCAA
epikol_01505	TAF1_BROMO_2	GGATGATGTAAACCTTATTC
epikol_01506	TAF1_BROMO_3	AACAGACGTTCACAATCTCC
epikol_01507	TAF1_GECKO_1	AAGAATCACCTGAGTGGCAA
epikol_01508	TAF1_GECKO_2	GATAAAATCTAGAATGATAG
epikol_01509	TET1_OXY_1	GGAGCATACTGCTTATAAAT
epikol_01510	TET1_OXY_2	AACTCTGTAAGTTATCTTCA
epikol_01511	TET1_OXY_3	GTTGCCCGAGAATGTCGGCT
epikol_01512	TET1_OXY_4	GCGGTTATCTTCTCGAGTTA
epikol_01513	TET1_OXY_5	GCTTATAAAGAGGTAGCACA
epikol_01514	TET2_OXY_1	CCAAGGAAGTTTAAGCTGCT
epikol_01515	TET2_OXY_2	TTGGTGCCATAAGAGTGGAC
epikol_01516	TET2_OXY_3	GCAAAACCTGTCCACTCTTA
epikol_01517	TET2_OXY_4	AGAGCACCAGAGTGCCGTCT
epikol_01518	TET2_OXY_5	TTCAGACCCAGACGGCACTC
epikol_01519	TET3_OXY_1	CTCGCAAGTTCCGCCTCGCA
epikol_01520	TET3_OXY_2	TCAACGGCTGCAAGTATGCT
epikol_01521	TET3_OXY_3	GCCGTTGAAGTACATGCTCC
epikol_01522	TET3_OXY_4	CGCTCCCCTGTACAAGCGAC
epikol_01523	TET3_OXY_5	GTACAGGGGAGCGACTTCGG
epikol_01524	TIP60_CHROM_1	GGCCGAGATCCTGAGCGTGA
epikol_01525	TIP60_CHROM_2	GCGTGAAGGACATCAGTGGC
epikol_01526	TIP60_CHROM_3	ATGGGTGACGCATGAGCGGC
epikol_01527	TIP60_CHROM_4	ATGAATGGGTGACGCATGAG
epikol_01528	TIP60_CHROM_5	CACTGATGTCCTTCACGCTC
epikol_01529	TIP60_NAT_1	GCTTGCCGTAGCCCCGGCGC
epikol_01530	TIP60_NAT_2	CTGCCTCCCTACCAGCGCCG
epikol_01531	TIP60_NAT_3	TCAGCAGCTTGCCGTAGCCC
epikol_01532	TIP60_NAT_4	ATCAACGGAAGACTACAATG
epikol_01533	TIP60_NAT_5	CCGGCGCTGGTAGGGAGGCA
epikol_01534	TRIM24_BROMO_1	TTACTGCCATGAAATGAGCC
epikol_01535	TRIM24_BROMO_2	GAACAGGGTCTTGAAAAGCC
epikol_01536	TRIM24_BROMO_3	AAATCAGCTACAAAATCTTC
epikol_01537	TRIM24_BROMO_4	GCATTGGCTACTTCTGAATC
epikol_01538	TRIM24_BROMO_5	GATTCAGAAGTAGCCAATGC
epikol_01539	TRIM33_BROMO_1	TACTTAATTCATGGCAATAG
epikol_01540	TRIM33_BROMO_2	CCACAAAGTCATCCGGGATT
epikol_01541	TRIM33_BROMO_3	CATCCGGGATTTGGTAGTGT
epikol_01542	TRIM33_BROMO_4	CTTGAAGATCAAACGGACAT
epikol_01543	TRIM33_BROMO_5	TGGACCTGTCAATCATCCGG
epikol_01544	TRIM66_BROMO_1	GGGCTGACAGGTTCATGGAA
epikol_01545	TRIM66_BROMO_2	GCTTCCTCCGGATGATTGAC
epikol_01546	TRIM66_BROMO_3	CGGATGATTGACAGGTCCAT
epikol_01547	TRIM66_BROMO_4	CCATGGGCCTCTTGATAATC
epikol_01548	TRIM66_BROMO_5	GCCTCTGCAACCTCGGAGTC
epikol_01549	TTF2_DEXD_1	GGATGAGCGCAATCATTGTC
epikol_01550	TTF2_DEXD_2	AGAAAAGCACAGCTTTGACG
epikol_01551	TTF2_DEXD_3	CTGGCACGTGAATCCCGGTT
epikol_01552	TTF2_DEXD_4	ATCTCTACCATGGGCCAAAC
epikol_01553	TTF2_DEXD_5	GATCACTACCTATAGCCTCG
epikol_01554	TTF2_HELIC_1	ATCTCTGTTGGCAGAATTGG
epikol_01555	TTF2_HELIC_2	CTGACTTATGCCACCATCGA
epikol_01556	TTF2_HELIC_3	GGGATTGACAGAGCCATCGA
epikol_01557	TTF2_HELIC_4	GAGGCATTTAACCACTCCAG
epikol_01558	TTF2_HELIC_5	GGTGTTGGTCTAAACCTGAC
epikol_01559	UBE2A_UBC_1	ACCATTATGTTGTTCTCGGA
epikol_01560	UBE2A_UBC_2	CATCATAGGTTGGACTCCAA
epikol_01561	UBE2A_UBC_3	TCCGTCCGAGAACAACATAA

epikol_01562	UBE2A_UBC_4	TCCTCCAGCCGGAGTCAGCG
epikol_01563	UBE2A_UBC_5	ATGGAAGACACATCATAGGT
epikol_01564	UBE2B_UBC_1	GGTGCGCCACTGACACCCAC
epikol_01565	UBE2B_UBC_2	TTACAAGAGGACCCACCTGT
epikol_01566	UBE2B_UBC_3	GATAAAAACCTAACAGTTGG
epikol_01567	UBE2B_UBC_4	TTGGACTCCATCGATTCTGA
epikol_01568	UBE2B_UBC_5	TTGGCTGGACTGTTAGGATT
epikol_01569	UBE2E1_UBC_1	GCCTCCAGGATCCGTGTATG
epikol_01570	UBE2E1_UBC_2	CCACCCTCATACACGGATCC
epikol_01571	UBE2E1_UBC_3	ACTTTAGAAATGGTTAGTGC
epikol_01572	UBE2E1_UBC_4	CAGTCAAGGTGTTATTTGCT
epikol_01573	UBE2E1_UBC_5	CTTCCCACCAAGGGGTCGGC
epikol_01574	UBE2I_UBC_1	TCGCCCAGGAGAGGAAAGCA
epikol_01575	UBE2I_UBC_2	AACTGGGAGTGCGCCATTCC
epikol_01576	UBE2I_UBC_3	ATGAGGTTCATCGTGCCATC
epikol_01577	UBE2I_UBC_4	GCACGATGAACCTCATGAAC
epikol_01578	UBE2I_UBC_5	ACCCGAATGTGTACCCTTCG
epikol_01579	UBR2_GECKO_1	ACTTAACACCTCTGAAATTG
epikol_01580	UBR2_GECKO_2	TGCATAACTTGAACTTTGAG
epikol_01581	UBR2_GECKO_3	CTCTTCTTCCTCAATTTCAG
epikol_01582	UBR2_GECKO_4	TACACCATCTCTAAATCTGC
epikol_01583	UBR2_GECKO_5	ATTGTCGCACATCAGAATTT
epikol_01584	UHRF1_1	TCCCGTCCATGGTCCGAACC
epikol_01585	UHRF1_2	GGACAGCGAGTCCACCGTGT
epikol_01586	UHRF1_3	GTGGATCCAGGTTCGGACCA
epikol_01587	UHRF1_4	TGGACAGCGAGTCCACCGTG
epikol_01588	UHRF1_5	GGCGGACCTCGTAGTCGAAG
epikol_01589	USP22_PC19_1	CTTCATGAACTGCATCGTGC
epikol_01590	USP22_PC19_2	AGTCCCGCAGAAGTGGCGTG
epikol_01591	USP22_PC19_3	GCCTGCTAGGTGCCTCGCGT
epikol_01592	USP22_PC19_4	ACCTGGTGTGGACCCACGCG
epikol_01593	USP22_PC19_5	GCAACCCGCCTGTGAAGATC
epikol_01594	USP22_UHYD_1	CTTCATGAACTGCATCGTGC
epikol_01595	USP22_UHYD_2	CTGCGTGGGCTGATCAACCT
epikol_01596	USP22_UHYD_3	GCCTGCTAGGTGCCTCGCGT
epikol_01597	USP22_UHYD_4	ACCTGGTGTGGACCCACGCG
epikol_01598	USP22_UHYD_5	GCAACCCGCCTGTGAAGATC
epikol_01599	USP44_PC19_1	TTGTTGGGCGTAACCACGAA
epikol_01600	USP44_PC19_2	TTACGCCCAACAAGACGCTC
epikol_01601	USP44_PC19_3	GCTTGATCTGAACCAATGGC
epikol_01602	USP44_PC19_4	CCACTGCATTGATACCTTTC
epikol_01603	USP44_PC19_5	TGGGCTTCTGTGAGTACAAC
epikol_01604	USP44_UHYD_1	TTGTTGGGCGTAACCACGAA
epikol_01605	USP44_UHYD_2	TTACGCCCAACAAGACGCTC
epikol_01606	USP44_UHYD_3	AAATTCCTGAGCGTCTTGTT
epikol_01607	USP44_UHYD_4	CCACTGCATTGATACCTTTC
epikol_01608	USP44_UHYD_5	TATCTATGACTTGTCCGCGG
epikol_01609	UTX_JMJC_1	CAAACCATTCACAGTCACCT
epikol_01610	UTX_JMJC_2	GAATGGTTTGTTGTTCCTGA
epikol_01611	UTX_JMJC_3	GTTGTTCCTGAAGGTTACTG
epikol_01612	UTX_JMJC_4	GTTCATTGGGTTCAGGCTAT
epikol_01613	UTX_JMJC_5	TGGGCCACCAAGAACCCATT
epikol_01614	UTY_JMJC_1	GTTGTACCTGAAGATTATTG
epikol_01615	UTY_JMJC_2	TGTTGTACCTGAAGATTATT
epikol_01616	UTY_JMJC_3	GTGCATTGGGTTCAAGCTGT
epikol_01617	UTY_JMJC_4	TTGCTTCATAAAGATCTTCA
epikol_01618	UTY_JMJC_5	TTGTTGTACCTGAAGATTAT
epikol_01619	WDR5_WD40_1	AAATTTGGGGCGCGTATGAT
epikol_01620	WDR5_WD40_2	ATCTGACGACCAGGCTACAT
epikol_01621	WDR5_WD40_3	CAAGACTTTGCCAGCTCACT
epikol_01622	WDR5_WD40_4	ATAGCTACTTGAAACTATCA
epikol_01623	WDR5_WD40_5	CAGGATGTATTTGCCGTTCG
epikol_01624	WDR82_WD40_1	TTTCAGCCCCAACGGCGAGA
epikol_01625	WDR82_WD40_2	ACGAATGAAGCTGCCGTTGG
epikol_01626	WDR82_WD40_3	CGTCTGATTGATGCATTCAA
epikol_01627	WDR82_WD40_4	CGAGATGACCGTCTCGCCGT
epikol_01628	WDR82_WD40_5	CTGCATGAGTGTATCTGATG
epikol_01629	ZMYND11_BROMO_1	ATTCATTGTCTCCCGCATGA
epikol_01630	ZMYND11_BROMO_2	ACAATAAACACCCGATGTAC
epikol_01631	ZMYND11_BROMO_3	ACACCCGATGTACAGGAGGC

epikol_01632	ZMYND11_BROMO_4	CGGTATTGTGGAGAAGCAAT
epikol_01633	ZMYND11_BROMO_5	GTGAGCAAGCTGACATTGCG
epikol_01634	ZMYND8_BROMO_1	AATGGCAAACTTGAGCAGGT
epikol_01635	ZMYND8_BROMO_2	ATTCCAGAAGCCCGTTCCAT
epikol_01636	ZMYND8_BROMO_3	GGGTGCTGTTCCAATGGAAC
epikol_01637	ZMYND8_BROMO_4	AAATCCACTTTGCATCAGCC
epikol_01638	ZMYND8_BROMO_5	TGGCTGCACAGAAGCCTTCC
epikol_01639	NonTargetingControlGuideForHuman_0001	ACGGAGGCTAAGCGTCGCAA
epikol_01640	NonTargetingControlGuideForHuman_0002	CGCTTCCGCGGCCCGTTCAA
epikol_01641	NonTargetingControlGuideForHuman_0003	ATCGTTTCCGCTTAACGGCG
epikol_01642	NonTargetingControlGuideForHuman_0004	GTAGGCGCGCCGCTCTCTAC
epikol_01643	NonTargetingControlGuideForHuman_0005	CCATATCGGGGCGAGACATG
epikol_01644	NonTargetingControlGuideForHuman_0006	TACTAACGCCGCTCCTACAG
epikol_01645	NonTargetingControlGuideForHuman_0007	TGAGGATCATGTCGAGCGCC
epikol_01646	NonTargetingControlGuideForHuman_0008	GGGCCCGCATAGGATATCGC
epikol_01647	NonTargetingControlGuideForHuman_0009	TAGACAACCGCGGAGAATGC
epikol_01648	NonTargetingControlGuideForHuman_0010	ACGGGCGGCTATCGCTGACT
epikol_01649	NonTargetingControlGuideForHuman_0011	CGCGGAAATTTTACCGACGA
epikol_01650	NonTargetingControlGuideForHuman_0012	CTTACAATCGTCGGTCCAAT
epikol_01651	NonTargetingControlGuideForHuman_0013	GCGTGCGTCCCGGGTTACCC
epikol_01652	NonTargetingControlGuideForHuman_0014	CGGAGTAACAAGCGGACGGA
epikol_01653	NonTargetingControlGuideForHuman_0015	CGAGTGTTATACGCACCGTT
epikol_01654	NonTargetingControlGuideForHuman_0016	CGACTAACCGGAAACTTTTT
epikol_01655	NonTargetingControlGuideForHuman_0017	CAACGGGTTCTCCCGGCTAC
epikol_01656	NonTargetingControlGuideForHuman_0018	CAGGAGTCGCCGATACGCGT
epikol_01657	NonTargetingControlGuideForHuman_0019	TTCACGTCGTCTCGCGACCA
epikol_01658	NonTargetingControlGuideForHuman_0020	GTGTCGGATTCCGCCGCTTA
epikol_01659	NonTargetingControlGuideForHuman_0021	CACGAACTCACACCGCGCGA
epikol_01660	NonTargetingControlGuideForHuman_0022	CGCTAGTACGCTCCTCTATA
epikol_01661	NonTargetingControlGuideForHuman_0023	TCGCGCTTGGGTTATACGCT
epikol_01662	NonTargetingControlGuideForHuman_0024	CTATCTCGAGTGGTAATGCG
epikol_01663	NonTargetingControlGuideForHuman_0025	AATCGACTCGAACTTCGTGT
epikol_01664	NonTargetingControlGuideForHuman_0026	CCCGATGGACTATACCGAAC
epikol_01665	NonTargetingControlGuideForHuman_0027	ACGTTCGAGTACGACCAGCT
epikol_01666	NonTargetingControlGuideForHuman_0028	CGCGACGACTCAACCTAGTC
epikol_01667	NonTargetingControlGuideForHuman_0029	GGTCACCGATCGAGAGCTAG
epikol_01668	NonTargetingControlGuideForHuman_0030	CTCAACCGACCGTATGGTCA
epikol_01669	NonTargetingControlGuideForHuman_0031	CGTATTCGACTCTCAACGCG
epikol_01670	NonTargetingControlGuideForHuman_0032	CTAGCCGCCCAGATCGAGCC
epikol_01671	NonTargetingControlGuideForHuman_0033	GAATCGACCGACACTAATGT
epikol_01672	NonTargetingControlGuideForHuman_0034	ACTTCAGTTCGGCGTAGTCA
epikol_01673	NonTargetingControlGuideForHuman_0035	GTGCGATGTCGCTTCAACGT
epikol_01674	NonTargetingControlGuideForHuman_0036	CGCCTAATTTCCGGATCAAT
epikol_01675	NonTargetingControlGuideForHuman_0037	CGTGGCCGGAACCGTCATAG
epikol_01676	NonTargetingControlGuideForHuman_0038	ACCCTCCGAATCGTAACGGA
epikol_01677	NonTargetingControlGuideForHuman_0039	AAACGGTACGACAGCGTGTG
epikol_01678	NonTargetingControlGuideForHuman_0040	ACATAGTCGACGGCTCGATT
epikol_01679	NonTargetingControlGuideForHuman_0041	GATGGCGCTTCAGTCGTCGG
epikol_01680	NonTargetingControlGuideForHuman_0042	ATAATCCGGAAACGCTCGAC
epikol_01681	NonTargetingControlGuideForHuman_0043	CGCCGGGCTGACAATTAACG
epikol_01682	NonTargetingControlGuideForHuman_0044	CGTCGCCATATGCCGGTGGC
epikol_01683	NonTargetingControlGuideForHuman_0045	CGGGCCTATAACACCATCGA
epikol_01684	NonTargetingControlGuideForHuman_0046	CGCCGTTCCGAGATACTTGA
epikol_01685	NonTargetingControlGuideForHuman_0047	CGGGACGTCGCGAAAATGTA
epikol_01686	NonTargetingControlGuideForHuman_0048	TCGGCATACGGGACACACGC
epikol_01687	NonTargetingControlGuideForHuman_0049	AGCTCCATCGCCGCGATAAT
epikol_01688	NonTargetingControlGuideForHuman_0050	ATCGTATCATCAGCTAGCGC
epikol_01689	NonTargetingControlGuideForHuman_0051	TCGATCGAGGTTGCATTCGG
epikol_01690	NonTargetingControlGuideForHuman_0052	CTCGACAGTTCGTCCCGAGC
epikol_01691	NonTargetingControlGuideForHuman_0053	CGGTAGTATTAATCGCTGAC
epikol_01692	NonTargetingControlGuideForHuman_0054	TGAACGCGTGTTTCCTTGCA
epikol_01693	NonTargetingControlGuideForHuman_0055	CGACGCTAGGTAACGTAGAG
epikol_01694	NonTargetingControlGuideForHuman_0056	CATTGTTGAGCGGGCGCGCT
epikol_01695	NonTargetingControlGuideForHuman_0057	CCGCTATTGAAACCGCCCAC
epikol_01696	NonTargetingControlGuideForHuman_0058	AGACACGTCACCGGTCAAAA
epikol_01697	NonTargetingControlGuideForHuman_0059	TTTACGATCTAGCGGCGTAG
epikol_01698	NonTargetingControlGuideForHuman_0060	TTCGCACGATTGCACCTTGG
epikol_01699	NonTargetingControlGuideForHuman_0061	GGTTAGAGACTAGGCGCGCG
epikol_01700	NonTargetingControlGuideForHuman_0062	CCTCCGTGCTAACGCGGACG
epikol_01701	NonTargetingControlGuideForHuman_0063	TTATCGCGTAGTGCTGACGT

epikol_01702	NonTargetingControlGuideForHuman_0064	TACGCTTGCGTTTAGCGTCC
epikol_01703	NonTargetingControlGuideForHuman_0065	CGCGGCCCACGCGTCATCGC
epikol_01704	NonTargetingControlGuideForHuman_0066	AGCTCGCCATGTCGGTTCTC
epikol_01705	NonTargetingControlGuideForHuman_0067	AACTAGCCCGAGCAGCTTCG
epikol_01706	NonTargetingControlGuideForHuman_0068	CGCAAGGTGTCGGTAACCCT
epikol_01707	NonTargetingControlGuideForHuman_0069	CTTCGACGCCATCGTGCTCA
epikol_01708	NonTargetingControlGuideForHuman_0070	TCCTGGATACCGCGTGGTTA
epikol_01709	NonTargetingControlGuideForHuman_0071	ATAGCCGCCGCTCATTACTT
epikol_01710	NonTargetingControlGuideForHuman_0072	GTCGTCCGGGATTACAAAAT
epikol_01711	NonTargetingControlGuideForHuman_0073	TAATGCTGCACACGCCGAAT
epikol_01712	NonTargetingControlGuideForHuman_0074	TATCGCTTCCGATTAGTCCG
epikol_01713	NonTargetingControlGuideForHuman_0075	GTACCATACCGCGTACCCTT
epikol_01714	NonTargetingControlGuideForHuman_0076	TAAGATCCGCGGGTGGCAAC
epikol_01715	NonTargetingControlGuideForHuman_0077	GTAGACGTCGTGAGCTTCAC
epikol_01716	NonTargetingControlGuideForHuman_0078	TCGCGGACATAGGGCTCTAA
epikol_01717	NonTargetingControlGuideForHuman_0079	AGCGCAGATAGCGCGTATCA
epikol_01718	NonTargetingControlGuideForHuman_0080	GTTCGCTTCGTAACGAGGAA

7. APPENDIX B - KUGBM8-EF drug screen

7.1. Introduction

Drug repurposing is the application of known drugs to other uses, which takes off years required to develop a new drug and provides a drastic economic benefit [214]. In addition, a repurposed drug already comes with the systemic toxicity knowledge, hence reducing cytotoxicity problems. Drug repurposing by using has provided many potential candidates for various diseases. For example, a screen in 1994 revealed Gefitinib (AstraZeneca) and Erlotinib (Roche) as specific inhibitor of the epidermal growth factor receptor tyrosine kinase, which were approved by FDA in 2003 and currently used in many cancer treatments [215].

With this in mind, a high throughput screen with a chemical library consisting of 1200 Food and Drug Administration (FDA) approved drugs were utilized for investigating novel therapeutic options for GBM.

7.2. Materials & methods

7.2.1. Cell culture, chemicals and reagents

KUGBM8-EF cell line was used grown in EF medium (Neurobasal medium (Gibco), L-Glutamine (Gibco), B27 and N2 supplements (Gibco), Pen-Strep (Gibco), Heparin (Stem Cell Technologies), FGF (Gibco, PHG0266) and EGF (Peprotech, AF-100-15)). Cells were kept in 37^{0}C humidified incubator with 5% CO_2. Cells were routinely checked for mycoplasma contamination by Lonza Mycoplasma Detection Kit.

The drug library composed of 1,200 FDA (Food and Drug Administration of USA) approved drugs were purchased from Prestwick Chemical (France). The list and structure of the drugs are provided in **Table 7.2**. Individual drugs, namely Astemizole, Camptothecine (S,+) Quinacrine dihydrochloride dihydrate, Mitoxantrone dihydrochloride, Daunorubicin hydrochloride, Doxorubicin and Topotecan were then separately supplied from Prestwick Chemicals in higher quantities.

7.2.2. Drug screen

For the optimal usage of reagents and having more technical replicates at once, 384 well plates (Corning) were chosen for the high throughput drug screen. For the drug

screen, KUGBM8-EF cells were automatically seeded to 384 well plates at the number of 1'500 cells/40 µl/well via Multidrop™ Combi Reagent Dispenser (Thermo-Scientific). Next day, fresh 50 µM drug plates were prepared with EF medium and added to 384 well plates with an automated pipettor (Matrix™ Multichannel Electronic Pipettes, Thermo Scientific) for a final concentration of 5µM. Each treatment was done in quadruplucates. Cell viability was determined 3 days after and normalization to untreated controls were done for statistical analysis.

7.2.3. Validation of chosen hits

For the chosen hits, cell viability was further investigated on black 96 well plates (Corning), with combination to Temozolomide. Cell viability was detected after 5 days by CTG.

7.3. Results & Discussion

Cells were treated with the respective drug at 5μM concentration for 3 days, and viability was detected by CTG. Percent viability was determined by normalization to untreated controls, and for hit determination a cut off value of 50% was utilized (**Figure 7.1A**).

30 drugs were found to decrease cell viability to at least 50%; Thonzonium bromide, Astemizole, Pyrvinium pamoate, Ivermectin, Quinacrine dihydrochloride dihydrate, Daunorubicin hydrochloride, Alexidine dihydrochloride, Methotrexate ,Doxorubicin hydrochloride ,Amethopterin (R,S), Thioguanosine, Methyl benzethonium chloride ,Alendronate sodium, Mercaptopurine, Topotecan, Thiostrepton, Avermectin B1a, Camptothecine (S,+), Chlorhexidine, Cycloheximide, Carbetapentane citrate, Proscillaridin A, Methiazole, Halofantrine hydrochloride, Sertindole, Azaguanine-8, Mitoxantrone dihydrochloride, Niclosamide and Flubendazol (**Figure 7.1B**).

When we categorize the hits into groups for their therapeutic effects, we observe that the major groups are infectiology and oncology (**Table 7.1**). We further studied some selected hits with combination to Temozolomide and observed Doxorubicin and Temozolomide has additive effects on cell viability (**Figure 7.2**).

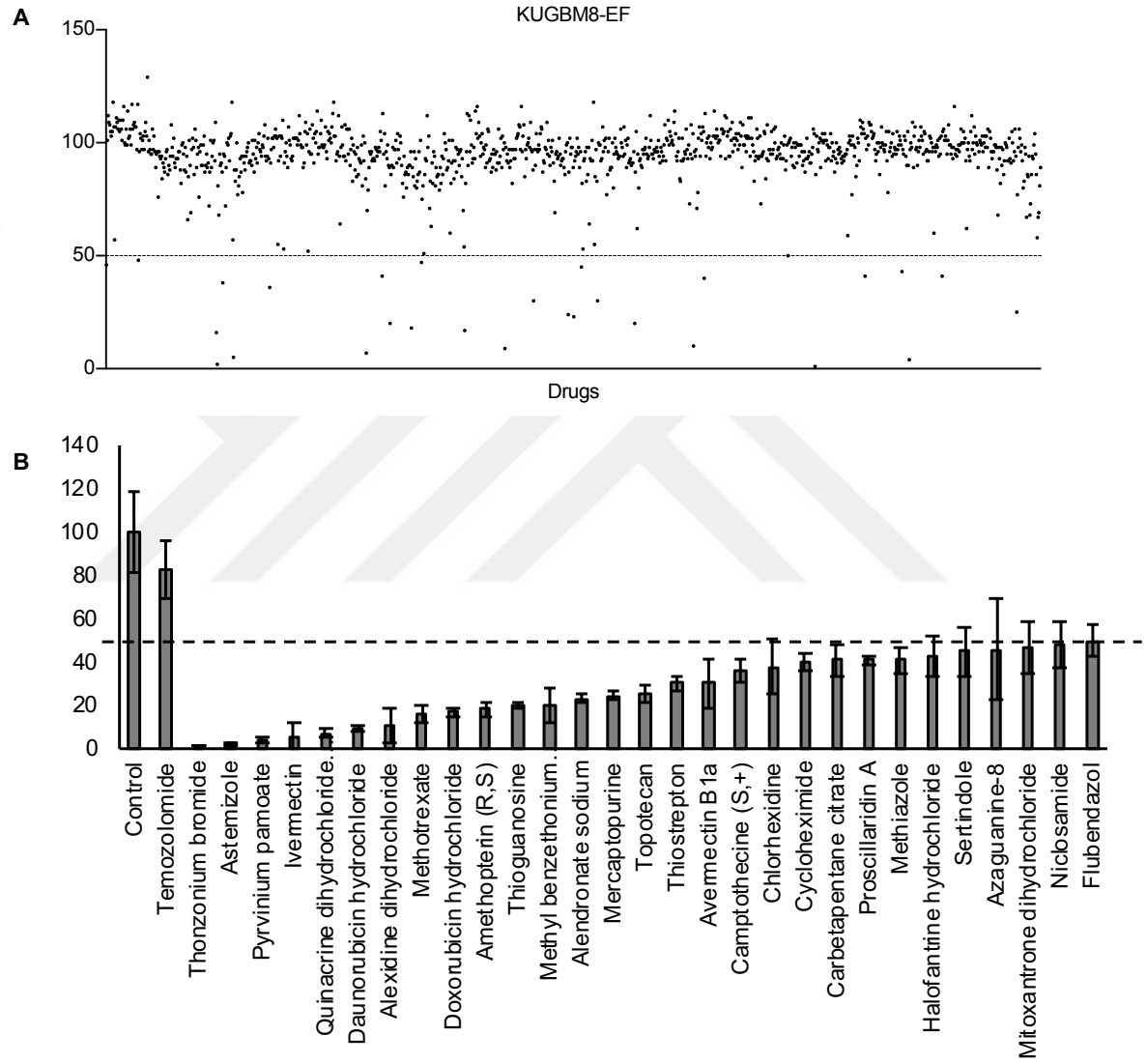

Figure 7.1 High-throughput drug repurposing screen on KUGBM8-EF cells. A) Cells were treated with 5μM of the respective drug for 72 hours. Cut off for hit identification was determined as 50% cell viability. **B)** Top 29 hits under 50% cut off viability. Temozolomide (500 μM) was used as a control. Viability was detected by CTG after 3 days and treated cells were normalized to untreated controls.

Table 7.1 Table of hits divided into therapeutic classes and effects.

Chemical name	Therapeutic class	Therapeutic effect
Astemizole	Allergology	Antihistaminic
Proscillaridin A	Cardiovascular	
Carbetapentane citrate	Central Nervous System	Antispastic, 'Local anesthetic
Sertindole	Central Nervous System	Antipsychotic
Thonzonium bromide	Dermatology	Antiseptic
Amethopterin (R,S)	Immunology, 'Oncology	Anti-inflammatory, 'Antineoplastic
Mercaptopurine	Immunology, 'Oncology	Immunosuppressant
Ivermectin	Infectiology	Antihelmintic
Alexidine dihydrochloride	Infectiology	Antibacterial
Methyl benzethonium chloride	Infectiology	Antibacterial
Thiostrepton	Infectiology	Antibacterial
Avermectin B1a	Infectiology	Antihelmintic
Chlorhexidine	Infectiology	Antibacterial, 'Antiseptic
Cycloheximide	Infectiology	Antibacterial
Methiazole	Infectiology	Antihelmintic
Niclosamide	Infectiology	Antihelmintic
Quinacrine dihydrochloride	Infectiology, Metabolism	Antihelmintic, Antiparasitic
Daunorubicin hydrochloride	Infectiology, Oncology	Antibacterial, 'Antineoplastic
Doxorubicin hydrochloride	Infectiology, Oncology	Antibacterial, 'Antineoplastic
Pyrvinium pamoate	Metabolism	
Thioguanosine	Metabolism	Antineoplastic
Alendronate sodium	Metabolism	Antiosteoporetic
Halofantrine hydrochloride	Metabolism	Antimalarial
Flubendazol	Metabolism	
Methotrexate	Oncology	Antineoplastic
Topotecan	Oncology	Antineoplastic
Camptothecine (S,+)	Oncology	Antineoplastic
Azaguanine-8	Oncology	Antineoplastic
Mitoxantrone dihydrochloride	Oncology	Antineoplastic

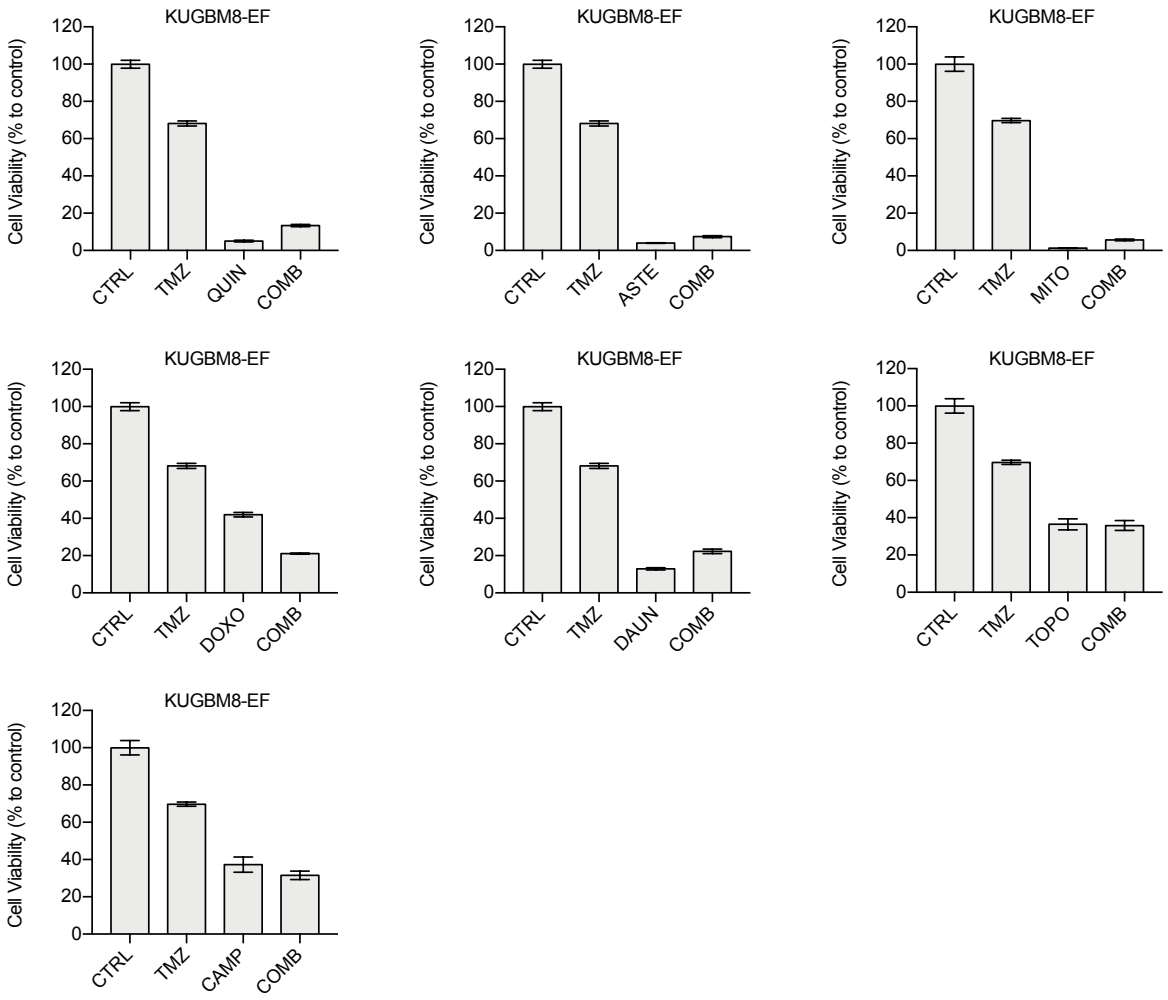

Figure 7.2 Selected hits are combined with Temozolomide. Cells were treated with 5 μM drug and 500 μM TMZ for 5 days.

In summary, we performed a high throughput screen using an FDA approved compound library with an attempt to provide useful therapeutic leads for GBM treatment. For this purpose, we used our own established cell line KUGBM8-EF. Further studies among the selected hits will be performed.

Table 7.2 List of drugs included in Prestwick Chemical Library

Prestwick Name	Chemical name	Therapeutic class
01A02	Azaguanine-8	Oncology
01A03	Allantoin	Dermatology
01A04	Acetazolamide	Metabolism
01A05	Metformin hydrochloride	Endocrinology
01A06	Atracurium besylate	Neuromuscular
01A07	Isoflupredone acetate	Endocrinology
01A08	Amiloride hydrochloride dihydrate	Metabolism
01A09	Amprolium hydrochloride	Infectiology
01A10	Hydrochlorothiazide	Metabolism
01A11	Sulfaguanidine	Infectiology, Metabolism
01B02	Meticrane	Metabolism
01B03	Benzonatate	Neuromuscular
01B04	Hydroflumethiazide	Metabolism
01B05	Sulfacetamide sodic hydrate	Infectiology, Metabolism
01B06	Heptaminol hydrochloride	Cardiovascular
01B07	Sulfathiazole	Infectiology, Metabolism
01B08	Levodopa	Central Nervous System
01B09	Idoxuridine	Infectiology
01B10	Captopril	Cardiovascular
01B11	Minoxidil	Cardiovascular
01C02	Sulfaphenazole	Infectiology, Metabolism
01C03	Panthenol (D)	Metabolism
01C04	Sulfadiazine	Infectiology, Metabolism
01C05	Norethynodrel	Endocrinology
01C06	Thiamphenicol	Infectiology, Metabolism
01C07	Cimetidine	Gastroenterology
01C08	Doxylamine succinate	Central Nervous System
01C09	Ethambutol dihydrochloride	Infectiology
01C10	Antipyrine	Central Nervous System
01C11	Antipyrine, 4-hydroxy	Metabolism
01D02	Chloramphenicol	Infectiology, Metabolism
01D03	Epirizole	Central Nervous System
01D04	Diprophylline	Cardiovascular, Respiratory
01D05	Triamterene	Metabolism
01D06	Dapsone	Infectiology
01D07	Troleandomycin	Infectiology
01D08	Pyrimethamine	Infectiology
01D09	Hexamethonium dibromide dihydrate	Cardiovascular
01D10	Diflunisal	Central Nervous System
01D11	Niclosamide	Infectiology
01E02	Procaine hydrochloride	Neuromuscular
01E03	Moxisylyte hydrochoride	Cardiovascular
01E04	Betazole hydrochloride	Gastroenterology
01E05	Isoxicam	Central Nervous System
01E06	Naproxen	Central Nervous System
01E07	Naphazoline hydrochloride	Cardiovascular
01E08	Ticlopidine hydrochloride	Hematology
01E09	Dicyclomine hydrochloride	Gastroenterology
01E10	Amyleine hydrochloride	Neuromuscular
01E11	Lidocaine hydrochloride	Cardiovascular
01F02	Trichlorfon	Infectiology
01F03	Carbamazepine	Central Nervous System
01F04	Triflupromazine hydrochloride	Central Nervous System
01F05	Mefenamic acid	Central Nervous System
01F06	Acetohexamide	Endocrinology
01F07	Sulpiride	Central Nervous System
01F08	Benoxinate hydrochloride	Neuromuscular
01F09	Oxethazaine	Neuromuscular
01F10	Pheniramine maleate	Allergology
01F11	Tolazoline hydrochloride	Cardiovascular
01G02	Morantel tartrate	Infectiology
01G03	Homatropine hydrobromide (R,S)	Diagnostic, Ophthalmology
01G04	Nifedipine	Cardiovascular
01G05	Chlorpromazine hydrochloride	Cardiovascular
01G06	Diphenhydramine hydrochloride	Allergology
01G07	Minaprine dihydrochloride	Central Nervous System
01G08	Miconazole	Infectiology, Metabolism
01G09	Isoxsuprine hydrochloride	Cardiovascular
01G10	Acebutolol hydrochloride	Cardiovascular
01G11	Tolnaftate	Infectiology
01H02	Todralazine hydrochloride	Cardiovascular
01H03	Imipramine hydrochloride	Central Nervous System
01H04	Sulindac	Central Nervous System
01H05	Amitryptiline hydrochloride	Central Nervous System
01H06	Adiphenine hydrochloride	Neuromuscular
01H07	Dibucaine	Neuromuscular
01H08	Prednisone	Endocrinology
01H09	Thioridazine hydrochloride	Central Nervous System
01H10	Diphemanil methylsulfate	Gastroenterology
01H11	Trimethobenzamide hydrochloride	Central Nervous System

02A02	Metronidazole	Infectiology, Metabolism
02A03	Fulvestrant	Endocrinology, Oncology
02A04	Edrophonium chloride	Diagnostic, Neuromuscular
02A05	Moroxidine hydrochloride	Infectiology
02A06	Baclofen (R,S)	Central Nervous System
02A07	Acyclovir	Metabolism
02A08	Diazoxide	Cardiovascular
02A09	Amidopyrine	Central Nervous System
02A10	Busulfan	Oncology
02A11	Pindolol	Cardiovascular
02B02	Khellin	Cardiovascular
02B03	Zimelidine dihydrochloride monohydrate	Central Nervous System
02B04	Azacyclonol	Central Nervous System
02B05	Azathioprine	Oncology
02B06	Lynestrenol	Endocrinology
02B07	Guanabenz acetate	Central Nervous System
02B08	Disulfiram	Metabolism
02B09	Acetylsalicylsalicylic acid	Central Nervous System
02B10	Mianserine hydrochloride	Cardiovascular
02B11	Nocodazole	Oncology
02C02	R(-) Apomorphine hydrochloride hemihydrate	Central Nervous System
02C03	Amoxapine	Central Nervous System
02C04	Cyproheptadine hydrochloride	Allergology, Central Nervous System
02C05	Famotidine	Gastroenterology
02C06	Danazol	Endocrinology
02C07	Nicorandil	Cardiovascular
02C08	Pioglitazone	Endocrinology
02C09	Nomifensine maleate	Central Nervous System
02C10	Dizocilpine maleate	Central Nervous System
02C11	Oxandrolone	Endocrinology
02D02	Naloxone hydrochloride	Central Nervous System
02D03	Metolazone	Cardiovascular
02D04	Ciprofloxacin hydrochloride monohydrate	Infectiology, Metabolism
02D05	Ampicillin trihydrate	Infectiology, Metabolism
02D06	Haloperidol	Central Nervous System
02D07	Naltrexone hydrochloride dihydrate	Central Nervous System
02D08	Chlorpheniramine maleate	Allergology, Central Nervous System
02D09	Nalbuphine hydrochloride	Central Nervous System
02D10	Picotamide monohydrate	Hematology
02D11	Triamcinolone	Endocrinology
02E02	Bromocryptine mesylate	Central Nervous System
02E03	Amfepramone hydrochloride	Central Nervous System
02E04	Dehydrocholic acid	Gastroenterology
02E05	Tioconazole	Infectiology
02E06	Perphenazine	Central Nervous System
02E07	Mefloquine hydrochloride	Infectiology
02E08	Isoconazole	Infectiology
02E09	Spironolactone	Endocrinology
02E10	Pirenzepine dihydrochloride	Gastroenterology
02E11	Dexamethasone acetate	Endocrinology
02F02	Glipizide	Endocrinology
02F03	Loxapine succinate	Central Nervous System
02F04	Hydroxyzine dihydrochloride	Allergology
02F05	Diltiazem hydrochloride	Cardiovascular
02F06	Methotrexate	Oncology
02F07	Astemizole	Allergology
02F08	Clindamycin hydrochloride	Infectiology
02F09	Terfenadine	Allergology
02F10	Cefotaxime sodium salt	Infectiology
02F11	Tetracycline hydrochloride	Infectiology
02G02	Verapamil hydrochloride	Cardiovascular
02G03	Dipyridamole	Cardiovascular
02G04	Chlorhexidine	Infectiology
02G05	Loperamide hydrochloride	Gastroenterology
02G06	Chlortetracycline hydrochloride	Infectiology
02G07	Tamoxifen citrate	Endocrinology, Oncology
02G08	Nicergoline	Cardiovascular
02G09	Canrenoic acid potassium salt	Endocrinology
02G10	Thioproperazine dimesylate	Central Nervous System
02G11	Dihydroergotamine tartrate	Central Nervous System
02H02	Erythromycin	Infectiology
02H03	Chloroxine	Dermatology
02H04	Didanosine	Infectiology
02H05	Josamycin	Infectiology
02H06	Paclitaxel	Oncology
02H07	Ivermectin	Infectiology
02H08	Gallamine triethiodide	Neuromuscular
02H09	Neomycin sulfate	Infectiology
02H10	Dihydrostreptomycin sulfate	Infectiology
02H11	Gentamicine sulfate	Infectiology
03A02	Isoniazid	Infectiology
03A03	Pentylenetetrazole	Central Nervous System
03A04	Chlorzoxazone	Central Nervous System
03A05	Ornidazole	Infectiology
03A06	Ethosuximide	Central Nervous System
03A07	Mafenide hydrochloride	Infectiology
03A08	Riluzole hydrochloride	Central Nervous System

03A09	Nitrofurantoin	Infectiology
03A10	Hydralazine hydrochloride	Cardiovascular
03A11	Phenelzine sulfate	Central Nervous System
03B02	Tranexamic acid	Hematology
03B03	Etofylline	Cardiovascular
03B04	Tranylcypromine hydrochloride	Central Nervous System
03B05	Alverine citrate salt	Neuromuscular
03B06	Aceclofenac	Central Nervous System
03B07	Iproniazide phosphate	Cardiovascular
03B08	Sulfamethoxazole	Infectiology
03B09	Mephenesin	Central Nervous System
03B10	Phenformin hydrochloride	Endocrinology
03B11	Flutamide	Oncology
03C02	Ampyrone	Central Nervous System
03C03	Levamisole hydrochloride	Immunology
03C04	Pargyline hydrochloride	Cardiovascular
03C05	Methocarbamol	Central Nervous System
03C06	Aztreonam	Infectiology
03C07	Cloxacillin sodium salt	Infectiology
03C08	Catharanthine	Oncology
03C09	Pentolinium bitartrate	Cardiovascular
03C10	Aminopurine, 6-benzyl	Endocrinology
03C11	Tolbutamide	Endocrinology
03D02	Midodrine hydrochloride	Cardiovascular
03D03	Thalidomide	Central Nervous System
03D04	Oxolinic acid	Metabolism
03D05	Nimesulide	Metabolism
03D06	Asenapine maleate	Central Nervous System
03D07	Pentoxifylline	Cardiovascular
03D08	Metaraminol bitartrate	Cardiovascular
03D09	Salbutamol	Neuromuscular
03D10	Prilocaine hydrochloride	Neuromuscular
03D11	Camptothecine (S,+)	Oncology
03E02	Ranitidine hydrochloride	Gastroenterology
03E03	Tiratricol, 3,3',5-triiodothyroacetic acid	Endocrinology
03E04	Flufenamic acid	Central Nervous System
03E05	Flumequine	Infectiology
03E06	Tolfenamic acid	Central Nervous System
03E07	Meclofenamic acid sodium salt monohydrate	Central Nervous System
03E08	Tibolone	Endocrinology
03E09	Trimethoprim	Infectiology
03E10	Metoclopramide monohydrochloride	Central Nervous System
03E11	Fenbendazole	Infectiology
03F02	Piroxicam	Central Nervous System
03F03	Pyrantel tartrate	Infectiology
03F04	Fenspiride hydrochloride	Respiratory
03F05	Gemfibrozil	Metabolism
03F06	Mefexamide hydrochloride	Central Nervous System
03F07	Tiapride hydrochloride	Central Nervous System
03F08	Mebendazole	Infectiology
03F09	Fenbufen	Central Nervous System
03F10	Ketoprofen	Central Nervous System
03F11	Indapamide	Metabolism
03G02	Norfloxacin	Infectiology
03G03	Antimycin A	Infectiology
03G04	Xylometazoline hydrochloride	Cardiovascular
03G05	Oxymetazoline hydrochloride	Respiratory
03G06	Nifenazone	Central Nervous System
03G07	Griseofulvin	Infectiology
03G08	Clemizole hydrochloride	Allergology
03G09	Tropicamide	Neuromuscular
03G10	Nefopam hydrochloride	Central Nervous System
03G11	Phentolamine hydrochloride	Cardiovascular
03H02	Etodolac	Central Nervous System
03H03	Scopolamin-N-oxide hydrobromide	Neuromuscular
03H04	Hyoscyamine (L)	Central Nervous System
03H05	Chlorphensin carbamate	Central Nervous System
03H06	Fadrozole hydrochloride	Oncology
03H07	Dilazep dihydrochloride	Cardiovascular
03H08	Ofloxacin	Infectiology
03H09	Lomefloxacin hydrochloride	Infectiology
03H10	Orphenadrine hydrochloride	Allergology
03H11	Proglumide	Gastroenterology
04A02	Mexiletine hydrochloride	Cardiovascular
04A03	Flavoxate hydrochloride	Metabolism
04A04	Bufexamac	Central Nervous System
04A05	Glutethimide, para-amino	Oncology
04A06	Dropropizine (R,S)	Respiratory
04A07	Pinacidil	Cardiovascular
04A08	Albendazole	Metabolism
04A09	Clonidine hydrochloride	Cardiovascular
04A10	Bupropion hydrochloride	Central Nervous System
04A11	Alprenolol hydrochloride	Cardiovascular
04B02	Chlorothiazide	Metabolism
04B03	Diphenidol hydrochloride	Central Nervous System
04B04	Norethindrone	Endocrinology
04B05	Nortriptyline hydrochloride	Central Nervous System

04B06	Niflumic acid	Central Nervous System
04B07	Isotretinoin	Dermatology
04B08	Retinoic acid	Dermatology
04B09	Antazoline hydrochloride	Allergology
04B10	Ethacrynic acid	Metabolism
04B11	Praziquantel	Infectiology
04C02	Ethisterone	Endocrinology
04C03	Triprolidine hydrochloride	Allergology
04C04	Doxepin hydrochloride	Allergology
04C05	Dyclonine hydrochloride	Neuromuscular
04C06	Dimenhydrinate	Allergology
04C07	Disopyramide	Cardiovascular
04C08	Clotrimazole	Infectiology
04C09	Vinpocetine	Cardiovascular
04C10	Clomipramine hydrochloride	Central Nervous System
04C11	Fendiline hydrochloride	Cardiovascular
04D02	Vincamine	Central Nervous System
04D03	Indomethacin	Central Nervous System
04D04	Cortisone	Endocrinology
04D05	Prednisolone	Endocrinology
04D06	Fenofibrate	Metabolism
04D07	Bumetanide	Metabolism
04D08	Labetalol hydrochloride	Cardiovascular
04D09	Cinnarizine	Allergology
04D10	Methylprednisolone, 6-alpha	Endocrinology
04D11	Quinidine hydrochloride monohydrate	Cardiovascular
04E02	Fludrocortisone acetate	Dermatology
04E03	Fenoterol hydrobromide	Neuromuscular
04E04	Homochlorcyclizine dihydrochloride	Allergology
04E05	Diethylcarbamazine citrate	Infectiology
04E06	Chenodiol	Gastroenterology
04E07	Perhexiline maleate	Cardiovascular
04E08	Oxybutynin chloride	Neuromuscular
04E09	Spiperone	Central Nervous System
04E10	Pyrilamine maleate	Allergology
04E11	Sulfinpyrazone	Hematology
04F02	Dantrolene sodium salt	Neuromuscular
04F03	Trazodone hydrochloride	Central Nervous System
04F04	Glafenine hydrochloride	Metabolism
04F05	Pimethixene maleate	Allergology
04F06	Pergolide mesylate	Central Nervous System
04F07	Acemetacin	Metabolism
04F08	Benzydamine hydrochloride	Central Nervous System
04F09	Fipexide hydrochloride	Central Nervous System
04F10	Mifepristone	Endocrinology
04F11	Diperodon hydrochloride	Neuromuscular
04G02	Lisinopril	Cardiovascular
04G03	Lincomycin hydrochloride	Infectiology
04G04	Telenzepine dihydrochloride	Gastroenterology
04G05	Econazole nitrate	Infectiology
04G06	Bupivacaine hydrochloride	Neuromuscular
04G07	Clemastine fumarate	Allergology
04G08	Oxytetracycline dihydrate	Infectiology
04G09	Pimozide	Central Nervous System
04G10	Amodiaquin dihydrochloride dihydrate	Infectiology
04G11	Mebeverine hydrochloride	Neuromuscular
04H02	Ifenprodil tartrate	Cardiovascular
04H03	Flunarizine dihydrochloride	Central Nervous System
04H04	Trifluoperazine dihydrochloride	Central Nervous System
04H05	Enalapril maleate	Cardiovascular
04H06	Minocycline hydrochloride	Infectiology
04H07	Glibenclamide	Endocrinology
04H08	Guanethidine sulfate	Central Nervous System
04H09	Quinacrine dihydrochloride dihydrate	Infectiology
04H10	Clofilium tosylate	Cardiovascular
04H11	Fluphenazine dihydrochloride	Central Nervous System
05A02	Streptomycin sulfate	Infectiology
05A03	Alfuzosin hydrochloride	Cardiovascular
05A04	Chlorpropamide	Endocrinology
05A05	Phenylpropanolamine hydrochloride	Respiratory
05A06	Ascorbic acid	Metabolism
05A07	Methyldopa (L,-)	Cardiovascular
05A08	Cefoperazone dihydrate	Infectiology
05A09	Zoxazolamine	Metabolism
05A10	Tacrine hydrochloride	Central Nervous System
05A11	Bisoprolol fumarate	Cardiovascular
05B02	Tremorine dihydrochloride	Central Nervous System
05B03	Practolol	Cardiovascular
05B04	Zidovudine, AZT	Infectiology
05B05	Sulfisoxazole	Infectiology
05B06	Zaprinast	Cardiovascular
05B07	Chlormezanone	Central Nervous System
05B08	Procainamide hydrochloride	Cardiovascular
05B09	N6-methyladenosine	Oncology
05B10	Guanfacine hydrochloride	Cardiovascular
05B11	Domperidone	Central Nervous System
05C02	Furosemide	Metabolism

05C03	Methapyrilene hydrochloride	Allergology
05C04	Desipramine hydrochloride	Central Nervous System
05C05	Clorgyline hydrochloride	Central Nervous System
05C06	Clenbuterol hydrochloride	Neuromuscular
05C07	Maprotiline hydrochloride	Central Nervous System
05C08	Thioguanosine	Metabolism
05C09	Chlorprothixene hydrochloride	Central Nervous System
05C10	Ritodrine hydrochloride	Neuromuscular
05C11	Clozapine	Central Nervous System
05D02	Chlorthalidone	Metabolism
05D03	Dobutamine hydrochloride	Cardiovascular
05D04	Moclobemide	Central Nervous System
05D05	Clopamide	Metabolism
05D06	Hycanthone	Infectiology
05D07	Adenosine 5'-monophosphate monohydrate	Cardiovascular
05D08	Amoxicillin	Metabolism
05D09	Pemirolast potassium	Ophthalmology
05D10	Dextromethorphan hydrobromide monohydrate	Central Nervous System
05D11	Droperidol	Central Nervous System
05E02	Bambuterol hydrochloride	Neuromuscular
05E03	Betamethasone	Endocrinology
05E04	Colchicine	Metabolism
05E05	Metergoline	Central Nervous System
05E06	Brinzolamide	Metabolism
05E07	Ambroxol hydrochloride	Respiratory
05E08	Benfluorex hydrochloride	Central Nervous System
05E09	Bepridil hydrochloride	Cardiovascular
05E10	Meloxicam	Metabolism
05E11	Benzbromarone	Cardiovascular
05F02	Ketotifen fumarate	Allergology
05F03	Debrisoquin sulfate	Cardiovascular
05F04	Amethopterin (R,S)	Immunology
05F05	Methylergometrine maleate	Neuromuscular
05F06	Methiothepin maleate	Central Nervous System
05F07	Clofazimine	Infectiology
05F08	Nafronyl oxalate	Cardiovascular
05F09	Bezafibrate	Metabolism
05F10	Nefazodone HCl	Central Nervous System
05F11	Clebopride maleate	Central Nervous System
05G02	Lidoflazine	Cardiovascular
05G03	Betaxolol hydrochloride	Cardiovascular
05G04	Nicardipine hydrochloride	Cardiovascular
05G05	Probucol	Metabolism
05G06	Mitoxantrone dihydrochloride	Oncology
05G07	GBR 12909 dihydrochloride	Central Nervous System
05G08	Carbetapentane citrate	Central Nervous System
05G09	Dequalinium dichloride	Infectiology
05G10	Ketoconazole	Infectiology
05G11	Fusidic acid sodium salt	Infectiology
05H02	Terbutaline hemisulfate	Respiratory
05H03	Ketanserin tartrate hydrate	Cardiovascular
05H04	Hemicholinium bromide	Neuromuscular
05H05	Kanamycin A sulfate	Infectiology
05H06	Amikacin hydrate	Infectiology
05H07	Etoposide	Oncology
05H08	Clomiphene citrate (Z,E)	Endocrinology
05H09	Oxantel pamoate	Infectiology
05H10	Prochlorperazine dimaleate	Central Nervous System
05H11	Hesperidin	Oncology
06A02	Testosterone propionate	Endocrinology
06A03	Haloprogin	Central Nervous System
06A04	Thyroxine (L)	Endocrinology
06A05	Idebenone	Oncology
06A06	Pepstatin A	Infectiology
06A07	Morpholinoethylamino-3-benzocyclohepta-(5,6-c)-pyridazine dihydrochloride	
06A08	Adamantamine fumarate	Infectiology
06A09	Butoconazole nitrate	Infectiology
06A10	Amiodarone hydrochloride	Cardiovascular
06A11	Amphotericin B	Infectiology
06B02	Androsterone	Endocrinology
06B03	Amifostine	Diagnostic
06B04	Carbarsone	Infectiology
06B05	Amlodipine	Cardiovascular
06B06	Modafinil	Central Nervous System
06B07	Bacampicillin hydrochloride	Infectiology
06B08	Lamivudine	Infectiology
06B09	Biotin	Metabolism
06B10	Bisacodyl	Gastroenterology
06B11	Erlotinib	Oncology
06C02	Suloctidil	Neuromuscular
06C03	Zotepine	Central Nervous System
06C04	Carisoprodol	Central Nervous System
06C05	Cephalosporanic acid, 7-amino	Infectiology
06C06	Chicago sky blue 6B	Central Nervous System
06C07	Buflomedil hydrochloride	Cardiovascular
06C08	Dibenzepine hydrochloride	Central Nervous System
06C09	Roxatidine Acetate HCl	Gastroenterology

06C10	Valacyclovir hydrochloride	Infectiology
06C11	Cisapride	Gastroenterology
06D02	Pefloxacine	Infectiology
06D03	Corticosterone	Endocrinology
06D04	Cyanocobalamin	Metabolism
06D05	Cefadroxil	Infectiology
06D06	Cyclosporin A	Immunology
06D07	Digitoxigenin	Cardiovascular
06D08	Digoxin	Cardiovascular
06D09	Doxorubicin hydrochloride	Infectiology
06D10	Carbimazole	Metabolism
06D11	Epiandrosterone	Endocrinology
06E02	Estradiol-17 beta	Endocrinology
06E03	Clobutinol hydrochloride	Central Nervous System
06E04	Gabazine bromide	Central Nervous System
06E05	Oxcarbazepine	Central Nervous System
06E06	Cyclobenzaprine hydrochloride	Neuromuscular
06E07	Carteolol hydrochloride	Cardiovascular
06E08	Hydrocortisone base	Endocrinology
06E09	Hydroxytacrine maleate (R,S)	Central Nervous System
06E10	Pilocarpine nitrate	Ophthalmology
06E11	Dicloxacillin sodium salt hydrate	Infectiology
06F02	Alizapride HCl	Central Nervous System
06F03	Stanozolol	Endocrinology
06F04	Calcipotriene	Dermatology
06F05	Linezolid	Infectiology
06F06	Mebhydroline 1,5-naphtalenedisulfonate	Allergology
06F07	Meclocycline sulfosalicylate	Infectiology
06F08	Meclozine dihydrochloride	Allergology
06F09	Melatonin	Central Nervous System
06F10	Butalbital	Central Nervous System
06F11	Dinoprost trometamol	Endocrinology
06G02	Tropisetron HCl	Central Nervous System
06G03	Cefixime	Infectiology
06G04	Metrizamide	Diagnostic
06G05	Quetiapine hemifumarate	Central Nervous System
06G06	Tosufloxacin hydrochloride	Infectiology
06G07	Efavirenz	Infectiology
06G08	Rifapentine	Infectiology
06G09	Neostigmine bromide	Diagnostic
06G10	Niridazole	Infectiology
06G11	Ceforanide	Infectiology
06H02	Vatalanib	Oncology
06H03	Itopride	Metabolism
06H04	Cefotetan	Infectiology
06H05	Fentiazac	Metabolism
06H06	Brompheniramine maleate	Allergology
06H07	Primaquine diphosphate	Infectiology
06H08	Progesterone	Endocrinology
06H09	Felodipine	Neuromuscular
06H10	Raclopride	Central Nervous System
06H11	Closantel	Infectiology
07A02	Serotonin hydrochloride	Central Nervous System
07A03	Cefotiam hydrochloride	Infectiology
07A04	Rofecoxib	Metabolism
07A05	Benperidol	Central Nervous System
07A06	Cefaclor hydrate	Infectiology
07A07	Colistin sulfate	Infectiology
07A08	Daunorubicin hydrochloride	Infectiology
07A09	Dosulepin hydrochloride	Central Nervous System
07A10	Ceftazidime pentahydrate	Infectiology
07A11	Iobenguane sulfate	Oncology
07B02	Metixene hydrochloride	Central Nervous System
07B03	Nitrofural	Infectiology
07B04	Omeprazole	Gastroenterology
07B05	Propylthiouracil	Metabolism
07B06	Terconazole	Infectiology
07B07	Tiaprofenic acid	Central Nervous System
07B08	Vancomycin hydrochloride	Infectiology
07B09	Artemisinin	Infectiology
07B10	Propafenone hydrochloride	Cardiovascular
07B11	Ethamivan	Central Nervous System
07C02	Vigabatrin	Central Nervous System
07C03	Biperiden hydrochloride	Central Nervous System
07C04	Cetirizine dihydrochloride	Allergology
07C05	Etifenin	Diagnostic
07C06	Metaproterenol sulfate, orciprenaline sulfate	Respiratory
07C07	Sisomicin sulfate	Infectiology
07C08	Sibutramine HCl	Central Nervous System
07C09	Acenocoumarol	Hematology
07C10	Bromperidol	Central Nervous System
07C11	Cyclizine hydrochloride	Allergology
07D02	Fluoxetine hydrochloride	Central Nervous System
07D03	Iohexol	Diagnostic
07D04	Norcyclobenzaprine	Gastroenterology
07D05	Pyrazinamide	Infectiology
07D06	Trimethadione	Central Nervous System

07D07	Lovastatin	Metabolism
07D08	Nystatine	Infectiology
07D09	Budesonide	Endocrinology
07D10	Imipenem	Infectiology
07D11	Sulfasalazine	Infectiology
07E02	Lofexidine	Cardiovascular
07E03	Thiostrepton	Infectiology
07E04	Miglitol	Endocrinology
07E05	Tiabendazole	Infectiology
07E06	Rifampicin	Infectiology
07E07	Ethionamide	Infectiology
07E08	Tenoxicam	Central Nervous System
07E09	Triflusal	Hematology
07E10	Mesoridazine besylate	Central Nervous System
07E11	Trolox	Metabolism
07F02	Pirenperone	Central Nervous System
07F03	Isoquinoline, 6,7-dimethoxy-1-methyl-1,2,3,4-tetrahydro, hydrochloride	
07F04	Phenacetin	Central Nervous System
07F05	Atovaquone	Infectiology
07F06	Methoxamine hydrochloride	Cardiovascular
07F07	(S)-(-)-Atenolol	Cardiovascular
07F08	Piracetam	Central Nervous System
07F09	Phenindione	Hematology
07F10	Thiocolchicoside	Central Nervous System
07F11	Clorsulon	Infectiology
07G02	Ciclopirox ethanolamine	Infectiology
07G03	Probenecid	Metabolism
07G04	Betahistine mesylate	Allergology
07G05	Tobramycin	Infectiology
07G06	Tetramisole hydrochloride	Immunology
07G07	Pregnenolone	Endocrinology
07G08	Molsidomine	Cardiovascular
07G09	Chloroquine diphosphate	Metabolism
07G10	Trimetazidine dihydrochloride	Cardiovascular
07G11	Parthenolide	Metabolism
07H02	Hexetidine	Infectiology
07H03	Selegiline hydrochloride	Central Nervous System
07H04	Pentamidine isethionate	Infectiology
07H05	Tolazamide	Metabolism
07H06	Nifuroxazide	Infectiology
07H07	Mirtazapine	Central Nervous System
07H08	Dirithromycin	Infectiology
07H09	Gliclazide	Metabolism
07H10	DO 897/99	Central Nervous System
07H11	Prenylamine lactate	Cardiovascular
08A02	Ziprasidone Hydrochloride	Central Nervous System
08A03	Mevastatin	Cardiovascular
08A04	Pyridostigmine iodide	Central Nervous System
08A05	Pentobarbital	Central Nervous System
08A06	Atropine sulfate monohydrate	Ophthalmology
08A07	Eserine hemisulfate salt	Central Nervous System
08A08	Itraconazole	Infectiology
08A09	Acarbose	Endocrinology
08A10	Entacapone	Central Nervous System
08A11	Nicotinamide	Dermatology
08B02	Tetracaïne hydrochloride	Neuromuscular
08B03	Mometasone furoate	Endocrinology
08B04	Troglitazone	Metabolism
08B05	Dacarbazine	Oncology
08B06	Tenatoprazole	Metabolism
08B07	Acetopromazine maleate salt	Central Nervous System
08B08	Escitalopram	Central Nervous System
08B09	Ropinirole HCl	Central Nervous System
08B10	Lacidipine	Cardiovascular
08B11	Argatroban	Hematology
08C02	Reboxetine mesylate	Central Nervous System
08C03	Camylofine chlorhydrate	
08C04	Papaverine hydrochloride	Cardiovascular
08C05	Yohimbine hydrochloride	Cardiovascular
08C06	Voriconazole	Infectiology
08C07	Alfacalcidol	Metabolism
08C08	Cilostazol	Hematology
08C09	Galanthamine hydrobromide	Central Nervous System
08C10	Azelastine HCl	Immunology
08C11	Etretinate	Dermatology
08D02	Emedastine	Allergology
08D03	Etofenamate	Metabolism
08D04	Zaleplon	Central Nervous System
08D05	Diclofenac sodium	Central Nervous System
08D06	Exemestane	Endocrinology
08D07	Fomepizole	Metabolism
08D08	Temozolomide	Oncology
08D09	Xylazine	Central Nervous System
08D10	Celiprolol HCl	Cardiovascular
08D11	Zopiclone	Central Nervous System
08E02	Tranilast	Allergology
08E03	Tizanidine HCl	Metabolism

08E04	Zafirlukast	Respiratory
08E05	Butenafine Hydrochloride	Infectiology
08E06	Carbadox	Infectiology
08E07	Rimantadine Hydrochloride	Infectiology
08E08	Eburnamonine (-)	Central Nervous System
08E09	Oxibendazol	Metabolism
08E10	Ipsapirone	Central Nervous System
08E11	Hydroxychloroquine sulfate	Metabolism
08F02	Loracarbef	Infectiology
08F03	Fenipentol	Metabolism
08F04	Diosmin	Cardiovascular
08F05	Carbidopa	Central Nervous System
08F06	(-)-Emtricitabine	Infectiology
08F07	Demecarium bromide	Ophthalmology
08F08	Quipazine dimaleate salt	Central Nervous System
08F09	Acipimox	Metabolism
08F10	Diflorasone Diacetate	Endocrinology
08F11	Acamprosate calcium	Central Nervous System
08G02	Mizolastine	Allergology
08G03	Amisulpride	Central Nervous System
08G04	Pyridoxine hydrochloride	Metabolism
08G05	Mercaptopurine	Immunology
08G06	Cytarabine	Oncology
08G07	Racecadotril	Gastroenterology
08G08	Folic acid	Metabolism
08G09	Benazepril HCl	Cardiovascular
08G10	Aniracetam	Central Nervous System
08G11	Dimethisoquin hydrochloride	Neuromuscular
08H02	Alendronate sodium	Metabolism
08H03	Dipivefrin hydrochloride	Ophthalmology
08H04	Thiorphan	Gastroenterology
08H05	Tomoxetine hydrochloride	Central Nervous System
08H06	Aceclidine Hydrochloride	Ophthalmology
08H07	Penciclovir	Infectiology
08H08	Levetiracetam	Central Nervous System
08H09	Dexfenfluramine hydrochloride	Central Nervous System
08H10	Etoricoxib	Central Nervous System
08H11	Sertindole	Central Nervous System
09A02	Sulmazole	Cardiovascular
09A03	Gefitinib	Oncology
09A04	Flunisolide	Endocrinology
09A05	N-Acetyl-DL-homocysteine Thiolactone	Respiratory
09A06	Flurandrenolide	Dermatology
09A07	Oxiconazole Nitrate	Infectiology
09A08	Rebamipide	Metabolism
09A09	Nilvadipine	Cardiovascular
09A10	Etanidazole	Oncology
09A11	Pinaverium bromide	Neuromuscular
09B02	Glimepiride	Endocrinology
09B03	Picrotoxinin	Central Nervous System
09B04	Mepenzolate bromide	Neuromuscular
09B05	Benfotiamine	Metabolism
09B06	Halcinonide	Dermatology
09B07	Lanatoside C	Cardiovascular
09B08	Benzamil hydrochloride	Metabolism
09B09	Suxibuzone	Central Nervous System
09B10	6-Furfurylaminopurine	Dermatology
09B11	Avermectin B1a	Infectiology
09C02	Pranlukast	Respiratory
09C03	Penicillamine	Central Nervous System
09C04	Zileuton	Respiratory
09C05	Loratadine	Allergology
09C06	Tetraethylenepentamine pentahydrochloride	Metabolism
09C07	Nisoldipine	Cardiovascular
09C08	Acefylline	Central Nervous System
09C09	Acitretin	Dermatology
09C10	Zonisamide	Central Nervous System
09C11	Irsogladine maleate	Metabolism
09D02	Dydrogesterone	Endocrinology
09D03	Sumatriptan succinate	Central Nervous System
09D04	Opipramol dihydrochloride	Central Nervous System
09D05	Nalidixic acid sodium salt	Infectiology
09D06	Oxacillin sodium	Infectiology
09D07	Beta-Escin	Metabolism
09D08	Thiamine hydrochloride	Immunology
09D09	Tazobactam	Infectiology
09D10	Ibandronate sodium	Metabolism
09D11	Warfarin	Hematology
09E02	Pranoprofen	Metabolism
09E03	Secnidazole	Infectiology
09E04	Pempidine tartrate	Cardiovascular
09E05	Clodronate	Metabolism
09E06	Ibutilide fumarate	Cardiovascular
09E07	Thimerosal	Infectiology
09E08	Tramadol hydrochloride	Central Nervous System
09E09	Estropipate	Endocrinology
09E10	Butylscopolammonium (n-) bromide	Central Nervous System

09E11	Irinotecan hydrochloride trihydrate	Oncology
09F02	Tylosin	Infectiology
09F03	Citalopram Hydrobromide	Central Nervous System
09F04	Promazine hydrochloride	Central Nervous System
09F05	Sulfamerazine	Infectiology
09F06	Venlafaxine	Central Nervous System
09F07	Ethotoin	Central Nervous System
09F08	3-alpha-Hydroxy-5-beta-androstan-17-one	Endocrinology
09F09	Tetrahydrozoline hydrochloride	Cardiovascular
09F10	Hexestrol	Endocrinology
09F11	Cefmetazole sodium salt	Infectiology
09G02	Trihexyphenidyl-D,L Hydrochloride	Central Nervous System
09G03	Succinylsulfathiazole	Infectiology
09G04	Famprofazone	Central Nervous System
09G05	Bromopride	Central Nervous System
09G06	Methyl benzethonium chloride	Infectiology
09G07	Chlorcyclizine hydrochloride	Allergology
09G08	Diphenylpyraline hydrochloride	Allergology
09G09	Benzethonium chloride	Infectiology
09G10	Trioxsalen	Dermatology
09G11	Doxofylline	Respiratory
09H02	Sulfabenzamide	Infectiology
09H03	Benzocaine	Neuromuscular
09H04	Dipyrone	Central Nervous System
09H05	Isosorbide dinitrate	Cardiovascular
09H06	Sulfachloropyridazine	Infectiology
09H07	Pramoxine hydrochloride	Neuromuscular
09H08	Finasteride	Endocrinology
09H09	Fluorometholone	Endocrinology
09H10	Cephalothin sodium salt	Infectiology
09H11	Cefuroxime sodium salt	Infectiology
10A02	Althiazide	Metabolism
10A03	Isopyrin hydrochloride	Central Nervous System
10A04	Phenethicillin potassium salt	Infectiology
10A05	Sulfamethoxypyridazine	Infectiology
10A06	Deferoxamine mesylate	Diagnostic
10A07	Mephentermine hemisulfate	Cardiovascular
10A08	Liranaftate	Infectiology
10A09	Sulfadimethoxine	Infectiology
10A10	Sulfanilamide	Infectiology
10A11	Balsalazide Sodium	Gastroenterology
10B02	Sulfaquinoxaline sodium salt	Infectiology
10B03	Streptozotocin	Oncology
10B04	Metoprolol-(+,-) (+)-tartrate salt	Cardiovascular
10B05	Flumethasone	Metabolism
10B06	Flecainide acetate	Cardiovascular
10B07	Cefazolin sodium salt	Metabolism
10B08	Atractyloside potassium salt	Oncology
10B09	Folinic acid calcium salt	Hematology
10B10	Levonordefrin	Cardiovascular
10B11	Ebselen	Metabolism
10C02	Nadide	Metabolism
10C03	Sulfamethizole	Metabolism
10C04	Medrysone	Metabolism
10C05	Flunixin meglumine	Central Nervous System
10C06	Spiramycin	Metabolism
10C07	Glycopyrrolate	Gastroenterology
10C08	Aprepitant	Metabolism
10C09	Monensin sodium salt	Infectiology
10C10	Isoetharine mesylate salt	Respiratory
10C11	Mevalonic-D, L acid lactone	Cardiovascular
10D02	Terazosin hydrochloride	Cardiovascular
10D03	Phenazopyridine hydrochloride	Central Nervous System
10D04	Demeclocycline hydrochloride	Metabolism
10D05	Fenoprofen calcium salt dihydrate	Metabolism
10D06	Piperacillin sodium salt	Metabolism
10D07	Diethylstilbestrol	Endocrinology
10D08	Chlorotrianisene	Endocrinology
10D09	Ribostamycin sulfate salt	Metabolism
10D10	Methacholine chloride	Diagnostic
10D11	Pipenzolate bromide	Gastroenterology
10E02	Butamben	Central Nervous System
10E03	Sulfapyridine	Metabolism
10E04	Meclofenoxate hydrochloride	Central Nervous System
10E05	Furaltadone hydrochloride	Infectiology
10E06	Ethoxyquin	Metabolism
10E07	Tinidazole	Infectiology
10E08	Guanadrel sulfate	Cardiovascular
10E09	Vidarabine	Metabolism
10E10	Sulfameter	Metabolism
10E11	Isopropamide iodide	Metabolism
10F02	Alclometasone dipropionate	Metabolism
10F03	Leflunomide	Immunology
10F04	Norgestrel-(-)-D	Endocrinology
10F05	Fluocinonide	Metabolism
10F06	Sulfamethazine sodium salt	Metabolism
10F07	Guaifenesin	Respiratory

10F08	Alexidine dihydrochloride	Infectiology
10F09	Proadifen hydrochloride	Neuromuscular
10F10	Zomepirac sodium salt	Metabolism
10F11	Cinoxacin	Metabolism
10G02	Clobetasol propionate	Metabolism
10G03	Podophyllotoxin	Metabolism
10G04	Clofibric acid	Metabolism
10G05	Bendroflumethiazide	Cardiovascular
10G06	Dicumarol	Hematology
10G07	Methimazole	Endocrinology
10G08	Merbromin	Infectiology
10G09	Hexylcaine hydrochloride	Dermatology
10G10	Drofenine hydrochloride	Neuromuscular
10G11	Cycloheximide	Infectiology
10H02	(R) -Naproxen sodium salt	Metabolism
10H03	Propidium iodide	Infectiology
10H04	Cloperastine hydrochloride	Respiratory
10H05	Eucatropine hydrochloride	Neuromuscular
10H06	Isocarboxazid	Central Nervous System
10H07	Lithocholic acid	Metabolism
10H08	Methotrimeprazine maleat salt	Central Nervous System
10H09	Dienestrol	Endocrinology
10H10	Pridinol methanesulfonate salt	Central Nervous System
10H11	Amrinone	Cardiovascular
11A02	Carbinoxamine maleate salt	Allergology
11A03	Methazolamide	Metabolism
11A04	Pyrithyldione	Central Nervous System
11A05	Spectinomycin dihydrochloride	Metabolism
11A06	Piromidic acid	Metabolism
11A07	Trimipramine maleate salt	Central Nervous System
11A08	Chloropyramine hydrochloride	Allergology
11A09	Furazolidone	Metabolism
11A10	Dichlorphenamide	Ophthalmology
11A11	Sulconazole nitrate	Metabolism
11B02	Auranofin	Metabolism
11B03	Cromolyn disodium salt	Allergology
11B04	Bucladesine sodium salt	Cardiovascular
11B05	Cefsulodin sodium salt	Metabolism
11B06	Fosfosal	Central Nervous System
11B07	Suprofen	Central Nervous System
11B08	Deflazacort	Immunology
11B09	Nadolol	Cardiovascular
11B10	Moxalactam disodium salt	Metabolism
11B11	Aminophylline	Cardiovascular
11C02	Azlocillin sodium salt	Metabolism
11C03	Clidinium bromide	Neuromuscular
11C04	Sulfamonomethoxine	Metabolism
11C05	Benzthiazide	Cardiovascular
11C06	Trichlormethiazide	Cardiovascular
11C07	Oxalamine citrate salt	Central Nervous System
11C08	Propantheline bromide	Neuromuscular
11C09	Viloxazine hydrochloride	Central Nervous System
11C10	Dimethadione	Central Nervous System
11C11	Ethaverine hydrochloride	Central Nervous System
11D02	Butacaine	Dermatology
11D03	Cefoxitin sodium salt	Metabolism
11D04	Ifosfamide	Oncology
11D05	Novobiocin sodium salt	Metabolism
11D06	Tetrahydroxy-1,4-quinone monohydrate	Dermatology
11D07	Indoprofen	Central Nervous System
11D08	Carbenoxolone disodium salt	Metabolism
11D09	Iocetamic acid	Diagnostic
11D10	Ganciclovir	Metabolism
11D11	Ethopropazine hydrochloride	Central Nervous System
11E02	Olanzapine	Central Nervous System
11E03	Trimeprazine tartrate	Allergology
11E04	Nafcillin sodium salt monohydrate	Metabolism
11E05	Procyclidine hydrochloride	Central Nervous System
11E06	Amiprilose hydrochloride	Immunology
11E07	Ethynylestradiol 3-methyl ether	Endocrinology
11E08	(-) -Levobunolol hydrochloride	Ophthalmology
11E09	Iodixanol	Diagnostic
11E10	Clinafloxacin	Infectiology
11E11	Equilin	Endocrinology
11F02	Paroxetine Hydrochloride	Central Nervous System
11F03	Nylidrin	Cardiovascular
11F04	Liothyronine	Endocrinology
11F05	Roxithromycin	Metabolism
11F06	Beclomethasone dipropionate	Metabolism
11F07	Tolmetin sodium salt dihydrate	Metabolism
11F08	(+) -Levobunolol hydrochloride	Ophthalmology
11F09	Doxazosin mesylate	Cardiovascular
11F10	Fluvastatin sodium salt	Cardiovascular
11F11	Methylhydantoin-5-(L)	Central Nervous System
11G02	Gabapentin	Central Nervous System
11G03	Raloxifene hydrochloride	Endocrinology
11G04	Etidronic acid, disodium salt	Metabolism

11G05	Methylhydantoin-5-(D)	
11G06	Simvastatin	Cardiovascular
11G07	Azacytidine-5	Oncology
11G08	Paromomycin sulfate	Metabolism
11G09	Acetaminophen	Central Nervous System
11G10	Phthalylsulfathiazole	Metabolism
11G11	Luteolin	Respiratory
11H02	Iopamidol	Diagnostic
11H03	Iopromide	Diagnostic
11H04	Theophylline monohydrate	Cardiovascular
11H05	Theobromine	Cardiovascular
11H06	Reserpine	Central Nervous System
11H07	Bicalutamide	Endocrinology
11H08	Scopolamine hydrochloride	Central Nervous System
11H09	Ioversol	Diagnostic
11H10	Rabeprazole Sodium salt	Metabolism
11H11	Carbachol	Cardiovascular
12A02	Niacin	Cardiovascular
12A03	Bemegride	Central Nervous System
12A04	Digoxigenin	Diagnostic
12A05	Meglumine	Metabolism
12A06	Dolasetron mesilate	Central Nervous System
12A07	Clioquinol	Metabolism
12A08	Oxybenzone	Dermatology
12A09	Promethazine hydrochloride	Allergology
12A10	Diacerein	Immunology
12A11	Esmolol hydrochloride	Cardiovascular
12B02	Cortisol acetate	Metabolism
12B03	Flubendazol	Metabolism
12B04	Felbinac	Central Nervous System
12B05	Butylparaben	Metabolism
12B06	Aminohippuric acid	Diagnostic
12B07	N-Acetyl-L-leucine	Central Nervous System
12B08	Pipemidic acid	Metabolism
12B09	Dioxybenzone	Dermatology
12B10	Adrenosterone	Endocrinology
12B11	Methylatropine nitrate	Neuromuscular
12C02	Hymecromone	Metabolism
12C03	Abacavir Sulfate	Infectiology
12C04	Diloxanide furoate	Metabolism
12C05	Metyrapone	Endocrinology
12C06	Urapidil hydrochloride	Cardiovascular
12C07	Fluspirilen	Central Nervous System
12C08	S-(+)-ibuprofen	Central Nervous System
12C09	Ethynodiol diacetate	Endocrinology
12C10	Nabumetone	Central Nervous System
12C11	Nisoxetine hydrochloride	Central Nervous System
12D02	(+)-Isoproterenol (+)-bitartrate salt	Respiratory
12D03	Monobenzone	Dermatology
12D04	2-Aminobenzenesulfonamide	Metabolism
12D05	Estrone	Endocrinology
12D06	Lorglumide sodium salt	Metabolism
12D07	Nitrendipine	Cardiovascular
12D08	Flurbiprofen	Central Nervous System
12D09	Nimodipine	Cardiovascular
12D10	Bacitracin	Metabolism
12D11	L(-)-vesamicol hydrochloride	Neuromuscular
12E02	Nizatidine	Metabolism
12E03	Thioperamide maleate	Central Nervous System
12E04	Xamoterol hemifumarate	Cardiovascular
12E05	Rolipram	Central Nervous System
12E06	Thonzonium bromide	Dermatology
12E07	Idazoxan hydrochloride	Central Nervous System
12E08	Quinapril HCl	Cardiovascular
12E09	Nilutamide	Oncology
12E10	Ketorolac tromethamine	Central Nervous System
12E11	Protriptyline hydrochloride	Central Nervous System
12F02	Propofol	Central Nervous System
12F03	S(-)Eticlopride hydrochloride	Central Nervous System
12F04	Primidone	Central Nervous System
12F05	Flucytosine	Metabolism
12F06	(-)-MK 801 hydrogen maleate	Central Nervous System
12F07	Bephenium hydroxynaphthoate	Metabolism
12F08	Dehydroisoandosterone 3-acetate	Endocrinology
12F09	Benserazide hydrochloride	Central Nervous System
12F10	Iodipamide	Diagnostic
12F11	Allopurinol	Metabolism
12G02	Pentetic acid	Oncology
12G03	Bretylium tosylate	Cardiovascular
12G04	Pralidoxime chloride	Neuromuscular
12G05	Phenoxybenzamine hydrochloride	Cardiovascular
12G06	Salmeterol	Respiratory
12G07	Altretamine	Oncology
12G08	Prazosin hydrochloride	Cardiovascular
12G09	Timolol maleate salt	Cardiovascular
12G10	(+,-)-Octopamine hydrochloride	Cardiovascular
12G11	Stavudine	Infectiology

12H02	Crotamiton	Dermatology
12H03	Toremifene	Endocrinology
12H04	(R)-(+)-Atenolol	Cardiovascular
12H05	Tyloxapol	Respiratory
12H06	Florfenicol	Metabolism
12H07	Megestrol acetate	Endocrinology
12H08	Deoxycorticosterone	Endocrinology
12H09	Urosiol	Metabolism
12H10	Proparacaine hydrochloride	Central Nervous System
12H11	Aminocaproic acid	Allergology
13A02	Denatonium benzoate	Neuromuscular
13A03	Canrenone	Endocrinology
13A04	Enilconazole	Metabolism
13A05	Methacycline hydrochloride	Metabolism
13A06	Floxuridine	Oncology
13A07	Sotalol hydrochloride	Cardiovascular
13A08	Gestrinone	Endocrinology
13A09	Decamethonium bromide	Neuromuscular
13A10	Darifenacin hydrobromide	Neuromuscular
13A11	Indatraline hydrochloride	Central Nervous System
13B02	Remoxipride Hydrochloride	Central Nervous System
13B03	THIP Hydrochloride	Central Nervous System
13B04	Pirlindole mesylate	Central Nervous System
13B05	Pronethalol hydrochloride	Cardiovascular
13B06	Naftopidil dihydrochloride	Cardiovascular
13B07	Tracazolate hydrochloride	Central Nervous System
13B08	Zardaverine	Respiratory
13B09	Memantine Hydrochloride	Central Nervous System
13B10	Ozagrel hydrochloride	Cardiovascular
13B11	Piribedil hydrochloride	Cardiovascular
13C02	Nitrocaramiphen hydrochloride	Central Nervous System
13C03	Nandrolone	Endocrinology
13C04	Dimaprit dihydrochloride	Metabolism
13C05	Oxfendazol	Metabolism
13C06	Guaiacol	Respiratory
13C07	Proscillaridin A	Cardiovascular
13C08	Pramipexole	Central Nervous System
13C09	Norgestimate	Endocrinology
13C10	Chlormadinone acetate	Endocrinology
13C11	Phenylbutazone	Metabolism
13D02	Gliquidone	Endocrinology
13D03	Pizotifen malate	Allergology
13D04	Ribavirin	Metabolism
13D05	Cyclopenthiazide	Cardiovascular
13D06	Fluvoxamine maleate	Central Nervous System
13D07	Prothionamide	Infectiology
13D08	Fluticasone propionate	Cardiovascular
13D09	Zuclopenthixol dihydrochloride	Central Nervous System
13D10	Proguanil hydrochloride	Metabolism
13D11	Lymecycline	Metabolism
13E02	Alfadolone acetate	Central Nervous System
13E03	Alfaxalone	Central Nervous System
13E04	Azapropazone	Central Nervous System
13E05	Meptazinol hydrochloride	Central Nervous System
13E06	Apramycin	Metabolism
13E07	Epitiostanol	Oncology
13E08	Fursultiamine Hydrochloride	Metabolism
13E09	Gabexate mesilate	Hematology
13E10	Pivampicillin	Metabolism
13E11	Talampicillin hydrochloride	Metabolism
13F02	Flucloxacillin sodium	Metabolism
13F03	Trapidil	Cardiovascular
13F04	Deptropine citrate	Allergology
13F05	Sertraline	Central Nervous System
13F06	Ethamsylate	Cardiovascular
13F07	Moxonidine	Cardiovascular
13F08	Etilefrine hydrochloride	Cardiovascular
13F09	Alprostadil	Cardiovascular
13F10	Tribenoside	Cardiovascular
13F11	Rimexolone	Metabolism
13G02	Isradipine	Cardiovascular
13G03	Tiletamine hydrochloride	Central Nervous System
13G04	Isometheptene mucate	Cardiovascular
13G05	Nifurtimox	Metabolism
13G06	Letrozole	Oncology
13G07	Arbutin	Metabolism
13G08	Tocainide hydrochloride	Cardiovascular
13G09	Benzathine benzylpenicillin	Metabolism
13G10	Risperidone	Central Nervous System
13G11	Torsemide	Cardiovascular
13H02	Halofantrine hydrochloride	Metabolism
13H03	Articaine hydrochloride	Central Nervous System
13H04	Nomegestrol acetate	Endocrinology
13H05	Pancuronium bromide	Neuromuscular
13H06	Molindone hydrochloride	Central Nervous System
13H07	Alcuronium chloride	Neuromuscular
13H08	Zalcitabine	Metabolism

13H09	Methyldopate hydrochloride	Cardiovascular
13H10	Levocabastine hydrochloride	Allergology
13H11	Pyrvinium pamoate	Metabolism
14A02	Etomidate	Central Nervous System
14A03	Tridihexethyl chloride	Neuromuscular
14A04	Penbutolol sulfate	Cardiovascular
14A05	Prednicarbate	Metabolism
14A06	Sertaconazole nitrate	Metabolism
14A07	Repaglinide	Endocrinology
14A08	Piretanide	Cardiovascular
14A09	Piperacetazine	Central Nervous System
14A10	Oxyphenbutazone	Metabolism
14A11	Quinethazone	Cardiovascular
14B02	Moricizine hydrochloride	Cardiovascular
14B03	Iopanoic acid	Diagnostic
14B04	Pivmecillinam hydrochloride	Metabolism
14B05	Levopropoxyphene napsylate	Central Nervous System
14B06	Piperidolate hydrochloride	Neuromuscular
14B07	Trifluridine	Metabolism
14B08	Oxprenolol hydrochloride	Cardiovascular
14B09	Ondansetron Hydrochloride	Central Nervous System
14B10	Propoxycaine hydrochloride	Central Nervous System
14B11	Oxaprozin	Central Nervous System
14C02	Phensuximide	Central Nervous System
14C03	Ioxaglic acid	Diagnostic
14C04	Naftifine hydrochloride	Infectiology
14C05	Meprylcaine hydrochloride	Neuromuscular
14C06	Milrinone	Cardiovascular
14C07	Methantheline bromide	Neuromuscular
14C08	Ticarcillin sodium	Infectiology
14C09	Thiethylperazine dimalate	Central Nervous System
14C10	Mesalamine	Metabolism
14C11	Vorinostat	Oncology
14D02	Imidurea	Infectiology
14D03	Lansoprazole	Metabolism
14D04	Bethanechol chloride	Metabolism
14D05	Cyproterone acetate	Endocrinology
14D06	(R)-Propranolol hydrochloride	Cardiovascular
14D07	Ciprofibrate	Metabolism
14D08	Formestane	Endocrinology
14D09	Benzylpenicillin sodium	Infectiology
14D10	Chlorambucil	Oncology
14D11	Methiazole	Infectiology
14E02	(S)-propranolol hydrochloride	Cardiovascular
14E03	(-)-Eseroline fumarate salt	Central Nervous System
14E04	Isosorbide mononitrate	Cardiovascular
14E05	Levalbuterol hydrochloride	Respiratory
14E06	Topiramate	Central Nervous System
14E07	D-cycloserine	Infectiology
14E08	2-Chloropyrazine	Cardiovascular
14E09	(+,-)-Synephrine	Cardiovascular
14E10	(S)-(-)-Cycloserine	Infectiology
14E11	Homosalate	Dermatology
14F02	Spaglumic acid	Allergology
14F03	Ranolazine	Cardiovascular
14F04	Misoprostol	Metabolism
14F05	Sulfadoxine	Infectiology
14F06	Cyclopentolate hydrochloride	Metabolism
14F07	Estriol	Endocrinology
14F08	(-)-Isoproterenol hydrochloride	Cardiovascular
14F09	Sarafloxacin	Infectiology
14F10	Nialamide	Central Nervous System
14F11	Toltrazuril	Infectiology
14G02	Perindopril	Cardiovascular
14G03	Fexofenadine HCl	Allergology
14G04	4-aminosalicylic acid	Infectiology
14G05	Clonixin Lysinate	Central Nervous System
14G06	Verteporfin	Ophthalmology
14G07	Meropenem	Infectiology
14G08	Ramipril	Cardiovascular
14G09	Mephenytoin	Central Nervous System
14G10	Rifabutin	Infectiology
14G11	Parbendazole	Infectiology
14H02	Mecamylamine hydrochloride	Cardiovascular
14H03	Procarbazine hydrochloride	Oncology
14H04	Viomycin sulfate	Infectiology
14H05	Saquinavir mesylate	Immunology
14H06	Ronidazole	Infectiology
14H07	Dorzolamide hydrochloride	Cardiovascular
14H08	Azaperone	Central Nervous System
14H09	Cefepime hydrochloride	Infectiology
14H10	Clocortolone pivalate	Endocrinology
14H11	Nadifloxacin	Infectiology
15A02	Buspirone hydrochloride	Central Nervous System
15A03	Anastrozole	Oncology
15A04	Doxycycline hydrochloride	Metabolism
15A05	Sulbactam	Infectiology

15A06	Fleroxacin	Infectiology
15A07	Clavulanate potassium salt	Infectiology
15A08	Valproic acid	Central Nervous System
15A09	Mepivacaine hydrochloride	Neuromuscular
15A10	Rifaximin	Infectiology
15A11	Estradiol Valerate	Endocrinology
15B02	Acetylcysteine	Metabolism
15B03	Melengestrol acetate	Endocrinology
15B04	Bromhexine hydrochloride	Respiratory
15B05	Anethole-trithione	Metabolism
15B06	Amcinonide	Metabolism
15B07	Caffeine	Central Nervous System
15B08	Carvedilol	Cardiovascular
15B09	Methenamine	Infectiology
15B10	Phentermine hydrochloride	Central Nervous System
15B11	Diclazuril	Metabolism
15C02	Famciclovir	Infectiology
15C03	Dopamine hydrochloride	Cardiovascular
15C04	Cefdinir	Infectiology
15C05	Carprofen	Metabolism
15C06	Celecoxib	Metabolism
15C07	Candesartan	Cardiovascular
15C08	Fludarabine	Oncology
15C09	Cladribine	Oncology
15C10	Vardenafil	Cardiovascular
15C11	Fluconazole	Metabolism
15D02	5-fluorouracil	Oncology
15D03	Mesna	Oncology
15D04	Mitotane	Endocrinology
15D05	Ambrisentan	Cardiovascular
15D06	Triclosan	Infectiology
15D07	Enoxacin	Infectiology
15D08	Olopatadine hydrochloride	Allergology
15D09	Granisetron	Endocrinology
15D10	Anthralin	Dermatology
15D11	Lamotrigine	Central Nervous System
15E02	Clofibrate	Metabolism
15E03	Cyclophosphamide	Immunology
15E04	Aripiprazole	Central Nervous System
15E05	Ethinylestradiol	Endocrinology
15E06	Fluocinolone acetonide	Metabolism
15E07	Sparfloxacin	Infectiology
15E08	Desloratadine	Allergology
15E09	Clarithromycin	Infectiology
15E10	Tripelennamine hydrochloride	Allergology
15E11	Tulobuterol	Respiratory
15F02	Topotecan	Oncology
15F03	Atorvastatin	Metabolism
15F04	Azithromycin	Infectiology
15F05	Ibudilast	Metabolism
15F06	Losartan	Cardiovascular
15F07	Benztropine mesylate	Central Nervous System
15F08	Vecuronium bromide	Metabolism
15F09	Telmisartan	Cardiovascular
15F10	Nalmefene hydrochloride	Central Nervous System
15F11	Bifonazole	Infectiology
15G02	Gatifloxacin	Infectiology
15G03	Bosentan	Cardiovascular
15G04	Gemcitabine	Oncology
15G05	Olmesartan	Cardiovascular
15G06	Racepinephrine HCl	Cardiovascular
15G07	Montelukast	Respiratory
15G08	Docetaxel	Oncology
15G09	Cilnidipine	Cardiovascular
15G10	Imiquimod	Dermatology
15G11	Fosinopril	Cardiovascular
15H02	Imatinib	Oncology
15H03	Moxifloxacin	Infectiology
15H04	Formoterol fumarate	Respiratory
15H05	Rufloxacin	Infectiology
15H06	Pravastatin	Metabolism
15H07	Rosiglitazone Hydrochloride	Metabolism
15H08	Rivastigmine	Central Nervous System
15H09	Sildenafil	Cardiovascular
15H10	Acetylsalicylic acid	Central Nervous System
15H11	Hexachlorophene	Infectiology

8. APPENDIX C - VIABILITY RESULTS OF PROBES SCREEN

Table 8.1 Percent viability results of Epigenetics Probes Screens

Drug	T98G				U373-1stscreen				U373-2ndscreen				DE-TMZR				TMZR			
	Drug		Drug+ TMZ (500 µM)		Drug		Drug+ TMZ (500 µM)		Drug		Drug+ TMZ (250 µM)		Drug		Drug+ TMZ (500 µM)		Drug		Drug+ TMZ (500 µM)	
	Viability(%)	STDEV(%)	Viability(%)	STDEV(%)	Viability(%)	STDEV(%)	Viability(%)	STDEV(%)	Viability(%)	STDEV(%)	Viability(%)	STDEV(%)	Viability(%)	STDEV(%)	Viability(%)	STDEV(%)	Viability(%)	STDEV(%)	Viability(%)	STDEV(%)
Control	100	2	87	3	100	1	60	1	100	4	86	0	100	0	86	0	100	2	95	0
(+)-JQ1	92	0	85	2	84	8	57	0	88	0	82	2	84	0	74	0	99	0	95	1
(-)-JQ1	99	0	91	2	96	8	74	3	96	1	86	1	90	1	80	3	97	1	93	4
PFI-1	85	0	79	0	72	5	46	2	69	2	57	2	58	0	42	3	82	2	70	3
I-BET	99	1	89	4	96	10	68	3	76	1	65	2	75	5	53	3	93	3	83	5
Bromosporine	88	2	82	1	76	6	51	4	76	4	71	1	70	3	57	4	92	1	87	2
CBP/BRD4	101	1	91	2	92	1	58	2	94	3	84	12	80	7	62	5	116	10	107	7
SGC-CBP30	101	1	94	1	97	8	67	1	95	2	84	2	95	2	74	1	101	3	97	4
I-CBP112	81	30	77	13	96	2	67	2	94	0	92	13	86	4	72	1	111	10	103	8
RVX-208	95	3	89	1	89	8	61	4	91	2	78	3	83	1	69	1	100	2	94	6
SMARCA	92	1	91	1	95	1	68	2	101	8	93	1	86	9	69	1	105	1	108	3
PFI-3	27	0	87	3	92	3	60	1	97	2	88	2	87	2	74	5	107	13	100	5
GSK2801	NA	NA	NA	NA	NA	NA	NA	NA	95	2	92	3	89	2	77	2	99	3	98	3
PFI-4	73	3	91	1	95	1	68	2	100	5	91	3	89	7	67	1	103	2	102	0
OF-1	63	1	85	1	90	5	66	0	98	7	88	1	85	3	69	0	97	3	99	10
Belinostat	48	2	25	0	52	1	9	6	50	3	3	1	7	0	2	0	15	0	9	1
CXD101	63	5	48	0	52	3	9	1	NA	NA	NA	NA	NA	NA	NA	NA	NA	NA	NA	NA
Valproicacid	98	3	93	4	97	0	68	0	105	5	92	0	91	0	72	0	119	9	104	4
Entinostat	97	5	94	1	100	10	78	0	105	3	68	4	91	1	88	0	103	0	99	1
SAHA	69	0	60	1	73	10	43	9	89	0	42	13	58	1	36	6	53	0	41	4
TrichostatinA	96	2	26	5	43	8	2	0	101	4	94	2	94	3	77	6	113	1	102	3
SRT1720	92	0	82	7	91	2	66	3	102	9	91	5	83	1	66	2	103	3	101	11
EX527	100	3	92	1	90	8	68	4	89	2	87	1	94	2	82	9	94	0	97	1
CI-994	96	0	88	1	97	1	74	2	103	4	82	1	89	4	77	5	109	5	106	3
CPI-360	92	2	87	0	99	2	69	0	102	5	83	7	89	2	78	7	113	12	104	1
UNC0638	97	4	82	2	91	9	67	5	95	1	85	5	85	11	76	3	98	1	94	2
UNC0642	96	1	71	16	85	7	69	8	90	0	85	5	81	2	69	2	94	0	96	8
A-366	35	8	93	1	97	1	64	1	101	6	95	6	94	2	71	1	103	1	108	2
Chaetocin	28	1	93	1	50	4	28	3	98	3	90	0	84	4	67	3	105	7	98	4
PFI-2	96	4	89	3	94	3	65	3	99	7	89	2	85	2	63	2	108	3	98	6
SGC0946	96	0	81	3	92	6	76	5	93	2	87	6	96	0	82	4	106	2	103	9
GSK343	94	14	85	2	96	3	73	1	105	10	77	14	86	3	71	5	100	2	106	4
UNC1999	93	1	89	1	98	3	70	2	101	7	90	2	89	4	71	3	116	3	101	5
LLY-507	92	1	77	2	89	5	71	4	93	2	88	2	94	5	76	4	95	4	99	0
Tranylcypromin	97	1	87	1	94	6	73	3	98	0	84	0	92	2	81	2	97	0	105	11
GSK-LSD)	38	2	83	1	93	1	69	1	101	9	93	2	86	3	74	8	98	1	105	5
GSKJ4	69	0	63	1	21	0	15	1	31	1	24	7	20	0	15	2	22	0	19	1
GSKJ5)	92	2	82	1	87	5	64	1	92	0	84	4	96	7	80	1	95	0	97	5
IOX	51	5	53	12	68	11	54	5	77	3	78	1	68	4	58	5	68	2	77	6
Methylstat	94	4	84	4	70	3	40	2	86	2	72	4	72	3	49	0	80	1	76	5
(E)-JIB-04	100	0	87	5	97	8	74	2	98	3	87	1	89	1	82	1	100	0	92	3
IOX2	86	1	89	2	73	1	56	5	99	5	95	3	85	4	65	3	110	5	101	4
OICR-9429	92	1	89	3	92	0	62	8	100	5	90	1	86	2	71	3	109	5	103	2
UNC1215	100	2	92	1	93	2	63	1	96	2	87	2	94	1	77	0	96	2	94	5
5-Azacitidine	71	11	68	0	97	4	73	2	84	0	58	10	68	2	53	11	72	2	70	1
5-Azadeoxycit.	94	4	91	8	83	7	50	0	81	3	49	6	72	4	53	0	74	4	58	0
Olaparib	93	2	66	1	65	1	45	0	95	1	29	0	92	3	23	0	96	3	17	2

Rucaparib	85	1	61	1	94	7	28	0	68	4	37	5	44	2	16	1	73	4	16	1
K00135	NA	NA	NA	NA	NA	NA	NA	NA	98	2	96	4	92	1	77	1	103	13	103	5
5-Iodotuber.	35	1	39	0	42	2	31	1	91	0	86	7	81	4	65	1	87	2	82	1
C646	96	8	87	1	95	0	63	1	99	4	89	0	86	3	73	1	108	2	97	5
GSK484	100	1	88	4	89	6	69	2	93	1	87	0	93	3	83	7	100	4	102	9
KDOBA67	54	1	51	1	32	1	18	1	43	0	32	2	24	0	15	2	18	2	17	0
BAZ2-ICR	96	2	90	1	95		69		99	6	92	3	86	2	69	0	111	5	100	4
NI-57	99	0	87	0	100	6	74	1	96	2	89	5	94	3	81	2	100	5	98	2
LP99	71	0	89	1	93	3	63	0	99	1	89	2	86	0	69	4	101	5	102	3
SGC707	96	0	85	0	95	4	69	2	93	2	89	2	97	5	81	0	97	0	99	1
RGFP966	88	0	85	2	92	2	65	3	99	3	88	1	75	3	69	0	103	10	103	2
PCI-34051	96	3	91	1	83	5	63	6	85	2	81	2	83	4	69	5	89	1	91	0
Ricolinostat	48	5	58	4	59	1	9	2	69	0	8	3	30	0	7	2	35	4	25	1
Tubastatin	2	3	84	2	78	0	60	6	89	2	74	10	91	4	69	6	89	3	89	6
KDOAM-25a	52	1	89	1	92	0	63	0	101	5	90	2	84	4	70	5	104	6	100	3
KDM5-C70	99	1	89	4	96	10	68	3	93	0	86	0	88	4	80	8	98	2	98	4
MAZ1805	82	3	65	2	64	3	53	1	82	11	63	22	59	1	52	1	54	9	48	3
MAZ1392	28	3	31	1	18	1	20	0	26	1	31	0	19	2	20	0	9	1	10	0
BI-9564	96	3	89	5	85	1	66	2	97	9	87	13	78	3	70	8	90	5	93	3
NVS-CECR2-1	100	0	89	1	94	5	68	3	96	1	83	6	92	5	78	1	97	1	97	2
GSK106	96	1	85	3	99	7	70	2	96	1	84	2	94	7	77	2	100	3	101	9
A-196	104	2	90	4	94	5	74	6	94	0	83	1	94	1	83	8	102	2	101	3
BAY-598	92	10	86	2	94	1	65	0	102	7	91	8	84	4	72	2	103	1	104	2
MS049	101	2	87	3	95	10	73	3	98	0	86	0	95	4	78	6	98	2	94	0
MS023	51	5	82	0	81	0	59	0	86	3	82	3	63	2	51	5	87	10	81	1
GSK591	78	4	88	3	87	1	67	0	88	1	93	9	75	5	62	3	91	10	96	9
SGI-1776	2	0	1	0	2	1	1	0	2	1	2	0	2	1	1	0	7	6	2	0
CHR-6494	99	1	40	2	58	2	42	0	81	2	82	1	88	2	61	2	103	2	98	3
CPI-169	6	1	86	1	95	3	70	2	103	5	83	9	96	2	78	1	103	2	108	4
UNC2400	100	1	86	7	95	10	74	1	97	0	86	4	86	6	83	1	95	3	95	7
GSK864	97	1	91	2	96	3	61	0	101	6	80	0	86	1	71	0	114	12	101	2
GSK8814	NA	NA	NA	NA	NA	NA	NA	NA	95	4	80	6	82	2	68	5	105	9	95	0
GSK8815	NA	NA	NA	NA	NA	NA	NA	NA	97	2	76	3	84	4	72	1	110	6	101	7
BAY-299	93	1	79	2	92	5	58	2	94	1	76	1	90	1	63	5	97	0	95	1
PCI-24781	14	8	5	0	6	0	1	0	12	0	2	0	2	0	1	0	2	0	2	0
Romidepsin	6	0	4	0	4	0	1	0	7	1	2	1	1	0	1	0	1	0	1	0
Mocetinostat	27	0	13	0	20	3	9	1	30	1	3	1	6	0	3	1	5	0	4	0
Santacruzama.	97	0	89	1	95	9	63	9	95	1	86	2	93	1	80	4	94	3	91	3
KDOAM32	97	2	87	3	94	6	69	2	96	1	88	2	91	3	79	2	95	2	90	2
MS409N	66	1	90	3	97	2	68	1	90	2	81	0	85	2	70	2	90	3	91	4
TP-064	85	2	89	3	91	1	64	3	93	2	82	3	81	5	71	0	87	2	84	2
TP-064N	93	6	90	2	95	0	71	1	95	1	85	2	77	2	71	0	90	2	85	6
A-395	98	1	93	2	97	8	69	7	95	3	81	3	94	5	76	8	91	0	95	2
A-395N	98	1	85	6	94	8	71	3	91	1	78	3	82	3	70	2	89	0	93	2
I-BRD9	85	5	70	2	68	6	44	2	66	2	57	11	50	4	42	2	69	0	55	8
TP-472	NA	NA	NA	NA	NA	NA	NA	NA	104	9	94	4	86	5	71	4	103	4	108	3
TP-472N	NA	NA	NA	NA	NA	NA	NA	NA	96	2	90	3	80	3	64	7	86	4	95	5
KDOPZ-32a	NA	NA	NA	NA	NA	NA	NA	NA	97	0	89	7	78	6	61	5	93	8	95	0
KDOOA012000	NA	NA	NA	NA	NA	NA	NA	NA	99	1	88	0	94	3	82	1	96	4	98	1
AMI-1	NA	NA	NA	NA	NA	NA	NA	NA	97	3	85	2	79	2	65	2	87	4	89	8
TMP269	NA	NA	NA	NA	NA	NA	NA	NA	93	6	66	1	80	1	63	1	91	2	87	3
AGK2	NA	NA	NA	NA	NA	NA	NA	NA	97	2	85	0	75	3	60	3	90	0	87	3